College de France lecture 2022: Interactions between atoms in quantum gases, from the two-body problem to the macroscopic case

Jean Dalibard

The interactions between atoms in quantum gases (II)

From the two-body problem to the macroscopic case

Jean Dalibard
Collège de France, chair *Atoms and radiation*

Course 2021-22

Contents

Introduction

How to go from the simple to the complex, from the individual to the collective, from the microscopic to the macroscopic? Does the knowledge of the properties of the basic constituents of ordinary matter, atoms and molecules, allow us to predict the behavior of an assembly of $N \gg 1$ particles, be it gaseous, liquid or solid?

This question arose as soon as the formalism of statistical physics was established. A famous example is the equation of state for a fluid of volume V, pressure P and temperature T written[1] by Johannes Diderik van der Waals in 1873 in his doctoral thesis, an equation which earned him the Nobel Prize in Physics in 1910:

$$\left(P + a' \frac{N^2}{V^2}\right)(V - Nb') = Nk_{\rm B}T. \tag{1}$$

In this equation, the parameters a' and b' are supposed to describe the microscopic physical processes which induce a deviation from the ideal gas, for which $PV = Nk_{\rm B}T$: a' characterizes the interactions between particles, in particular the van der Waals interactions, and b' the volume occupied by each one, considered as a hard impenetrable sphere.

An important prediction of this equation is the universality of phenomena characteristic of fluids described by classical physics, such as the existence of a liquid-gas transition and a critical point where the distinction between liquid and vapor disappears[2]. The van der Waals equation of state also provides relations between the properties of various fluids, as long as reduced units are used that eliminate the microscopic parameters a' and b'. If we denote P_c, T_c and n_c as the pressure, temperature and density $n = N/V$ at the critical point, we can put this equation in the form

$$\frac{P}{P_c} = F\left(\frac{T}{T_c}, \frac{n}{n_c}\right) \tag{3}$$

where F is an identical function for all fluids.

This universality, called the law of corresponding states, is illustrated in figure 1 from the article by Guggenheim (1945). Here, the author has plotted for eight different fluids the density of the gas and the density of the liquid for a range of temperatures below the critical temperature. The densities are measured in units of n_c and the temperatures in units of T_c, so that the universality expressed by (3) should lead to one and the same curve for the different fluids. This is indeed what happens, to a good approximation, for the eight fluids considered.

The van der Waals equation and its generalization by Guggenheim (1945) are entirely classical approaches. They are valid at high temperature, more precisely at low phase space density:

$$n\lambda^3 \ll 1 \qquad \text{with} \quad \lambda = \left(\frac{2\pi\hbar^2}{mk_{\rm B}T}\right)^{1/2}, \tag{4}$$

where λ is the thermal wavelength.

In this course we will focus on the opposite point of view, in which quantum effects play an essential role. This point of view is of course mo-

[1] The variables used by van der Waals were the number of moles and the ideal gas constant R. One passes from one notation system to the other by a multiplication by the Avogadro number.

[2] Let us recall that this critical point is obtained by finding the inflection point of the set of isothermal curves $P(V)$ at a given T. It is therefore necessary to solve

$$\text{Critical point:} \qquad \left(\frac{\partial P}{\partial V}\right)_T = 0 \qquad \left(\frac{\partial^2 P}{\partial V^2}\right)_T = 0, \tag{2}$$

expressing in particular that the compressibility of the fluid is infinite at this point.

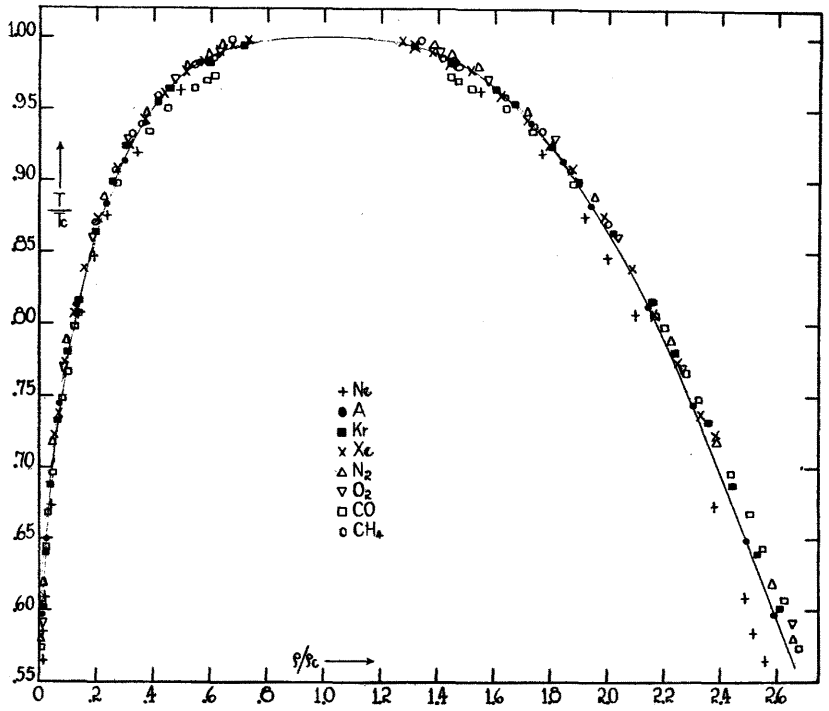

Figure 1. *The "universal" character of liquid-gas coexistence for a series of different fluids, represented here on a density-temperature diagram. The density of the gas (left branch) and that of the liquid (right branch) are plotted on this graph. The densities and temperatures are expressed in units of the critical values for each fluid, n_c (noted here ρ_c) and T_c. At the critical point, at the top of the graph, the two curves meet. Note that the fits indicated by a solid line differ quantitatively from the prediction for the van der Waals equation of state, even though the general shape of the results is consistent with what is expected for (1). Figure from Guggenheim (1945).*

tivated by the considerable development of research in the physics of gases at very low temperatures that has taken place over the last twenty years. Thanks to the combination of laser and evaporative cooling of atoms, it is possible to produce highly degenerate bosonic or fermionic fluids. For these fluids, the interactions must be described by quantum physics. More precisely, the collisions occur essentially in the partial wave of zero angular momentum, the s-wave. They are therefore characterized by a number, the scattering length a, whose value can, for some atomic species, be adjusted to an arbitrary value, possibly $a = \pm\infty$, thanks to scattering resonances called Fano–Feshbach resonances.

Our goal will be to understand to what extent we can find a quantum universality, similar in principle to the one shown in figure 1. This universality should allow us to link the macroscopic properties of the fluid, such as its energy, to the microscopic quantity a. We will proceed step by step according to the following plan:

- Chapter 1 will be devoted to the weakly degenerate case, $n\lambda^3 \lesssim 1$, which can be approached by the virial expansion, i.e. an expansion of the equation of state in powers of $n\lambda^3$.

- Chapters 2, 3 and 4 will be devoted to the case of the strongly degenerate Bose gas, $n\lambda^3 \gg 1$, but relatively weakly interacting in the sense that $na^3 \ll 1$. We will start with a detailed presentation of the Bogoliubov method, then we will study higher order corrections, such as the Lee-Huang-Yang correction (Lee, Huang, et al. 1957). We will describe several recent experiments providing quantitative tests of these theories. We will also explain how these corrections allow to stabilize "liquid" states, i.e. states with density independent of the number of particles (Petrov 2015).

- In chapters 5 and 6, we will discuss the case of strongly interacting systems, in which a scattering resonance allows to realize a situation such as $na^3 \gtrsim 1$, while remaining in the dilute regime $nb^3 \ll 1$ where b is the range of the potential. We will present the contact concept introduced by S. Tan (Tan 2008a; Tan 2008c) and show how it allows to link one- or two-body physics, for example the momentum distribution $n(\boldsymbol{k})$ and the spatial correlation function $g_2(r)$, to N-body physics through thermodynamic functions.

In this course we will use a number of notions that were developed in detail in last year's course: s-wave collision and scattering length, Born expansion, Fano–Feshbach resonances. We will recall as we go along the essential ingredients to use these notions and we refer the reader to the notes of the course 2020-21 to deepen them if needed.

I thank Jérôme Beugnon, Markus Holzmann, Raphael Lopes, Sylvain Nascimbene, Félix Werner and Willi Zwerger for many discussions on the points covered in this course.

Chapter I

Weakly degenerate quantum gases : the virial expansion approach

In this chapter we discuss a first method to relate few-body physics and macroscopic properties of a fluid. This method, which is called virial expansion, is usable for weakly degenerate fluids, i.e. a phase-space density $n\lambda^3 \ll 1$, where n is the spatial density and $\lambda = \sqrt{2\pi\hbar^2/mk_{\rm B}T}$ the thermal wavelength, T denoting the temperature.

This virial approach consists in an expansion of a thermodynamic function of the macroscopic fluid, the pressure for example, in powers of the density n or of the fugacity[1] $z = \exp(\mu/k_{\rm B}T)$, where μ is the chemical potential. This type of expansion was proposed by Kamerlingh Onnes at the very beginning of the twentieth century for a fluid described by classical thermodynamics, then extended to a quantum description by Uhlenbeck & Beth (1936) and Beth & Uhlenbeck (1937). Remarkably, the coefficient of the n-th order term (with in practice n from 2 to 5) is computable provided that one knows how to treat exactly the n-body problem, thus a "small" system, far from the macroscopic case [*cf.* figure 1].

We begin this chapter by recalling the basics of the thermodynamic description of an ideal quantum gas, obeying Bose or Fermi statistics. We then find a first source of deviation of the coefficients of the virial expansion with respect to a Boltzmann gas. In the second part, we are interested in the first non-trivial virial coefficient, noted b_2. We detail its calculation in the case of "standard" interactions and we recover a famous result of Beth & Uhlenbeck (1937). We then discuss the case of binary resonant interactions. The third part is devoted to the case of the spin 1/2 Fermi gas in the unitary regime, i.e. with resonant $\uparrow\downarrow$ interactions. This is a system which currently plays a central role in quantum gas physics, as it allows to test in a very fine way different theoretical approaches by confronting them with experimental results. We describe these experiments and present the different known results for the coefficients b_3, b_4 and b_5 of the expansion.

[1] For an expansion in powers of z, some authors prefer to use the term *cluster expansion*. We will keep here the most common terminology, virial expansion.

1 The virial expansion

1-1 Equation of state of a fluid

The state of a fluid at thermodynamic equilibrium is characterized by the value of a number of thermodynamic variables. For a gas of particles without spin, we generally use the following three variables:

- the temperature T or its conjugate variable, the entropy S.
- the volume L^3 or its conjugate variable, the pressure P.

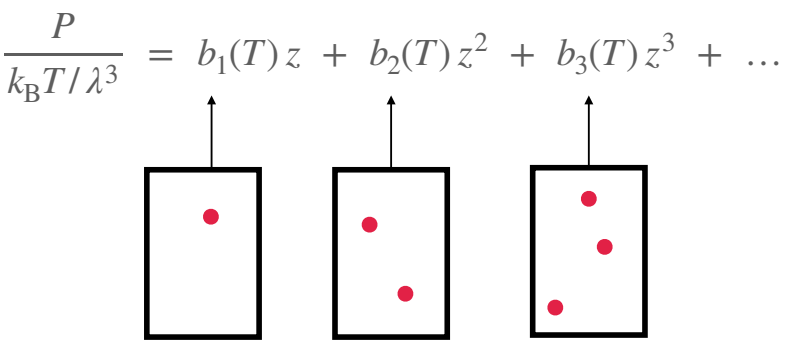

Figure 1. *Principle of virial expansion. We express the pressure P (in units of $k_B T/\lambda^3$) as an expansion in powers of the fugacity $z = \exp(\mu/k_B T)$. The coefficient of order n, $b_n(T)$, is computed by solving the corresponding n-body problem. We thus make the link between the macroscopic properties of the fluid and the few-body problem (n typically ranging from 2 to 5), at least in the weakly degenerate case: $n\lambda^3 \sim z \ll 1$.*

- the number of particles N or its conjugate variable, the chemical potential μ

The equation of state of a fluid consists in expressing a thermodynamic function, the energy $E(S, L^3, N)$ or the grand potential $\Omega(T, L^3, \mu)$ for example, in terms of a triplet formed from these variables. At first, we will use the grand potential $\Omega(T, L^3, \mu)$, whose total differential is written:

$$\boxed{\mathrm{d}\Omega = -S\,\mathrm{d}T \; - P\,\mathrm{d}L^3 \; - \; N\,\mathrm{d}\mu} \tag{1}$$

It is shown in statistical physics [see for example Landau & Lifshitz (1975)] that Ω is related to the partition function in the grand-canonical set Z_{GC}

$$\Omega = -k_B T \log Z_{GC} \tag{2}$$

with

$$Z_{\mathrm{GC}} = \sum_{N=0}^{\infty} z^N Z_N, \tag{3}$$

where we introduced the fugacity $z = \exp(\mu/k_B T)$ and where Z_N is the partition function of the N-particle canonical ensemble, with $Z_0 = 1$ by convention. Recall the definition of Z_N:

$$Z_N = \sum_j \mathrm{e}^{-E_j/k_B T} \tag{4}$$

where the sum relates to all the ϕ_j states of the N particle system. In practice, due to the Boltzmann factor $\mathrm{e}^{-E_j/k_B T}$, only the ground state of energy E_0 and the excited states of energy $E_j - E_0 \lesssim$ some $k_B T$ contribute significantly to Z_N.

Once we know grand potential $\Omega(L^3, T, \mu)$, we deduce the conjugate thermodynamic quantities of the three variables, the entropy S, the pressure P and the average number of particles N (or the spatial density n):

$$S = -\left(\frac{\partial\Omega}{\partial T}\right)_{L^3,\mu} \qquad P = -\left(\frac{\partial\Omega}{\partial L^3}\right)_{T,\mu} \qquad n = \frac{N}{L^3} = -\frac{1}{L^3}\left(\frac{\partial\Omega}{\partial\mu}\right)_{T,L^3}. \tag{5}$$

We consider here a fluid in which the range of interaction is sufficiently short for the grand potential Ω to be an extensive function, i.e. proportional to the volume when we keep T and μ constant. The interest of the choice of the grand potential is then clear: the relation between Ω and P can only be the linear relation

$$\boxed{\Omega = -PL^3} \tag{6}$$

In other words, a possible equation of state for the fluid is the expression of the pressure P in terms of the temperature and the chemical potential. To work with dimensionless quantities, we can look at, for example

$$\frac{P\lambda^3}{k_B T}. \tag{7}$$

By Legendre transformation, we can then calculate other thermodynamic potentials like the free energy $F(L^3, T, N) = \Omega + \mu N$ or the internal energy $E(L^3, S, N) = \Omega + TS + \mu N$.

1-2 The classical ideal gas (Boltzmann)

The classical ideal gas corresponds to an assembly of particles of mass m, non-interacting and uncorrelated, and it obeys the Boltzmann statistics. If

we take periodic boundary conditions in the box of volume L^3, a basis of eigenstates for a particle is given by the plane waves

$$\frac{1}{\sqrt{L^3}}\mathrm{e}^{\mathrm{i}\boldsymbol{k}\cdot\boldsymbol{r}}, \qquad \boldsymbol{k}=\frac{2\pi}{L}\boldsymbol{n}, \quad n\in\mathbb{Z}^3, \tag{8}$$

of energy $\hbar^2k^2/2m$ The partition function at a particle is then

$$Z_1=\sum_{\boldsymbol{k}}\mathrm{e}^{-\hbar^2k^2/2mk_{\mathrm{B}}T}=\frac{L^3}{(2\pi)^3}\int\mathrm{e}^{-\hbar^2k^2/2mk_{\mathrm{B}}T}\,\mathrm{d}^3k \tag{9}$$

or

$$\boxed{Z_1=\frac{L^3}{\lambda^3}} \tag{10}$$

Since the particles are not correlated, the N-particle partition function is equal to the product of N functions Z_1, up the $1/N!$ factor necessary for the resolution of the Gibbs paradox. We thus have

$$Z_{\mathrm{GC}}=\sum_{N=0}^{\infty}\frac{(zZ_1)^N}{N!}=\exp(zZ_1) \tag{11}$$

and therefore

$$\Omega=-k_{\mathrm{B}}T\;z\;Z_1=-k_{\mathrm{B}}T\;z\;\frac{L^3}{\lambda^3}. \tag{12}$$

We deduce from (6) the expression of the pressure

$$\boxed{\text{Classical ideal gas}: \qquad \frac{P\lambda^3}{k_{\mathrm{B}}T}=z} \tag{13}$$

The spatial density is deduced from (5):

$$n\lambda^3=z. \tag{14}$$

For the classical ideal gas, the fugacity is equal to the phase-space density.

1-3 The Quantum Ideal Gases

In our physical world, the classical ideal gas studied above does not exist. Even if the particles do not interact (ideal gas), the fact that they obey the Bose or Fermi statistics introduces correlations between them. For example, the Pauli principle forbids that two fermions of the same spin occupy the same $\boldsymbol{k}$ state.

For quantum particles without interaction, the calculation (2) of the grand potential Ω from the grand-canonical partition function Z_{GC} is treated in all the statistical physics books. Let us state here the result:

$$\text{Ideal gas (Bose)}: \qquad \Omega=k_{\mathrm{B}}T\sum_j\log\left(1-z\,\mathrm{e}^{-E_j/k_{\mathrm{B}}T}\right) \tag{15}$$

$$\text{Ideal gas (Fermi)}: \qquad \Omega=-k_{\mathrm{B}}T\sum_j\log\left(1+z\,\mathrm{e}^{-E_j/k_{\mathrm{B}}T}\right) \tag{16}$$

where the sum covers all single-particle states ϕ_j (spin and orbital), of energy E_j.

Let us take a gas of spinless or polarized particles, so that the spin degree of freedom does not intervene. The ϕ_j states are the plane waves and we find, by replacing the discrete sum over $\boldsymbol{k}$ by an integral:

$$\Omega=\pm k_{\mathrm{B}}T\frac{L^3}{(2\pi)^3}\int\log\left(1\mp z\,\mathrm{e}^{-\hbar^2k^2/2mk_{\mathrm{B}}T}\right)\mathrm{d}^3k \tag{17}$$

By using the series expansion

$$\log(1-x)=-\sum_{j=1}^{\infty}\frac{x^j}{j}, \tag{18}$$

we arrive at

$$\boxed{\text{Ideal gas (polarized bosons)}: \qquad \frac{P\lambda^3}{k_{\mathrm{B}}T}=\sum_{j=1}^{+\infty}\frac{1}{j^{5/2}}\,z^j} \tag{19}$$

and

$$\boxed{\text{Ideal gas (polarized fermions)}: \qquad \frac{P\lambda^3}{k_{\mathrm{B}}T}=\sum_{j=1}^{+\infty}\frac{(-1)^{j+1}}{j^{5/2}}\,z^j} \tag{20}$$

The first term ($j=1$) of the expansions (19) and (20) coincides with the classical gas result (13). The appearance of the following terms ($j\geq 2$) in the case of bosons or fermions reflects the emergence of correlations between particles due to quantum statistics.

1-4 The principle of virial expansion

We now consider a gas of spinless or polarized particles, interacting with each other and confined in a box of volume L^3. The virial expansion is based on the series in powers of the fugacity z:

$$\boxed{\frac{P\lambda^3}{k_{\rm B}T} = \sum_{j=1}^{\infty} b_j(T)\, z^j} \tag{21}$$

This expansion is useful when the fugacity z is small in front of 1, i.e. negative μ with $|\mu| \gg k_{\rm B}T$. As we have seen in the case of the classical ideal gas [*cf.* (14)], this corresponds to a weakly degenerate gas, with a small phase-space density $n\lambda^3$. We can then restrict ourselves to the first terms of the expansion, which we assume to converge in the limit $z \ll 1$ (Lebowitz & Penrose 1964).

Once the expansion of the pressure is known, we deduce from (5) the other thermodynamic quantities such as the density n:

$$n = \left(\frac{\partial P}{\partial \mu}\right)_{T,L^3}, \tag{22}$$

which leads to

$$\boxed{n\lambda^3 = \sum_{j=1}^{\infty} j\, b_j(T)\, z^j} \tag{23}$$

The different coefficients $b_j(T)$ are obtained by identifying term by term the powers of z in the equality

$$\frac{P\lambda^3}{k_{\rm B}T} = \frac{\lambda^3}{L^3} \log Z_{\rm GC} \tag{24}$$

that is:

$$b_1(T)\, z + b_2(T)\, z^2 + \ldots = \frac{\lambda^3}{L^3} \log\left(1 + zZ_1 + z^2 Z_2 + \ldots\right) \tag{25}$$

We can then immediately see that the first virial coefficient $b_1(T)$ involves only the one-body partition function Z_1 and therefore contains no contribution from the interactions:

$$b_1(T) = \frac{\lambda^3}{L^3} Z_1 \tag{26}$$

or by using the relation $Z_1 = L^3/\lambda^3$:

$$\boxed{b_1(T) = 1} \tag{27}$$

The second virial coefficient $b_2(T)$ requires the knowledge of Z_2, thus of two-body physics:

$$\boxed{b_2(T) = \frac{1}{Z_1}\left(Z_2 - \frac{Z_1^2}{2}\right)} \tag{28}$$

and we similarly find:

$$\boxed{b_3(T) = \frac{1}{Z_1}\left(Z_3 - Z_1 Z_2 + \frac{Z_1^3}{3}\right)} \tag{29}$$

More generally, the coefficient of order j, $b_j(T)$, involves the solution of problems with at most j bodies, and only them! We thus have the following remarkable property: the virial expansion, when it converges, allows us to link in a natural way the few-body physics and the macroscopic properties of the fluid. In the following paragraph, we will focus on two-body processes, i.e. the first deviation from the ideal gas.

2 The second virial coefficient

According to the results stated in the previous paragraph, the second virial coefficient $b_2(T)$ contains the first corrections to the classical ideal gas. These corrections correspond to the emergence of correlations between particles caused by

- the simple effects of quantum statistics, with

$$b_2^{(0)} = \pm\frac{1}{2^{5/2}} \tag{30}$$

  as we saw in (19) and (20). The superscript $^{(0)}$ indicates here that the result is obtained for an ideal gas.

- the interactions between particles, which we will focus on in the following paragraphs.

According to (28), the correction to b_2 related to the interactions is directly proportional to the correction to Z_2, which we will note ΔZ_2.

The quantum effects for b_2. Before turning to the role of interactions, it is instructive to check that one can recover directly the coefficient $b_2^{(0)}$. For bosons, a basis of possible states is given by the pairs $(\boldsymbol{k}_1, \boldsymbol{k}_2)$, counting only once the pair $(\boldsymbol{k}_1, \boldsymbol{k}_2) \equiv (\boldsymbol{k}_2, \boldsymbol{k}_1)$ and without restriction for the state $\boldsymbol{k}_1 = \boldsymbol{k}_2$. For polarized fermions, we also count only once each pair but the $\boldsymbol{k}_1 = \boldsymbol{k}_2$ state is excluded. We can group the two cases by writing:

$$Z_2 = \frac{1}{2} \sum_{\boldsymbol{k}_1, \boldsymbol{k}_2} \mathrm{e}^{-\hbar^2(k_1^2+k_2^2)/(2mk_{\mathrm{B}}T)} \pm \frac{1}{2} \sum_{\boldsymbol{k}} \mathrm{e}^{-\hbar^2 k^2/(mk_{\mathrm{B}}T)} = \frac{Z_1^2}{2} \pm \frac{Z_1}{2^{5/2}} \quad (31)$$

with sign $+$ for bosons and $-$ for fermions. We thus recover

$$\boxed{\text{Ideal quantum gas:} \qquad b_2^{(0)} = \pm \frac{1}{2^{5/2}}} \quad (32)$$

2-1 "Center of mass" and "relative motion" separation

Let us consider a gas of polarized bosons with binary interactions through the potential $V(r)$, assumed to be isotropic. We rewrite here the two-particle partition function Z_2 in the form:

$$Z_2 = \left(\sum_{\boldsymbol{K}} \mathrm{e}^{-\hbar^2 K^2/(4mk_{\mathrm{B}}T)} \right) \left(\sum_j \mathrm{e}^{-E_j/k_{\mathrm{B}}T} \right). \quad (33)$$

We have separated the free motion of the center of mass, parametrized by its momentum $\boldsymbol{K} = \boldsymbol{k}_1 + \boldsymbol{k}_2$ associated to the total mass $2m$, and the motion of the relative variable, characterized by its eigenstates $\psi_j(\boldsymbol{r})$ of energy E_j, and associated to the reduced mass $m_{\mathrm{r}} = m/2$.

The center of mass part is calculated as before to give:

$$\boxed{Z^{\mathrm{CdM}} = \sum_{\boldsymbol{K}} \mathrm{e}^{-\hbar^2 K^2/(4mk_{\mathrm{B}}T)} = 2^{3/2} Z_1} \quad (34)$$

The sum in the relative variable part

$$Z^{\mathrm{rel}} = \sum_j \mathrm{e}^{-E_j/k_{\mathrm{B}}T} \quad (35)$$

contains the contribution of all angular momentum states (partial waves) $\ell = 0, 2, 4, \ldots$ allowed by the symmetrization principle:

$$Z^{\mathrm{rel}} = \sum_\ell Z_\ell^{\mathrm{rel}}. \quad (36)$$

We will assume here that the gas of bosons is cold enough for only the s-wave interactions to play a role (recall that polarized fermions have no interaction in this channel). The contribution of the partial waves $\ell \neq 0$ to this sum is therefore identical to that of an ideal gas and we will not write it explicitly. Concerning the contribution $Z_{\ell=0}^{\mathrm{rel}}$ of the angular momentum channel $\ell = 0$ (s wave), let us recall that it contains both the contribution of the bound states (diatomic molecules) and of the asymptotically free scattering states.

2-2 s wave interactions away from resonance

In this paragraph, we place ourselves in a "normal" situation of the interaction between two atoms, i.e. a scattering length a comparable to the range of the van der Waals potential[2] $b \equiv R_{\mathrm{vdW}}$. This assumption simplifies the calculation of the b_2 coefficient, both for the contribution of scattering and bound states [see figure 2]:

- The free states that contribute significantly to Z_2^{rel} are such that $\hbar^2 k^2/2m \lesssim$ a few $k_{\mathrm{B}}T$, that is, $k \lesssim 1/\lambda$. But the thermal energies $k_{\mathrm{B}}T$ of quantum gases are much lower than $E_{\mathrm{vdW}} \equiv \hbar^2/mR_{\mathrm{vdW}}^2$, which is of the order of a least a few ten microkelvin (or even more for light

[2] Recall that the van der Waals radius is defined from the mass of an atom and the coefficient C_6 describing the van der Waals interaction by

$$R_{\mathrm{vdW}} = \frac{1}{2} \left(\frac{mC_6}{\hbar^2} \right)^{1/4}. \quad (37)$$

For the atomic species used in the experiments, this van der Waals radius is of the order of a few nanometers.

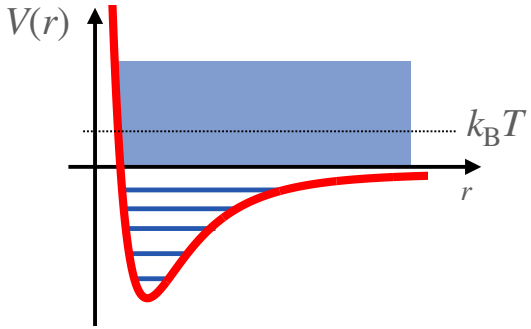

Figure 2. *Scattering states and bound states for the two-body problem. In the non-resonant case ($|a| \ll \lambda$), we will focus essentially on the scattering states, and more particularly on those whose energy does not exceed a few $k_B T$. In the resonant case ($|a| \gg \lambda$), we will also take into account the contribution of the last bound state, whose energy $\sim -\hbar^2/ma^2$ may be (in absolute value) small compared to $k_B T$.*

atoms). Actually, if this were not the case, collisions would not occur only in the s wave channel. We have therefore $a \ll \lambda$, that is to say for all relevant $\boldsymbol{k}$ wave vectors the relation $ka \ll 1$.

- The interaction potential between two atoms generally contains many bound states, and the energy of the last bound state in the absence of a scattering resonance is of the order of $-E_{\rm vdW}$. As we have just said, this binding energy is in absolute value large compared to $k_B T$. If there were a collision process in the gas that established an equilibrium between the populations of free and bound states, essentially all atoms would be in the form of dimers (or trimers, tetramers, etc.). Fortunately, this is not the case: the formation of dimers can occur, but it is a marginal process on the time scale of the experiments. Moreover, as soon as they are formed, these dimers generally escape from the trap confining the atoms because the energy released during their formation is greater than the depth of the trap.

Thanks to these two remarks, we limit the calculation of $Z^{\rm rel}_{\ell=0}$ to the

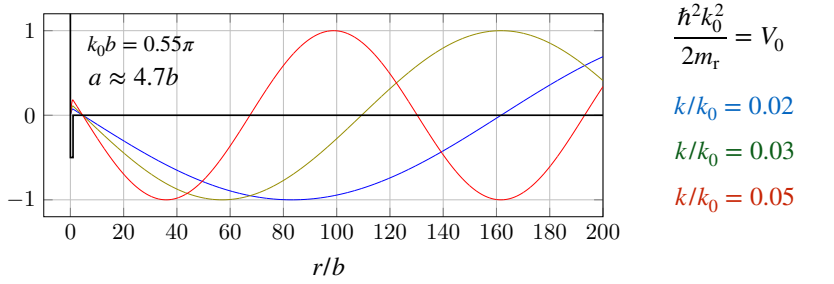

Figure 3. *Scattering states in a square well of depth V_0 and width b, with a (nearly) common node of the wave functions in $r = a$.*

contribution of the s-wave scattering states, identified by their momentum $\hbar k$ and their energy $\hbar^2 k^2/2m_{\rm r} = \hbar^2 k^2/m$. The only difficulty is to count them correctly, knowing that the asymptotic behavior of their reduced wave function is for $ka \ll 1$ (see figure 3):

$$u(r) \approx \sin[k(r-a)]. \tag{38}$$

The presence of the $-ka$ term in the sine does indeed modify their density of states. Suppose that the relative particle is inserted in the center of a sphere of radius R, with Dirichlet boundary conditions on the walls of the sphere. The wave numbers k must then satisfy the quantization condition

$$k_n = n\frac{\pi}{R-a}, \qquad n \text{ positive integer}, \tag{39}$$

instead of $k_n = n\pi/R$ in the absence of interaction. The passage from a discrete sum to an integral for the calculation of $Z^{\rm rel}_{\ell=0}$ then gives:

$$\begin{aligned} Z^{\rm rel}_{\ell=0} &= \sum_n \mathrm{e}^{-\hbar^2 k_n^2/(mk_B T)} = \frac{R-a}{\pi}\int_0^{+\infty} \mathrm{e}^{-\hbar^2 k^2/(mk_B T)}\,\mathrm{d}k \\ &= \frac{R-a}{\sqrt{2}\,\lambda}. \end{aligned} \tag{40}$$

The contribution in R/λ would be present even in the absence of interactions and it has to be added to that of the other partial waves to give, all calculations done, the partition function Z_2 of the ideal quantum gas. The

interesting term here is the one related to the interactions, in a/λ. When multiplied by $Z^{\rm CdM} = 2^{3/2} Z_1$ [*cf.* (34)], this term leads to the contribution of the interactions to the Z_2 partition function:

$$\Delta Z_2 = -2 Z_1 \frac{a}{\lambda} \tag{41}$$

from which we deduce the second virial coefficient

$$\boxed{\text{Bosons out of resonance } (a \ll \lambda) : \qquad b_2(T) = \frac{1}{2^{5/2}} - \frac{2a}{\lambda}} \tag{42}$$

with the two contributions $b_2^{(0)} = 2^{-5/2}$ from quantum statistics and $b_2^{(\rm int.)} = -2a/\lambda$ coming from the interactions.

2-3 Pressure and internal energy of gas

As we explained in z, the knowledge of the grand potential (at a given order in z) allows to find the other thermodynamic potentials at the same order. We will use here the virial expansion to order 2 to find the expression of the interaction energy in the weakly degenerate regime.

We start from the expression of Ω:

$$\Omega(T, L^3, \mu) \approx -k_{\rm B} T \frac{L^3}{\lambda^3} \left[z + b_2(T) z^2 \right] \tag{43}$$

from which we deduce the average number of particles

$$N = -\left(\frac{\partial \Omega}{\partial \mu} \right)_{L^3, T} \approx \frac{L^3}{\lambda^3} \left(z + 2 b_2 z^2 \right) \tag{44}$$

and entropy:

$$\frac{S}{k_{\rm B}} = -\left(\frac{\partial \Omega}{\partial (k_{\rm B} T)} \right)_{L^3, \mu} \approx \frac{L^3}{\lambda^3} \left[\frac{5}{2} (z + b_2 z^2) - \frac{\mu}{k_{\rm B} T} (z + 2 b_2 z^2) + z^2 T \frac{{\rm d}b_2}{{\rm d}T} \right]. \tag{45}$$

At this order of calculation, the relationship (44) between the number of particles and the fugacity can be inverted to give :

$$z \approx n\lambda^3 - 2 b_2 (n\lambda^3)^2, \tag{46}$$

which gives for the pressure-density relationship at this order:

$$\frac{P\lambda^3}{k_{\rm B} T} \approx \left[n\lambda^3 - 2 b_2 (n\lambda^3)^2 \right] + b_2 (n\lambda^3)^2 = n\lambda^3 - b_2 (n\lambda^3)^2. \tag{47}$$

If we limit ourselves to the corrections linked to quantum statistics, $b_2(T) = \pm 2^{-5/2}$, we see that there is, for a fixed density and temperature, a decrease of pressure for bosons ($b_2 > 0$) and an increase for fermions ($b_2 < 0$), compared to the case of a classical ideal gas. This can be understood from the postulate of (anti)symmetrization. For example, for fermions, preventing two particles from being present at the same place constitutes in some way a decrease of the accessible space, hence an increase of the pressure.

Let us now express the internal energy of the gas as a function of T, L^3 and N (or $n = N/L^3$):

$$\boxed{E = \Omega + TS + \mu N = N k_{\rm B} T \left[\frac{3}{2} + n\lambda^3 \left(T \frac{{\rm d}b_2}{{\rm d}T} - \frac{3 b_2}{2} \right) \right]} \tag{48}$$

We find of course the dominant term $\frac{3}{2} k_{\rm B} T$ corresponding to the kinetic energy of a classical ideal gas. Let us examine the corrections to this classical model by reviewing the two contributions to $b_2(T)$ found in (42).

- The term related to quantum statistics, $b_2^{(0)} = 2^{-5/2}$, does not depend on the temperature. It corresponds to a lowering of the energy (for bosons) given by

  $$\text{Bosons :} \qquad \Delta E^{(0)} = -\frac{3}{2^{7/2}} N k_{\rm B} T \; n\lambda^3. \tag{49}$$

  We would find the same contribution for a gas of polarized fermions, up to a change of sign:

  $$\text{Fermions :} \qquad \Delta E^{(0)} = +\frac{3}{2^{7/2}} N k_{\rm B} T \; n\lambda^3. \tag{50}$$

  Here, the small parameter of the expansion, the phase space density $n\lambda^3$, appears explicitely.

- The term related to the interactions, coming from $b_2^{(\rm int.)} = -2a/\lambda$, leads to the modification of the energy

  $$\boxed{\text{Bosons :} \qquad \Delta E^{(\rm int.)} = gnN \qquad \text{with} \quad g = \frac{4\pi\hbar^2 a}{m}} \tag{51}$$

This term would be absent for a gas of polarized fermions (no s-wave interaction).

The form found for $\Delta E^{(\mathrm{int.})}$ is interesting for at least two reasons. First, it allows to verify that the scattering length a is indeed the only parameter of the interaction potential $V(r)$ that plays a role in the N-body problem, at least in the weakly degenerate regime. This important result does not require that the potential $V(r)$ is treated by the Born approximation.

Moreover, the numerical coefficient appearing in (51) is instructive. In this course, we will frequently model the interaction potential by a contact interaction (possibly regularized), leading to the same scattering length a as the real potential. This means replacing the interaction Hamiltonian

$$\hat{H}_{\mathrm{int}} = \frac{1}{2} \iint \hat{n}(\boldsymbol{r})\, \hat{n}(\boldsymbol{r}')\, V(|\boldsymbol{r}-\boldsymbol{r}'|)\, \mathrm{d}^3 r\, \mathrm{d}^3 r' \tag{52}$$

where $\hat{n}(\boldsymbol{r})$ is the operator associated with the density at the point $\boldsymbol{r}$, by

$$\hat{H}_{\mathrm{int}} = \frac{g}{2} \int [\hat{n}(\boldsymbol{r})]^2 \ \mathrm{d}^3 r \qquad \text{with} \quad g = \frac{4\pi\hbar^2 a}{m}. \tag{53}$$

For a homogeneous system, we expect for the average of the interaction energy

$$\Delta E^{(\mathrm{int.})} = \langle \hat{H}_{\mathrm{int}} \rangle = \frac{g}{2} \langle n^2(0) \rangle L^3 \tag{54}$$

which leads, by comparison with (51), that we have in the weakly degenerate regime:

$$\langle n^2(0) \rangle = 2n^2. \tag{55}$$

We find here the bunching discovered by Hanbury-Brown & Twiss (1956) for photons, characteristic of a classical field with Gaussian fluctuations .

2-4 The neighborhood of a scattering resonance

A scattering resonance is characterized by an abnormally large scattering length a, i.e. $|a| \gg b$ where b is the range of the potential. In the vicinity of such a resonance, the evaluation of the b_2 coefficient must be modified.

Let us first recall the nature of these resonances, assuming that one can finely modify one of the parameters of the interaction potential $V(r)$ by

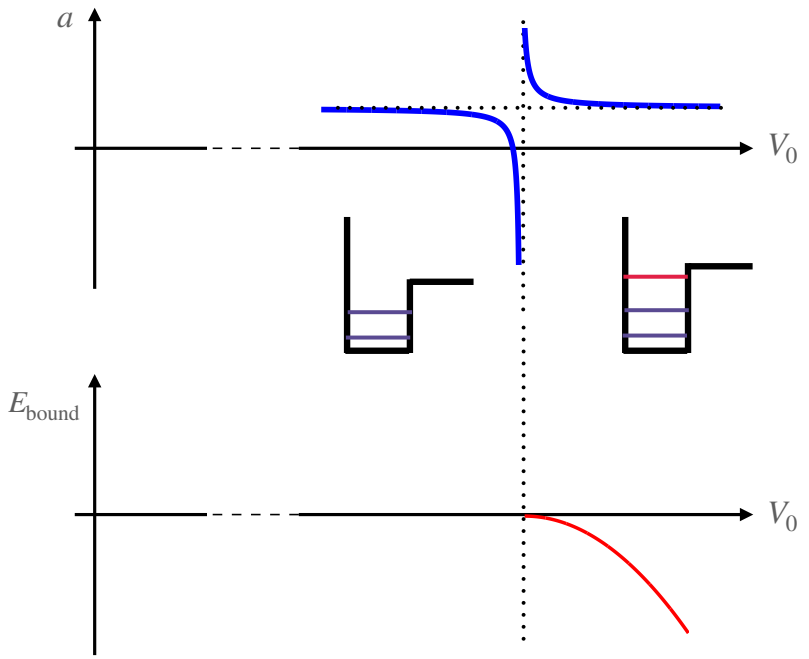

Figure 4. *Appearance of a bound state and divergence of the scattering length a at a scattering resonance.*

making a new bound state appear in this potential[3]. We have the following general result, known as Levinson's theorem [*cf.* figure 4]:

- Just before the bound state appears, the scattering length is large and negative.
- At the threshold of the bound state, the scattering length is infinite.
- Just after the appearance of the bound state, the scattering length is large and positive.

[3]The following description applies without modification to the case of a Fano-Feshbach resonance, at least for the case of a broad resonance. For a study in the case of a narrow resonance, one may consult Endo & Castin (2016b).

Under these conditions, it is essential to take into account the contribution of this weakly bound state to the partition function because its wave function is very large ($\sim a$) and it can be significantly populated during collisions between atoms. Moreover, its (negative) energy :

$$E_{\rm bound} \approx -\frac{\hbar^2}{ma^2} \tag{56}$$

can become very small in front of $k_{\rm B}T$ and a significant population of this bound state is possible without the gas being entirely in dimer form.

Around the resonance, the phase shift $\delta_0(k)$ varies very quickly with k and it is no longer legitimate to assume $\delta_0(k) \approx -ka$ as we did in (38). We must return to the expression

$$u(r) \approx \sin\left[kr + \delta_0(k)\right] \tag{57}$$

where the phase shift is deduced from the general expression

$$\tan[\delta_0(k)] = -ka. \tag{58}$$

As in the non-resonant case, the interactions change the density of states involved in the summation over all possible wave numbers. Taking again Dirichlet boundary conditions in a spherical box of radius R, we now have the quantization condition on k:

$$k_n R + \delta_0(k_n) = n\pi, \qquad n \text{ positive integer} \tag{59}$$

so that the interval between two successive values of k verifies

$$(k_{n+1} - k_n)\left(R + \frac{{\rm d}\delta_0}{{\rm d}k}\right) = \pi. \tag{60}$$

We can then resume the calculation of the partition function $Z^{\rm rel}_{\ell=0}$ as in (40) to find:

$$Z^{\rm rel}_{\ell=0} = (\dots) + \frac{1}{\pi}\int_0^{+\infty} \frac{{\rm d}\delta_0}{{\rm d}k} {\rm e}^{-\hbar^2k^2/mk_{\rm B}T}\,{\rm d}k \;+\; \left[{\rm e}^{-E_{\rm lie}/k_{\rm B}T}\right]. \tag{61}$$

In this expression, the first term $(\dots)$ represents the contribution of the sphere radius R: it is independent of the interactions and will thus be omitted in what follows. The last term corresponds to the contribution

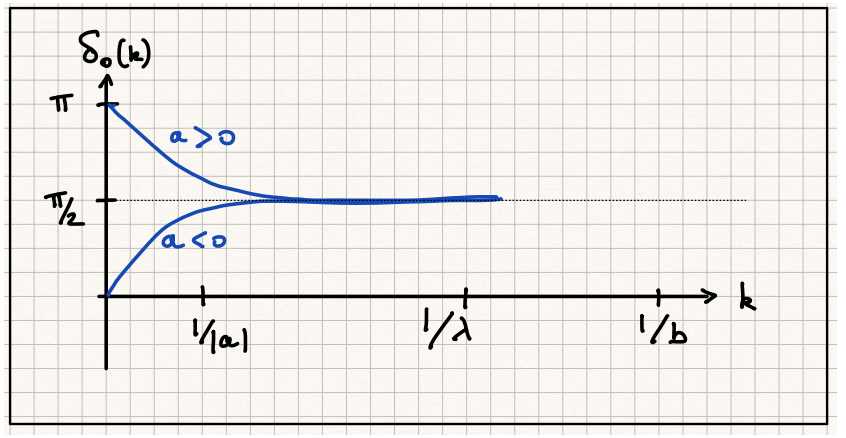

Figure 5. *Schematic representation of the variation of the s-wave phase shift $\delta_0(k)$ in the vicinity of a scattering resonance ($|a| \gg \lambda$).*

of the possible bound state: this contribution must be taken into account only on the $a > 0$ side, since this state does not exist when a is negative; the brackets around this term indicate this restriction. In what follows, we will multiply this contribution by the Heaviside function $\Theta(a)$ to take into account both possibilities.

Using the partition function expression for the center of mass, $Z^{\rm CdM} = 2^{3/2}Z_1$ [*cf.* (34)], we then find the contribution of the interactions to the second virial coefficient[4]:

$$b_2^{\rm (int)} = \frac{2^{3/2}}{\pi}\int_0^{+\infty} \frac{{\rm d}\delta_0}{{\rm d}k} {\rm e}^{-\hbar^2k^2/mk_{\rm B}T}\,{\rm d}k \;+\; 2^{3/2}{\rm e}^{-E_{\rm lie}/k_{\rm B}T}\Theta(a). \tag{63}$$

Let us explicitly compute the integral on k in the case of a scattering

[4] We find here a particular case of the general formula of Beth & Uhlenbeck (1937)

$$b_2^{\rm (int)} = \frac{2^{3/2}}{\pi}\sum_\ell (2\ell+1)\int_0^{\infty} \frac{{\rm d}\delta_\ell}{{\rm d}k} {\rm e}^{-\hbar^2k^2/mk_{\rm B}T}\,{\rm d}k \;+\; 2^{3/2}\sum_j {\rm e}^{-E_j/k_{\rm B}T} \tag{62}$$

restricted here to the case of the s-wave, $\ell = 0$. The discrete sum over j corresponds to the bound states.

resonance. We take the derivative of the relation $\tan[\delta_0(k)] = -ka$:

$$\frac{\mathrm{d}\delta_0}{\mathrm{d}k} = \frac{-a}{1+k^2a^2}. \tag{64}$$

The variation of $\delta_0(k)$ with k is represented on figure 5. For $a < 0$, $\delta_0(k)$ is an increasing function which starts from the value 0 in $k = 0$ to reach a value close to $\pi/2$ when k becomes greater than $1/a$. For $a > 0$, $\delta_0(k)$ is a decreasing function, which starts from π in $k = 0$ to tend also to $\pi/2$ at large k.

If we define the resonance as the region where the scattering length $|a|$ is much larger than the thermal wavelength λ, we see that in this case the variations of the integrand of (63) are dominated by $\frac{\mathrm{d}\delta_0}{\mathrm{d}k}$ and one can take $\mathrm{e}^{-\hbar^2k^2/mk_\mathrm{B}T} \approx 1$ in this integral. Moreover, the bound state when it exists ($a > 0$) also has a very simple contribution to (63): $\mathrm{e}^{-E_\mathrm{bound}/k_\mathrm{B}T} \approx 1$. So we find (Ho & Mueller 2004):

$$b_2^{(\mathrm{int})} \approx \frac{2^{3/2}}{\pi}\int_0^{+\infty} \frac{-a}{1+k^2a^2}\,\mathrm{d}k \;+\; 2^{3/2}\Theta(a) \tag{65}$$

that is:

$$a<0: \qquad b_2^{(\mathrm{int})} \approx \sqrt{2} \qquad \text{(no bound state)} \tag{66}$$

and

$$a>0: \qquad b_2^{(\mathrm{int})} \approx -\sqrt{2}+2^{3/2} \;=\; \sqrt{2}. \tag{67}$$

The coefficient b_2 related to the interactions does not present any discontinuity at the passage to the resonance and it takes at this point a "universal" value, i.e. independent of the temperature:

$$\boxed{\text{Bosons at resonance:} \qquad b_2^{(\mathrm{int})} = \sqrt{2}} \tag{68}$$

We will find this same behavior, within a factor of 2, for the two-component Fermi gas in the unitary regime. Adding the statistical contribution, we have:

$$\boxed{\text{Bosons at resonance:} \qquad b_2 = \frac{1}{2^{5/2}} \;+\; \sqrt{2}} \tag{69}$$

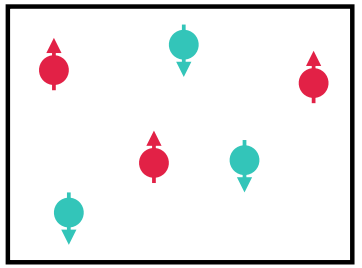

Figure 6. *A two-component Fermi gas, composed of ↑ and ↓ spin atoms.*

3 The unitary Fermi gas

We are interested in a gas of particles with spin (or pseudo-spin) equal to 1/2, sufficiently cold for the interactions to be in the s-wave regime (figure 6). This gas exhibits a scattering resonance so that the ↑↓ interaction corresponds to an infinite a scattering length (figure 4). Moreover, we assume that the gas is sufficiently dilute so that the distance between particles remains large in front of the range b of the potential (or its effective range r_0) so that b and r_0 are not involved in the physics of the problem. We then speak of a unitary Fermi gas since the interactions reach the largest possible value, given the constraint imposed by the unitarity of quantum physics. Recall that there is no s wave interaction for a ↑↑ or ↓↓ pair, because of the exchange antisymmetry between two fermions.

This paradigm of the unitary Fermi gas is found in several circumstances in nature, at least in an approximate way. It is found for example in neutron stars: the scattering length a is of the order of 18 fm while the effective range r_0 is only 2.8 fm. One can thus consider configurations where the distance between particles is large in front of r_0 (thus a dilute system), but small in front of a (thus a strong interaction). Other physical systems approaching the regime of a unitary Fermi gas are the quark-gluon plasma or some superconductors at high critical temperature.

The unitary Fermi gas is a universal system in that it has no length scale associated with the interactions[5]. It is thus a remarkable testbed for

[5]For the unitary Bose gas, effects related to the Efimov phenomenon (appearance of an

the different approaches to systems of strongly correlated particles. For the virial expansion that interests us here, this scale invariance is reflected by the fact that the b_n coefficients of the expansion are pure numbers. We have already noted this point in paragraph § 2-4 on the case of polarized bosons for the b_2 coefficient, but for the case of the unitary Fermi gas, it is in fact valid for all b_n as we will explain in § 3-2.

Considerable efforts have been made over the last 15 years to go beyond the b_2 coefficient. We now have reliable theoretical values for b_3 and for b_4, validated (at least to some extent) by experiment. We will not detail here the complex calculations that led to these predictions, but simply sketch the progress that has been made during the last few years. The reader wishing to go deeper into the question can consult the review articles of Liu (2013) and Endo (2020).

3-1 Virial expansion for a spinor gas

To describe the thermodynamic equilibrium of a gas with two components, we have to introduce a chemical potential for each of them, which we will note μ_+ and μ_-. We assume here that the two components have the same mass and the same energy for the single-particle ground state $\boldsymbol{k} = 0$. They are at the same temperature and occupy the same volume L^3 so that the grand-canonical partition function is now written

$$Z_{\rm GC} = \sum_{N_+,N_-} z_+^{N_+} z_-^{N_-} Z_{N_+,N_-}. \tag{70}$$

The canonical partition function Z_{N_+,N_-} describes a system of N_+ particles in the $\uparrow$ state and N_- particles in the $\downarrow$ state, both at temperature T. The relation between $Z_{\rm GC}$ and the grand potential is unchanged:

$$\Omega = -k_{\rm B}T \ \log Z_{\rm GC}, \tag{71}$$

infinite series of three-body bound states when $|a| = +\infty$) introduce a specific length scale, which breaks the scale invariance. We refer the interested reader to the article by Castin & Werner (2013) which explains how to obtain the b_3 coefficient in this case. A similar situation occurs if the two (pseudo)spin states of the unitary Fermi gas have very different masses. We will assume here that the two masses $m_\uparrow$ and $m_\downarrow$ are equal; hence there is no Efimov effect, hence the announced universality.

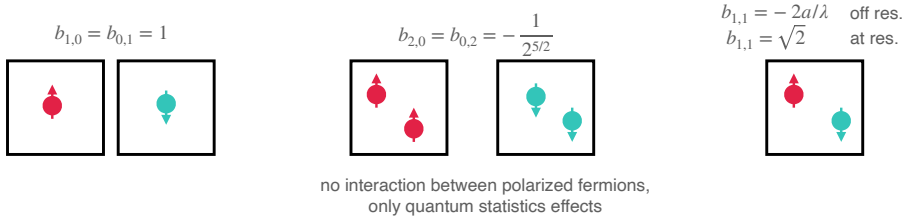

Figure 7. *The first coefficients of the virial expansion for a spin 1/2 gas.*

so that we arrive at an expansion for Ω

$$\Omega = -k_{\rm B}T \ \frac{L^3}{\lambda^3} \sum_{i,j} b_{i,j} \ z_+^i \ z_-^j \tag{72}$$

which we assume to be convergent, at least at low densities in phase space.

The value of the first two coefficients $b_{1,0}$ and $b_{0,1}$ is obtained by putting a single particle ($\uparrow$ or $\downarrow$) in the box of volume L^3 and is therefore unchanged from the one-component case (*cf.* figure 7):

$$\boxed{b_{1,0} = b_{0,1} = 1} \tag{73}$$

To evaluate the terms of order 2, let's separate the two possible cases:

- The two particles are in the same spin state, $N_+ = 2, N_- = 0$ or $N_+ = 0, N_- = 2$. We are then brought back to the previously studied case of polarized fermions, without interaction in the s wave. The corresponding virial coefficient is only due to statistical effects and we have [*cf.* (32)]

$$\boxed{b_{2,0} = b_{0,2} = -\frac{1}{2^{5/2}}} \tag{74}$$

- The two particles are in opposite spin states $N_+ = 1, N_- = 1$. We can consider:
  - Symmetric spin states, hence antisymmetric spatial states (odd partial waves), for which there will be no s-wave interaction and a contribution to $b_{1,1}$ due to quantum statistics in $-2^{-5/2}$ as above.

- Antisymmetric spin states, therefore symmetric spatial states (even partial waves). We then find the same result as for polarized bosons [*cf.* (42) and (68)] with a contribution due to quantum statistics in $+2^{-5/2}$ and a contribution due to interactions equal to $-2a/\lambda$ off-resonance and to $\sqrt{2}$ at resonance.

By summing up the contributions of these two classes of states, we arrive at

$$\boxed{\text{Out of resonance :} \quad b_{1,1} = -\frac{2a}{\lambda} \qquad \text{At resonance :} \quad b_{1,1} = \sqrt{2}} \tag{75}$$

In the following, we will consider a balanced Fermi gas, for which $z_+ = z_- \equiv z$. Noting $n_s = 2$ the number of spin states, the grand potential is then written to order 2 included in fugacity:

$$\Omega \approx -n_s\, k_{\rm B} T\, \frac{L^3}{\lambda^3} \left[z + b_2 z^2 \right] \tag{76}$$

with the effective coefficient b_2:

$$b_2 = \frac{1}{2} \left(b_{2,0} + b_{0,2} + b_{1,1} \right). \tag{77}$$

We find then out of resonance :

$$\boxed{\text{Balanced Fermi gas out of resonance:} \qquad b_2 = -\frac{1}{2^{5/2}} - \frac{a}{\lambda}} \tag{78}$$

and at resonance (Ho & Mueller 2004)

$$\boxed{\text{Resonant balanced Fermi gas:} \qquad b_2 = -\frac{1}{2^{5/2}} + \frac{1}{\sqrt{2}} = \frac{3}{4\sqrt{2}}} \tag{79}$$

i.e. an effect of the interactions divided by 2 compared to the bosonic case: each particle interacts only with half of the assembly of particles, namely those which have a spin opposite to its own.

Internal energy. As we have done in the case of polarized bosons, it is interesting to study the expression of the internal energy of the gas as a function of the densities n_+ and n_-. We place ourselves here in the non-resonant case and we start from the grand potential at order two included

$$\Omega \approx -k_{\rm B} T\, \frac{L^3}{\lambda^3} \left[z_+ + z_- - \frac{1}{2^{5/2}} (z_+^2 + z_-^2) - \frac{2a}{\lambda} z_+ z_- \right]. \tag{80}$$

The calculation proceeds as in the bosonic case. We begin by evaluating the average numbers of particles $N_\pm$ and the entropy S by deriving Ω with respect to $\mu_\pm$ and T. In particular, we arrive at (Ho & Mueller 2004)

$$z_+ \approx n_+ \lambda^3 + \frac{1}{2^{3/2}} \left(n_+ \lambda^3 \right)^2 + \frac{2a}{\lambda} \left(n_+ \lambda^3 \right) \left(n_- \lambda^3 \right) \tag{81}$$

and a similar result for z_-, which gives the contribution of the interactions to the internal energy:

$$\Delta E^{(\rm int)} = g\, n_+ n_-\, L^3 \qquad \text{with} \quad g = \frac{4\pi\hbar^2 a}{m}. \tag{82}$$

This result corresponds well to that expected for a contact interaction between the two components:

$$\hat{H}_{\rm int} = g \int \hat{n}_+(\boldsymbol{r})\, \hat{n}_-(\boldsymbol{r})\, {\rm d}^3 r, \tag{83}$$

with uncorrelated fluctuations in the spatial densities of the two components.

3-2 The b_3 coefficient

The calculation of the b_3 coefficient (and the following ones) is notoriously more difficult since it involves solving the (at least) three-body problem, with the determination of all its eigenenergies (figure 8). We will concentrate in the following on the resonant case ($|a| = +\infty$) which is the most discriminating situation with respect to the validity of the different possible approaches.

Because of the scale invariance that appears in the unitary regime, the coefficient $b_3(T)$ – as well as all the other virial coefficients – can only be a pure number. Indeed, $b_n(T)$ is by construction a function of the temperature only, and not of the chemical potential μ. Moreover, it is dimensionless and the temperature can therefore only intervene in an adimensional

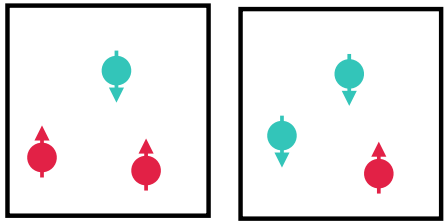

Figure 8. *The two situations to be taken into account for the calculation of the b_3 coefficient. These two situations lead to identical results if $m_\uparrow = m_\downarrow$.*

way. When the scattering length is not infinite, it provides the energy scale $E_a = \hbar^2/ma^2$ and we can therefore find $b_n(T)$ as a function of the variable $x = k_\mathrm{B}T/E_a$. This is indeed what happened when we arrived at the result $b_2^{(\mathrm{int})} = -2a/\lambda$ in the non-resonant case. On the other hand, in the resonant case, the only possible dimensionless quantity that would allow us to provide a variable for $b_n(T)$ is $k_\mathrm{B}T/\mu$, but it is not eligible since it depends on μ. The coefficients $b_n(T)$ are therefore numbers independent of T in the unitary regime.

The calculation of this coefficient b_3 in the unitary regime has been done only quite recently, with contradictory results at the beginning. The first published result (Rupak 2007), $b_3 \approx 1.11$, which is now known to be incorrect, used a "field theory" approach. Two years later, Liu, Hu, et al. (2009) published the value now considered correct and confirmed by experiment

$$\boxed{\text{Balanced Fermi gas on resonance:} \qquad b_3 = \frac{1}{3^{5/2}} - 0.3551\ldots = -0.2910\ldots} \tag{84}$$

They built on a previous work by Werner & Castin (2006), who had succeeded in calculating quasi-analytically the entire spectrum of three identical particles in an isotropic harmonic trap, for a zero range and resonant interaction. Liu, Hu, et al. (2009) then calculated the three-body partition function in a trap of frequency ω and deduced the corresponding $b_{3,\mathrm{trap}}$ coefficient. The case of a homogeneous gas was obtained via a local density

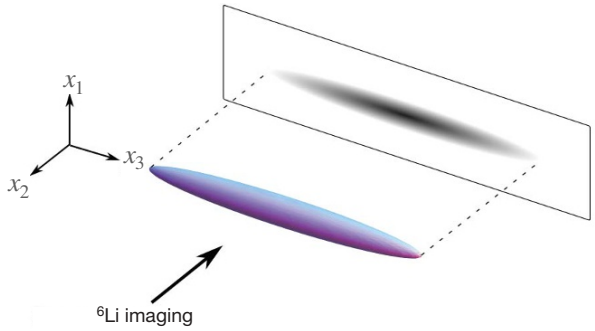

Figure 9. *Imaging a unitary Fermi gas of lithium 6. The length of the trapped gas along the x_3 direction is a few hundred micrometers. Figure extracted from Nascimbène, Navon, et al. (2010).*

approximation which becomes exact in the $\omega \to 0$ limit and leads to :

$$\boxed{b_n = n^{3/2}\, b_{n,\mathrm{trap}}} \tag{85}$$

The result of Liu, Hu, et al. (2009) was then confirmed theoretically by several authors, either from methods using field theory (Kaplan & Sun 2011; Leyronas 2011), or by a numerical solution of the three-body problem (Rakshit, Daily, et al. 2012). As we will see in the following paragraph, this result is also in excellent agreement with the experiment.

3-3 Experimental Results

The first measurement of the thermodynamics of the Fermi gas in the unitary regime was carried out in 2009-10 in the group of Christophe Salomon and Frédéric Chevy at ENS (Nascimbène, Navon, et al. 2010). The experiment is carried out on an assembly of about 10^5 atoms of ^{6}Li, placed in a magnetic field $B = 834\,\mathrm{G}$ (center of a large Fano–Feshbach resonance) and prepared in an equilibrated mixture of the two lowest energy Zeeman states. A $1/2$ pseudospin system is thus realized. The temperature range explored is from 150 nK to 1.3 μK. The atoms are confined in an elongated

harmonic trap in the direction [6] x_3 (*cf.* figure 9), with the potential:

$$V(\boldsymbol{x}) = \frac{1}{2}m\omega^2(x_1^2 + x_2^2) + \frac{1}{2}m\omega_3^2 x_3^2. \tag{86}$$

One measures the total density of the gas, $\bar{n}(x_3) = \bar{n}_+(x_3) + \bar{n}_-(x_3)$, integrated along the axes x_1 and x_2:

$$\bar{n}(x_3) = \iint n(x_1, x_2, x_3)\, \mathrm{d}x_1\, \mathrm{d}x_2. \tag{87}$$

The integration along the x_2 imaging axis is a natural result of the imaging procedure, and that along the x_1 axis is done numerically from the two-dimensional images in the (x_1, x_3) plane. This measurement provides the pressure $P(\mu, T)$ thanks to an ingenious remark published by Ho & Zhou (2010), and established independently by Sylvain Nascimbene:

- We use the relation between density and pressure, deduced from the thermodynamic relations already mentioned:

$$n_+ = \left(\frac{\partial P}{\partial \mu_+}\right)_{T,\mu_-} \tag{88}$$

  and idem for n_-. Here, as the gas is balanced, we will take $\mu_+ = \mu_-$ and thus

$$n = \left(\frac{\partial P}{\partial \mu}\right)_T. \tag{89}$$

- It is assumed that the gas is sufficiently large to be well described by the local density approximation, i.e. that the equilibrium state at a point $\boldsymbol{x}$ is that of a homogeneous gas of chemical potential $\mu(\boldsymbol{x}) = \mu_c - V(\boldsymbol{x})$, where μ_c is the chemical potential at the center of the trap ($\boldsymbol{x} = 0$ with by convention $V(0) = 0$).

- We then transform the integral on the space of (87) into an integral over the chemical potential:

$$\bar{n}(x_3) = 2\pi \int_0^\infty n(r, x_3)\, r\, \mathrm{d}r = \frac{2\pi}{m\omega^2} \int_{-\infty}^{\mu(x_3)} \left(\frac{\partial P}{\partial \mu}\right)_T \mathrm{d}\mu = \frac{2\pi}{m\omega^2}\, P[T, \mu(x_3)]. \tag{90}$$

[6] We note here the three space coordinates x_1, x_2, x_3 rather than x, y, z to avoid confusion with the fugacity z.

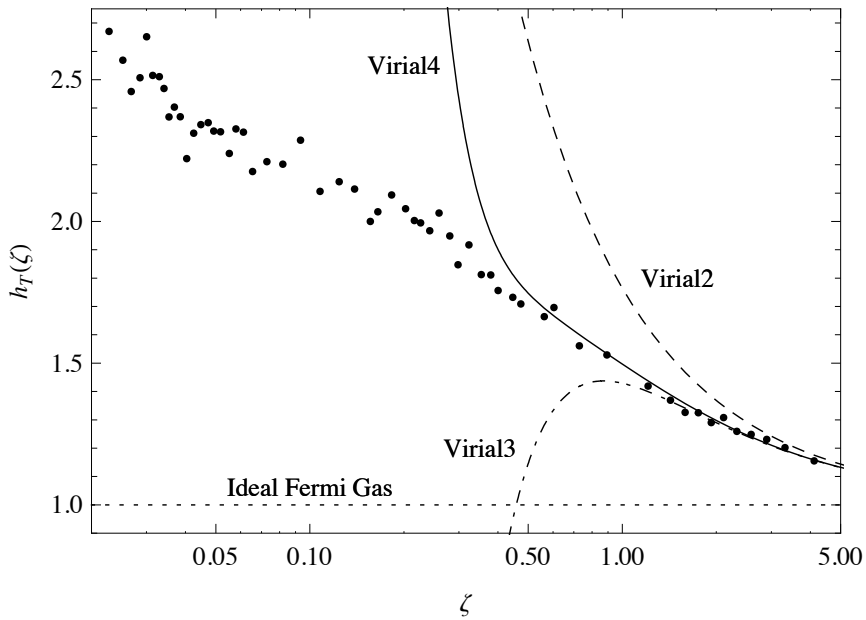

Figure 10. *Experimental measurement of the pressure P of a Fermi gas in the unitary regime by the ENS group [*cf. *Nascimbène, Navon, et al. (2010)]. We have plotted here $h = P/P_{\mathrm{ideal}}$ as a function of the inverse of the fugacity $\zeta = 1/z$. The region of small fugacities (large ζ) is fitted by a polynomial of degree 4 in z. The result of this fit leads to $b_4 = -4^{-5/2} + 0.096 = 0.065$. Figure extracted from Sylvain Nascimbene's thesis.*

We have thus directly access to the expected pressure for a homogeneous gas of parameters $[T, \mu(x_3) = \mu_c - m\omega_3^2 x_3^2/2]$. Given the scale invariance, this quantity is in fact only a function of $\mu(x_3)/k_{\mathrm{B}}T$ so that a single image is in principle sufficient to obtain the whole equation of state from $z = 0$ (at the edges of the trap where $\mu \to -\infty$) to $z = \exp(\mu_c/k_{\mathrm{B}}T)$.

The gas temperature is measured by inserting a small fraction of impurities (a few thousand lithium 7 atoms) and measuring their velocity distribution by a time-of-flight method (Spiegelhalder, Trenkwalder, et al.

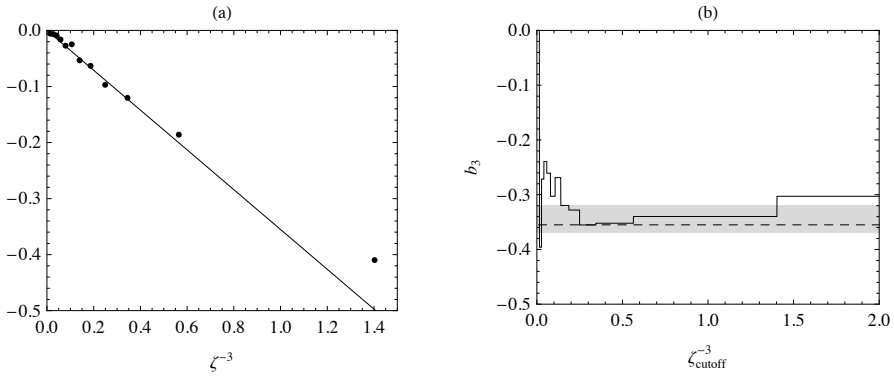

Figure 11. *Determination of b_3 (see text). Figure extracted from Sylvain Nascimbene's thesis.*

2009a).

An example of this result is shown in figure 10, extracted from Sylvain Nascimbene's thesis. We plot the variations of the pressure, normalized by the pressure of the ideal Fermi gas, $h(z) = P(z)/P_{\rm ideal}(z)$, as a function of the variable $\zeta = 1/z$. The applicability domain of the virial expansion ($z \lesssim 1$) corresponds therefore to the $\zeta \gtrsim 1$ area. We show a fit of the data with a polynomial of degree 4:

$$h(z) = b_1 z + b_2 z^2 + b_3 z^3 + b_4 z^4, \tag{91}$$

the first three coefficients being fixed at their known values at the time :

$$b_1 = 1 \qquad b_2 = \frac{3}{4\sqrt{2}} \qquad b_3 = -0.2910. \tag{92}$$

We then deduce from this fit a value of b_4: $b_4 = 0.065\,(15)$.

The verification of the value of b_3 is detailed on the figure 11. We show on the left the deviation of the pressure (in units of $P_{\rm ideal}$) from the law $z + b_2 z^2$, as a function of z^3. The fit by a $b_3 z^3$ function depends on the $z_{\rm cutoff}$ value used. The gray rectangle indicates the values of b_3 compatible with the data.

Two years later, a new set of data was published by Martin Zwierlein's group at MIT, also from a lithium 6 gas (Ku, Sommer, et al. 2012). We will not go into the detailed description of this experiment, of which we give one of the main results in figure 12. In the area of interest here, $z \lesssim 1$, the agreement with the ENS data is excellent and leads to a compatible value for b_4: $b_4 = 0.065\,(10)$.

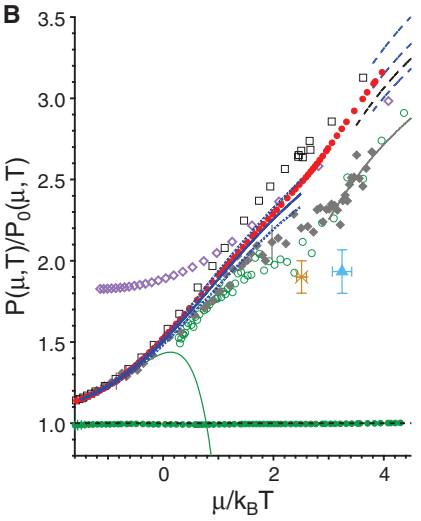

Figure 12. *Pressure of a ^{6}Li Fermi gas in the unitary regime, normalized by the ideal gas pressure. Red dots: data from the MIT group (Ku, Sommer, et al. 2012), gray diamonds: data from the ENS group (Nascimbène, Navon, et al. 2010). The virial expansion at order 4 with the parameters given in (92) and $b_4 = 0.065$ is represented by the green continuous line. The other points or lines correspond to theoretical predictions in the degenerate regime, not described in this chapter. Figure extracted from Ku, Sommer, et al. (2012).*

3-4 Beyond three-body effects

Once the value for b_4 was deduced from the two experiments we have just described, the ball was in the theorists' court to refine the calculations of this quantity. The challenge is of course considerable since it is a question of determining the exact spectrum of 4 fermions interacting with two

configurations of different nature, $\uparrow\uparrow\downarrow\downarrow$ and $\uparrow\uparrow\uparrow\downarrow$ (or its symmetric).

The outcome of this series of work is described by Endo (2020):

- At the time the MIT experimental paper was published, only one prediction was available: $b_4 = -0.047(4)$, in clear disagreement with the experiment (Rakshit, Daily, et al. 2012). This work used the variational method to find the energy of particles in a harmonic trap and then extrapolated the results to zero stiffness, corresponding to the homogeneous gas.

- Ngampruetikorn, Parish, et al. (2015) used a field theory method in the homogeneous case to arrive at $b_4 \approx 0.03$.

- Endo & Castin (2016a) used a Fadeev ansatz, inspired by the solution of the three-body problem, to treat quasi-analytically the case of trapped particles. At the cost of a conjecture[7] (not yet proven to our knowledge), they arrived at a precise value of b_4: $b_4 = 0.031\,(1)$.

- Yan & Blume (2016) used a Monte Carlo method based on the path integral to numerically compute the spectrum of the trapped four-particle Hamiltonian, and then proceeded to a zero-stiffness extrapolation to find the value of b_4 in the homogeneous case: $b_4 = 0.047\,(18)$.

- Hou & Drut (2020) [see also Hou, Morrell, et al. 2021] have developed a partially analytical method to evaluate the Boltzmann weights involved in the partition function, using a Trotter decomposition (alternating evolutions due to kinetic energy and interaction energy). They confirmed the result (93) of Endo & Castin (2016a), while noting that the result for b_4 of Ngampruetikorn, Parish, et al. (2015), while broadly consistent with (93), corresponds to notably different values for each of the two components $\uparrow\uparrow\downarrow\downarrow$ and $\uparrow\uparrow\uparrow\downarrow$. In contrast, these individual components have compatible values in both the Endo & Castin (2016a) and Hou & Drut (2020) approaches. We will therefore retain the value:

[7] The calculation involves the integration in the complex plane of a function whose analytical properties are not completely known. The conjecture is necessary to apply the residue theorem.

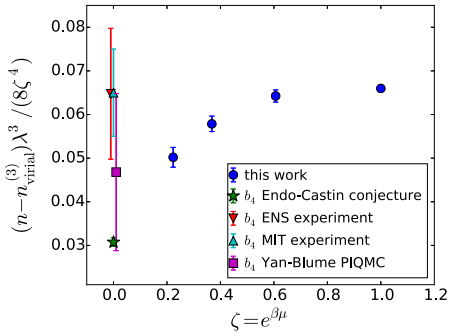

Figure 13. *Calculation of the density of a unitary Fermi gas as a function of its fugacity. The calculation is done by summation of a series of Feynman diagrams, associated with a diagrammatic Monte Carlo method up to order 9. Figure extracted from Rossi, Ohgoe, et al. (2018).*

$$\text{Balanced Fermi gas on resonance:} \qquad b_4 = -\frac{1}{4^{5/2}} + 0.062 = 0.031\,(1) \tag{93}$$

Note that this value is significantly different from the one found experimentally ($b_4 = 0.065$, see figure 10). Let us also note that Hou & Drut (2020) propose a value for b_5: $b_5 = 5^{-5/2} + 0.78 = 0.80\,(6)$.

The determination of b_4 is thus clearly a difficult problem, and Endo (2020) gives at least one reason for this difficulty on the theoretical level: when this coefficient is first computed in a harmonic trap, the behavior of $b_4(\omega)$ is not monotonous which makes the numerical passage to the $\omega \to 0$ limit used by several authors very tricky. On the experimental side, a potential difficulty is illustrated on figure 13, taken from Rossi, Ohgoe, et al. (2018). This figure shows the deviation between the density calculated by resummation of Feynman diagrams and the $n^{(3)}$ density calculated by virial expansion to order 3. It shows an apparent plateau for values of the fugacity between 0.6 and 1.1. An extrapolation of this plateau at zero fugacity gives the value compatible with experimental results. However, the data obtained for even smaller values of the fugacity seem rather compatible with the value $b_4 = 0.031$ given by Endo & Castin (2016a).

Chapter II

The Quantum Bogoliubov Approach

In this chapter we discuss the description of a powerful method for treating the case of an interacting Bose gas, the Bogoliubov approach[1] (Bogoliubov 1947). This approach allows to describe the ground state of the gas as well as its excitation spectrum at low energy, with a number of approximations that we will detail in the following lectures. This method starts from a binary interaction potential between the particles

$$\hat{\mathcal{V}} = \sum_{i<j} V(\hat{\boldsymbol{r}}_i - \hat{\boldsymbol{r}}_j), \tag{1}$$

and is based on the assumption that the action of this potential "does not change much" – in a sense that we will specify – the ground state of the fluid compared to the case of the ideal gas.

The Bogoliubov method, although a commonly used tool, has some subtleties that we will highlight in the following chapters. One of these subtleties comes from the fact that it is difficult to use the Bogoliubov method with the real interatomic potential. For all the atomic species used in the laboratory, this potential contains many two-particle bound states. The true ground state of the system is thus very different from the Bose–Einstein condensate formed from the monoatomic gas found in the non-interacting case, and also very far from the fluid prepared, in a metastable state, in the cold atom experiments.

[1] We have already discussed this method in the context of a description in terms of classical fields in the 2015-16 course, but the quantum aspect of the treatment changes the approach very significantly, even if some results are similar.

The Bogoliubov method is frequently used with a contact potential $V(\boldsymbol{r}) = g\,\delta(\boldsymbol{r})$, thus of zero range b. The coupling g is then defined from the scattering length a of the physical problem by:

$$g \equiv \frac{4\pi\hbar^2 a}{m}. \tag{2}$$

However, we know (*cf.* course 2020-21) that such a potential leads to divergences already at order 2 of the Born series. *A fortiori*, it does not allow to describe in a "safe way" the interaction between N particles. Some expressions, like the speed of sound or the quantum depletion, can be calculated without difficulty while others, like the ground state energy, diverge. For a mathematically well-established version of a zero-range potential, one can use[2] the pseudo-potential $\hat{V}_{\rm pp}$, defined by its action on a wave function $\psi(\boldsymbol{r})$ by:

$$\hat{V}_{\rm pp}\left[\psi(\boldsymbol{r})\right] = g\,\delta(\boldsymbol{r})\,\frac{\partial}{\partial r}\left[r\,\psi(\boldsymbol{r})\right]. \tag{3}$$

This is the approach followed in the original article of Lee, Huang, et al. (1957), but the calculations are then relatively subtle. Indeed, as we explained in the 2020-21 course, the use of the pseudopotential amounts to changing the domain of the Hamiltonian. When using $\hat{V}_{\rm pp}$, any two-body wave function $\Psi(\boldsymbol{r}_1, \boldsymbol{r}_2)$ must not be regular when $r = |\boldsymbol{r}_1 - \boldsymbol{r}_2| \to 0$, but

[2] See Olshanii & Pricoupenko (2001) for a general class of such potentials.

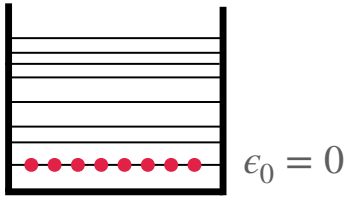

Figure 1. *Bose gas ground state without interaction: all particles accumulate in the state of zero momentum and zero energy (for periodic boundary conditions), and $N_0 = N$.*

must vary as

$$r \to 0 : \qquad \Psi(\boldsymbol{r}_1, \boldsymbol{r}_2) \approx \left(\frac{1}{r} - \frac{1}{a}\right) \Phi(\boldsymbol{R}) \qquad \text{with} \quad \boldsymbol{R} = (\boldsymbol{r}_1 + \boldsymbol{r}_2)/2. \quad (4)$$

We will describe the spirit of this approach in Chapter 3.

The approach we will explore here is to use a regular potential $V(\boldsymbol{r})$, of range b, whose Fourier transform $\tilde{V}_{\boldsymbol{k}}$ is also regular for all $\boldsymbol{k}$:

$$\tilde{V}_{\boldsymbol{k}} = \int V(\boldsymbol{r})\, \mathrm{e}^{-\mathrm{i}\boldsymbol{k}\cdot\boldsymbol{r}}\, \mathrm{d}^3 r. \quad (5)$$

We will assume that the action of this two-body potential can be described in the Born approximation. For the low energy regime of interest here, this leads in particular to the following link between the zero momentum Fourier transform, $\tilde{V}_0$, and the coupling g defined in (2):

$$\text{Born approximation:} \qquad \tilde{V}_0 = \int V(\boldsymbol{r})\, \mathrm{d}^3 r \;\approx\; g. \quad (6)$$

Recall that a condition for the validity of the Born approximation is that the scattering length deduced from (6) is small in front of the range b of the potential $V(\boldsymbol{r})$.

In a Bose gas without interaction, the ground state is obtained by placing the N particles in the single-particle ground state $\boldsymbol{k} = 0$ (figure 1). In other words, the population N_0 of this $\boldsymbol{k} = 0$ state is equal to N. In what follows, we will start (§ 1) by using the fact that the potential can be treated as a weak perturbation to perform a systematic expansion of the N-body Hamiltonian, assuming that the average population $\langle N_0 \rangle$ of the $\boldsymbol{k} = 0$ state remains close to 1:

$$\frac{N - \langle N_0 \rangle}{N} \ll 1. \quad (7)$$

This will allow us to obtain an approximate expression of the Hamiltonian containing only quadratic terms in $a^\dagger_{\boldsymbol{k}}$ and $a_{\boldsymbol{k}}$, the creation and destruction operators of a particle in the momentum state $\hbar\boldsymbol{k} \neq 0$. More precisely, the structure of the Hamiltonian will show a sum of independent terms, each of them dealing with a pair $\{+\boldsymbol{k}, -\boldsymbol{k}\}$. In § 2, we will focus on a given pair to detail the Bogoliubov method, which uses a canonical transformation to diagonalize this Hamiltonian. Finally in § 3, we will illustrate this diagonalization method on the case of a spinor gas in the single spatial mode approximation.

The return to an infinite number of pairs $\{+\boldsymbol{k}, -\boldsymbol{k}\}$, with the problems of convergence which may then arise, will be discussed in chapter 3, as will the discussion of the validity of the expansion in powers of $(N - \langle N_0 \rangle)/N$, which we shall see amounts to imposing $\sqrt{na^3} \ll 1$.

1 The quadratic approximation for $\hat{H}$

We consider here an assembly of particles with binary interactions. The Hamiltonian written in the second quantization formalism using the basis of plane waves then involves products of four creation or annihilation operators $a_{\boldsymbol{k}}$ or $a^\dagger_{\boldsymbol{k}}$ (see appendix). In this form, it is not possible to find analytically the eigenstates and the eigenenergies of the system. The Bogoliubov method consists in assuming that a particular mode, in this case the plane wave $\boldsymbol{k} = 0$, is macroscopically populated. Under these conditions, one can neglect the operator character of a_0 and $a^\dagger_0$, and then limit oneself to terms involving only binary products of the other operators $a_{\boldsymbol{k}}$ and $a^\dagger_{\boldsymbol{k}}$ with $\boldsymbol{k} \neq 0$. The mathematical study of the resulting quadratic Hamiltonian is then not difficult, as we will see in the following sections.

In what follows we will make the assumption that $V(\boldsymbol{r})$ is invariant by rotation, $V(\boldsymbol{r}) = V(r)$, with $r = |\boldsymbol{r}|$. This assumption is not necessary, but will simplify the notations. It follows that the Fourier transform $\tilde{V}_{\boldsymbol{k}}$ is also

invariant by rotation: $\tilde{V}_{\boldsymbol{k}} = \tilde{V}_k$.

1-1 Preliminary : Hartree term, Fock term

Let us start by considering the case of two identical particles, prepared in well-defined momentum states $\hbar\boldsymbol{k}_a, \hbar\boldsymbol{k}_b$, with $\boldsymbol{k}_a \neq \boldsymbol{k}_b$. Let us assume that these particles are spin-polarized so that the corresponding degree of freedom does not play a role here. We are interested in the average of a potential $V(|\boldsymbol{r}_{12}|)$, depending only on the distance r_{12} between the two particles.

The two-particle state is written

$$|\Psi\rangle = \frac{1}{\sqrt{2}}\left(|1:\boldsymbol{k}_a\ ,\ 2:\boldsymbol{k}_b\rangle \ \pm\ |1:\boldsymbol{k}_b\ ,\ 2:\boldsymbol{k}_a\rangle\right) \tag{8}$$

where the signs $+$ and $-$ are associated respectively to bosons and fermions. The average value of $\hat{V}$ in this state is a sum of four terms

$$\begin{aligned}\langle V\rangle = \langle\Psi|\hat{V}|\Psi\rangle \quad &= \quad \frac{1}{2}\Big(\langle 1:\boldsymbol{k}_a\ ,\ 2:\boldsymbol{k}_b|\hat{V}|1:\boldsymbol{k}_a\ ,\ 2:\boldsymbol{k}_b\rangle \\ &\qquad \pm\langle 1:\boldsymbol{k}_b\ ,\ 2:\boldsymbol{k}_a|\hat{V}|1:\boldsymbol{k}_a\ ,\ 2:\boldsymbol{k}_b\rangle + \ldots\Big)\end{aligned} \tag{9}$$

Using the definition of the plane wave of momentum $\hbar\boldsymbol{k}$ in the quantization volume L^3 with periodic boundary conditions:

$$\langle\boldsymbol{r}|\boldsymbol{k}\rangle = \frac{1}{\sqrt{L^3}}\mathrm{e}^{\mathrm{i}\boldsymbol{k}\cdot\boldsymbol{r}}, \qquad \boldsymbol{k} = \frac{2\pi}{L}\boldsymbol{n}, \quad \boldsymbol{n}\in\mathbb{Z}^3, \tag{10}$$

the two terms written explicitly in this equation are calculated to give

$$\langle 1:\boldsymbol{k}_a\ ,\ 2:\boldsymbol{k}_b|\hat{V}|1:\boldsymbol{k}_a\ ,\ 2:\boldsymbol{k}_b\rangle = \frac{1}{L^3}\,\tilde{V}_0 \tag{11}$$

and

$$\langle 1:\boldsymbol{k}_b\ ,\ 2:\boldsymbol{k}_a|\hat{V}|1:\boldsymbol{k}_a\ ,\ 2:\boldsymbol{k}_b\rangle = \frac{1}{L^3}\,\tilde{V}_{\boldsymbol{k}_a-\boldsymbol{k}_b}. \tag{12}$$

The two other terms intervening in (9) and represented by "..." are equal to the two terms given above, so that the average sought is written:

$$\boxed{\langle V\rangle = \frac{1}{L^3}\left(\tilde{V}_0 \pm \tilde{V}_k\right) \qquad \boldsymbol{k} = \boldsymbol{k}_a - \boldsymbol{k}_b} \tag{13}$$

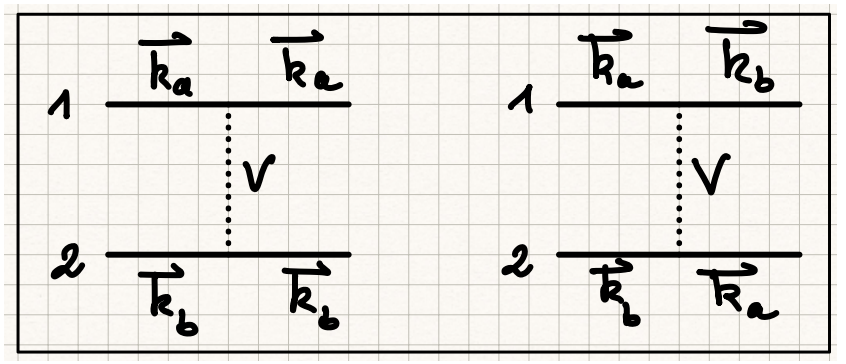

Figure 2. *Hartree term and Fock term involved in the calculation of the average value $\langle\Psi|\hat{V}|\Psi\rangle$ of a two-particle state, with both plane waves $\boldsymbol{k}_a$ and $\boldsymbol{k}_b$ occupied [*cf. *(13).*

There are thus two contributions to $\langle V\rangle$, the first is called *Hartree's term*, the second *Fock's term* (figure 2).

The structure of this result is characteristic of a problem of indistinguishable particles in quantum mechanics. If the particles were discernible, the initial state would be written

$$\text{Discernible particles:} \qquad |\Psi\rangle = |1:\boldsymbol{k}_a\ ,\ 2:\boldsymbol{k}_b\rangle \tag{14}$$

and only the first contribution to (13), the Hartree term still called *direct term*, would be present in the average $\langle V\rangle$. The Fock term, also called *exchange term*, has its origin in the fundamental impossibility of knowing whether the pair of particles $(1,2)$ is in the state $(\boldsymbol{k}_a,\boldsymbol{k}_b)$ or $(\boldsymbol{k}_b,\boldsymbol{k}_a)$.

Note that in the case of a pair of bosons prepared in the same momentum state $\hbar\boldsymbol{k}_a$, the initial state is $|\Psi\rangle = |1:\boldsymbol{k}_a\ ,\ 2:\boldsymbol{k}_a\rangle$ and the exchange term also disappears from the result (13).

1-2 N body Hamiltonian in second quantization

We now consider an assembly of N bosons (spinless or polarized) with two-body interactions described by the potential $V(r)$. The Hamiltonian is

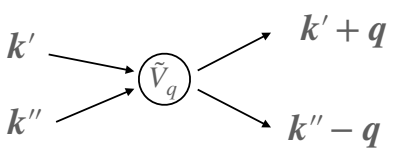

Figure 3. *Representation of the interaction term of (16), for which the conservation of the total momentum appears explicitly.*

written in first quantization for particles of mass m

$$\hat{H} = \sum_{i=1}^{N} \frac{\hat{\boldsymbol{p}}_i^2}{2m} + \frac{1}{2}\sum_i \sum_{j\neq i} V(|\hat{\boldsymbol{r}}_i - \hat{\boldsymbol{r}}_j|) \tag{15}$$

and we can show with the definitions recalled in the appendix of this chapter that its version in second quantization is [3]

$$\hat{H} = \sum_{\boldsymbol{k}} \epsilon_k \, a^\dagger_{\boldsymbol{k}} \, a_{\boldsymbol{k}} + \frac{1}{2L^3} \sum_{\boldsymbol{k}',\boldsymbol{k}'',\boldsymbol{q}} \tilde{V}_q \, a^\dagger_{\boldsymbol{k}'+\boldsymbol{q}} \, a^\dagger_{\boldsymbol{k}''-\boldsymbol{q}} \, a_{\boldsymbol{k}''} \, a_{\boldsymbol{k}'}. \tag{16}$$

where we introduced the kinetic energy at a particle associated to the plane wave of wave vector $\boldsymbol{k}$

$$\epsilon_k \equiv \frac{\hbar^2 k^2}{2m}. \tag{17}$$

A diagrammatic representation of the interaction term is given in figure 3.

In particular, we can verify that we recover the Hartree and Fock terms when we compute the average value of the interaction term in the $|\boldsymbol{k}_a, \boldsymbol{k}_b\rangle$ state. There are indeed 4 triples $(\boldsymbol{k}, \boldsymbol{k}', \boldsymbol{q})$ which contribute in the sum involved in (16):

- The choice $\boldsymbol{q} = 0$ with the two possibilities $(\boldsymbol{k}', \boldsymbol{k}'') = (\boldsymbol{k}_a, \boldsymbol{k}_b)$ and $(\boldsymbol{k}', \boldsymbol{k}'') = (\boldsymbol{k}_b, \boldsymbol{k}_a)$: we find the Hartree term of (13).
- The choice $\boldsymbol{q} = \boldsymbol{k}'' - \boldsymbol{k}'$ with the two possibilities $(\boldsymbol{k}', \boldsymbol{k}'') = (\boldsymbol{k}_a, \boldsymbol{k}_b)$ and $(\boldsymbol{k}', \boldsymbol{k}'') = (\boldsymbol{k}_b, \boldsymbol{k}_a)$: we find the Fock term of (13).

[3] To simplify the notations, we will not put ˆ above the symbols $a_{\boldsymbol{k}}$ and $a^\dagger_{\boldsymbol{k}}$ although they are operators.

1-3 The assumptions of the Bogoliubov approach

The expression (16) of the Hamiltonian is valid whatever the regime of the gas, weakly or strongly degenerate. We will now assume that a particular state of the gas, the $\boldsymbol{k} = 0$ zero momentum state, is strongly populated:

$$\langle N_0 \rangle \gg 1. \tag{18}$$

An argument[4] introduced by Bogoliubov (1947) and taken up in practically all approaches to this problem consists in positing that under these conditions, the difference between the prefactor $\sqrt{N_0}$ intervening for a_0 and the prefactor $\sqrt{N_0+1}$ intervening in $a_0^\dagger$ should not play a significant role. We can then neglect the fact that the commutator between a_0 and $a_0^\dagger$ is nonzero, and replace these operators by $\sqrt{N_0}$.

This approach consists therefore (with one subtlety for the canonical point of view, see next paragraph) in treating the particle condensate in the $\boldsymbol{k} = 0$ state as a classical field. This field will be able to generate or absorb in arbitrary numbers particles coming from the other $\boldsymbol{k} \neq 0$ momentum states.

Let us further assume that the number of particles outside the $\boldsymbol{k} = 0$ state is small in front of N:

$$N - \langle N_0 \rangle \ll N. \tag{19}$$

We can then truncate the Hamiltonian (16) to keep in the interaction term only the terms that are at least linear in N_0, i.e. the terms $a^\dagger_{\boldsymbol{k}+\boldsymbol{q}} \, a^\dagger_{\boldsymbol{k}'-\boldsymbol{q}} \, a_{\boldsymbol{k}'} \, a_{\boldsymbol{k}}$ involving at least two operators a_0 or $a_0^\dagger$. We then arrive at an approximate Hamiltonian $\hat{H}'$ quadratic with respect to $a_{\boldsymbol{k}}$, $a^\dagger_{\boldsymbol{k}}$ with $\boldsymbol{k} \neq 0$:

$$\begin{aligned} \hat{H}' \;=\; & \frac{N_0^2}{2L^3}\tilde{V}_0 + \sum_{\boldsymbol{k}\neq 0} \left[\epsilon_k + n_0\tilde{V}_0 + n_0\tilde{V}_k\right] a^\dagger_{\boldsymbol{k}} a_{\boldsymbol{k}} \\ & + \frac{1}{2}\sum_{\boldsymbol{k}\neq 0} n_0 \tilde{V}_k \left(a^\dagger_{\boldsymbol{k}} a^\dagger_{-\boldsymbol{k}} + a_{\boldsymbol{k}} a_{-\boldsymbol{k}}\right) \end{aligned} \tag{20}$$

where we introduced the spatial density in the condensed mode $n_0 = N_0/L^3$.

[4] Bogoliubov cites Dirac's book, *The Principles of Quantum mechanics*, as a source of inspiration for this argument.

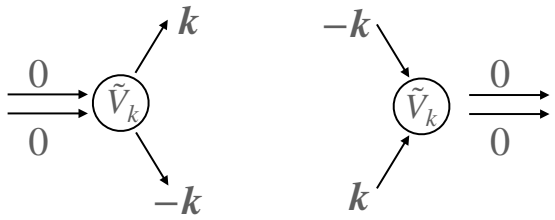

Figure 4. *Creation and annihilation of a pair $\{+\boldsymbol{k}, -\boldsymbol{k}\}$ appearing in the second line of (20).*

The first line of this expression shows first the energy of the particles occupying the $\boldsymbol{k} = 0$ mode interacting with each other (no Fock term since they are all in the same state), then a first contribution of the non-condensed particles, with their kinetic energy ϵ_k and the Hartree and Fock terms in $\tilde{V}_0$ and $\tilde{V}_k$. On the second line, we can see that the interaction will induce in addition correlations between the $\boldsymbol{k}$ and $-\boldsymbol{k}$ modes, through terms that create or annihilate pairs of particles in these modes. The corresponding diagrams are shown in figure 4.

At this stage, there is no guarantee that the two hypotheses made above, $N_0 \gg 1$ and $N - N_0 \ll N$ are legitimate. It will therefore be once the analysis has been completed that we will be able to verify what constraints these hypotheses impose on the potential $V(r)$ or its Fourier transform $\tilde{V}_q$, in association with the total spatial density $n = N/L^3$.

Non-conservation of the number of particles. An immediate counterpart of the $a_0^\dagger \approx a_0 \approx N_0$ approximation is that the total number of particles is no longer a conserved quantity for the Hamiltonian $\hat{H}'$ whereas it was for the Hamiltonian $\hat{H}$ written in (16). Even if this point does not pose a problem on the mathematical level, it can raise difficulties when interpreting certain results physically. Leggett (2001) [see also Leggett (2006)] proposes for this an alternative approach, based on the variational method with a N-particle test function (N is assumed here to be even)

$$|\Psi\rangle \propto \left(a_0^\dagger a_0^\dagger - \sum_{\boldsymbol{k}\neq 0} c(\boldsymbol{k}) a_{\boldsymbol{k}}^\dagger a_{-\boldsymbol{k}}^\dagger \right)^{N/2} |0\rangle, \tag{21}$$

the coefficients $c(\boldsymbol{k})$ being parameters to be optimized in order to minimize the average energy of the gas in the state $|\Psi\rangle$. Thanks to this ansatz, we force the emergence of correlations between the $\boldsymbol{k}$ and $-\boldsymbol{k}$ modes. The corresponding calculations are carried out in detail in the complement $\mathrm{E_{XVII}}$ of Cohen-Tannoudji, Diu, et al. (2021). The result of this approach is identical to that of the "standard" method that we will develop here. Let us also mention the approaches of Gardiner (1997) and Castin & Dum (1998), which also use Hamiltonians conserving the number of particles, these approaches being well adapted to the case of gases of non uniform density.

1-4 Grand canonical vs. canonical approach

In what follows, we are essentially interested in the ground state of the Bose gas Hamiltonian, and we thus want to minimize the energy associated with the Hamiltonian $\hat{H}'$ written in (20). As always in statistical physics, several statistical ensembles can be used for this. Two ensembles are particularly relevant:

- The grand-canonical ensemble which corresponds to the case where the gas (condensate + non-condensed part) is coupled to a reservoir of particles which imposes its chemical potential μ. It is then a question of minimizing the quantity $\langle \hat{H}' - \mu \hat{N} \rangle$ at μ fixed. The value of μ is then adjusted to correctly describe the physical situation we are interested in. This point of view is used for example by Nozières & Pines (1990).

- The canonical ensemble in which we consider that the gas (condensate + non-condensed part) is isolated from the point of view of the number of particles, even if an energy exchange with a reservoir remains possible to impose a certain temperature. The total number of particles N is thus fixed and we must impose the constraint

$$\boxed{N = \hat{N}_0 + \sum_{\boldsymbol{k}\neq 0} a_{\boldsymbol{k}}^\dagger a_{\boldsymbol{k}}} \tag{22}$$

  This leads us to (slightly) take up the assimilation of N_0 to a classical field. This is the point of view used by Pethick & Smith (2008) and by Pitaevskii & Stringari (2016).

We take here the canonical point of view. The constraint on the number of atoms written in (22) imposes to be vigilant towards the dominant term of $\hat{H}'$, $N_0^2\tilde{V}_0/2L^3$. It would be inaccurate to treat N_0 simply as a fixed number for this term because the error made would be comparable to the other terms of $\hat{H}'$. To perform an expansion in $(N-N_0)/N$, we must rewrite this term in the form:

$$\frac{N_0^2\tilde{V}_0}{2L^3} = \frac{\tilde{V}_0}{2L^3}\left(N - \sum_{\boldsymbol{k}\neq 0} a_{\boldsymbol{k}}^\dagger a_{\boldsymbol{k}}\right)^2 \approx \frac{N^2\tilde{V}_0}{2L^3} - n_0\tilde{V}_0 \sum_{\boldsymbol{k}\neq 0} a_{\boldsymbol{k}}^\dagger a_{\boldsymbol{k}}. \tag{23}$$

Once this approximation is made, the expression of the Hamiltonian $\hat{H}'$ simplifies: the terms in $\tilde{V}_0\, a_{\boldsymbol{k}}^\dagger a_{\boldsymbol{k}}$ are eliminated so that $\hat{H}'$ is written:

$$\boxed{\hat{H}' = \frac{1}{2}nN\tilde{V}_0 + \hat{H}''} \tag{24}$$

with

$$\boxed{\hat{H}'' = \sum_{\substack{\text{pairs}\\ \{\boldsymbol{k},-\boldsymbol{k}\}}} \left[\epsilon_k + n\tilde{V}_k\right]\left(a_{\boldsymbol{k}}^\dagger a_{\boldsymbol{k}} + a_{-\boldsymbol{k}}^\dagger a_{-\boldsymbol{k}}\right) + n\tilde{V}_k\left(a_{\boldsymbol{k}}^\dagger a_{-\boldsymbol{k}}^\dagger + a_{\boldsymbol{k}} a_{-\boldsymbol{k}}\right)} \tag{25}$$

In this sum, each pair $\{\boldsymbol{k},-\boldsymbol{k}\}$ (with $\boldsymbol{k}\neq 0$) is counted only once. In an equivalent way, we can sum over all $\boldsymbol{k}\neq 0$ and multiply the result by $1/2$. Note that we have replaced in $\hat{H}''$ the condensed density n_0 by the total density n, which is legitimate at this order of calculation.

2 The two-mode Bogoliubov Hamiltonian

The Hamiltonian (25) found in the previous paragraph is quadratic with respect to the creation and annihilation operators $a_{\boldsymbol{k}}$ and $a_{\boldsymbol{k}}^\dagger$. It is always possible to diagonalize exactly this kind of Hamiltonian, either for bosons or fermions, by means of canonical transformations. In the 2017-18 course (chapter 2), we had studied the problem for fermions in the framework of the Kitaev model. In what follows, we will focus on the case of bosonic particles.

In order to clarify the essential steps of the method to follow, we will work here on a two-mode model, characterized by the operators $(a_1^\dagger, a_1)$ and $(a_2^\dagger, a_2)$, and consider the Hamiltonian

$$\hat{H} = \hat{H}_0 + \hat{V} \tag{26}$$

with

$$\hat{H}_0 = \hbar\omega_0\left(a_1^\dagger a_1 + a_2^\dagger a_2 + 1\right) \qquad \hat{V} = \hbar\kappa\left(a_1^\dagger a_2^\dagger + a_1 a_2\right), \tag{27}$$

where the real parameters ω_0 and κ each have the dimension of a frequency. The quantity ω_0 is assumed positive so that the spectrum of $\hat{H}_0$ is simply $(n_1+n_2+1)\hbar\omega_0$, with eigenstates $|n_1,n_2\rangle$. We have chosen here the origin of the energies so that the ground state of $\hat{H}_0$ has energy

$$E_{\text{grnd}}^{(0)} = \hbar\omega_0, \tag{28}$$

i.e. the sum of the zero-point energies $\hbar\omega_0/2$ for each of the modes a_1 and a_2. This ground state is obtained for $n_1 = n_2 = 0$.

Note that this Hamiltonian is found in many quantum optics problems and is the basis for the generation of two-mode squeezed vacuum states, by populating modes 1 and 2 with rigorously equal numbers of photons from a pump laser described as a classical field (Walls & Milburn 2007). It can also be found in the description of superconducting circuits (Nation, Johansson, et al. 2012) and in the description of the dynamics of spin gases, where modes (1,2) correspond to different spin states, as we will see in 3.

In this section, we will treat exactly the $\hat{V}$ coupling between the two modes but we start by addressing the problem by perturbation theory.

2-1 Perturbative approach

We are interested here in the ground state of the two-mode system. Starting from the unperturbed ground state $|\Psi_0\rangle = |0,0\rangle$, we immediately see that the average of $\hat{V}$ in this state is zero, so that the energy of the ground state is unchanged at order 1:

$$\Delta E^{(1)} = \langle\Psi_0|\hat{V}|\Psi_0\rangle = 0. \tag{29}$$

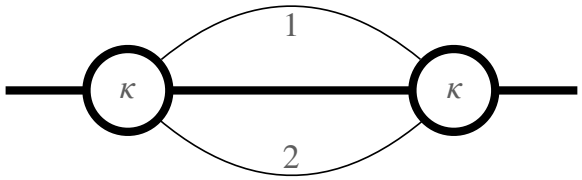

Figure 5. *A diagram contributing to the ground state energy of the Hamiltonian (26) at order 2 in κ/ω_0. The thick horizontal line represents the "reservoir" from which $(1,2)$ pairs can be created. Each disk represents the creation or destruction of a pair under the influence of the potential $\hat{V} \propto \kappa$.*

Let's go to the second order in $\hat{V}$. The general formula of the perturbation theory is written

$$\Delta E^{(2)} = \sum_{j\neq 0} \frac{|\langle \Psi_j | \hat{V} | \Psi_0 \rangle|^2}{E_0 - E_j} \tag{30}$$

where the sum carries *a priori* over all excited states. In this case, only one excited state contributes, $n_1 = n_2 = 1$, this state having energy $3\hbar\omega_0$. We deduce:

$$\Delta E^{(2)} = -\frac{\hbar\kappa^2}{2\omega_0}. \tag{31}$$

We have represented on the figure 5 the corresponding diagram. Starting from the unperturbed ground state, represented by a thick line, we create the pair of excitations $n_1 = n_2 = 1$ which is then destroyed.

One could continue to apply the perturbation theory to higher orders. At order $2n$ in κ/ω_0, one will in particular have to consider the coupling between the ground state and the $|n,n\rangle$ state resulting from the application of the operator $\hat{V}^n$ which creates n pairs of bosons. However, it is simpler to use the formalism of canonical transformations, which amounts to resuming the infinite series provided by the perturbation theory pushed to arbitrarily high orders.

2-2 Canonical transformation

The principle of this method consists in introducing two new couples of bosonic operators $(b_1^\dagger, b_1)$ and $(b_2^\dagger, b_2)$, linear combinations of the initial operators $(a_i^\dagger, a_i)$ with $i = 1, 2$, so that the Hamiltonian $\hat{H}$ is "diagonal" with respect to b_i, i.e. it is written as a sum of $b_i^\dagger b_i$ and a constant term.

Given the particular form of the coupling $\hat{V}$, we can look for the b_i in the form

$$\boxed{b_1 = ua_1 + va_2^\dagger \qquad b_2 = ua_2 + va_1^\dagger} \tag{32}$$

where u and v are real numbers. The bosonic character[5] of these new operators imposes that:

$$[b_i, b_i^\dagger] = 1 \quad \Rightarrow \quad u^2 - v^2 = 1 \tag{33}$$

which means that we can look for the numbers u and v in the form

$$u = \cosh\lambda \qquad v = \sinh\lambda \tag{34}$$

where λ is itself a real number. Moreover, the form chosen in (32) ensures the independence of the two new modes:

$$[b_1, b_2] = 0 \qquad [b_1, b_2^\dagger] = 0. \tag{35}$$

The relation (32) defining the b_i is inverted to give

$$a_1 = ub_1 - vb_2^\dagger \qquad a_2 = ub_2 - vb_1^\dagger \tag{36}$$

so that the Hamiltonian $\hat{H}$ is written in terms of b_i:

$$\begin{aligned} \hat{H} &= \hbar\omega_0 \left[(u^2+v^2)\left(b_1^\dagger b_1 + b_2^\dagger b_2\right) - 2uv\left(b_1^\dagger b_2^\dagger + b_1 b_2\right) + 2v^2 + 1 \right] \\ &+ \hbar\kappa \left[-2uv\left(b_1^\dagger b_1 + b_2^\dagger b_2\right) + (u^2+v^2)\left(b_1^\dagger b_2^\dagger + b_1 b_2\right) - 2uv \right]. \end{aligned} \tag{37}$$

The choice of the numbers u and v is made in order to cancel the contribution of $b_1^\dagger b_2^\dagger$ and $b_1 b_2$ to this expression. Using the form (34) for these numbers, we have to impose

$$\boxed{\tanh(2\lambda) = \frac{\kappa}{\omega_0}} \tag{38}$$

[5] The adjective "canonical" means precisely that the new operators b_i satisfy the commutation relations associated to bosons.

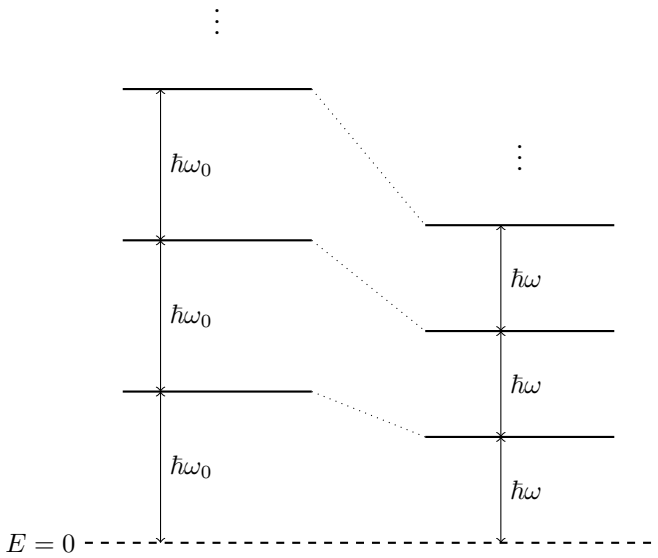

Figure 6. *Spectrum of the unperturbed Hamiltonian $\hat{H}_0$ and the pair Hamiltonian $\hat{H} = \hat{H}_0 + \hat{V}$ given in (26-27) and (40).*

which is only possible if

$$\boxed{|\kappa| < \omega_0} \tag{39}$$

We will come back to this condition in a moment.

Once this choice is made, we obtain the desired form:

$$\boxed{\hat{H} = \hbar\omega \left(b_1^\dagger b_1 + b_2^\dagger b_2 + 1 \right) \qquad \text{with} \quad \omega = \sqrt{\omega_0^2 - \kappa^2}} \tag{40}$$

We obtain two independent bosonic modes, each with a frequency ω smaller than the initial frequency. We have thus succeeded in completely diagonalizing the problem and found the spectrum of the Hamiltonian $\hat{H}$, which is written $(n_1 + n_2 + 1)\hbar\omega$ [*cf.* figure 6]. We will detail the structure of the ground state of energy $\hbar\omega$ in the following paragraph. The excited states are obtained by acting with the operators $b_1^\dagger$ and $b_2^\dagger$ on this ground state.

It will be useful to have the following expressions for ω

$$\boxed{\omega = \sqrt{\omega_0^2 - \omega_0^2 \tanh^2(2\lambda)} = \frac{\omega_0}{\cosh(2\lambda)}} \tag{41}$$

and for the coefficients u and v:

$$\boxed{\begin{array}{rcl} u^2 & = & \cosh^2\lambda = \dfrac{1}{2}\left[\cosh(2\lambda) + 1\right] = \dfrac{1}{2}\left(\dfrac{\omega_0}{\omega} + 1\right) \\ v^2 & = & \sinh^2\lambda = \dfrac{1}{2}\left[\cosh(2\lambda) - 1\right] = \dfrac{1}{2}\left(\dfrac{\omega_0}{\omega} - 1\right) \end{array}} \tag{42}$$

Condition on $|\kappa|$. The condition $|\kappa| < \omega_0$ given in (39) reflects the instability that may appear when the coupling between the two initial modes a_1 and a_2 is increased too much: when $|\kappa| \to \omega_0$ from below, the frequency of the eigenmodes b_i of the system tends to 0. The value of ω given in (40) would become purely imaginary if $|\kappa|$ were to exceed this value. The system is in fact unstable for $|\kappa| > \omega_0$: starting from the $|0,0\rangle$ state, the number of pairs in the a_i modes increases exponentially with time and the system has no stationary state.

"Usual" coupling of two oscillators. We have found here the spectrum $(n_1+n_2+1)\hbar\omega$ of two coupled oscillators via the term $\hat{V} = \hbar\kappa(a_1^\dagger a_2^\dagger + a_1 a_2)$. This spectrum is similar to the spectrum of the Hamiltonian $\hat{H}_0$, except for the rescaling $\omega_0 \to \omega$; in particular, it presents the same degeneracies. The result is very different from the one obtained for the more usual coupling

$$\hat{H}_0 = \hbar\omega_0 \left(a_1^\dagger a_1 + a_2^\dagger a_2 + 1 \right) \qquad \hat{V}' = \hbar\kappa(a_1^\dagger a_2 + a_2^\dagger a_1). \tag{43}$$

In this case, the operators allowing the diagonalization are

$$b_1 = \frac{1}{\sqrt{2}}(a_1 + a_2), \qquad b_2 = \frac{1}{\sqrt{2}}(a_1 - a_2) \tag{44}$$

and the frequencies of the two modes resulting from the coupling are no longer degenerate :

$$\omega_1 = \omega_0 + \kappa, \qquad \omega_2 = \omega_0 - \kappa. \tag{45}$$

The ground state of the system is then not modified and its energy remains equal to $\hbar\omega_0 = \frac{1}{2}\hbar\omega_1 + \frac{1}{2}\hbar\omega_2$ [*cf.* figure 7].

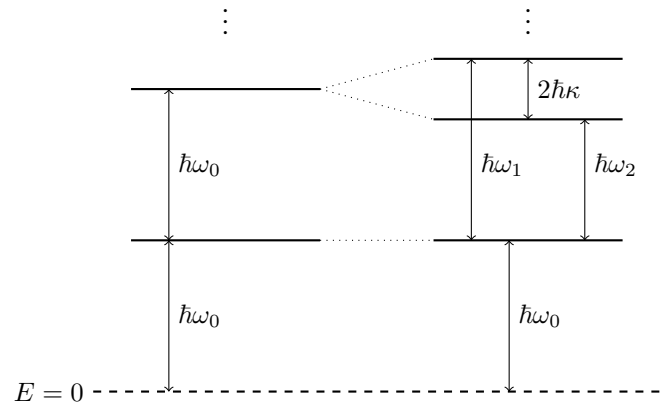

Figure 7. *Spectrum of the unperturbed Hamiltonian $\hat{H}_0$ and of the Hamiltonian with the "usual" coupling $\hat{H} = \hat{H}_0 + \hat{V}'$ given in (43). The ground state is not modified in this case.*

2-3 Ground state of the Hamiltonian

The ground state $|\Psi\rangle$ of the Hamiltonian $\hat{H}$ is obtained by placing the two eigenmodes b_1 and b_2 in their ground state. Its energy

$$\boxed{E_{\rm grnd} = \hbar\omega \qquad \text{with} \quad \omega = \sqrt{\omega_0^2 - \kappa^2}} \tag{46}$$

corresponds to the sum of the zero-point energies $\hbar\omega/2$ of the modes b_1 and b_2 [*cf.* figure 8]. It is lower than the energy $\hbar\omega_0$ of the ground state of $\hat{H}_0$ [*cf.* 28]:

$$E_{\rm grnd} - E^{(0)}_{\rm grnd} = \hbar(\omega - \omega_0) \ \leq 0, \tag{47}$$

as one would expect given the average value of $\hat{H}$ in the unperturbed $|\Psi_0\rangle$ state (the eigenstate of $\hat{H}_0$):

$$\langle\Psi_0|\hat{H}|\Psi_0\rangle = \langle\Psi_0|\hat{H}_0|\Psi_0\rangle + \langle\Psi_0|\hat{V}|\Psi_0\rangle = \hbar\omega_0. \tag{48}$$

Indeed, the theorem at the basis of the variational method entails that the energy of the ground state of $\hat{H}$ is necessarily lower than this average value:

$$E_{\rm grnd} = \langle\Psi|\hat{H}|\Psi\rangle \ \leq \ \langle\Psi_0|\hat{H}|\Psi_0\rangle. \tag{49}$$

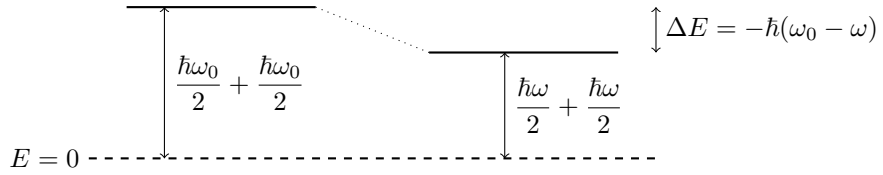

Figure 8. *Lowering the ground state energy of the two-mode system due to the coupling $\hat{V} = \hbar\kappa\left(a_1^\dagger a_2^\dagger + a_1 a_2\right)$, with $\omega = \sqrt{\omega_0^2 - \kappa^2}$.*

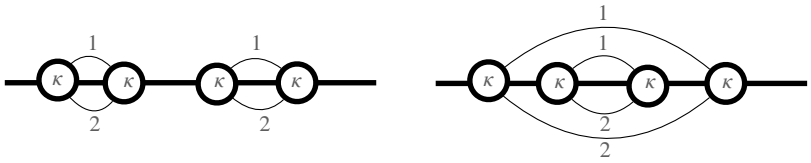

Figure 9. *The two diagrams contributing to the ground state energy of the Hamiltonian (26) at order 4 in κ/ω_0.*

Link with perturbation theory. By performing an expansion of the general expression (46) up to order 2 in κ, we recover the result (31) obtained by perturbation theory. As we have indicated, this general expression can be seen as a resummation of the perturbation series at all orders in κ. For example, we find at order 4 in κ/ω_0:

$$E_{\rm grnd} \approx \omega_0 - \frac{\kappa^2}{2\omega_0} - \frac{\kappa^4}{8\omega_0^3} \tag{50}$$

corresponding for order 2 to the diagram of the figure 5 and for order 4 to the two diagrams of the figure 9.

Expansion of the ground state on the Fock basis. The ground state $|\Psi\rangle$ of the Hamiltonian $\hat{H}$ can be decomposed on the eigenbasis $|n_1, n_2\rangle$ of $\hat{H}_0$

as

$$|\Psi\rangle = \sum_{n_1,n_2} c(n_1,n_2)\ |n_1,n_2\rangle. \tag{51}$$

The values of the coefficients $c(n_1,n_2)$ are deduced from the relations:

$$b_1|\Psi\rangle = 0 \qquad b_2|\Psi\rangle = 0 \tag{52}$$

which impose respectively

$$\frac{c(n_1+1,n_2+1)}{c(n_1,n_2)} = -\frac{v}{u}\left(\frac{n_2+1}{n_1+1}\right)^{1/2} \tag{53}$$

and

$$\frac{c(n_1+1,n_2+1)}{c(n_1,n_2)} = -\frac{v}{u}\left(\frac{n_1+1}{n_2+1}\right)^{1/2}. \tag{54}$$

We deduce that only the states with $n_1 = n_2$ are populated, which was expected given the form of the coupling $\hat{V}$ which excites the two modes a_1 and a_2 in pairs. We therefore rewrite this ground state as

$$|\Psi\rangle = \sum_n c(n)\ |n,n\rangle \tag{55}$$

with the recursion relation on c_n:

$$\frac{c_{n+1}}{c_n} = -\frac{v}{u} = -\tanh\lambda \tag{56}$$

i.e.

$$c_n = c_0\,(-\tanh\lambda)^n\,. \tag{57}$$

After normalization, the ground state is written:

$$\boxed{|\Psi\rangle = \frac{1}{\cosh\lambda}\sum_n (-\tanh\lambda)^n\,|n,n\rangle} \tag{58}$$

This state is well known in quantum optics under the name *Two-mode squeezed vacuum state*. It is generically written as

$$|\Psi\rangle = \frac{1}{\sqrt{\mathcal{N}}}\sum_{n=0}^{\infty}\eta^n|n,n\rangle \qquad \text{with} \quad \mathcal{N} = \sum_n \eta^{2n} = \frac{1}{1-\eta^2}. \tag{59}$$

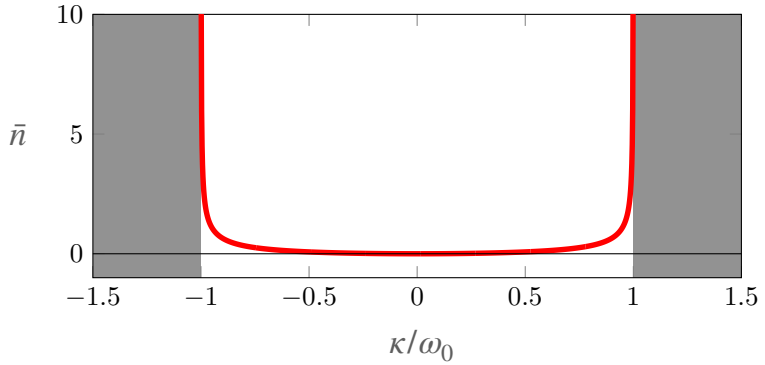

Figure 10. *Variation of the average number of pairs as a function of the ratio κ/ω_0.*

The probability law for observing the n-pair state $|n,n\rangle$ in an occupancy number measurement is:

$$\mathcal{P}(n) = \frac{\eta^{2n}}{\mathcal{N}} = \left(1-\eta^2\right)\,\eta^{2n}. \tag{60}$$

The notion of squeezing comes from the fact that there is a perfect correlation between the occupancies of the modes a_1 and a_2:

$$\Delta\,(n_1-n_2) = 0 \qquad \text{with} \quad \hat{n}_i = a_i^\dagger a_i. \tag{61}$$

This absence of fluctuation of the variable $n_1 - n_2$ allows to design measurements with a noise much lower than the one expected for two independent coherent states for modes 1 and 2, which would lead to $\Delta^2(n_1-n_2) = \Delta^2(n_1) + \Delta^2(n_2) = \bar{n}_1 + \bar{n}_2$.

When $|\kappa| \ll \omega_0$, i.e., $|\lambda| \ll 1$, the ground state (58) is close to the ground state $|\Psi_0\rangle = |0,0\rangle$ of $\hat{H}_0$. On the other hand, when $|\kappa|$ becomes comparable to ω_0, λ becomes arbitrarily large and many $|n,n\rangle$ states are significantly populated. More precisely, we find the average number of pairs:

$$\boxed{\bar{n} = \frac{\sum_n n\,(\tanh\lambda)^{2n}}{\sum_n (\tanh\lambda)^{2n}} = \sinh^2\lambda = v^2} \tag{62}$$

This mean number is plotted as a function of the ratio $\kappa/\omega_0 = \tanh(2\lambda)$ in

figure 10. The variance of this distribution is given by:

$$\boxed{\Delta n^2 = \bar{n}\,(1+\bar{n})} \tag{63}$$

so that we find the standard deviation $\Delta n \approx \bar{n}$ as soon as $\bar{n}$ becomes significantly larger than 1. Note that the statistical law for $\mathcal{P}(n)$ found in (60) is formally identical to the one giving the occupancy of an individual quantum state in the Bose–Einstein law at non-zero temperature.

3 Example : spin 1 gas in "zero dimension"

Before returning to the N-body problem of the three-dimensional Bose gas in the next chapter, it is interesting to consider a direct application of the two-mode model we have just described. We will consider the case of a collection of spin-1 atoms strongly confined in a trap, so that the three spatial degrees of freedom of the atoms are "frozen": only spin dynamics remains possible, in particular through spin exchange collisions:

$$(m=0)\ +(m=0)\ \leftrightarrows\ (m=+1)\ +(m=-1), \tag{64}$$

where we introduced the quantum number $m = 0, \pm 1$ characterizing the projection of the spin of an atom on a given axis. This process is formally equivalent to the parametric conversion in optics (Walls & Milburn 1988) and is also found in superconducting circuits (Nation, Johansson, et al. 2012). The squeezed two-mode vacuum state thus produced is among those frequently considered for quantum metrology (Pezzè, Smerzi, et al. 2018).

In the context of quantum gas experiments, this process was proposed by Duan, Sørensen, et al. (2000) and Pu & Meystre (2000), then highlighted by Klempt, Topic, et al. (2010), Gross, Zibold, et al. (2010) and Bookjans, Hamley, et al. (2011) (see also Sadler, Higbie, et al. (2006)). We will focus here on the recent experimental and numerical study by Evrard, Qu, et al. (2021), which explored different regimes, from the reversible evolution predicted by the Bogoliubov approach to a chaotic regime allowing to discuss the hypothesis that a (quasi-)arbitrary eigenstate can be seen as a representation – in the micro-canonical sense – of the thermalized system (*Eigenstate thermalization hypothesis*). The theoretical model that we will use is directly inspired by the article of Mias, Cooper, et al. (2008).

3-1 s-wave interactions between two spin-1 atoms

We consider here bosonic atoms whose total spin (electrons+nucleus) of the ground state is $s = 1$. This is notably the case for several alkaline species used in the laboratory: ^{7}Li, ^{23}Na, ^{39}K and ^{41}K, ^{87}Rb. The value 1 of the spin is obtained in this case by coupling the spin $1/2$ of the external electron and the spin $3/2$ of the nucleus.

During a collision between two identical atoms of spin $s_1 = s_2 = 1$, three channels are possible corresponding to the three possible values $s = 0, 1, 2$ for the spin $\boldsymbol{s} = \boldsymbol{s}_1 + \boldsymbol{s}_2$ of the pair of atoms. We can verify that[6] that the spin state $s = 1$ is obtained by an antisymmetric combination of the two spins $\boldsymbol{s}_1$ and $\boldsymbol{s}_2$. Since we are dealing with bosons, the total orbital+spin state must be symmetric by exchange of the two particles, which means that the space wave function must be antisymmetric for a total spin $s = 1$. As we are interested here in the very low temperature regime, where only s-wave collisions are significant, this $s = 1$ channel does not contribute to the interaction between particles.

The two remaining channels, $s = 0$ and $s = 2$, correspond to spin-symmetric states and s-wave collisions are allowed. These channels are therefore each characterized by a scattering length, a_0 and a_2. We can then model the interaction between atoms by a contact term:

$$\hat{V}_{\text{int.}} = \delta(\boldsymbol{r}_1 - \boldsymbol{r}_2) \otimes (g_0 \mathcal{P}_0 \ + \ g_2 \mathcal{P}_2) \qquad \text{with} \quad g_i = \frac{4\pi\hbar^2 a_i}{m}, \tag{65}$$

where $\mathcal{P}_i$ is the projector onto the total spin subspace $s = i$, with $i = 0, 2$. Note that the Dirac distribution $\delta(\boldsymbol{r})$ must in fact be regularized in the form of the pseudo-potential as shown in (3). This interaction can be written in an equivalent way

$$\boxed{\hat{V}_{\text{int.}} = \delta(\boldsymbol{r}_1 - \boldsymbol{r}_2) \otimes \left(\bar{g}\hat{1} + g_s \hat{\boldsymbol{s}_1} \cdot \hat{\boldsymbol{s}_2}\right) (\mathcal{P}_0 + \mathcal{P}_2)} \tag{66}$$

[6] For $m = \pm 1$ we find that:

$$\sqrt{2}\,|s=1, m\rangle = |s_1, m\,;\, s_2, 0\rangle - |s_1, 0\,;\, s_2, m\rangle$$

and for $m = 0$

$$\sqrt{2}\,|s=1, 0\rangle = |s_1, +1\,;\, s_2, -1\rangle - |s_1, -1\,;\, s_2, +1\rangle.$$

where we have posed:

$$\bar{g} = \frac{1}{3}(g_0 + 2g_2) \qquad g_s = \frac{1}{3}(g_2 - g_0)\,. \tag{67}$$

To demonstrate the passage from (65) to (66), it is sufficient to note that the scalar product

$$\hat{\boldsymbol{s}}_1 \cdot \hat{\boldsymbol{s}}_2 = \frac{1}{2}\left(\hat{s}^2 - \hat{s}_1^2 - \hat{s}_2^2\right) = \frac{1}{2}\hat{s}^2 - 2 \tag{68}$$

is equal to -2 when it acts on a $s = 0$ spin state, and to $+1$ when it acts on a $s = 2$ spin state.

We will consider in what follows the case of sodium atoms, for which we find for the scattering lengths $\bar{a}$ and a_s associated respectively to $\bar{g}$ and g_s:

$$\bar{a} = 52.66\, a_0 = 2.8\,\text{nm} \qquad a_s = 1.88\, a_0 = 98\,\text{pm}. \tag{69}$$

The form of the interaction in $\hat{\boldsymbol{s}}_1 \cdot \hat{\boldsymbol{s}}_2$ is reminiscent of magnetic dipole interactions, but it is important to emphasize that its origin is purely electrostatic, since it results from van der Waals interactions. Magnetic interactions are also present but they are much weaker, at least for alkali atoms, and we will neglect them in what follows.

3-2 The single mode approximation

We now consider a condensate of N atoms confined in a trap of high stiffness (figure 11); we note R the spatial size of the cloud and n the average density of the gas. For simplicity, we consider an isotropic harmonic trap of frequency ω. We will assume in the following that the interaction energy, function of $N\bar{g}$ and Ng_s, is low enough for the atoms to accumulate essentially in the ground state $\psi_0(\boldsymbol{r})$ of the trap, the Gaussian function of extension $a_{\text{ho}} = \sqrt{\hbar/m\omega}$ (figure 12). The spatial dynamics is thus frozen and only the spin dynamics can lead to an evolution of the system. This is the single mode approximation (SMA); in other words, we have realized a spin gas of "zero spatial dimension".

The Hamiltonian governing the spin dynamics from the interaction term (66) is obtained by averaging the initial Hamiltonian over the density distribution $|\psi_0(\boldsymbol{r})|^2$:

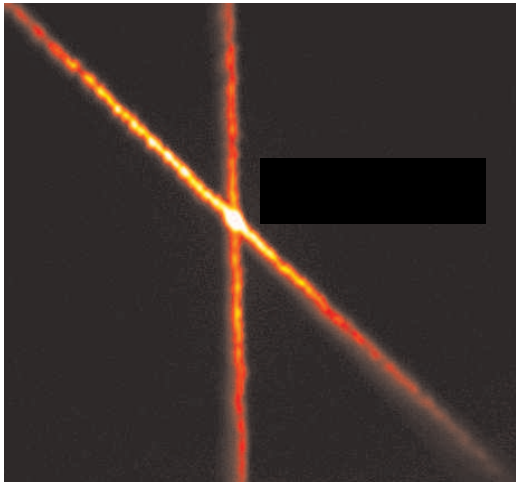

Figure 11. *Dipole trap obtained at the intersection of two detuned laser beams on the red of the atomic resonance line. The atoms (sodium) are visible because they are excited here by additional beams creating an optical molasses. This type of trap ensures a confinement with similar frequencies along the three eigenaxes of the trap. Figure extracted from David Jacob's thesis.*

$$\hat{V}_{\text{int.}}^{\text{SMA}} = \frac{U_s}{2N}\sum_{i,j\neq i}\hat{\boldsymbol{s}}_i \cdot \hat{\boldsymbol{s}}_j = \frac{U_s}{2N}\hat{\boldsymbol{S}}^2 + \ldots \tag{70}$$

where $\hat{\boldsymbol{S}} = \sum_{i=1}^{N}\hat{\boldsymbol{s}}_i$ is the total spin operator, where $\ldots$ represents a constant additive term, and where we have posed:

$$U_s = Ng_s\int |\psi_0(\boldsymbol{r})|^4\,\mathrm{d}^3r. \tag{71}$$

In the following, it will be useful to express this interaction Hamiltonian in terms of the creation $a_m^\dagger$ and annihilation a_m operators of an atom in the ψ_0 orbital state and in the $m = -1, 0, +1$ spin state, with a given quantization axis. We also introduce the occupation number operator of a

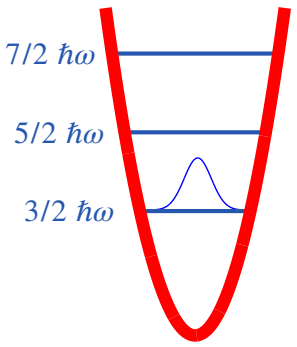

Figure 12. *Single mode approximation: it is assumed here that the interactions and the temperature are sufficiently low that the atoms essentially occupy the ground state of the harmonic trap which confines them. Under these conditions, only the dynamics related to the spin degree of freedom is relevant.*

given m state: $\hat{N}_m = a_m^\dagger a_m$. The result is written after a somewhat tedious calculation (Law, Pu, et al. 1998):

$$\begin{aligned}\hat{V}_{\text{int.}}^{\text{SMA}} &= \frac{U_s}{2N}\left[(\hat{N}_{+1}-\hat{N}_{-1})^2+(2\hat{N}_0-1)\left(\hat{N}_{+1}+\hat{N}_{-1}\right)\right] \\ &+\frac{U_s}{N}\left[a_{+1}^\dagger a_{-1}^\dagger a_0 a_0 + \text{H.c.}\right], \end{aligned} \tag{72}$$

again up to an additive constant.

The expression (72) is instructive. The first line depends only on the occupation numbers $\hat{N}_m = a_m^\dagger a_m$ and therefore does not induce spin dynamics. This dynamics comes from the second line which describes the spin exchange collision:

$$\boxed{(m=0)\ +(m=0) \leftrightarrows\ (m=+1)\ +(m=-1)} \tag{73}$$

From a pair of atoms initially in the $m=0$ state, an elastic collision can create a pair of atoms in the $m=+1$ and $m=-1$ states, and conversely. This is an essential ingredient of Bogoliubov's formalism, which we will explore in the next paragraph.

Remark. The large difference between $\bar{g}$ and g_s for the sodium atoms (factor ~ 30 as shown in (69)) allows to relax somewhat the constraints on the initial state for the single mode approximation. Even if the product $N\bar{g}$ is such that the initial condensate is described rather in the Thomas-Fermi approximation and has an extension $R \gg a_{\text{ho}}$, the single mode approximation is valid if

$$\xi_s \gg R \qquad \text{with} \quad \xi_s = \frac{1}{\sqrt{8\pi n a_s}}. \tag{74}$$

ξ_s is called then *spin healing length*. In general, for a scalar condensate of density n and scattering length a, the healing length $\xi = 1/\sqrt{8\pi n a}$ represents the shortest length scale on which the fluid can react to an external perturbation (obstacle, impurity, ...). For a spin gas, the condition (74) leads to the fact that it would be too energetically expensive to form spin domains within the R size domain.

3-3 Zeeman effect and Bogoliubov Hamiltonian

In what follows, we will assume that the spinor gas is immersed in a magnetic field $\boldsymbol{B}$ of fixed z axis, which we take as the quantization axis. We will further assume that the N atoms are initially prepared in the $m=0$ state. Under the effect of elastic collisions (73), the $m=\pm 1$ states will be populated under the constraint $N_{+1} = N_{-1}$.

Let us focus on the regime where the $m=0$ state is sparsely populated, i.e. $N_{\pm 1} \ll N_0 \approx N$. By treating $\hat{N}_0$ as a number equal to N, we can then simplify the expression for the interaction Hamiltonian (72) to:

$$\hat{V}_{\text{int.}}^{\text{SMA}} \approx U_s\left(\hat{N}_{+1}+\hat{N}_{-1}+a_{+1}^\dagger a_{-1}^\dagger + a_{+1}a_{-1}\right) \tag{75}$$

Let's now look at the magnetic energy of the gas (figure 13) :

- At order 1 in magnetic field, the two states $m=\pm 1$ are displaced by opposite quantities, $\pm\mu B$. A pair of atoms $\{m=+1, m=-1\}$ has therefore, at this order in magnetic field, the same energy as the initial pair $\{m=0, m=0\}$: the linear Zeeman effect has no consequence on the dynamics of the system and can be forgotten.

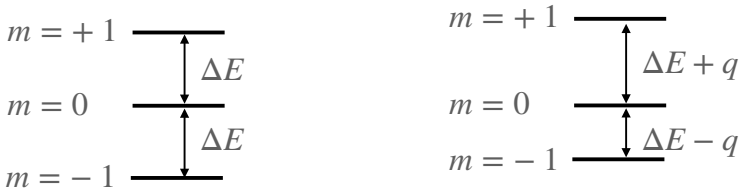

Figure 13. *Zeeman effect for an atom of spin 1. On the left, only the linear Zeeman effect with $\Delta E = \mu B$; on the right, the quadratic Zeeman effect, characterized by the energy $q \propto B^2$, has been added.*

- At order 2 in a magnetic field, the $m = \pm 1$ states are displaced by the same amount[7] $q > 0$ proportional to B^2 compared to the $m = 0$ state. This shift affects the pair creation process (73) since the energy of the right-hand side member differs from that of the left-hand side by the quantity $2q$.

For the magnetic fields considered here, we can limit ourselves to the second order in B and write the contribution of the Zeeman effect in the form

$$V_{\text{Zeem.}} = q\left(\hat{N}_{+1} + \hat{N}_{-1}\right), \tag{76}$$

which gives the total Hamiltonian:

$$\boxed{\hat{H} = (q + U_s)\left(a^\dagger_{+1}a_{+1} + a^\dagger_{-1}a_{-1}\right) + U_s\left(a^\dagger_{+1}a^\dagger_{-1} + a_{+1}a_{-1}\right)} \tag{77}$$

This is exactly the starting point for the Bogoliubov method. We deduce from the analysis made in the previous section that in the approximation of a weak depletion of the $m = 0$ mode, the spectrum of the N-body system is composed of equidistant levels separated by the energy

$$\boxed{\hbar\omega = \left[(q + U_s)^2 - U_s^2\right]^{1/2} = \sqrt{q\,(q + 2U_s)}} \tag{78}$$

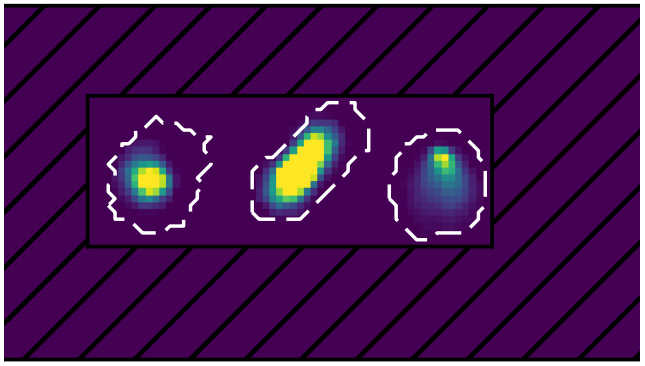

Figure 14. *Measurement of the occupation numbers of the three Zeeman sub-levels $m = -1, 0, +1$. A Stern and Gerlach experiment followed by an optical molasses phase allows to count the atoms with an accuracy of the order of one atom, by analyzing the fluorescence light collected in the three spots. Figure extracted from Bertrand Evrard's thesis.*

3-4 Response of the gas to a magnetic field jump

To test the predictions of the Bogoliubov approach, Evrard, Qu, et al. (2021) started with a sodium condensate of $N \sim 5000$ atoms in the $m = 0$ state. The condensate is initially placed in a large magnetic field ($B \sim 1\,\text{G}$, leading to $q/h \sim 280\,\text{Hz}$) and is confined in a trap such that $U_s/h = 17\,\text{Hz}$. Under these conditions, $q \gg U_s$ and the number of pairs in the $m = \pm 1$ states is notably less than 1. The experiment, which measures the population of each spin state with a precision close to the single-atom level (figure 14), confirms this prediction. The magnetic field is then suddenly lowered to a much lower value, corresponding to $q = 0.3\,\text{Hz}$ (thus $q \ll U_s$), and we are interested in the evolution of the system.

On the theoretical side, as the Bogoliubov Hamiltonian is quadratic with respect to the operators a_m and $a^\dagger_m$, the simplest way to study the evolution of the system is to use the Heisenberg picture. We find for the

[7] For the sodium atom, the quadratic Zeeman effect is $277\,\text{Hz/G}^2$.

pair of operators $a_1, a_{-1}^\dagger$:

$$i\hbar\frac{da_1}{dt} = [a_1, \hat{H}] = (q+U_s)a_1 + U_s a_{-1}^\dagger \quad (79)$$

$$i\hbar\frac{da_{-1}^\dagger}{dt} = [a_{-1}^\dagger, \hat{H}] = -(q+U_s)a_{-1}^\dagger - U_s a_1 \quad (80)$$

or

$$i\hbar\frac{d}{dt}\begin{pmatrix} a_1 \\ a_{-1}^\dagger \end{pmatrix} = [M]\begin{pmatrix} a_1 \\ a_{-1}^\dagger \end{pmatrix} \quad \text{with} \quad M = \begin{pmatrix} q+U_s & U_s \\ -U_s & -(q+U_s) \end{pmatrix} \quad (81)$$

and similar coupled equations for the pair $a_{-1}, a_1^\dagger$. The eigenvalues of the matrix $[M]$ are $\pm\hbar\omega$ and solving this differential system gives the result:

$$\begin{pmatrix} a_1 \\ a_{-1}^\dagger \end{pmatrix}(t) = \begin{pmatrix} C - i(q+U_s)S/\hbar\omega & -iU_sS/\hbar\omega \\ iU_sS/\hbar\omega & C + i(q+U_s)S/\hbar\omega \end{pmatrix}\begin{pmatrix} a_1 \\ a_{-1}^\dagger \end{pmatrix}(0) \quad (82)$$

where we put $C = \cos(\omega t)$ and $S = \sin(\omega t)$. Starting from the vacuum (i.e. all the atoms in the state $m = 0$) at time $t = 0$, we deduce the average number of pairs $(+1, -1)$ at time t:

$$N_p(t) = \frac{1}{2}\sum_{m=\pm1}\langle 0|a_m^\dagger(t)a_m(t)|0\rangle = \frac{1}{2}\sum_{m=\pm1}||a_m(t)|0\rangle||^2 \quad (83)$$

or

$$\boxed{\bar{N}_p(t) = \left(\frac{U_s}{\hbar\omega}\right)^2 \sin^2(\omega t)} \quad (84)$$

Note that it is also possible to use the Schrödinger point of view and to compute the state vector of the system $|\Psi(t)\rangle$. It can be shown [see for example Mias, Cooper, et al. (2008)] that this state is at each instant a two-mode squeezed vacuum state as defined in (58), characterized by the mean value $\bar{N}_p(t)$ given in (84).

The experiment confirms the prediction of this reversible and oscillating evolution of a N-body system (figure 15, left). We verify that the numbers of atoms in $m = \pm1$ remain equal to each other in the course of time, within the measurement uncertainties. The dependence of the frequency ω with the magnetic field (characterized by the value of the parameter q) is also in agreement with the prediction (78) of the Bogoliubov theory (figure 15, right).

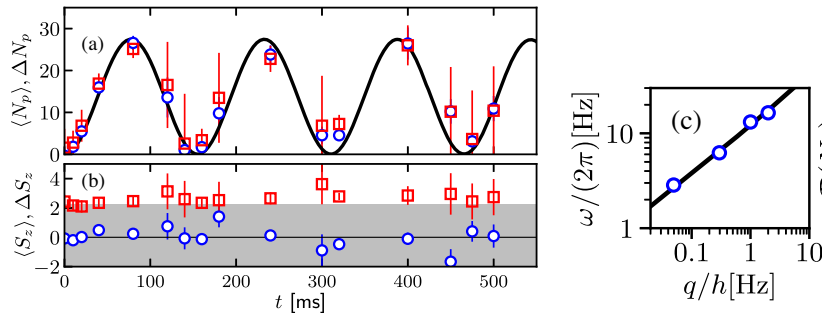

Figure 15. *Left, top: Mean value and standard deviation of the number of pairs created in a spin 1 assembly, under the effect of spin exchange collisions (73). The solid line is the prediction (84) obtained from the Bogoliubov approach. Left, bottom: the magnetization $S_z = N_{+1} - N_{-1}$ remains zero during the evolution, within measurement uncertainties. Right: variation of the frequency ω of the oscillations with the parameter q characterizing the magnetic field. The continuous line corresponds to the prediction (78). Figures extracted from Evrard, Qu, et al. (2021).*

Depletion of the $m = 0$ state. Bogoliubov's method is based on the assumption that the population of the $m = 0$ state remains close to the total number of atoms. It is interesting to see what happens when this assumption is no longer valid. In the case of the N-body problem, it is the problem of quantum depletion, which we will address in the next chapter.

For the case of a spin 1 gas in the single mode approximation, the assumption of weak depletion of the $m = 0$ state is verified if the amplitude of the $N_p(t)$ oscillations written in (84) is small in front of N, which imposes $q \gg U_s/N$. Recall that $q \lesssim U_s$ is required for the number of pairs to be greater than unity and for a signal to be detected.

When we take a final value of q very small in front of U_s/N, we leave the Bogoliubov regime and the dynamics of the system which follows the sudden change of magnetic field is no longer a reversible dynamics. It is simple to model the $q = 0$ case, for which the Hamiltonian is simply (still in the single spatial mode approximation) $\hat{H} = \frac{U_s}{2N}\hat{S}^2$ [*cf.* (70)]. The spectrum of this N-body Hamiltonian is no longer linear as in the Bogoliubov regime, but $\sim$ quadratic with energy levels in $(U_s/2N)S(S+1)$. The evo-

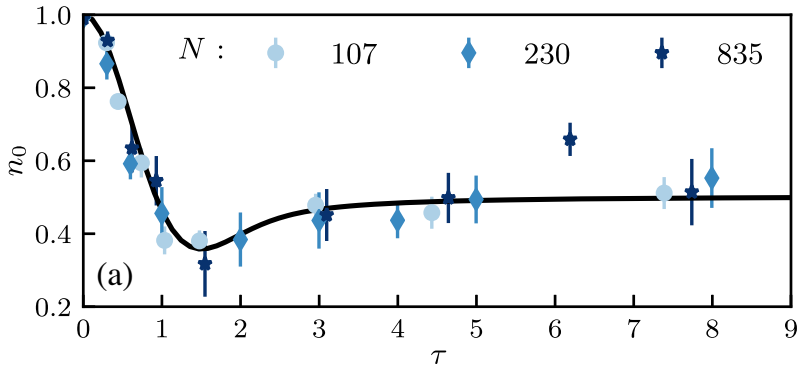

Figure 16. *The "universal" evolution obtained in the $q \ll U_s/N$ regime, for which the population of the $m = 0$ state becomes strongly depleted. In this regime, the Bogoliubov method does not apply anymore. The solid line corresponds to the theoretical prediction (85). Figure extracted from Evrard, Qu, et al. (2021).*

lution then becomes irreversible and characterized by a universal function of time t:

$$N_0(t) = N\left[1 - \tau D(\tau)\right] \qquad \text{with} \quad \tau = \sqrt{\frac{2}{N}}\frac{U_s t}{\hbar} \tag{85}$$

where $D(\tau)$ is the Dawson function (figure 16).

A last point studied by Evrard, Qu, et al. (2021) concerns the addition of an extra term to the Hamiltonian (77) which allows to reach a chaotic regime. It is then possible to test numerically if the dynamics leads to a thermalization of the spin assembly, as predicted by the *Eigenstate thermalization hypothesis (ETH)*. We will not describe these results here because they are not related to the general topic of Bogoliubov's method and we refer the interested reader to the article of Evrard, Qu, et al. (2021) and the references therein.

Appendix : the formalism of the second quantization

In non-relativistic physics, the number of particles is conserved and it is in principle possible to carry out the Bogoliubov analysis in the wave function formalism. Nevertheless, the calculations become disproportionate, because of the simple writing of the $N!$ terms which result from the symmetrization of a N body wave function.

It is very preferable to use the formalism of the second quantization which we recall here for bosons. We give ourselves a basis $= \{|\alpha\rangle, |\beta\rangle, \ldots\}$ of the one-particle Hilbert space, noted $\mathcal{E}^{(1)}$, for example the plane wave basis characterized by the wave vectors $\boldsymbol{k}$. A basis of the N-particle state space, noted $\mathcal{E}^{(N)}$, is obtained by considering all states

$$|n_\alpha, n_\beta, \ldots\rangle \qquad \sum_\alpha n_\alpha = N \tag{86}$$

The integer $n_\alpha \geq 0$ denotes the number of particles in the α state.

We work in the Fock space, direct sum of Hilbert spaces with a given number of particles:

$$\mathcal{E} = \mathcal{E}^{(0)} \oplus \mathcal{E}^{(1)} \oplus \ldots \oplus \mathcal{E}^{(N)} \oplus \ldots \tag{87}$$

The space $\mathcal{E}^{(0)}$ is the vacuum of particles; it is a space of dimension 1 corresponding to the state noted $|0\rangle$.

We introduce the creation operator of a particle in one of these states

$$\begin{aligned} &a_\mu^\dagger : \mathcal{E}^{(N)} \longrightarrow \mathcal{E}^{(N+1)} \\ &a_\mu^\dagger |n_\alpha, n_\beta, \ldots, n_\mu, \ldots\rangle = \sqrt{n_\mu + 1}\,|n_\alpha, n_\beta, \ldots, n_\mu + 1, \ldots\rangle \end{aligned} \tag{88}$$

and the associated destruction operator

$$\begin{aligned} &a_\mu : \mathcal{E}^{(N)} \longrightarrow \mathcal{E}^{(N-1)} \\ &a_\mu |n_\alpha, n_\beta, \ldots, n_\mu, \ldots\rangle = \sqrt{n_\mu}\,|n_\alpha, n_\beta, \ldots, n_\mu - 1, \ldots\rangle \quad \text{if } n_\mu \neq 0 \\ &\qquad\qquad = 0 \quad \text{if } n_\mu = 0 \end{aligned} \tag{89}$$

The algebra thus obtained is formally identical to that of a harmonic oscillator. In particular, the prefactors $\sqrt{n_\mu + 1}$ and $\sqrt{n_\mu}$ allow a considerable simplification in the writing of the operators. They also lead to the value of the commutators:

$$[a_\mu, a_\nu] = 0 \quad [a_\mu^\dagger, a_\nu^\dagger] = 0 \quad [a_\nu, a_\mu^\dagger] = \delta_{\mu\nu}. \tag{90}$$

In this course, we use the plane wave basis $\boldsymbol{k}$ to write the creation and annihilation operators which thus become $a_{\boldsymbol{k}}^\dagger, a_{\boldsymbol{k}}$.

Chapter III

Lee-Huang-Yang energy and quantum depletion

The previous chapter was devoted to the implementation of the Bogoliubov formalism for a Bose gas. The interaction potential between the N atoms is chosen of the form

$$\hat{\mathcal{V}} = \sum_{i<j} V(|\hat{\boldsymbol{r}}_i - \hat{\boldsymbol{r}}_j|) \tag{1}$$

and the binary potential $V(r)$, which is assumed to be spherically symmetric to simplify the notations, has the Fourier transform

$$\tilde{V}_k = \int V(r)\, \mathrm{e}^{-\mathrm{i}\boldsymbol{k}\cdot\boldsymbol{r}}\, \mathrm{d}^3 r. \tag{2}$$

$V(r)$ is assumed to be regular and sufficiently small for the Born expansion to converge. Starting from the N-body Hamiltonian written in second quantization,

$$\hat{H} = \sum_{\boldsymbol{k}} \epsilon_k\, a^\dagger_{\boldsymbol{k}}\, a_{\boldsymbol{k}} + \frac{1}{2L^3} \sum_{\boldsymbol{k}',\boldsymbol{k}'',\boldsymbol{q}} \tilde{V}_q\, a^\dagger_{\boldsymbol{k}'+\boldsymbol{q}}\, a^\dagger_{\boldsymbol{k}''-\boldsymbol{q}}\, a_{\boldsymbol{k}''}\, a_{\boldsymbol{k}'} \tag{3}$$

with $\epsilon_k = \hbar^2 k^2/2m$, we made a quadratic approximation consisting (i) in treating the condensate in $\boldsymbol{k} = 0$ as a classical field and (ii) in keeping only the terms of degree at most 2 in an expansion in powers of the creation and destruction operators $a^\dagger_{\boldsymbol{k}}$ and $a_{\boldsymbol{k}}$ for $\boldsymbol{k} \neq 0$. After this approximation, the Hamiltonian is written

$$\hat{H}' = \frac{1}{2} nN\tilde{V}_0 + \hat{H}'' \tag{4}$$

with

$$\hat{H}'' = \sum_{\substack{\text{pairs}\\ \{\boldsymbol{k},-\boldsymbol{k}\}}} \left(\epsilon_k + n\tilde{V}_k\right)\left(a^\dagger_{\boldsymbol{k}} a_{\boldsymbol{k}} + a^\dagger_{-\boldsymbol{k}} a_{-\boldsymbol{k}}\right) + n\tilde{V}_k \left(a^\dagger_{\boldsymbol{k}} a^\dagger_{-\boldsymbol{k}} + a_{\boldsymbol{k}} a_{-\boldsymbol{k}}\right), \tag{5}$$

where $n = N/L^3$ denotes the spatial density of the gas.

The Hamiltonian $\hat{H}''$ consists of a sum of independent Hamiltonians, each of them dealing with a pair $\{+\boldsymbol{k}, -\boldsymbol{k}\}$. We have shown that each of these Hamiltonians can be diagonalized by a canonical transformation

$$b_{\boldsymbol{k}} = u_k a_{\boldsymbol{k}} + v_k a^\dagger_{-k} \qquad b_{-\boldsymbol{k}} = u_k a_{-\boldsymbol{k}} + v_k a^\dagger_{\boldsymbol{k}} \tag{6}$$

with

$$u_k = \cosh\lambda_k \qquad v_k = \sinh\lambda_k \qquad \tanh(2\lambda_k) = \frac{n\tilde{V}_k}{\epsilon_k + \tilde{V}_k}. \tag{7}$$

The Hamiltonian $\hat{H}''$ is then written in terms of the operators $b^\dagger_{\boldsymbol{k}}, b_{\boldsymbol{k}}$:

$$\hat{H}'' = \sum_{\boldsymbol{k}\neq 0} \left[\hbar\omega_k\, b^\dagger_{\boldsymbol{k}} b_{\boldsymbol{k}} \;+\; \frac{1}{2}\hbar\left(\omega_k - \omega_{0,k}\right)\right] \tag{8}$$

with

$$\hbar\omega_k = \left[\left(\epsilon_k + n\tilde{V}_k\right)^2 - \left(n\tilde{V}_k\right)^2\right]^{1/2} = \left(\epsilon_k^2 + 2n\tilde{V}_k\epsilon_k\right)^{1/2} \tag{9}$$

$$\hbar\omega_{0,k} = \epsilon_k + n\tilde{V}_k. \tag{10}$$

We have thus reduced the problem to a collection of independent modes of frequency ω_k. We immediately notice an effect of the pair creation and destruction terms $\{+\boldsymbol{k}, -\boldsymbol{k}\}$ in the Hamiltonian $\hat{H}''$ written in (5): it lowers the energy of the ground state for each pair by the quantity $\hbar\omega_k - \hbar\omega_{0,k} < 0$. The other important result from the previous chapter, which we will use to evaluate the *quantum depletion*, concerns the structure of this ground state, and in particular the average number of pairs $\{+\boldsymbol{k}, -\boldsymbol{k}\}$ present in this ground state:

$$\bar{n}_k = v_k^2 = \frac{\omega_{0,k} - \omega_k}{2\omega_k}. \tag{11}$$

We immediately notice that this average number of pairs can become large when $\omega_k \to 0$, i.e. according to (9) when the kinetic energy $\epsilon_k = \hbar^2 k^2/2m$ is much smaller than $n\tilde{V}_k$.

In this chapter, we will exploit this set of results to study the ground state of the Bose gas. First, we will continue to work with a potential $V(\boldsymbol{r})$ for which the Born expansion is valid. We will discuss successively the excitation spectrum of the system, the energy E_0 of the ground state and the quantum depletion, i.e. the fraction of atoms n'/n outside the condensate $\boldsymbol{k} = 0$. Concerning the quantum depletion, we will establish the following result:

$$\boxed{\frac{n'}{n} \approx \frac{8}{3\sqrt{\pi}}\sqrt{na^3}} \tag{12}$$

Recall that this fraction must be much smaller than 1 for the expansion of the complete Hamiltonian (3) to the approximate Hamiltonian (4) to be justified. Concerning the ground state energy, we will show that:

$$\boxed{\frac{E_0}{L^3} = \frac{1}{2}gn^2\left[1 + \frac{128}{15\sqrt{\pi}}\sqrt{na^3} + \dots\right] \qquad \text{with} \quad g \equiv \frac{4\pi\hbar^2 a}{m}} \tag{13}$$

The first term is simply the mean field energy already encountered in the previous chapter. The second term, which is small in front of the first one because of the condition $n'/n \ll 1$, is the correction calculated for the first time by Lee, Huang and Yang (Lee, Huang, et al. 1957) which is also written, noting L^3 the volume occupied by the gas:

$$\boxed{\frac{E_{\rm LHY}}{L^3} = \frac{1}{2}gn^2 \times \frac{128}{15\sqrt{\pi}}\sqrt{na^3} = \frac{8}{15\pi^2}\frac{m^{3/2}}{\hbar^3}(gn)^{5/2}} \tag{14}$$

It is important to note that the potential $V(\boldsymbol{r})$ enters in the energy E_0 only through the scattering length[1] a (or the coupling coefficient g which is proportional to it).

Once these results are established, we will turn to another type of interaction, the pseudo-potential $\hat{V}_{\rm pp}$, which is of zero range. The results obtained in the Born approximation and indicated above will remain formally valid, but we will point out some difficulties specific to $\hat{V}_{\rm pp}$. Let us also mention the recent publication of Carlen, Holzmann, et al. (2021), who develop a rigorous alternative approach to the Bose gas for the case of a purely repulsive potential, both for the low and high density cases, and who present detailed comparisons with Monte Carlo calculations. Finally, we will describe a number of recent experiments which have provide precise measurements of the different physical quantities we have just mentioned.

1 Preliminary remarks

1-1 Preliminary 1: The Born expansion

As in the previous chapter, we consider in this section a regular two-body interaction potential of range b. We assume that the interaction of two atoms under this potential can be treated by the Born approach, the scattering length being written as an expansion in powers of V:

$$a = a^{(1)} + a^{(2)} + \dots\,, \qquad g = g^{(1)} + g^{(2)} + \dots \tag{16}$$

with $g \equiv 4\hbar^2 a/m$.

Let us briefly recall the nature of this approximation and its validity criterion at low energy. In a binary collision, the scattering amplitude of

[1] The next term in the bracket expansion is (Wu 1959):

$$\left[1 + \frac{128}{15\sqrt{\pi}}\sqrt{na^3} + 8\left(\frac{4\pi}{3} - \sqrt{3}\right)na^3\ln(na^3) + \dots\right] \tag{15}$$

and thus also depends only on the scattering length a. The term which follows in the expansion and represented by $\dots$ is proportional to n; it involves the effective range r_e and a three-body parameter computed by Tan (2008d).

the relative particle from $\boldsymbol{k}_i$ to $\boldsymbol{k}_f$ is given by the matrix element of $\hat{T}(E)$ between these two states, with $\hat{H}_0 = \hat{p}^2/2m_{\rm r}$ and $E = \hbar^2 k_i^2/2m_{\rm r}$ ($\hat{p}$ and $m_{\rm r} = m/2$ represent the momentum and mass of the relative particle):

$$\hat{T}(E) = \hat{V} + \hat{V}\frac{1}{E - \hat{H}_0 + {\rm i}0_+}\hat{V} + \dots \tag{17}$$

The Born approximation consists in keeping only the first term of this expansion:

$$\langle \boldsymbol{k}_f|\hat{T}(E)|\boldsymbol{k}_i\rangle \approx \langle \boldsymbol{k}_f|\hat{V}|\boldsymbol{k}_i\rangle = \frac{\tilde{V}_{\boldsymbol{k}_f-\boldsymbol{k}_i}}{L^3}. \tag{18}$$

We are interested in the regime of low energy collisions (s-wave collisions). Taking the limit $|\boldsymbol{k}_i| = |\boldsymbol{k}_f| \to 0$, we find the result already used in the previous chapter:

$$g^{(1)} \equiv \frac{4\pi\hbar^2 a^{(1)}}{m} = \tilde{V}_0. \tag{19}$$

A necessary condition for this approximation to be valid is that the next term in the Born expansion is small compared to the first-order contribution. The matrix element of the next term is easily calculated by introducing a closure relation in momentum space:

$$\begin{aligned}\langle \boldsymbol{k}_f|\hat{V}\frac{1}{E - \hat{H}_0 + {\rm i}0_+}\hat{V}|\boldsymbol{k}_i\rangle &= \frac{L^3}{(2\pi)^3}\int \frac{\langle \boldsymbol{k}_f|\hat{V}|\boldsymbol{k}\rangle\,\langle \boldsymbol{k}|\hat{V}|\boldsymbol{k}_i\rangle}{E - \frac{\hbar^2k^2}{2m_{\rm r}} + {\rm i}0_+}\,{\rm d}^3k \\ &= \frac{1}{(2\pi)^3 L^3}\int \frac{\tilde{V}_{\boldsymbol{k}_f-\boldsymbol{k}}\,\tilde{V}_{\boldsymbol{k}-\boldsymbol{k}_i}}{E - \frac{\hbar^2k^2}{2m_{\rm r}} + {\rm i}0_+}\,{\rm d}^3k. \end{aligned}\tag{20}$$

Let's take the limit $|\boldsymbol{k}_i| = |\boldsymbol{k}_f| \to 0$ in this equation, using $m_{\rm r} = m/2$:

$$\begin{aligned}\langle \boldsymbol{k}_f|\hat{V}\frac{1}{E - \hat{H}_0 + {\rm i}0_+}\hat{V}|\boldsymbol{k}_i\rangle &\approx -\frac{m}{(2\pi)^3\hbar^2 L^3}\int \frac{\tilde{V}_k^2}{k^2}\,{\rm d}^3k \\ &= -\frac{m}{2\pi^2\hbar^2 L^3}\int_0^\infty \tilde{V}_k^2 {\rm d}k, \end{aligned}\tag{21}$$

this integral converging as soon as $|\tilde{V}_k|$ decreases faster than $1/\sqrt{k}$ at infinity. As $|\tilde{V}_k|$ takes significant values for values of k up to $\sim 1/b$, the corresponding value of the integral is, up to a numerical coefficient depending on the precise shape of the potential:

$$\langle \boldsymbol{k}_f|\hat{V}\frac{1}{E - \hat{H}_0 + {\rm i}0_+}\hat{V}|\boldsymbol{k}_i\rangle \sim -\frac{m}{2\pi^2\hbar^2 L^3}\frac{\tilde{V}_0^2}{b}. \tag{22}$$

The contribution of this term (always negative) to the scattering length a is small compared to the dominant contribution if

$$\frac{m}{2\pi^2\hbar^2}\frac{\tilde{V}_0^2}{b} \ll \tilde{V}_0 \qquad \Leftrightarrow \quad a^{(1)} \ll b. \tag{23}$$

This is the criterion needed for the Born approximation at low energy (19) to be valid.

The above analysis allows us to give the first correction to the Born approximation, which will be useful in the following:

$$g^{(2)} \equiv \frac{4\pi\hbar^2 a^{(2)}}{m} = -\frac{1}{(2\pi)^3}\int \frac{|\tilde{V}_k|^2}{2\epsilon_k}\,{\rm d}^3k \tag{24}$$

with as before $\epsilon_k = \hbar^2k^2/2m$, this correction $\sim a^{(1)} \times \left(a^{(1)}/b\right)$ being always negative.

1-2 Preliminary 2: The different sectors for k

The different physical quantities mentioned in the introduction, such as the ground state energy or the quantum depletion, involve integrals over the wave vector $\boldsymbol{k}$. It is therefore important to identify now the behaviors of the two main terms, $n\tilde{V}_k$ and ϵ_k, that will intervene in all these integrals in order to compare them.

We have made the assumption that the potential $V(r)$ is regular of range b. We will assume in what follows that its Fourier transform $\tilde{V}_k$ is approximately constant and equal to $\tilde{V}_0$ as long as $k \ll 1/b$, then decreases and tends to 0 when k becomes significantly larger than b. An example of variation for $V(r)$ and $\tilde{V}_k$ is given in figure 1 in the case of a Gaussian potential.

In the expression (9) of the frequency of the mode associated with the pair $\{+\boldsymbol{k}, -\boldsymbol{k}\}$, the sum

$$\epsilon_k + 2n\tilde{V}_k \tag{25}$$

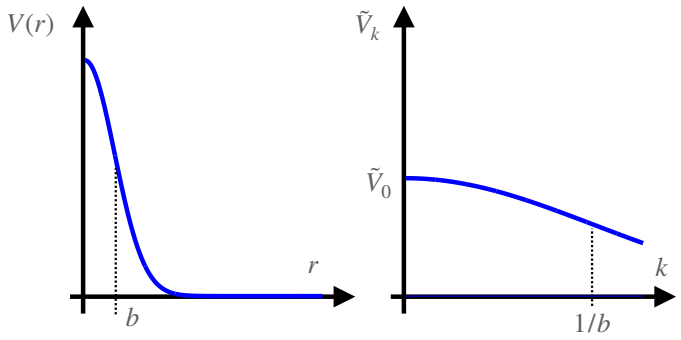

Figure 1. *A potential $V(r)$ of range b and its Fourier transform $\tilde{V}_k$ of range $1/b$.*

appears, with $\epsilon_k = \hbar^2 k^2/2m$; it is then useful to determine which of these two terms is preponderant:

- When $k \to 0$, $\epsilon_k \to 0$, while $\tilde{V}_k$ tends to the non-zero value $\tilde{V}_0$. The dominant term is $n\tilde{V}_k \approx n\tilde{V}_0$.
- When $k \to \infty$, ϵ_k diverges whereas $\tilde{V}_k \to 0$. It is then ϵ_k which dominates.

We must now evaluate the point from which ϵ_k becomes dominant with respect to $n\tilde{V}_k$. To do this, let's start by defining the value k_0 for which ϵ_k is equal to $n\tilde{V}_0$:

$$\frac{\hbar^2 k_0^2}{2m} = n\tilde{V}_0 \quad \Rightarrow \quad k_0 = \frac{\sqrt{2mn\tilde{V}_0}}{\hbar}. \tag{26}$$

The question is to know if $\tilde{V}_k$ is still close to $\tilde{V}_0$ for $k = k_0$, or if it has already strongly decreased. We will be in the first case if $k_0 \ll 1/b$ and in the opposite case if $k_0 \gg 1/b$. These two limiting cases are represented in figure 2.

Using the link (19) between scattering length and $\tilde{V}_0$, the definition of k_0 is

$$k_0 = \sqrt{8\pi n a} \equiv \frac{1}{\xi} \tag{27}$$

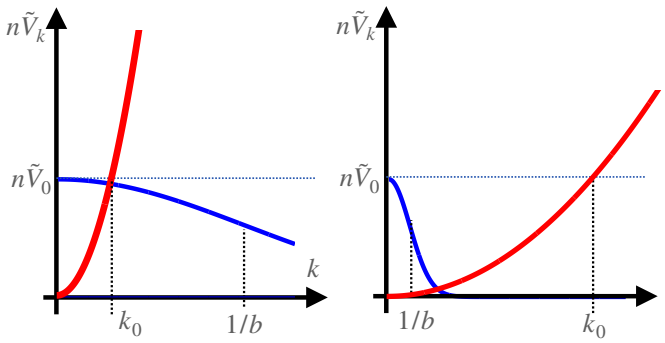

Figure 2. *The two possible situations to reach the equality between the single-particle kinetic energy $\epsilon_k = \hbar^2 k^2/2m$ (in red) and the interaction energy $n\tilde{V}_k$ (in blue).*

where ξ is called *healing length*. The condition $k_0 \ll 1/b$ can then be written:

$$k_0 \ll 1/b \quad \Leftrightarrow \quad 8\pi n a b^2 \ll 1. \tag{28}$$

In all this paragraph, we will assume that the condition (28) is realized and that one is thus in the case of the left diagram of figure 2. This assumption can be seen as a low density condition. More precisely, we can write nab^2 in the form

$$nab^2 = nb^3 \times \frac{a}{b}. \tag{29}$$

We explained in the first chapter that we will consider here dilute gases in the sense of $nb^3 \ll 1$, and the validity of the Born expansion requires moreover that $a/b \ll 1$.

In the regime represented on the left-hand diagram of figure 2, we can identify three distinct domains for k (see figure 3):

- Domain 1, $k \ll k_0 = 1/\xi$: the term $n\tilde{V}_k$ dominates the kinetic energy ϵ_k and we can also take $\tilde{V}_k \approx \tilde{V}_0$.
- Domain 2, $k_0 \ll k \ll 1/b$: the kinetic energy ϵ_k is dominant and $\tilde{V}_k$ remains close to its value at the origin $\tilde{V}_0$.

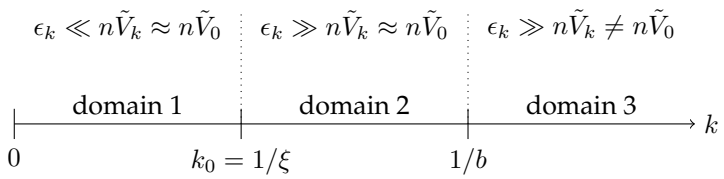

Figure 3. *The three relevant domains for the wavenumber k when the low density condition (28) is met.*

- Domain 3, $1/b \ll k$: the kinetic energy ϵ_k is dominant and $\tilde{V}_k$ tends to 0 when $k \to \infty$ (this domain will be absent for the pseudopotential).

Remark. Even if the quantum gases correspond to the case we have just discussed, it is interesting to consider the opposite case represented on the diagram on the right of figure 2, obtained for a high density situation, $8\pi nab^2 \gg 1$. In order to specify the parameters in this case, it is preferable to choose a specific form of potential, such as the Yukawa potential [see for example Ceperley, Chester, et al. (1978) and Campana, D'Auria, et al. (1979)]

$$\tilde{V}_k = \frac{\tilde{V}_0}{1+k^2b^2}, \qquad V(r) = V_0\,\frac{\mathrm{e}^{-r/b}}{r/b}, \qquad \tilde{V}_0 = 4\pi b^3\,V_0. \tag{30}$$

One might worry about the validity of Bogoliubov's approach in this high density regime, but there is in fact no problem. Indeed, we can show that the quantum depletion is written in this case:

$$\text{High density:} \qquad \frac{n'}{n} \sim \frac{1}{(nab^2)^{1/4}} \times \frac{a}{b}. \tag{31}$$

and it is thus all the smaller that the density is larger ! More precisely, the first term of the product intervening in the right-hand side is less than 1 by definition of the high density situation, and the second term is small in front of 1 because of the validity criterion of the Born approximation. Note that one can take the limit of an infinite range b, i.e. a Coulomb potential. This problem was initially studied by Foldy (1961) and Girardeau (1962). The Bose–Einstein condensed phase is then in competition with the formation of a Wigner crystal, but for the high density limit considered here, it can be shown that the Bose–Einstein condensed phase leads to a lower energy (Ceperley, Chester, et al. 1978; Halinen, Apaja, et al. 2000).

1-3 Illustration: the excitation spectrum

Once the Bogoliubov Hamiltonian is put into the form

$$\hat{H}' = \sum_{\boldsymbol{k}\neq 0} \hbar\omega_k\, b^\dagger_{\boldsymbol{k}} b_{\boldsymbol{k}} \;+\; \text{constante}, \qquad \hbar\omega_k = \left(\epsilon_k^2 + 2n\tilde{V}_k\epsilon_k\right)^{1/2}, \tag{32}$$

the simplest physical quantity to study is its excitation spectrum, i.e. the energy and the momentum that it is necessary to bring to the system to make it pass from its ground state to an excited state.

The elementary excitations of the system are obtained by making one of the operators $b^\dagger_{\boldsymbol{k}}$ act on the ground state of the system. Such an operation gives the fluid the energy $\hbar\omega_k$ and the momentum $\hbar\boldsymbol{k}$, since $b^\dagger_{\boldsymbol{k}}$ is a linear combination of $a^\dagger_{\boldsymbol{k}}$ (which brings $\hbar\boldsymbol{k}$) and $a_{-\boldsymbol{k}}$ (which removes $-\hbar\boldsymbol{k}$). We will now discuss the different possible regimes for this elementary excitation, based on the different domains of k values we have just identified.

- **Domain 1.** In this domain, we have $n\tilde{V}_k \approx n\tilde{V}_0 \gg \epsilon_k$ and we find

  $$\omega_k \approx ck \qquad \text{with} \quad c = \sqrt{n\tilde{V}_0/m}. \tag{33}$$

  We find the well-known phonon spectrum, which also appears in a Bogoliubov theory conducted with classical fields [cf. course 2015-16]. Recall that this linear spectrum is a key element of the superfluidity of the gas; it allows indeed a localized impurity to propagate in the gas without dissipating energy, provided that its velocity is sufficiently low.

- **Domain 2.** In this domain, we have $\epsilon_k \gg n\tilde{V}_k \approx n\tilde{V}_0$ and we find

  $$\hbar\omega_k \approx \epsilon_k + n\tilde{V}_0. \tag{34}$$

This result is simply interpreted from the Hartree and Fock contributions calculated in the previous chapter. It corresponds to the energy that must be provided to make a particle of the condensate pass from the state of zero momentum, with an interaction energy with its neighbors equal to $n\tilde{V}_0$ [only the Hartree term, since the Fock term (exchange) is zero in this case], to an excited state of momentum $\hbar\boldsymbol{k}$ and an interaction energy $2n\tilde{V}_0$ [Hartree+Fock]. This energy to be provided is therefore $\epsilon_k + 2n\tilde{V}_0 - n\tilde{V}_0$, as indicated in (34).

- **Domain 3.** In this domain, we have $\epsilon_k \gg n\tilde{V}_k \neq n\tilde{V}_0$ and we find

$$\hbar\omega_k \approx \epsilon_k + n\tilde{V}_k \tag{35}$$

The result can again be interpreted from the Hartree–Fock contributions. The initial energy of the particle when it is part of the condensate is $n\tilde{V}_0$as above, and the final energy is $\epsilon_k + n(\tilde{V}_0 + \tilde{V}_k)$. The initial and final Hartree terms cancel each other out, leaving only the kinetic energy and the Fock term.

We will see in the rest of this chapter and in the next one that it is possible to add terms that were neglected so far in the Bogoliubov approximation, and to reach in this way a resummation of the Born series describing two-body collisions. This procedure, initially discussed by Beliaev (1958b), amounts to taking into account for example virtual processes like

$$(\boldsymbol{k}) + (0) \;\longleftrightarrow\; (\boldsymbol{k}-\boldsymbol{q}) + (\boldsymbol{q}) \tag{36}$$

which corresponds to the application of the operator $a^\dagger_{\boldsymbol{k}-\boldsymbol{q}} a^\dagger_{\boldsymbol{q}} a_{\boldsymbol{k}} a_0$ and its conjugate. The effect of this resummation is to replace $\tilde{V}_0$ by a term proportional to the low energy scattering amplitude $f(k=0) = -a$, more precisely by the coupling $g = 4\pi\hbar^2 a/m$. The results (33) and (34) become respectively

$$\text{Domain 1:} \qquad \omega_k \approx ck \qquad \text{with} \quad c = \sqrt{ng/m} \tag{37}$$

$$\text{Domain 2:} \qquad \hbar\omega_k \approx \epsilon_k + ng. \tag{38}$$

2 LHY energy and quantum depletion

2-1 The energy of the ground state

In this paragraph, we will evaluate the ground state energy of the approximate Hamiltonian $\hat{H}'$ given in (4). Our goal will be to make the Born expansion (16) appear in the expression of this energy. In particular, we wish to go to order 2 included in V for the dominant term, representing the mean field energy.

The ground state is obtained by placing each mode described by the operators $b^\dagger_{\boldsymbol{k}}, b_{\boldsymbol{k}}$ in its ground state, so that the sought energy is written:

$$E_{\text{grnd}} = \frac{1}{2} nN\tilde{V}_0 \;+\; \frac{1}{2}\sum_{\boldsymbol{k}\neq 0} \hbar\omega_k - \hbar\omega_{0,k}. \tag{39}$$

Using the values (9-10) of ω_k and $\omega_{0,k}$, and replacing the discrete sum by an integral, we obtain:

$$\frac{E_{\text{grnd}}}{L^3} = \frac{1}{2} n^2\tilde{V}_0 \;+\; \frac{1}{2\,(2\pi)^3}\int \left[\left(\epsilon_k^2 + 2n\tilde{V}_k\epsilon_k\right)^{1/2} - \epsilon_k - n\tilde{V}_k\right] \mathrm{d}^3k. \tag{40}$$

It is important to make sure that the integral involved in this expression converges. At large k, as explained in § 1-2, $n\tilde{V}_k$ tends to 0 while ϵ_k grows. We can therefore carry out the expansion:

$$\sqrt{1+x} = 1 + \frac{x}{2} - \frac{x^2}{8} + \frac{x^3}{16} + \mathcal{O}(x^4). \tag{41}$$

of the square root contributing to the integral

$$\begin{aligned}\left(\epsilon_k^2 + 2n\tilde{V}_k\epsilon_k\right)^{1/2} &= \epsilon_k\left(1 + \frac{2n\tilde{V}_k}{\epsilon_k}\right)^{1/2} \\ &\approx \epsilon_k + n\tilde{V}_k - \frac{n^2\tilde{V}_k^2}{2\epsilon_k} + \frac{n^3\tilde{V}_k^3}{2\epsilon_k^2} + \dots\end{aligned} \tag{42}$$

Here, the dominant term of the integrand is

$$-\frac{n^2\tilde{V}_k^2}{2\epsilon_k}, \tag{43}$$

i.e. the same term as the one appearing in $a^{(2)}$, the second order of the Born expansion (24) of the scattering length. The criterion of convergence is therefore always a decay of $|\tilde{V}_k|^2$ faster than $1/k$, which we assume here.

At this point, the dominant term of $E_{\rm grnd}$ given in (40) is the first contribution of the right-hand member, $\frac{1}{2}n^2\tilde{V}_0$, with $\tilde{V}_0 = g^{(1)}$. As announced in the introduction of this paragraph, we wish to express this term as a function of g with a precision better than $g^{(1)}$, and go to order 2 in V. For this purpose, we can rewrite this dominant term in the form:

$$\frac{1}{2}n^2\tilde{V}_0 = \frac{1}{2}n^2\left(g^{(1)} + g^{(2)}\right) - \frac{1}{2}n^2 g^{(2)} \tag{44}$$

and then feed the second term $-\frac{1}{2}n^2 g^{(2)}$ back into the integral over k using the expression (24) of $g^{(2)}$. We then arrive at:

$$E_{\rm grnd} = E_{\rm mean\,field} + E_{\rm LHY} \tag{45}$$

with

$$\frac{E_{\rm mean\,field}}{L^3} = \frac{1}{2}n^2\left(g^{(1)} + g^{(2)}\right) \approx \frac{1}{2}gn^2 \tag{46}$$

and

$$\frac{E_{\rm LHY}}{L^3} = \frac{1}{2\,(2\pi)^3}\int\left[\left(\epsilon_k^2 + 2n\tilde{V}_k\epsilon_k\right)^{1/2} - \epsilon_k - n\tilde{V}_k + \frac{n^2\tilde{V}_k^2}{2\epsilon_k}\right]\,{\rm d}^3k. \tag{47}$$

2-2 Calculation of the energy $E_{\rm LHY}$

An important point regarding the expression (47) of the energy $E_{\rm LHY}$ concerns the behavior at large k of the integrand. While the dominant term of the integrand appearing in (40) involved $\tilde{V}_k^2/\epsilon_k$ [see (43)], this dominant term is exactly offset by the contribution of $g^{(2)}$. The integrand of $E_{\rm LHY}$ now tends to 0 much faster at large k, with the dominant term

$$\text{Dominant term for } \epsilon_k \gg \tilde{V}_k : \qquad \frac{n^3\tilde{V}_k^3}{2\epsilon_k^2}. \tag{48}$$

Even if $\tilde{V}_k$ decreases only very slowly at infinity, the convergence of the integral is now assured by the presence of $\epsilon_k^2 \propto k^4$ in the denominator.

It is therefore interesting to look further into the values of k which contribute significantly to this integral. Let's take again the figure 3 on which we have distinguished three sectors:

- Domain 1 of small k values, where $\epsilon_k \ll n\tilde{V}_k \approx n\tilde{V}_0$.
- Domain 2 of intermediate k values, where $\epsilon_k \gg n\tilde{V}_k \approx n\tilde{V}_0$.
- Domain 3 of large k values, where ϵ_k is dominant and $\tilde{V}_k$ differs significantly from $\tilde{V}_0$.

Given the rapid decay of the integrand involved in $E_{\rm LHY}$ [*cf.* (48)], zone 3 has a negligible contribution. Limiting ourselves to the contribution of zones 1 and 2, we can therefore replace $\tilde{V}_k$ in $\tilde{V}_0$ in the integral:

$$\frac{E_{\rm LHY}}{L^3} = \frac{1}{2\,(2\pi)^3}\int\left[\left(\epsilon_k^2 + 2n\tilde{V}_0\epsilon_k\right)^{1/2} - \epsilon_k - n\tilde{V}_0 + \frac{n^2\tilde{V}_0^2}{2\epsilon_k}\right]\,{\rm d}^3k. \tag{49}$$

To finish the calculation, let us note that the energy $E_{\rm LHY}$ is a small correction to the mean field term. We can systematically replace $a^{(1)}$ by a, or equivalently $g^{(1)} = \tilde{V}_0$ by g. In this way, we obtain an expression as a function of a or g which corresponds to a systematic expansion in powers of V, to order 2 included. Let us insist on the fact that this is only possible thanks to the fast decay of the integrand of (47). This would not have been the case if we had tried to compute explicitly the integral of (40): the full form of the k-dependence of $\tilde{V}_k$ would have contributed. Fortunately, this contribution is reintegrated in the second order term of the Born expansion, $a^{(2)}$.

After the change of variable $x = k(\hbar^2/2mn\tilde{V}_0)^{1/2}$ [or $x = k\xi$ with $\xi = 1/\sqrt{8\pi na}$] in the integral (49), we obtain

$$\frac{E_{\rm LHY}}{L^3} = \frac{\hbar^2}{m}\,(na)^{5/2}\,\mathcal{I} \tag{50}$$

where we have posed

$$\mathcal{I} = 16\sqrt{2\pi}\int_0^{+\infty}\left[x^2 + 1 - \left(x^2+2x\right)^{1/2} - \frac{1}{2x}\right]\,{\rm d}x. \tag{51}$$

After an explicit calculation of this integral, we arrive at:

$$\frac{E_{\rm LHY}}{L^3} = \frac{1}{2}gn^2 \times \frac{128}{15\sqrt{\pi}}\sqrt{na^3}, \tag{52}$$

which is the result announced in (13). As indicated in the introduction, the energy $E_{\rm LHY}$ is small in front of the mean field energy as soon as the "low density" validity condition of the Bogoliubov approach, $\sqrt{na^3} \ll 1$, is satisfied.

We have thus seen how the Born expansion for the scattering length appears. The first and second order contributions must be taken into account for the dominant mean field term, whereas the first order contribution is sufficient for the LHY term. One may seek to go further[2] and include all terms of the Born expansion to express the final result solely in terms of $a = \sum_{j=1}^{\infty} a^{(j)}$. We will not do this resummation here for an arbitrary potential $V(\boldsymbol{r})$ because it is very technical [see for example Beliaev (1958b), Hugenholtz & Pines (1959), Gavoret & Nozieres (1964) and Nozières & Pines (1990)]. Moreover, the convergent character of the series that we sum up is not easy to establish, especially in the presence of bound states in the potential $V(r)$ that we have to ignore to treat only the case of a gas of free atoms. Thus Lieb, Seiringer, et al. (2005) write about these methods[3] : *They all rely on some special assumptions about the ground state that have never been proved, or on the selection of special terms from a perturbation series which likely diverges.*

2-3 Quantum depletion

The last step of our treatment is the validation of the approximation at the basis of the Bogoliubov method. Is it correct to assume that the number of particles N' outside the $\boldsymbol{k} = 0$ state is small in front of the total number N?

To evaluate N', we can directly use the result of the two-mode model developed in the previous chapter. The average number of pairs $\{+\boldsymbol{k}, -\boldsymbol{k}\}$ in the ground state of the system is given by v_k^2, where the coefficient v_k is recalled in (11). Summing up the contribution of all pairs, we thus find the number of atoms N':

$$N' = \sum_{\boldsymbol{k}\neq 0} v_k^2 = \frac{1}{2}\,\frac{L^3}{(2\pi)^3}\int \left[\frac{\epsilon_k + n\tilde{V}_k}{\left(\epsilon_k^2 + 2n\tilde{V}_k\epsilon_k\right)^{1/2}} - 1\right] \mathrm{d}^3k. \qquad (53)$$

As in the calculation of the energy of the ground state, it is important to verify the convergence of this integral:

- In the neighborhood of the origin, thanks to the Jacobian in $\mathrm{d}^3k = 4\pi k^2\,\mathrm{d}k$, there is no divergence problem although the content of the bracket diverges as $1/k$.
- At large values of k, the dominant term of the integrand is [4] :

$$\frac{n_0^2\tilde{V}_k^2}{2\,\epsilon_k^2}. \qquad (54)$$

  This asymptotic behavior is the same as the one found above for the energy $E_{\rm LHY}$ in the framework of the Born expansion [see (48)] and the conclusion is identical: even if $\tilde{V}_k$ decreases only very slowly at infinity, the integral will be convergent thanks to the factor $\epsilon_k^2 \propto k^4$ which appears in the denominator.

The procedure is therefore similar to that used to calculate $E_{\rm LHY}$. Among the three domains of k values identified in figure 3, only domains 1 and 2 contribute significantly to the integral (53). In these domains, we can make the approximation $\tilde{V}_k \approx \tilde{V}_0 \approx g$ and arrive at the expression for the uncondensed density $n' = N/L^3$:

$$n' = (na)^{3/2}\,\frac{4\sqrt{2}}{\sqrt{\pi}}\int_0^{+\infty}\left(\frac{x^2+1}{\sqrt{x^2+2}} - x\right) x\,\mathrm{d}x, \qquad (55)$$

where we set $x = k\xi$. The integral in this expression can be calculated analytically and the result is

$$\frac{n'}{n} = \frac{8}{3\sqrt{\pi}}\sqrt{na^3}. \qquad (56)$$

[2] This possibility was mentioned by Bogoliubov in his original paper (Bogoliubov 1947), and he thanked Landau for this "important remark".

[3] One can also consult the discussion on pages 463-464 of Gavoret (1963).

[4] We use the expansion $(1+2u)^{-1/2} = 1 - u + \frac{3}{2}u^2 + \ldots$ and $(1+u)(1+2u)^{-1/2} = 1 + \frac{1}{2}u^2 + \ldots$ with $u = n\tilde{V}_k/\epsilon_k$.

We see appearing here the small parameter $\sqrt{na^3}$ announced in introduction. The result (56) involves only the scattering length and its scope goes beyond the case of a regular potential described by the Born approximation; it extends to the case of any potential, in particular the pseudo-potential, as we shall verify in the next paragraph.

To make the connection with the low density condition established in § 1-2 [*cf.* (28)], it is interesting to rewrite this result as :

$$\frac{n'}{n} \sim \sqrt{nab^2}\ \frac{a}{b} \tag{57}$$

which is the product of two terms, each small compared to 1: the smallness of the first term $\sqrt{nab^2}$ comes from the condition (28), and that of the second term a/b comes from the validity criterion of the Born approximation.

3 Bogoliubov Hamiltonian for $\hat{V}_{\rm pp}$

After studying in detail the effect of the coupling created by a regular potential $V(r)$, in the limit $|a| \ll b$ allowing to use the Born expansion, we move to the case of the pseudo-potential, of range $b = 0$, but of arbitrary scattering length a. The results (12) and (13) for quantum depletion and ground state energy will be unchanged, but the approach to be followed has some specific subtleties that we will discuss.

3-1 Contact potential and pseudo-potential $\hat{V}_{\rm pp}$

We studied in detail in last year's course how to obtain such a zero range potential in three dimensions in quantum physics. The simplest choice seems to be the contact potential

$$V(\boldsymbol{r}) = g\,\delta(\boldsymbol{r}) \qquad \Leftrightarrow \qquad \forall k: \quad \tilde{V}_k = g. \tag{58}$$

But this potential leads to a divergence of the scattering amplitude and is therefore not usable as is. This singular behavior can be observed for example on the Born expansion: the first order is regular and gives

$$a_1 = \frac{mg}{4\pi\hbar^2}, \tag{59}$$

but the second order a_2 given in (24) is proportional to the integral $\int (1/k^2)\ \mathrm{d}^3k$, which is divergent.

The pseudo-potential $\hat{V}_{\rm pp}$ allows to cure this divergence while keeping a zero range. We define its action[5] on a wave function $\psi(\boldsymbol{r})$ by:

$$\boxed{\hat{V}_{\rm pp}\left[\psi(\boldsymbol{r})\right] = g\,\delta(\boldsymbol{r})\ \frac{\partial}{\partial r}\left[r\,\psi(\boldsymbol{r})\right]\Big|_{\boldsymbol{r}=0}} \tag{60}$$

This expression allows us to give a meaning to the potential when it acts on regular functions in $\boldsymbol{r} = 0$ and also on functions diverging like $1/r$. More precisely, we find that $\hat{V}_{\rm pp}$ "erases" any term diverging like $1/r$:

$$\boxed{\psi(\boldsymbol{r}) = \frac{\alpha}{r} + \psi_{\rm reg}(\boldsymbol{r}) \quad \Rightarrow \quad \hat{V}_{\rm pp}\left[\psi(\boldsymbol{r})\right] = g\,\psi_{\rm reg}(0)\,\delta(\boldsymbol{r})} \tag{61}$$

where $\psi_{\rm reg}(\boldsymbol{r})$ is regular in $\boldsymbol{r} = 0$. The action of $\hat{V}_{\rm pp}$ on regular functions (such as plane waves $\mathrm{e}^{\mathrm{i}\boldsymbol{k}\cdot\boldsymbol{r}}$) is thus identical to that of the contact potential (58), but $\hat{V}_{\rm pp}$ also has a well-defined action on spherical waves that play an essential role in scattering theory:

$$\hat{V}_{\rm pp}\left[\frac{\mathrm{e}^{\mathrm{i}kr}}{r}\right] = \hat{V}_{\rm pp}\left[\frac{1}{r} + \frac{\mathrm{e}^{\mathrm{i}kr}-1}{r}\right] = \mathrm{i}kg\,\delta(\boldsymbol{r}). \tag{62}$$

We can thus completely solve the problem of a two-body collision interacting via this pseudo-potential and we find in particular that the scattering length a is always related to the coupling constant g by the relation $g = 4\pi\hbar^2 a/m$.

3-2 The subtleties of the pseudopotential

When manipulating the pseudo-potential, it is important to keep in mind several subtleties in its action. An example is provided by the action of $\hat{V}_{\rm pp}$ on an infinite sum of terms. Consider the identity:

$$\frac{1}{r} = \frac{1}{2\pi^2}\int \frac{\mathrm{e}^{\mathrm{i}\boldsymbol{k}\cdot\boldsymbol{r}}}{k^2}\ \mathrm{d}^3k \tag{63}$$

and apply $\hat{V}_{\rm pp}$ on both members:

[5] See Olshanii & Pricoupenko (2001) for a generalization of this definition.

- On the left member, the action of $\hat{V}_{\rm pp}$ is by definition:

$$\hat{V}_{\rm pp}\left[\frac{1}{r}\right] = 0. \tag{64}$$

- On the right hand side, if we allow ourselves to swap the action of $\hat{V}_{\rm pp}$ and the integral on $\boldsymbol{k}$ (which is in fact incorrect), we find

$$\begin{aligned}\hat{V}_{\rm pp}\left[\frac{1}{2\pi^2}\int \frac{\mathrm{e}^{\mathrm{i}\boldsymbol{k}\cdot\boldsymbol{r}}}{k^2}\,\mathrm{d}^3k\right] &\stackrel{?}{=} \frac{1}{2\pi^2}\int \frac{\hat{V}_{\rm pp}\left[\mathrm{e}^{\mathrm{i}\boldsymbol{k}\cdot\boldsymbol{r}}\right]}{k^2}\,\mathrm{d}^3k \\ &= \frac{g\,\delta(\boldsymbol{r})}{2\pi^2}\int \frac{1}{k^2}\,\mathrm{d}^3k = \frac{g\,\delta(\boldsymbol{r})}{2\pi^2}\int 4\pi\,\mathrm{d}k\end{aligned} \tag{65}$$

  which is a divergent integral in $k = +\infty$!

It is therefore necessary to be careful as soon as we want to calculate the action of $\hat{V}_{\rm pp}$ on a function that we express in terms of its Fourier transform, as in (63). This point appears when we consider the action of $\hat{V}_{\rm pp}$ in second quantization

$$\hat{\mathcal{V}} = \frac{1}{2}\int \hat{\Psi}^\dagger(\boldsymbol{r}')\,\hat{\Psi}^\dagger(\boldsymbol{r})\,\hat{V}_{\rm pp}\left[\hat{\Psi}(\boldsymbol{r})\,\hat{\Psi}(\boldsymbol{r}')\right]\,\mathrm{d}^3r\,\mathrm{d}^3r' \tag{66}$$

where $\hat{\Psi}(\boldsymbol{r})$ is the field operator which destroys a particle at point $\boldsymbol{r}$. The expression of this operator on the plane wave basis is written:

$$\hat{\psi}(\boldsymbol{r}) = \frac{1}{L^{3/2}}\sum_{\boldsymbol{k}} \mathrm{e}^{\mathrm{i}\boldsymbol{k}\cdot\boldsymbol{r}}\,a_{\boldsymbol{k}} \tag{67}$$

If we insert this expression in (66) and permute the action of $\hat{V}_{\rm pp}$ and the summation on $\boldsymbol{k}$, we get

$$\hat{\mathcal{V}} = \frac{g}{2L^3}\sum_{\boldsymbol{k},\boldsymbol{k}',\boldsymbol{q}} a^\dagger_{\boldsymbol{k}+\boldsymbol{q}}a^\dagger_{\boldsymbol{k}'-\boldsymbol{q}}a_{\boldsymbol{k}'}a_{\boldsymbol{k}}. \tag{68}$$

This is exactly the form that we would have deduced from the general expression

$$\frac{1}{2L^3}\sum_{\boldsymbol{k},\boldsymbol{k}',\boldsymbol{q}} \tilde{V}_q\,a^\dagger_{\boldsymbol{k}+\boldsymbol{q}}\,a^\dagger_{\boldsymbol{k}'-\boldsymbol{q}}\,a_{\boldsymbol{k}'}\,a_{\boldsymbol{k}}. \tag{69}$$

by taking $\tilde{V}_q = g$ for any moment $\boldsymbol{q}$, which in fact corresponds to the naive contact potential $g\,\delta(\boldsymbol{r})$ given in (58). By passing from (66) to (68), one has omitted the subtle difference between $\hat{V}_{\rm pp}$ and a pure contact potential, which opens the way to divergences.

To eliminate these discrepancies, two strategies are possible. One can forbid oneself from interchanging the action of $\hat{V}_{\rm pp}$ with any infinite sum on $\boldsymbol{k}$, and to work only with operators of the type (66) (Lee, Huang, et al. 1957). The other approach, which is validated by a treatment using the renormalization group (Braaten, Kusunoki, et al. 2008), consists in carrying out the calculations with the "plane wave" expression of $\hat{V}_{\rm pp}$ [i.e. the expression (68)] while watching for the appearance of divergent terms of the form

$$\frac{g}{L^3}\sum_{\boldsymbol{k}\neq 0}\frac{1}{k^2} = \frac{g}{(2\pi)^3}\int 4\pi\,\mathrm{d}k. \tag{70}$$

These terms will "sign" the result of applying $\hat{V}_{\rm pp}$ to a function proportional to $1/r$, which in fact gives a zero result, and so they should simply be subtracted from the final result:

$$\boxed{\frac{g}{L^3}\sum_{\boldsymbol{k}\neq 0}\frac{1}{k^2}\;\longrightarrow\;0} \tag{71}$$

More generally, let us recall that the pseudo-potential changes the domain of acceptable functions: for the two-body problem with a regular interaction potential, the space of wave functions $\psi(\boldsymbol{r}_1,\boldsymbol{r}_2)$ is composed of the continuous functions of the two variables $\boldsymbol{r}_1,\boldsymbol{r}_2$. When we use the pseudopotential to describe the interaction, the domain of the Hamiltonian is modified. It is now the set of functions satisfying *the Bethe–Peierls* boundary condition, i.e. behaving as

$$r\to 0: \qquad \Psi(\boldsymbol{r}_1,\boldsymbol{r}_2) \approx \left(\frac{1}{r}-\frac{1}{a}\right)\Phi(\boldsymbol{R}) \tag{72}$$

with

$$\boldsymbol{R} = (\boldsymbol{r}_1+\boldsymbol{r}_2)/2, \qquad \boldsymbol{r} = \boldsymbol{r}_1-\boldsymbol{r}_2. \tag{73}$$

This Bethe–Peierls boundary condition plays an important role in the choice of test functions if one wishes to approach the problem by the variational method.

3-3 Bogoliubov method for the pseudo-potential

Once the expression of the $\hat{\mathcal{V}}$ operator describing the interaction between particles is established, the Bogoliubov approach proceeds in the same way as for a regular $V(\boldsymbol{r})$ potential. We assume that the majority of the particles occupy the condensed state $\boldsymbol{k} = 0$ and we treat the operators a_0 and $a_0^\dagger$ as classical numbers, neglecting their commutator. We then arrive at the approximate Hamiltonian:

$$\boxed{\hat{H}' = \frac{1}{2} gnN + \hat{H}''} \tag{74}$$

and

$$\boxed{\hat{H}'' = \sum_{\substack{\text{pairs} \\ \{\boldsymbol{k},-\boldsymbol{k}\}}} [\epsilon_k + gn] \left(a_{\boldsymbol{k}}^\dagger a_{\boldsymbol{k}} + a_{-\boldsymbol{k}}^\dagger a_{-\boldsymbol{k}} \right) + gn \left(a_{\boldsymbol{k}}^\dagger a_{-\boldsymbol{k}}^\dagger + a_{\boldsymbol{k}} a_{-\boldsymbol{k}} \right)} \tag{75}$$

The dominant term of $\hat{H}$ is the constant energy $\frac{1}{2}gnN$: it is the mean field energy calculated by assuming that all particles occupy the state $\boldsymbol{k} = 0$.

The diagonalization of $\hat{H}''$ is done with the same canonical transformation as before, $b_{\boldsymbol{k}} = u_k a_{\boldsymbol{k}} + v_k a_{-\boldsymbol{k}}^\dagger$ with the coefficients (u_k, v_k) given by

$$u_k = \cosh \lambda_k \qquad v_k = \sinh \lambda_k, \tag{76}$$

the auxiliary variable λ_k being defined by

$$\sinh(2\lambda_k) = \frac{gn}{\hbar\omega_k} \qquad \cosh(2\lambda_k) = \frac{\epsilon_k + gn}{\hbar\omega_k} \tag{77}$$

i.e.

$$\boxed{\tanh(2\lambda_k) = \frac{gn}{gn + \epsilon_k} = \frac{1}{1 + k^2\xi^2}} \tag{78}$$

where the healing length ξ is given by

$$\xi = \frac{1}{\sqrt{8\pi a n}} = \frac{\hbar}{\sqrt{2mgn}}. \tag{79}$$

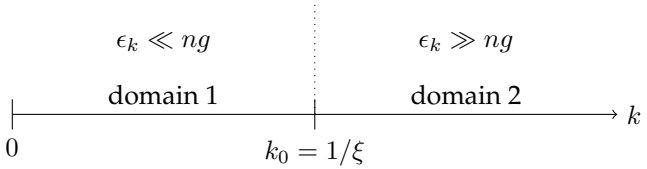

Figure 4. *The two domains of k values for the pseudo-potential.*

The Hamiltonian $\hat{H}$ is written as a function of $b_{\boldsymbol{k}}, b_{\boldsymbol{k}}^\dagger$:

$$\boxed{\hat{H} = \sum_{\boldsymbol{k}\neq 0} \hbar\omega_k \, b_{\boldsymbol{k}}^\dagger b_{\boldsymbol{k}} + E_0 \qquad \text{with} \quad \hbar\omega_k = \sqrt{\epsilon_k^2 + 2gn\epsilon_k}} \tag{80}$$

The frequency ω_k and the energy gn can also be put in the form:

$$\hbar\omega_k = \epsilon_k \, \mathrm{e}^{2\lambda_k} \qquad gn = \frac{1}{2}\epsilon_k \left(\mathrm{e}^{4\lambda_k} - 1 \right). \tag{81}$$

In principle, the energy of the ground state can be deduced from the previous general result:

$$\Delta E = \sum_{\boldsymbol{k}\neq 0} \left(\frac{1}{2}\hbar\omega_k - \frac{1}{2}\hbar\omega_{0,k} \right) \tag{82}$$

which leads to:

$$E_{\rm grnd} \stackrel{?}{=} \frac{1}{2} gnN + \frac{1}{2} \sum_{\boldsymbol{k}\neq 0} \left(\hbar\omega_k - \epsilon_k - gn \right). \tag{83}$$

We put a question mark on this last result, because we will see that it presents in fact a divergence of the type (71), which we will have to erase before giving the correct result to this order of the calculation.

Because of the zero range of this potential, there are only two domains to consider for k instead of three (*cf.* figure 4) :

- The small k domain, for which $\epsilon_k \ll gn$ that is $k\xi \ll 1$. It corresponds to the phononic regime

$$\boxed{\omega_k \approx ck \qquad \text{with} \quad c = \frac{1}{\sqrt{2}} \frac{\hbar}{m\xi}, \qquad u_k \approx v_k \approx \frac{1}{2^{3/4}\sqrt{k\xi}}} \tag{84}$$

- The domain of almost free particles, $\epsilon_k \gg gn$, that is $k\xi \gg 1$, for which

$$\boxed{\hbar\omega_k \approx \epsilon_k + gn \qquad u_k \approx 1 + \frac{1}{8k^4\xi^4}, \qquad v_k \approx \frac{1}{2k^2\xi^2}} \tag{85}$$

The calculation of the quantum depletion is unchanged from that of the previous chapter. Indeed, the k states contributing to the depletion are essentially such that $k \lesssim 1/\xi$ and their contribution is not affected by the $\tilde{V}_k \to \tilde{V}_0$ substitution. Thus we find:

$$\boxed{\frac{n'}{n} = \frac{1}{N}\sum_{\boldsymbol{k}\neq 0} v_k^2 = \frac{8}{3\sqrt{\pi}}\sqrt{na^3}} \tag{86}$$

Note that the condition of validity of Bogoliubov's approach, $\sqrt{na^3} \ll 1$, ensures the hierarchy of length scales in the problem:

$$a \;\ll\; d \equiv n^{-1/3} \;\ll\; \xi. \tag{87}$$

The average distance between particles d must be large compared to the scattering length a, but small compared to the healing length ξ since

$$\frac{d}{\xi} = n^{-1/3}\sqrt{8\pi a n} = \sqrt{8\pi}(na^3)^{1/6} \ll 1. \tag{88}$$

3-4 The energy of the ground state

Let us now return to the expression (83) of the energy of the ground state which is put in the form

$$E_{\rm grnd} \stackrel{?}{=} \frac{1}{2}gnN + \frac{1}{2}\sum_{\boldsymbol{k}\neq 0}\left[\left(\epsilon_k^2 + 2gn\epsilon_k\right)^{1/2} - \epsilon_k - gn\right]. \tag{89}$$

At large values of k, the dominant terms in the argument of the sum are:

$$-\frac{g^2n^2}{2\epsilon_k} + \frac{g^3n^3}{2\epsilon_k^2} \tag{90}$$

The first term $\propto \sum_{\boldsymbol{k}\neq 0} 1/k^2$ leads to the characteristic divergence we reported in § 3-2 and related to the fact that by switching to the plane wave basis, we identified $\hat{V}_{\rm pp}$ to a pure contact potential [*cf.* 68]. Recall that this term results from an abusive inversion of the action of $\hat{V}_{\rm pp}$ and the Fourier series expansion of a function proportional to $1/r$. As explained before, this kind of term must simply be removed from the final result since $\hat{V}_{\rm pp}(1/r)$ is in fact zero:

$$g\sum_{\boldsymbol{k}\neq 0}\frac{1}{k^2} \longrightarrow 0. \tag{91}$$

Once this subtraction is done, we find the expression for the energy shift of the ground state under the effect of the pseudopotential:

$$E_{\rm grnd} = \frac{1}{2}gnN + \frac{1}{2}\sum_{\boldsymbol{k}\neq 0}\left[\left(\epsilon_k^2 + 2gn\epsilon_k\right)^{1/2} - \epsilon_k - gn + \frac{g^2n^2}{2\epsilon_k}\right]. \tag{92}$$

At large values of k, the dominant term in the argument of this sum is now

$$\frac{g^3n^3}{2\epsilon_k^2} \;\propto\; \frac{1}{k^4} \tag{93}$$

which leads to a convergent three-dimensional integral on $\boldsymbol{k}$.

In fact, the second member of the expression (92) is identical to the term (49) obtained for a regular potential and the result of the calculation $E_{\rm LHY}$, given in (52), is unchanged. Once the first term $\frac{1}{2}gnN$ of (92) is added, we arrive again at the result (13) announced in the introduction of this chapter.

The similarity between the results of the calculations carried out with a regular potential or with the pseudo-potential should not, however, hide an important subtlety of $\hat{V}_{\rm pp}$:

- Calculation for $V(r)$ regular: The energy E'' written in (40) is always negative. To bring out the Born expansion of g, we added to the dominant term $\frac{1}{2}nN\tilde{V}_0 = \frac{1}{2}nNg^{(1)}$ the order 2 correction $\frac{1}{2}nNg^{(2)}$, a contribution which we simultaneously subtracted from E''. This led to a positive value for $E_{\rm LHY}$ (recall that the correction $g^{(2)}$ is always negative):

$$\begin{aligned}\frac{1}{2}nN\tilde{V}_0 \;&\to\; \frac{1}{2}nN\tilde{V}_0 + \underbrace{E''}_{<0}\\ &=\; \underbrace{\frac{1}{2}nN\tilde{V}_0 + \frac{1}{2}nNg^{(2)}}_{\frac{1}{2}gnN} + \underbrace{E'' - \frac{1}{2}nNg^{(2)}}_{E_{\rm LHY}>0}\end{aligned} \tag{94}$$

- Calculation for $\hat{V}_{\rm pp}$: Starting from $\hat{H}' = \frac{1}{2}gnN + \hat{H}''$, we arrived at the energy:

$$\frac{1}{2}gnN \to \frac{1}{2}gnN + \underbrace{E_{\rm LHY}}_{>0}. \tag{95}$$

  Taking into account $\hat{H}''$ for the pseudo-potential thus increases the energy of the ground state instead of decreasing it, which seems to constitute a violation of the variational theorem. The explanation of this paradox lies in the change of the domain of the Hamiltonian when passing from $\frac{1}{2}gnN$ to $\frac{1}{2}gnN + \hat{H}''$. Since we are no longer working in the same Hilbert space, the theorem in question no longer applies and this increase in energy can occur. We refer the reader to the course 2020-21 (chapter 3), where this point is discussed in more detail with the corresponding bibliographic references.

4 Measures of quantum depletion

In the previous sections, we have presented the Bogoliubov method, both for a regular potential for which the Born expansion converges, and for the pseudopotential. In the low density limit $na^3 \ll 1$, the quantum depletion n'/n and the LHY energy take in both cases the same values, given in (12) and in (13). In this section, we will discuss some measurements of quantum depletion as well as related experiments, such as the observation of correlated pairs of excitations. We will describe the measurements of $E_{\rm LHY}$ in the next chapter.

4-1 The case of liquid helium

Measurements of quantum depletion, i.e. the fraction of atoms outside the zero momentum component, have been conducted with remarkable accuracy on liquid helium. The most robust protocol uses inelastic neutron scattering; it gives access to the dynamical structure factor $S(\boldsymbol{k}, \omega)$, where $\hbar\boldsymbol{k}$ and $\hbar\omega$ are the momentum and energy deposited by a neutron in the fluid [see figure 5, taken from the original proposal by Hohenberg & Platzman (1966)].

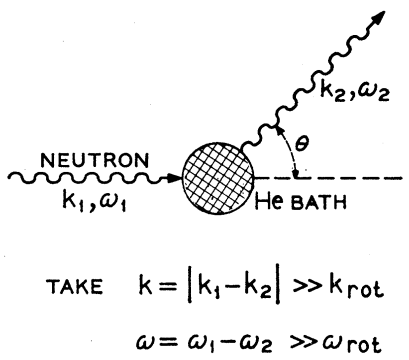

Figure 5. *Inelastic scattering of neutrons by liquid helium. The analysis of the distribution of scattered neutrons gives access to the momentum $\hbar\boldsymbol{k}$ and the energy $\hbar\omega$ transferred to the liquid. Figure extracted from Hohenberg & Platzman (1966).*

To access the quantum depletion, the neutrons must be fast enough that the wave number k is larger than $1/d$, where d is the average distance between atoms in the fluid. In this way, one does not probe the collective properties of the fluid, but the properties of individual atoms, in particular their momentum distribution $n(p)$.

More precisely, we place ourselves in the regime of the *impulse approximation*, where the duration of the neutron-atom scattering is sufficiently short that we can, in a first approximation, neglect the interaction of the atom with its neighbors during this time. We then have simply

$$\boldsymbol{p}_{\rm at}^{\rm fin} \;=\; \boldsymbol{p}_{\rm at}^{\rm ini} \;+\; \hbar\boldsymbol{k}, \qquad \frac{(\boldsymbol{p}_{\rm at}^{\rm fin})^2}{2m_{\rm at}} \;=\; \frac{(\boldsymbol{p}_{\rm at}^{\rm ini})^2}{2m_{\rm at}} \;+\; \hbar\omega, \tag{96}$$

from which we deduce

$$\hbar\omega = \frac{\hbar^2 k^2}{2m_{\rm at}} + \frac{\boldsymbol{p}_{\rm at}^{\rm ini}\cdot\boldsymbol{k}}{m_{\rm at}}, \tag{97}$$

i.e. the sum of the recoil energy $\hbar\omega_{\rm rec} \equiv \hbar^2k^2/2m_{\rm at}$ and a term describing the Doppler effect related to the initial motion of the atom. The signal obtained by measuring the momentum and energy of the scattered neutrons

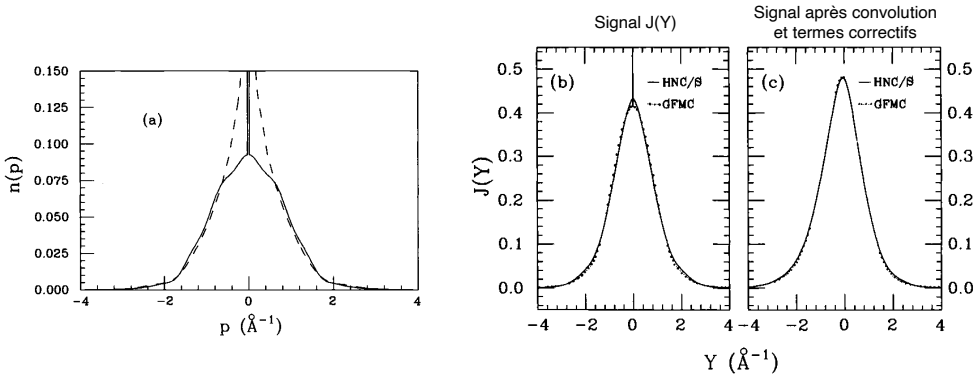

Figure 6. *Expected signal (right) for two very different $n(p)$ distributions (left). See text for more details. Figure taken from Sokol (1995).*

is written as

$$I(\boldsymbol{k},\omega) \;\propto\; \int \mathrm{d}^3p\, n(p)\, \delta\left[\hbar(\omega-\omega_{\mathrm{rec}}) - \frac{\boldsymbol{p}\cdot\boldsymbol{k}}{m_{\mathrm{at}}}\right] \tag{98}$$

where we noted $\boldsymbol{p} = \boldsymbol{p}_{\mathrm{at}}^{\mathrm{ini}}$.

After passing in spherical coordinates and angular integration, we arrive at

$$I(\boldsymbol{k},\omega) \propto \; J\,(Y) \;\propto\; \int_{|Y|}^{+\infty} p\, n(p)\, \mathrm{d}p \tag{99}$$

where the variable Y is defined by

$$Y = \frac{\omega-\omega_{\mathrm{rec}}}{k}. \tag{100}$$

A serious experimental difficulty comes from the fact that the signal $J(Y)$ obtained after integration on $p\,n(p)$ masks to a large extent the desired effect, namely the presence of a very narrow peak at $p = 0$. We have plotted on figure 6 an example from Sokol (1995) which shows on the left two very different theoretical predictions for the same system, superfluid helium at low temperature. One of the curves, obtained with a quantum Monte Carlo approach, shows the narrow peak at $p = 0$ corresponding to a condensate; the other curve, which results from a variational approach, is regular at

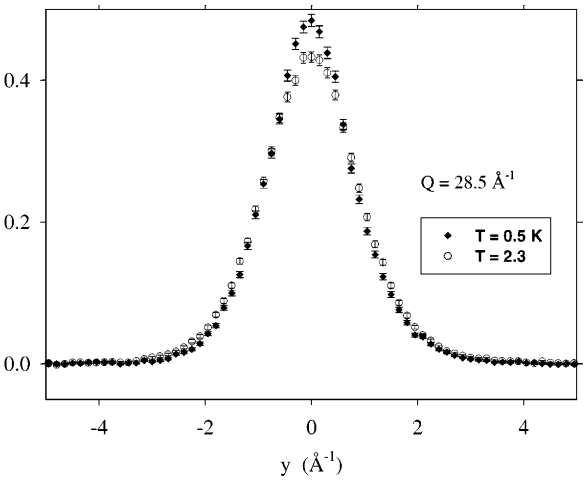

Figure 7. *$J(Y)$ distributions measured in the superfluid case ($T = 0.5\,K$) and in the normal case ($T = 2.3\,K$). The difference in the center is explained by the presence of a condensed fraction in the superfluid case. Figure extracted from Glyde, Azuah, et al. (2000).*

$p = 0$. The function $J(Y)$ given in (99), shown on the middle panel still allows to differentiate the two predictions. On the other hand, after convolution by the experimental resolution and corrections taking into account the interaction of the scattering atom with its neighbors, the predictions for the two $n(p)$ distributions become almost indistinguishable (right panel of figure 6).

Nevertheless, one can finely analyze the experimentally measured $J(Y)$ curves to deduce the condensed fraction. The recent results of Glyde, Azuah, et al. (2000) and Glyde, Diallo, et al. (2011) (see figure 7) lead in the limit $T \to 0$ to a condensed fraction $n_0/n = 7.25\,(0.75)\%$ at the saturating vapor pressure. We are thus very far from the limit of applicability of the Bogoliubov method, which requires a condensed fraction n_0/n close to 100%.

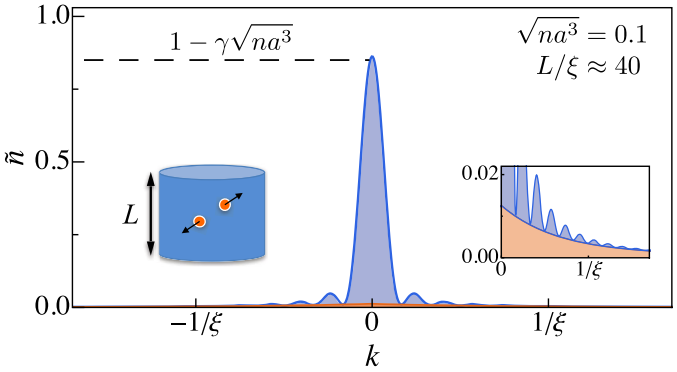

Figure 8. *Momentum distribution for the ground state of a Bose gas confined in a box of length $L = 50\,\mu$m and diameter $60\,\mu$m. For a gas without interaction, we expect an ideal condensate with a distribution limited simply by the Heisenberg relation (blue colored area). For an interacting gas, additional wings on both sides of the $k = 0$ momentum appear due to the quantum depletion (in orange). Figure extracted from Lopes, Eigen, et al. (2017b).*

4-2 Measurement on an atomic gas

Quantitative measurement of quantum depletion with cold atoms "suffers" from an inverse problem of liquid helium. The atomic densities there are low, less than 10^{15} atoms/cm^3. With a typical scattering length a of the order of a few nanometers, one arrives at na^3 of the order of 10^{-5}: the non-condensed fraction is then less than 1%. To increase it and to be able to measure it with a good precision, it is necessary to use either a local increase of the density induced for example by an optical lattice (Xu, Liu, et al. 2006), or to increase a thanks to a scattering resonance. We will describe here this second strategy.

We are interested in the measurement made by the Cambridge group (Lopes, Eigen, et al. 2017b) on a gas of potassium atoms (isotope ^{39}K) for which a Fano-Feshbach resonance (magnetic field $\sim 400\,$G) allows to increase the scattering length a up to about a hundred nanometers without the atomic losses by inelastic collisions becoming troublesome. The gas is confined in a cylindrical box potential (see figure 8). The gas is probed by Bragg spectroscopy by illuminating it with two light beams of frequencies and wave vectors $\omega_1, \boldsymbol{k}_1$ and $\omega_2, \boldsymbol{k}_2$. By an absorption – stimulated emission process, one transfers the momentum $\hbar q = \hbar(\boldsymbol{k}_2 - \boldsymbol{k}_1)$ and the energy $\hbar\omega = \hbar(\omega_2 - \omega_1)$ to the gas.

The gas is prepared in the equilibrium state corresponding to an interaction between atoms characterized by the scattering length a. Just before the Bragg spectroscopy measurement, the scattering length is suddenly brought to 0, so that one obtains a gas without interaction, but with the momentum distribution corresponding to a. As in the case of neutron scattering by liquid helium, the atoms that are affected by Bragg spectroscopy are those for which momentum and energy conservation are possible, i.e. those of initial momentum $\boldsymbol{p}_i$ and final momentum $\boldsymbol{p}_f$ such that

$$\boldsymbol{p}_f = \boldsymbol{p}_i + \hbar\boldsymbol{q} \qquad \frac{p_f^2}{2m} = \frac{p_i^2}{2m} + \hbar\omega, \tag{101}$$

or by eliminating $\boldsymbol{p}_f$:

$$\frac{\boldsymbol{p}_i \cdot \boldsymbol{q}}{m} + \frac{\hbar q^2}{2m} = \hbar\omega. \tag{102}$$

In practice, the transferred momentum $\hbar q$ is aligned with the axis of the cylinder and we choose $\omega = \hbar q^2/2m$, so that the transfer will be done for atoms of zero initial velocity along this axis. The non-transferred atoms can have three origins:

- These are the atoms corresponding to the desired quantum depletion.
- These are atoms whose non-zero momentum comes from the finite size of the box along the z direction: the Heisenberg inequality imposes indeed that the momentum distribution of the single particle ground state along z is not a $\delta(z)$, but rather a power function of a cardinal sine.
- These are atoms corresponding to a thermal excitation. They play a weak role, taking into account the extremely low temperature of the gas (see the inset of figure 9).

After deconvolution of the different effects, Lopes, Eigen, et al. (2017b) arrived at the result shown in Figure 9, giving the diffracted fraction η as a

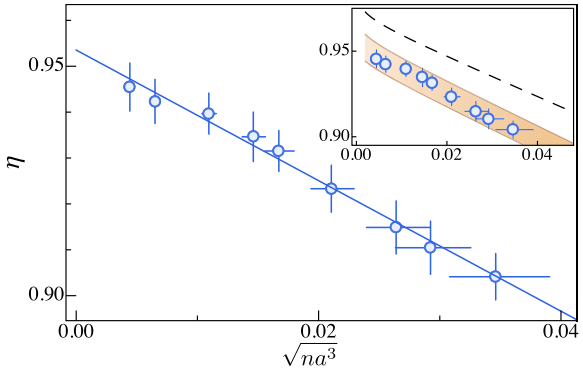

Figure 9. *Maximum diffracted fraction by a Bragg pulse of frequency $\omega = \hbar q^2/2m$. The linear fit corresponds to $\eta_0 = 0.954\,(5)$ and $\gamma = 1.5\,(2)$. The inset shows the result of numerical simulations, done at $T = 0$ (dashed line) and for T between 3.5 and 5 nK, area colored in orange. Figure extracted from Lopes, Eigen, et al. (2017b).*

function of the scattering length. These data are well fitted by the function

$$\eta = \eta_0 \left(1 - \gamma\sqrt{na^3}\right) \tag{103}$$

with $\gamma = 1.5\,(2)$ in agreement with the prediction $8/(3\sqrt{\pi}) = 1.505$. Further analysis of the systematic effects in this experiment leads to a quantitative confirmation of the prediction (56), with a statistical error of 15 % and a systematic error of 20 %.

4-3 Pairs of atoms in the Bogoliubov vacuum

An important prediction of the Bogoliubov approach is the correlation between particles of opposite momenta. This correlation originates in the very form of the coupling involved in $\hat{H}'$, in $a^\dagger_{\boldsymbol{k}} a^\dagger_{-\boldsymbol{k}}$. As we pointed out in our analysis of the two-mode system, these correlations appear in a simultaneous measurement of the occupation numbers n_1 and n_2 of the two modes in question: these two numbers are in principle always equal, $n_1 - n_2 = 0$, even if the sum $n_1 + n_2$ can have a wide distribution.

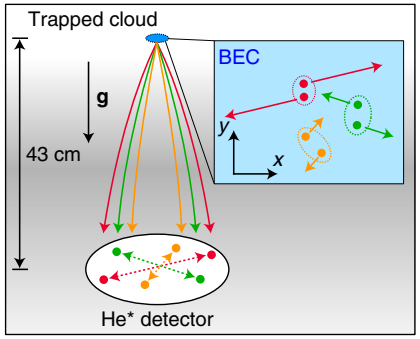

Figure 10. *Left: time-of-flight experiment conducted on a Bose–Einstein condensate of metastable helium atoms. For each realization of the experiment, we deduce the $\boldsymbol{v}_j$ velocities of the atoms. Right: Ω area (colored in green) selected for data analysis. Figure extracted from Tenart, Hercé, et al. (2021).*

Recently, Tenart, Hercé, et al. (2021) have succeeded in directly measuring the correlation between these $(\boldsymbol{k}, -\boldsymbol{k})$ pairs [see also Cayla, Butera, et al. (2020)]. The experiment is performed with helium atoms placed in a metastable electronic state. The atoms are detected after time of flight thanks to a microchannel plate with an efficiency of 53 %. This plate is placed in the vacuum chamber, 45 cm under the condensate (time of flight of 300 ms). The impact of a metastable atom generates an electron pulse that propagates on the surface of the plate; the very precise measurement of the arrival times of this pulse on the plate periphery gives access to the x, y coordinates and the t time of the atom's impact, which then allows to trace the three components of the atom's initial velocity.

For each realization of the experiment, one selects the detections outside the peak corresponding to the condensate itself (green zone Ω of the figure 10, right). There are about 100 atoms and 0.5 correlated pairs in this area. The experiment is reproduced 2000 times to obtain a significant average for the correlation function

$$g^{(2)}(\delta\boldsymbol{k}) = \frac{\int_\Omega \langle n(\boldsymbol{k}) n(\delta\boldsymbol{k} - \boldsymbol{k})\rangle \, \mathrm{d}^3k}{\int_\Omega \langle n(\boldsymbol{k})\rangle \, \langle n(\delta\boldsymbol{k} - \boldsymbol{k})\rangle \, \mathrm{d}^3k}, \tag{104}$$

where $\langle \ldots \rangle$ means an average over the different realizations of the experiment. With this definition, the pairs $(\boldsymbol{k}, -\boldsymbol{k})$ should appear as a peak in

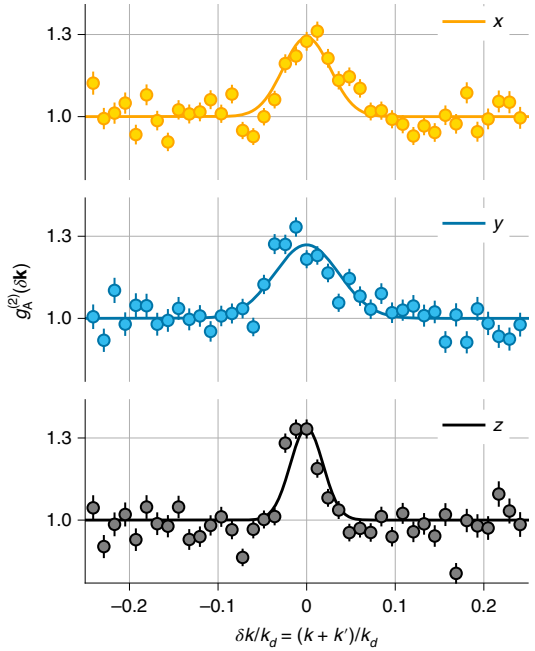

Figure 11. *Correlation function $g^{(2)}(\delta\boldsymbol{k})$ measured along the three directions of space, clearly highlighting the correlations between pairs of opposite momenta. Figure extracted from Tenart, Hercé, et al. (2021).*

$\delta\boldsymbol{k} = 0$. Note that to increase the quantum depletion, Tenart, Hercé, et al. (2021) have placed the atoms in an optical lattice, which has the effect of concentrating the atoms at the minima of the potential and thus increasing the effective density n, hence $\sqrt{na^3}$.

An example of the result is shown in figure 11. The correlation peak in $\delta\boldsymbol{k} = 0$ appears clearly. This figure was obtained at very low temperature, for a condensed fraction of 84%. Tenart, Hercé, et al. (2021) studied the dependence of the height of this peak with temperature and showed that it becomes almost undetectable when approaching the critical condensation temperature. They also verified that its height varied as $1/\rho_\Omega$, where the density ρ_Ω is defined by $\rho_\Omega = \int_\Omega \langle n(\boldsymbol{k})\rangle \ \mathrm{d}^3k$; this is the expected dependence if we assume a perfect correlation between $n(\boldsymbol{k})$ and $n(-\boldsymbol{k})$.

Chapter IV

The ground state of the Bose gas : LHY, excitation spectrum and quantum droplets

In this chapter we continue the study of the dilute Bose gas by looking at both its ground state energy and its excitation spectrum. Thanks to the Bogoliubov approach, we know the expression of the energy E_0 of the ground state for a gas of density $n = N/L^3$:

$$\frac{E_0}{L^3} = \frac{1}{2} g n^2 \left[1 + \alpha \sqrt{n a^3} + \dots\right] \qquad \text{with} \quad \alpha = \frac{128}{15\sqrt{\pi}} \approx 4.8, \tag{1}$$

where a is the scattering length characterizing the s wave interactions and $g \equiv 4\pi\hbar^2 a/m$. The dominant term $gn^2/2$ represents the mean field term and the following term is the LHY correction describing (at lowest order) the effect of quantum fluctuations (Lee, Huang, et al. 1957).

The expression (1) results from a quadratic approximation of the Hamiltonian with respect to the operators $a_{\boldsymbol{k}}$ and $a^\dagger_{\boldsymbol{k}}$ with $\boldsymbol{k} \neq 0$, destroying and creating a particle in a non-zero momentum state. This quadratic approximation is valid when the quantum depletion $n'/n = (N - N_0)/N$ giving the fraction of atoms outside the $\boldsymbol{k} = 0$ state is small. The Bogoliubov approach allows to estimate this depletion:

$$\frac{n'}{n} \approx \frac{8}{3\sqrt{\pi}} \sqrt{n a^3}. \tag{2}$$

The self-consistency condition of the Bogoliubov approach is thus written

$$\sqrt{n a^3} \ll 1. \tag{3}$$

The excitation spectrum is deduced from the expression of the Hamiltonian after the canonical Bogoliubov transformations, which introduce new bosonic operators $b_{\boldsymbol{k}}, b^\dagger_{\boldsymbol{k}}$:

$$\hat{H} = E_0 + \sum_{\boldsymbol{k} \neq 0} \hbar\omega_k \; b^\dagger_{\boldsymbol{k}} b_{\boldsymbol{k}} \tag{4}$$

with for the pseudo-potential approach:

$$\hbar\omega_k = \left[\epsilon_k \left(\epsilon_k + 2gn\right)\right]^{1/2}, \qquad \epsilon_k = \frac{\hbar^2 k^2}{2m}. \tag{5}$$

The action of $b^\dagger_{\boldsymbol{k}}$ on the Bogoliubov vacuum thus creates a quasiparticle of momentum $\hbar\boldsymbol{k}$ and energy $\hbar\omega_k$. The k dependence of ω_k allows to identify the characteristic value k_0 (see figure 1)

$$\frac{\hbar^2 k_0^2}{2m} = gn \quad \Rightarrow \quad k_0 = \frac{1}{\xi} = \sqrt{8\pi n a}. \tag{6}$$

For $k \ll k_0$, we find the phononic regime $\omega_k \approx ck$, with the speed of sound $c = \hbar k_0/\sqrt{2}\, m$. For $k \gg k_0$, we find the free particle regime $\hbar\omega_k \approx \epsilon_k + gn$. Let us recall the origin of the energy shift gn in this regime: it must be understood as the difference $gn = 2gn - gn$. The first term $2gn$ represents the total interaction energy (direct term + exchange term) of the excited

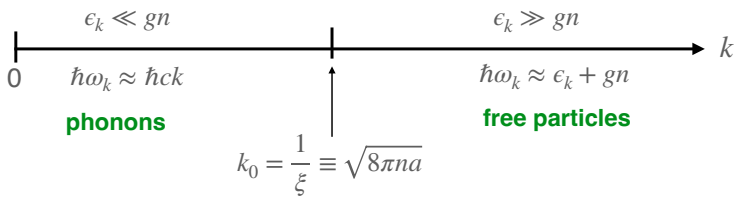

Figure 1. *The two regimes of k values for the pseudo-potential in the Bogoliubov approach. Another characteristic value of k, of the order of $1/a \gg k_0$, will appear later. Moreover, for a potential of finite range b, the scale $k \sim 1/b$ can also play an important role (see Lecture 3).*

particle of momentum $\hbar k$ with the condensate of density n ; the second term corresponds to the initial energy gn of the particle when it is part of the condensate (direct term).

This dispersion relation, plotted in figure 2, is obtained by assuming a fluid of low density [*cf.* 3] and therefore does not allow the description of strongly interacting systems such as liquid helium: in particular, it does not contain its famous *roton-maxon* structure plotted in figure 3. On the other hand, it is in principle well adapted to the description of gaseous Bose-Einstein condensates, at least as long as one does not get too close to a scattering resonance.

In this chapter, we will first describe the experimental measurements of the LHY energy made on dilute atomic gases. We will then move on to measurements of the excitation spectrum: we will first present the now classic results of Steinhauer, Ozeri, et al. (2002) which are very well described by (5). These measurements were made in both the phonon regime and the free particle regime, but always keeping $ka \ll 1$. We will then look at more recent experiments conducted in Boulder (Papp, Pino, et al. 2008) and Cambridge (Lopes, Eigen, et al. 2017a), which extended the measurement range to the $ka \sim 1$ region, leading to notable deviations from (5).

The last part of this chapter will be devoted to the case of a mixture of two quantum gases noted 1 and 2. Depending on the values of the three interaction parameters g_{ij} with $i, j = 1, 2$, this mixture can be miscible or immiscible in the framework of the mean field theory. In particular, immis-

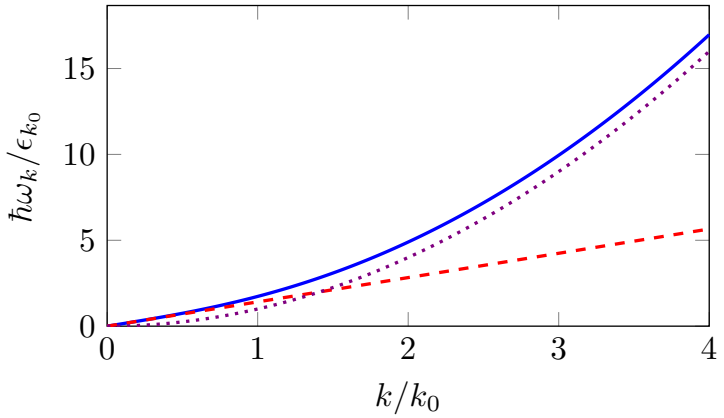

Figure 2. *Bogoliubov dispersion relation (5) in solid blue line with $k_0 = 1/\xi = \sqrt{8\pi na}$ and $\epsilon_{k_0} = \hbar^2 k_0^2/2m$. The red dashed line corresponds to the phonon regime. The purple dashed curve gives the dispersion relation of a free particle $\epsilon_k = \hbar^2 k^2/2m$.*

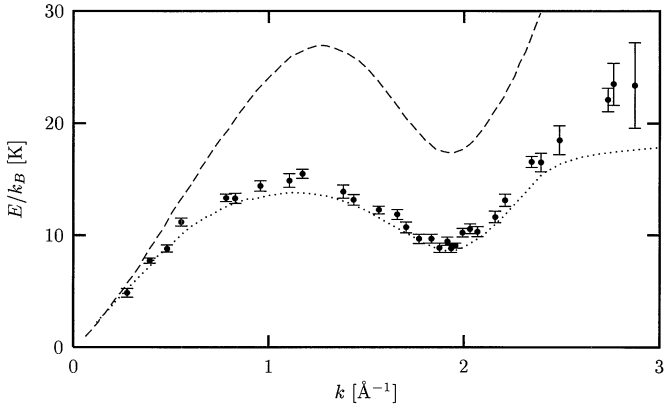

Figure 3. *Excitation spectrum for superfluid liquid helium; the dotted line represents the experimental data of Donnelly, Donnelly, et al. (1981) and the points with error bar the results of the quantum Monte Carlo calculation of Moroni, Galli, et al. (1998). The dashed line is an upper bound obtained from the Feynman approach. Figure taken from Pitaevskii & Stringari (2016).*

cibility occurs when the dispersion relation of the homogeneous mixture, which generalizes (5), gives rise to complex frequencies ω, leading to exponential divergences from a small initial perturbation. We will then see, following the proposal of Petrov (2015), how it is possible to use LHY effects to stabilize this mixture in the form of quantum droplets.

1 LHY energy measurements

1-1 The three-body loss problem

The quantitative measurement of the LHY energy is not easy since it is by definition (at least for a one-component gas) only a small correction to the mean field energy. One could think of increasing experimentally its relative contribution by momentarily increasing the scattering length a thanks to a Feshbach resonance, even if it means giving up the Bogoliubov approach to describe precisely the system. One could then take advantage of the fact that E_{LHY} grows as $a^{5/2}$ [*cf.* (1)] while the mean field energy only grows as a.

Nevertheless, this increase of a cannot be done in practice up to arbitrarily large values. One is indeed limited by the three-body recombination losses, whose rate varies as $L_3 \sim a^4/m$, to within a multiplicative factor, in the vicinity of a scattering resonance (Fedichev, Reynolds, et al. 1996). In this process, two of the atoms form a molecule of size $\sim a$ and energy $\sim -\hbar^2/ma^2$, with the third body carrying away the energy released during the formation of the weakly bound dimer. This dimer can then relax to a more strongly bound molecular state and escape from the confining trap. For a reliable measurement of the LHY energy, it is necessary that the increase of a is made only for a short duration τ, such that $L_3 n^2 \tau \ll 1$, thus ensuring that the density varies little during the measurement. But the duration τ must also be at least equal to the time it takes the system to reach its equilibrium for the new value of a, typically $\hbar/\mu$. As an order of magnitude, we can take here the value of the chemical potential given by the mean field theory, $\mu = gn$. The conjunction of these two inequalities leads to:

$$\frac{\hbar}{\mu} < \tau < \frac{1}{L_3 n^2} \qquad \Rightarrow \qquad na^3 \ll 1. \tag{7}$$

At zero temperature[1], the study of a Bose gas at equilibrium can only be done for small values of na^3 (for a review, see Chevy & Salomon (2016)). We now detail some of the lines that have been explored to highlight this LHY energy.

1-2 Use of the breathing mode

This approach takes advantage of an important theoretical result established by Pitaevskii & Rosch (1997). Consider a condensate described by mean-field theory, confined in a two-dimensional isotropic harmonic trap in the xy plane, (i) in the form of a disk or (ii) in the form of a very elongated cigar of axis z. In both cases, the breathing mode in the xy plane always has frequency $\omega_{\mathrm{brea.}} = 2\omega$, where ω is the trap frequency. This result can be proved relatively simply by studying the evolution of $\langle r^2 \rangle(t)$ from the Gross–Pitaevskii equation in 2D:

$$\mathrm{i}\hbar \frac{\partial \psi}{\partial t} = -\frac{\hbar^2}{2m}\nabla^2\psi + gN|\psi|^2\psi + \frac{1}{2}m\omega^2 r^2 \psi \tag{8}$$

whatever the value of the product Ng (ψ is normalized to unity). It was verified experimentally for the first time by Chevy, Bretin, et al. (2001).

Any deviation of $\omega_{\mathrm{brea.}}$ from the 2ω frequency thus signals a beyond mean-field contribution to the energy of the gas. This is the principle of the experiment of Altmeyer, Riedl, et al. (2007), carried out on a gas of ^{6}Li, the fermionic isotope of lithium. The authors prepared the gas in the vicinity of a Feshbach resonance (834 G), on the $a > 0$ side of the resonance. To a first approximation, the gas in its equilibrium state is then essentially formed of $^6\mathrm{Li}_2$ dimers, bosonic molecules that form a Bose–Einstein condensate. This gas is confined in a hybrid trap: the harmonic confinement in the xy plane is ensured by a laser beam of wavelength 1030 nm and waist $54\,\mu$m. The frequency $\omega/2\pi$ is adjusted between 290 and 590 Hz by varying the power of this laser. The confinement along the z axis is ensured by a magnetic trap, of frequency $\omega_z/2\pi = 22.4$ Hz.

The excitation of the breathing mode is done by reducing the power of the confining laser for a short time interval. The gas is then allowed to

[1] We will see in a later chapter that this condition can be relaxed at higher temperatures, in the non-degenerate regime, and becomes $n\lambda^3 \ll 1$.

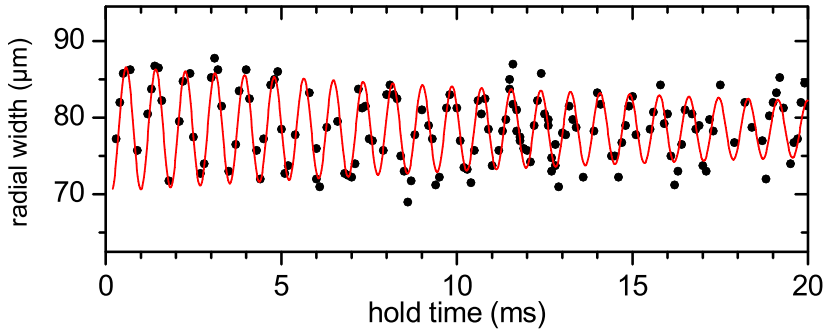

Figure 4. *Evolution of $\sqrt{\langle r^2\rangle(t)}$ (breathing mode) for a ^{6}Li gas (fermions) in the neighborhood of a Feshbach resonance. The gas is prepared on the $a > 0$ side of the resonance so that the ^{6}Li atoms are present essentially as $^6Li_2$ bosonic molecules. The frequency (here 1185 Hz) is measured with a precision $\sim 10^{-3}$. Figure extracted from Altmeyer, Riedl, et al. (2007).*

oscillate in the trap for an adjustable amount of time before its radius is measured. An example of the oscillation is shown in figure 4.

This experiment is repeated for different values of the scattering length a and the ratio $\omega_{\text{brea.}}/\omega$ is plotted as a function of $1/a$ in figure 5. In the molecular condensate regime ($k_F a \lesssim 1$), this ratio is notably above 2, and the deviation from 2 is in good agreement with a numerical calculation based on a quantum Monte Carlo approach (figure 5, top). Note that the experimental data have been (slightly) corrected to take into account the non-isotropy of the trap ($\sim 7\,\%$) as well as its anharmonicity.

The fact that the gas is prepared in the vicinity of a Feshbach resonance complicates the attribution of the non-zero value of $\omega_{\text{brea.}} - 2\omega$ to LHY effects alone. We have reported in figure 5 (bottom) an analysis made by S. Nascimbene from the theoretical predictions of Stringari (2004). It shows that for the values of $1/k_F a$ explored here, which remain relatively small, one is still far from the prediction for a "simple" Bose–Einstein condensate.

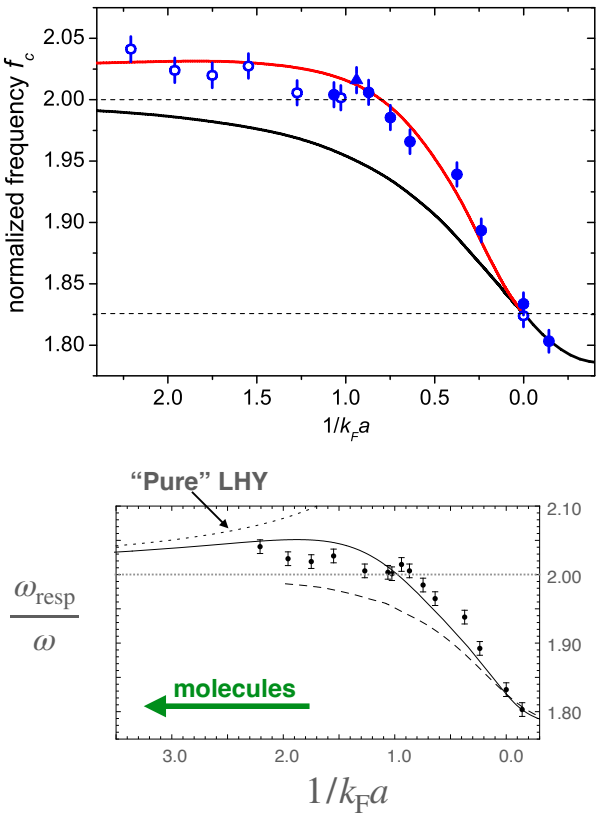

Figure 5. *Top: Variation of $f_c = \omega_{\text{brea.}}/\omega$ as a function of $1/k_F a$ with $k_F = \left(24m^3\omega^2\omega_z N/\hbar^3\right)^{1/6}$. The open (resp. full) disks were obtained with $\omega/2\pi =$ 290 Hz (resp. 590 Hz). The black curve is the prediction of the mean field theory and is compatible with a limit $\omega_{\text{brea.}} = 2\omega$ in the limit $k_F a \ll 1$, corresponding to a weakly interacting molecular condensate. The red curve is a quantum Monte Carlo calculation, taking into account the LHY corrections. Figure extracted from Altmeyer, Riedl, et al. (2007). Bottom: same experimental data, with in dashed line the contribution of the LHY effects only. The continuous curve is deduced from the equation of state measured by Nascimbène, Navon, et al. (2010). Figure adapted from S. Nascimbene's thesis.*

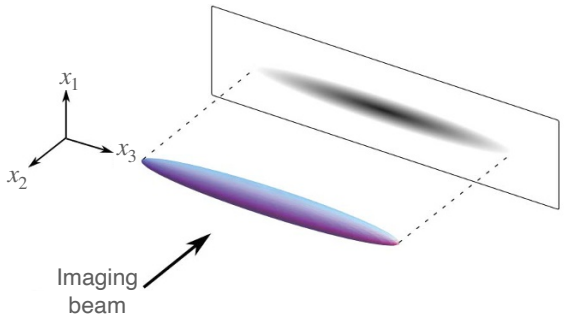

Figure 6. *Measure of the equation of state $P(\mu)$ from the image of a gas confined in a harmonic trap. Using the local density approximation, the pressure P is obtained from $\int n(x_1, x_2, x_3)\, \mathrm{d}x_1\, \mathrm{d}x_2$ (*cf. *chapter 1).*

1-3 Determination of the equation of state

We described in chapter 1 the measure of the equation of state of a gas confined in a harmonic trap from its integrated density profile along two spatial directions (Nascimbène, Navon, et al. 2010) [see figure 6]. In chapter 1, we were interested in the low phase space density limit and we described how some coefficients of the virial expansion could be extracted from these experiments. The same type of experiment allows one to study the equation of state at very low temperature, in the strongly degenerate regime.

Navon, Piatecki, et al. (2011) used a gas of $\sim$ 60 000 atoms of ^{7}Li (a bosonic isotope of lithium) that they prepared to a "standard" value for the scattering length, $a \sim 10\,\mathrm{nm}$. They then modified the magnetic field to approach a Fano-Feshbach resonance ($B = 738\,\mathrm{G}$) and measured the gas pressure for different values of a, ranging from 30 to 100 nm. These measurements are made at very low temperature so that the only thermodynamic variable relevant from a grand-canonical point of view is the chemical potential μ, which can be measured in units of the energy scale $\hbar^2/ma^2$.

The results for pressure, measured in units of $P_a = \hbar^2/ma^5$, are shown in figure 7. The prediction of the mean field theory is $P = gn^2/2$ and

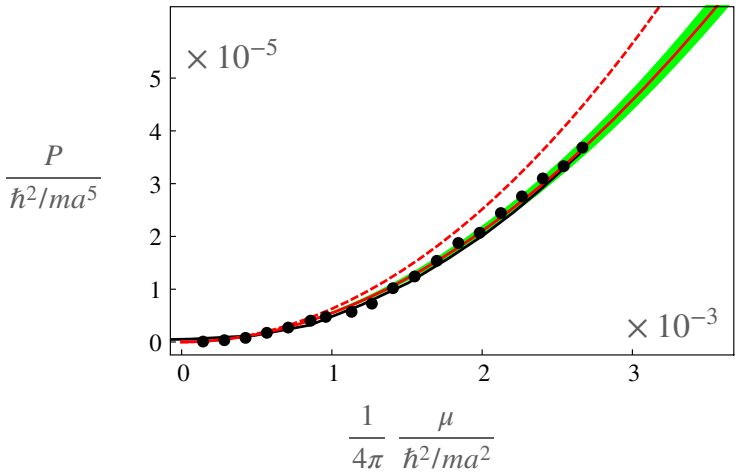

Figure 7. *Equation of state for a ^{7}Li Bose gas: measurement of the pressure P as a function of the chemical potential μ. Red solid and dashed lines: analytical prediction including or not the LHY correction. Black line: numerical results obtained by a quantum Monte Carlo method. The region colored in green delimits the uncertainty zone related to the determination of a. Figure extracted from Navon, Piatecki, et al. (2011).*

$\mu = gn$ [with $g = 4\pi\hbar^2 a/m$], and it thus corresponds to the quadratic law $P = \mu^2/2g$. This prediction, indicated by the red dashed line, is clearly not in agreement with the experimental results for larger values of μ.

Quantum fluctuations are taken into account using the LHY result given in (1) and the thermodynamic relations taken here at zero entropy (ground state):

$$P = -\left(\frac{\partial E}{\partial L^3}\right)_{S,N} = \frac{1}{2}gn^2\left(1 + \frac{3}{2}\alpha\sqrt{na^3} + \ldots\right) \quad (9)$$

$$\mu = \left(\frac{\partial E}{\partial N}\right)_{S,L^3} = gn\left(1 + \frac{5}{2}\alpha\sqrt{na^3} + \ldots\right) \quad (10)$$

from which we deduce by elimination of na^3:

$$\boxed{P = \frac{\mu^2}{2g}\left(1 - \alpha\sqrt{\mu a^3/g}\right)} \tag{11}$$

This LHY prediction, shown as a red solid line in figure 7, is in excellent agreement with the data, as are the Monte Carlo results (black solid line) obtained assuming a temperature $T \lesssim T_c/4$, where T_c is the condensation temperature of the ideal gas.

1-4 Momentum distribution and kinetic energy

We now return to the momentum distribution deduced from the Bogoliubov approximation and discuss the total kinetic energy derived from it. For this analysis, we momentarily leave the pseudo-potential approach and return to a regular interaction potential $V(r)$ of Fourier transform $\tilde{V}_k$.

In the calculation of the quantum depletion (Chapter 3), we obtained the value of the population $\bar{n}_k$ of each momentum state $\hbar\boldsymbol{k}$:

$$\bar{n}_k = |v_k|^2 = \frac{1}{2}\left[\frac{\epsilon_k + n\tilde{V}_k}{\sqrt{\epsilon_k^2 + 2n\tilde{V}_k\epsilon_k}} - 1\right], \tag{12}$$

from which we can deduce the kinetic energy

$$E_{\rm kin} = \sum_{\boldsymbol{k}} \frac{\hbar^2 k^2}{2m}\,\bar{n}_k. \tag{13}$$

The population $\bar{n}_k$ represents the momentum distribution of the gas, as it can be measured in a time-of-flight experiment, if we abruptly switch off the interaction potential at the beginning of the ballistic expansion.

For a regular potential, we explained in the previous chapter that one can distinguish three domains for k, which we recall in figure 8 :

- The phonon domain, $k \ll \xi^{-1}$, which leads to $\bar{n}_k \propto 1/k\xi$. These states are thus highly populated without leading to a divergence of the quantum depletion or the kinetic energy due to the Jacobian in $k^2\,\mathrm{d}k$ which appears in the 3D integration volume element.

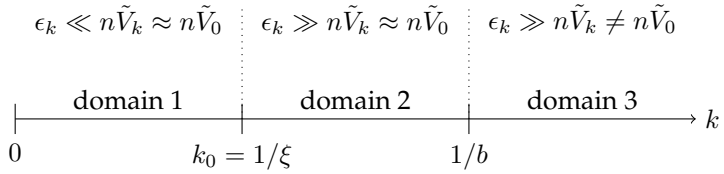

Figure 8. *The three domains relevant to the k wavenumber.*

- The intermediate domain $\xi^{-1} \ll k \ll b^{-1}$, in which the kinetic energy term ϵ_k dominates the interaction term $\tilde{V}_k$, but where we can still replace $\tilde{V}_k$ by its value at the origin $\tilde{V}_0$. We then obtain a power law for the momentum distribution:

$$\bar{n}_k \approx \frac{n^2\tilde{V}_0^2}{4\epsilon_k^2} = \frac{C/L^3}{k^4} \qquad \text{with} \quad C \equiv (4\pi a)^2 nN. \tag{14}$$

  This law in k^{-4} is an important characteristic of interacting gases. We will find it again when we study the formalism of the *contact of Tan*.

- The very large momentum domain, $b^{-1} \ll k$. The decay of $\tilde{V}_k$ then becomes significant and the momentum distribution decays faster than in the intermediate domain:

$$\bar{n}_k \propto \frac{\tilde{V}_k^2}{k^4}. \tag{15}$$

  This zone of very high momentum is absent for the pseudo-potential, since the latter amounts to taking $\tilde{V}_k$ constant equal to g for all values of k.

The faster than k^{-4} decay of $\bar{n}_k$ is essential to ensure that the kinetic energy of the gas takes a finite value. Indeed, in three dimensions, a momentum distribution varying like C/k^4 up to infinity leads to a divergence of the integral

$$\int \frac{\hbar^2 k^2}{2m}\,\frac{C}{k^4}\,\mathrm{d}^3k = \int \frac{\hbar^2 k^2}{2m}\,\frac{C}{k^4}\,4\pi k^2\,\mathrm{d}k. \tag{16}$$

Such a divergence, which leads to an infinite kinetic energy, will occur if we model $V(\boldsymbol{r})$ as a contact potential since we will then have $\tilde{V}_k = \tilde{V}_0$ for all k.

As the total energy E_{LHY} is finite, this means that the positive divergence of the kinetic energy must be compensated by a negative divergence of the interaction energy. This last point is easily verified; let us write the interaction potential involved in the Bogoliubov Hamiltonian as

$$\hat{V} = gn\left(\hat{N}' + \hat{O}\right) \tag{17}$$

where $\hat{N}' = \sum_{\boldsymbol{k}\neq 0} a^\dagger_{\boldsymbol{k}} a_{\boldsymbol{k}}$ is the operator number of particles outside $\boldsymbol{k} = 0$ and

$$\hat{O} = \frac{1}{2}\sum_{\boldsymbol{k}\neq 0} a_{\boldsymbol{k}} a_{-\boldsymbol{k}} + \text{H.c.} \tag{18}$$

The divergence comes from the contribution of $\langle\hat{O}\rangle$ which is written in the Bogoliubov vacuum:

$$\langle\hat{O}\rangle = -\frac{1}{2}\sum_{\boldsymbol{k}\neq 0} u_k v_k \langle b_{\boldsymbol{k}} b^\dagger_{\boldsymbol{k}}\rangle + \text{c.c.} = -\sum_{\boldsymbol{k}\neq 0} u_k v_k. \tag{19}$$

The argument of the sum indeed behaves like k^{-2} at large $\boldsymbol{k}$, so that the three-dimensional integral on k (with its Jacobian in $4\pi k^2\,\mathrm{d}k$) diverges. We will come back to these two divergences of the kinetic energy and the potential energy when we study the contact.

2 The excitation spectrum of a condensate

2-1 Summing the Born expansion

The diagonalization of the Bogoliubov Hamiltonian carried out in the previous chapters led us to the expression of the dispersion relation for the elementary excitations of the gas. We treated two different cases: for a regular potential in the Born approximation, we found

$$\text{regular potential (Born):} \qquad \hbar\omega_k = \left[\epsilon_k\left(\epsilon_k + 2n\tilde{V}_k\right)\right]^{1/2} \tag{20}$$

and for the pseudo-potential :

$$\text{Pseudo-pot.:} \quad \hbar\omega_k = \left[\epsilon_k\left(\epsilon_k + 2ng\right)\right]^{1/2} \qquad \text{with} \quad g = \frac{4\pi\hbar^2 a}{m}. \tag{21}$$

Let us look at the first of these two relations, concerning the case of a regular potential. We see that it involves the Fourier transform of the potential k. If we restrict ourselves to momenta k small in front of $1/b$, where b is the range of the potential, we can use

$$k \ll \frac{1}{b}: \qquad \tilde{V}_k \approx \tilde{V}_0 = \frac{4\pi\hbar^2 a^{(1)}}{m} \tag{22}$$

where $a^{(1)}$ is the scattering length, at order 1 of the Born expansion. Recall that it is only legitimate to restrict to this first order if the scattering length a is very small in front of the range b, i.e. $\frac{1}{b} \ll \frac{1}{a}$. In fact, as we explained in the previous chapter, it is possible to go further in Born's expansion and to sum the whole Born series (Beliaev 1958a; Beliaev 1958b). This requires going beyond the Bogoliubov Hamiltonian: to study the interaction between an atom with momentum $\hbar\boldsymbol{k}$ and an atom of the condensate with zero momentum, one must take into account the passage through a virtual state where both atoms have momentum $\boldsymbol{k}_1, \boldsymbol{k}_2$ with $\boldsymbol{k} = \boldsymbol{k}_1 + \boldsymbol{k}_2$:

$$\boldsymbol{k}, N-1:0 \quad \longrightarrow \quad \boldsymbol{k}_1, \boldsymbol{k}_2, N-2:0 \quad \longrightarrow \quad \boldsymbol{k}, N-1:0 \tag{23}$$

which is only possible by the action of terms like $a^\dagger_{\boldsymbol{k}_1} a^\dagger_{\boldsymbol{k}_2} a_{\boldsymbol{k}} a_0$ for the first arrow and $a^\dagger_{\boldsymbol{k}} a^\dagger_0 a_{\boldsymbol{k}_1} a_{\boldsymbol{k}_2}$ for the second. These terms, which contain only one operator a_0 or $a^\dagger_0$, have been neglected when restricting the N-body Hamiltonian to its quadratic approximation.

Once this resummation is done, we arrive at an expression formally identical to the one obtained in the case of the pseudopotential in (21). The constraint $a \ll b$ has no more reason to exist if all the terms of the Born expansion are taken into account (provided that this expansion converges, of course) and we arrive for the regular potential at the same result as the one obtained for the pseudo-potential:

$$k \ll \frac{1}{a}, \frac{1}{b}: \qquad \hbar\omega_k = \left[\epsilon_k\left(\epsilon_k + 2ng\right)\right]^{1/2}. \tag{24}$$

2-2 Measurement of the Bogoliubov spectrum

We will briefly describe here the quantitative measurement of the Bogoliubov spectrum made by Steinhauer, Ozeri, et al. (2002) [see also course

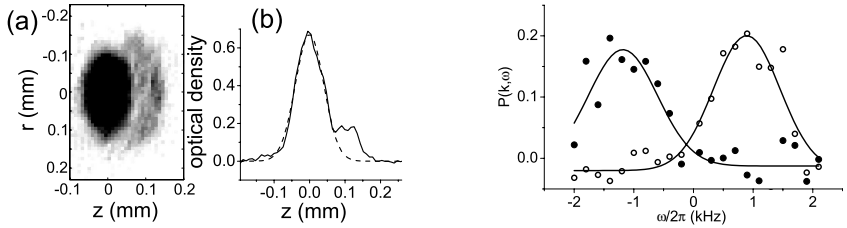

Figure 9. *Left: Image of an atomic cloud after a Bragg pulse. The diffracted cloud is moving in the $x > 0$ direction. Right: resonance curve. Both types of symbols correspond to diffracted clouds moving in the $x > 0$ or $x < 0$ direction. Figure extracted from Steinhauer, Ozeri, et al. (2002).*

2016]. This experiment is based on Bragg spectroscopy, which we have already described in the previous chapter. Recall that this experimental technique consists in studying the linear response of the fluid to a probe that can transfer a momentum $\hbar\boldsymbol{q}$ and an energy $\hbar\omega$. For cold atomic gases, this probe is generally[2] formed by a pair of light beams of wave vectors $\boldsymbol{k}_1$ and $\boldsymbol{k}_2$, the atoms gaining momentum $\hbar\boldsymbol{q} = \hbar(\boldsymbol{k}_1 - \boldsymbol{k}_2)$ and energy $\hbar\omega = \hbar(\omega_1 - \omega_2)$ in an "absorption – stimulated emission" process.

Steinhauer, Ozeri, et al. (2002) worked with a rubidium 87 condensate, and a pair of light beams whose angle varies between 3 and 130 degrees, which corresponds to q between 0.4 and 15 μm^{-1}. The healing length is $\xi \approx 0.25\,\mu\text{m}$, so that $q\xi$ varies between 0.1 (phonon regime) and 4 (free particle regime). A typical example of the result is shown in figure 9 for $q = 2.8\,\mu\text{m}^{-1}$. This image taken after a time of flight clearly shows the (small) fraction of atoms excited by the light pulse, on the right side of the condensate.

If we assume that the observed signal corresponds to the creation of a single elementary excitation for each elementary Bragg process (we will come back to this assumption later), the resonance curve of these processes gives direct access to the desired dispersion relation ω_q. The results are presented in figure 10. The agreement with Bogoliubov's prediction (24) is remarkable, both in the phononic and in the free particle regime.

[2]For another type of probe, however, see Guarrera, Würtz, et al. (2011)

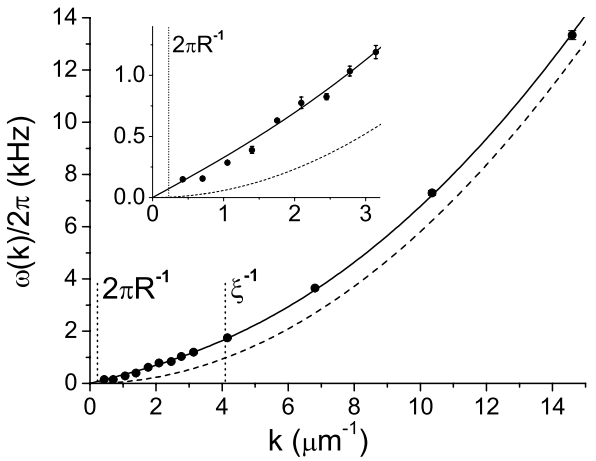

Figure 10. *Excitation spectrum measured by Bragg spectroscopy. The solid curve shows the prediction (24) for the Bogoliubov spectrum. Figure extracted from Steinhauer, Ozeri, et al. (2002).*

One may wonder about the effect of the LHY terms on this excitation spectrum:

- In the phononic case, these effects will modify the speed of sound in the condensate. Let us start from the general relation

$$c = \sqrt{\frac{1}{m}\left(\frac{\partial P}{\partial n}\right)_S}, \tag{25}$$

where the derivative is taken at constant entropy, i.e. for the ground state in the case of interest here. The pressure P was given in (9) and we deduce:

$$c = \sqrt{\frac{gn}{m}}\left[1 + \frac{8}{\sqrt{\pi}}\sqrt{na^3} + \dots\right]. \tag{26}$$

This result coincides with the one found by Beliaev by the method of Green's functions [see also Mohling & Sirlin (1960)].

- In the free particle regime $k\xi \gg 1$ (but $ka \ll 1$), Mohling & Sirlin (1960) write the dispersion relation of an excitation in the form

$$\xi^{-1} \ll k \ll a^{-1} : \qquad \hbar\omega(k) \approx \epsilon_k + 2gn - \mu, \tag{27}$$

where μ is the chemical potential of the condensate given in (10). The physical interpretation of (27) is in line with that proposed above in this regime: this relation represents the difference between the energy of the particle in its final state, $\epsilon_k + 2gn$, unmodified by terms beyond the mean field at this order of the calculation[3], and the energy required to extract a particle from the condensate, i.e. the chemical potential μ.

For each of these two regimes, phonon and free particle, it seems difficult to detect beyond mean-field effects in a weakly interacting Bose gas, given the present accuracy of the measurements.

2-3 Boulder and Cambridge experiments: $q \gtrsim 1/a$

Using rubidium 85 and potassium 39, respectively, Papp, Pino, et al. (2008) and Lopes, Eigen, et al. (2017a) have extended the measurement of the response of a condensate by Bragg spectroscopy to much larger values of qa, taking advantage of the existence of a Feshbach resonance for these atomic species.

The results of Papp, Pino, et al. (2008) are shown in figure 11. The top figure shows the deviation $\hbar\omega_q - \epsilon_q$ as a function of the scattering length a. In the $q\xi \gg 1$ regime, the Bogoliubov spectrum (24) predicts $\hbar\omega_q - \epsilon_q \approx gn$, i.e. a linear variation of this gap with a, which is not consistent with observations.

This type of experiment was repeated over a wider range of qa values by Lopes, Eigen, et al. (2017a). In this experiment, three values of q were used, corresponding to three possible relative orientations of the $\boldsymbol{k}_1$ and $\boldsymbol{k}_2$ vectors. An example of resonance is shown in figure 12. The results for different values of a and q are grouped together[4] in figure 13. The plotted

[3] This can be understood by noting that the domain contributing to the integral for the LHY correction is $k \lesssim 1/\xi$.

[4] For this data set, the maximum value of the small parameter $\sqrt{na^3}$ is about 0.05.

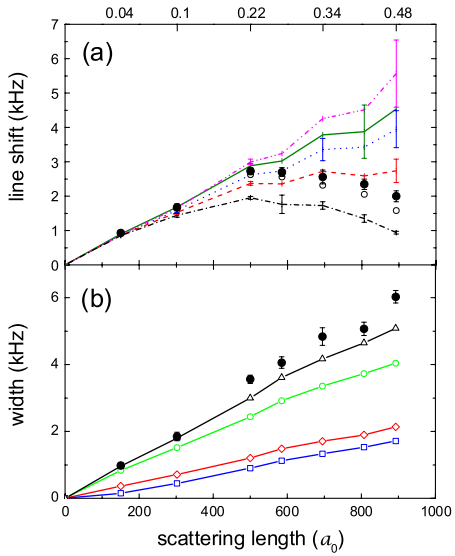

Figure 11. *Top: Bragg spectroscopy of a ^{85}Rb condensate, showing the resonance frequency $\omega_{\rm res}/2\pi$ measured after subtraction of the "one particle" frequency ϵ_q/h. The open symbols correspond to the direct measurements and the closed symbols are the corrected data, once the contribution of the thermal part of the cloud is taken into account. The lines correspond to different theoretical models. Bottom: width of the Bragg resonance giving access, at least qualitatively, to the lifetime of the excitations. Figure extracted from Papp, Pino, et al. (2008).*

quantity is

$$\alpha = qa\,\frac{\hbar\omega_{\rm res}(q) - \epsilon_q}{gn} \tag{28}$$

and the experimental results are remarkably well fitted by the law:

$$\alpha = qa\left(1 - \frac{\pi}{4}qa\right), \tag{29}$$

which leads to a cancellation of α in $qa = 4/\pi \approx 1.3$. At this point, the resonance frequency for the Bragg process is equal to the single atom frequency, ϵ_q/h.

We will explain the rationale for this choice of the quadratic law (29) in

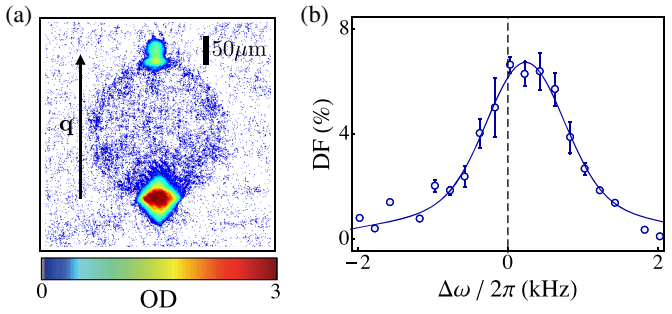

Figure 12. *Left: Image of a cloud of ^{39}K atoms after Bragg spectroscopy. The cloud at the bottom of the figure corresponds to the initial condensate. The smaller cloud at the top of the figure corresponds to the diffracted atoms, having gained the momentum $\hbar\boldsymbol{q}$. Right: Example of a resonance curve allowing to determine $\omega_{\rm res}(q)$. The dashed line gives the position of the "bare" resonance: $\hbar\omega = \epsilon_q$. Figure taken from Lopes, Eigen, et al. (2017a).*

§ 2-5, but note that it is not compatible with the Bogoliubov single-particle excitation spectrum (24), which predicts $\hbar\omega_q = \epsilon_q + gn$, and thus the linear law $\alpha = qa$ plotted as a dashed straight line on figure 13.

2-4 Back to Beliaev's approach

A first clue to explain the experimental results of Boulder and Cambridge is provided by Beliaev's approach, which has recently been generalized to an arbitrary value of na^3 by Hofmann & Zwerger (2017) using the OPE (*Operator Product Expansion*) technique. We will give here some elements to explore this track, to conclude that it cannot alone explain the experimental results.

In his article already quoted above, Beliaev (1958b) explains how to take into account at all orders in V the interaction between the elementary excitation of momentum $\hbar\boldsymbol{k}$ and an atom of the condensate at zero momentum. The result of this resummation of the Born expansion is expressed in terms of the scattering amplitude $f(k_r)$ between the two partners, with the relative momentum $k_r = k/2$. Assuming that a is large in front of the effective

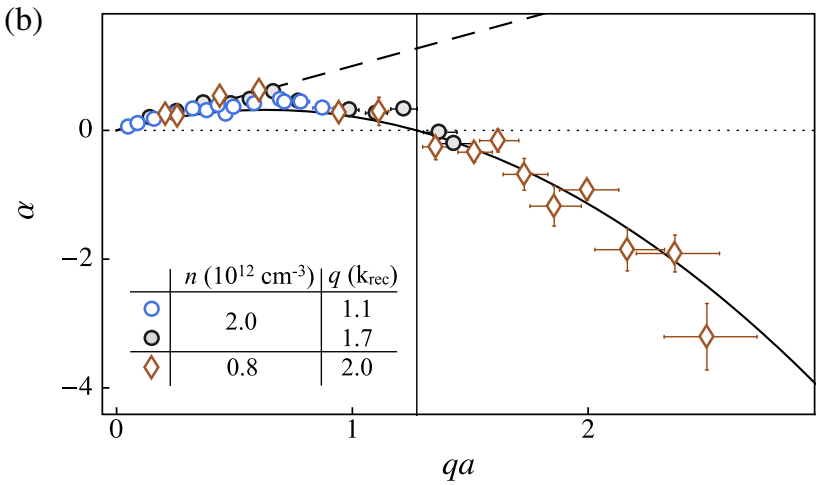

Figure 13. *Positions $\omega_{\rm res}(q)$ of the resonances as a function of qa for three different values of q, with α defined in (28). The solid line represents the prediction (29) based on Feynman's formula (*cf. *§,2-5). The straight dashed line represents the prediction for an elementary Bogoliubov excitation $\alpha = qa$. Figure taken from Lopes, Eigen, et al. (2017a).*

range, we have [*cf.* course 2021]:

$$f(k_r) \approx \frac{-a}{1 + \mathrm{i}k_r a}. \tag{30}$$

At low energy, $k \ll 1/a$ and we find $f(k_r) \approx -a$, which leads to the Bogoliubov spectrum given in (24). On the other hand, when k_r becomes comparable to $1/a$, the corrections related to the denominator of (30) become significant. Beliaev shows that the excitation spectrum is related to the real part of $f(k_r)$ which is modified as:

$$\mathcal{R}\mathrm{e}\left[f(0)\right] = -a \qquad \longrightarrow \qquad \mathcal{R}\mathrm{e}\left[f(k_r)\right] = \frac{-a}{1 + (ka/2)^2}. \tag{31}$$

More precisely, the energy balance already mentioned in the regime [5] $k\xi \gg$

[5] We will not give here the general expression found by Beliaev (1958b) [*cf.* eq. (4.7) of this

1 becomes:

$$\boxed{\hbar\omega_k = (\epsilon_k + 2\,gn) - gn \quad \longrightarrow \quad \hbar\omega_k = \left(\epsilon_k + \frac{2\,gn}{1+(ka/2)^2}\right) - gn} \tag{32}$$

This prediction constitutes a significant deviation from the Bogoliubov dispersion relation (24). In particular, we see that the difference $\hbar\omega_k - \epsilon_k$ can now cancel and change sign. However, the point of cancellation does not correspond to what was measured in Cambridge: according to (32), it should occur for $ka = 2$, whereas it is found experimentally around $ka = 1.3$. The same kind of disagreement occurs when one tries to fit the data of the Boulder experiment with the result (32) [see Hofmann & Zwerger (2017)].

Lifetime of the excitations. The Beliaev analysis also allows to calculate the lifetime of an elementary excitation from the imaginary part of the scattering amplitude (30). This lifetime corresponds to a process in which an excitation decays into two excitations of lower energy. In the free particle regime, this can correspond simply to the elastic collision process between the particle with momentum $\hbar\boldsymbol{k}$ and an atom of the condensate

$$(\hbar\boldsymbol{k}) + (\boldsymbol{0}) \;\longrightarrow (\hbar\boldsymbol{k}_1) + (\hbar\boldsymbol{k}_2) \tag{33}$$

with $|\boldsymbol{k}_1|, |\boldsymbol{k}_2| < |\boldsymbol{k}|$. The result of these s-wave collisions is clearly visible in figure 12 and it leads to the lifetime (Mohling & Sirlin 1960; Hofmann & Zwerger 2017):

$$1/\xi \ll k \lesssim 1/a : \qquad \tau^{-1} \sim n(8\pi a^2)\frac{\hbar k_r}{m} = \frac{gn}{\hbar}\,ka. \tag{34}$$

We note that to have a measurement of the resonance with an accuracy at least equal to gn (necessary to discriminate between $\hbar\omega_k$ and ϵ_k), the measurement time must be at least equal to $\hbar/gn$, which is comparable to the lifetime τ of an excitation when $ka \sim 1$. An accurate description of the Bragg measurement process in the high energy regime should therefore take into account this finite lifetime.

article]. Ronen (2009) has studied in detail how to adapt this general result to the case of a van der Waals interaction potential between atoms [see also Hofmann & Zwerger (2017)].

2-5 The Feynman Formula

Feynman (1954) developed a powerful approach to study the excitation spectrum of interest here. This approach provides the center of gravity of the absorption line:

$$\bar{\omega}(\boldsymbol{q}) = \frac{\int_{-\infty}^{+\infty} \omega\;\Gamma(\boldsymbol{q},\omega)\;\mathrm{d}\omega}{\int_{-\infty}^{+\infty}\;\Gamma(\boldsymbol{q},\omega)\;\mathrm{d}\omega} \tag{35}$$

by putting it in the form

$$\boxed{\hbar\bar{\omega}(q) = \frac{\epsilon_q}{S(q)}} \tag{36}$$

with as always $\epsilon_q = \hbar^2q^2/2m$ and the *static structure factor* $S(q)$ given by:

$$\boxed{S(q) = 1 + n\int [g_2(r) - 1]\,\mathrm{e}^{-\mathrm{i}\boldsymbol{q}\cdot\boldsymbol{r}}\;\mathrm{d}^3r} \tag{37}$$

The spatial correlation function $g_2(r)$ gives the probability density to find two particles separated by the distance r within the fluid. It is calculated from:

$$g_2(r) = \frac{1}{n^2}\langle\hat{\Psi}^\dagger(0)\,\hat{\Psi}^\dagger(\boldsymbol{r})\,\hat{\Psi}(\boldsymbol{r})\,\hat{\Psi}(0)\rangle. \tag{38}$$

This function characterizes the density fluctuations of the fluid, in particular a possible bunching or antibunching of particles, and it is normalized so that it tends to 1 when $r \to \infty$.

The proof of Feynman's formula for the problem we are interested in is detailed in the appendix of this chapter. We indicate here the main ingredients. We consider a quantum fluid with N particles which is subjected to a time-dependent, monochromatic perturbation:

$$\hat{V}(t) = \hat{V}^{(+)}\;\mathrm{e}^{-\mathrm{i}\omega t} + \mathrm{H.c.} \tag{39}$$

where the operator $\hat{V}^{(+)}$ transfers the momentum $\hbar\boldsymbol{q}$ to one of the particles of the fluid:

$$\hat{V}^{(+)} = \hbar\kappa\;\sum_{j=1}^{N}\mathrm{e}^{\mathrm{i}\boldsymbol{q}\cdot\hat{\boldsymbol{r}}_j}. \tag{40}$$

At the lowest order of perturbation theory, one can use Fermi's golden rule to evaluate the probability per unit time $\Gamma(\boldsymbol{q},\omega)$ for the fluid to absorb a quantum of momentum $\hbar\boldsymbol{q}$ and energy $\hbar\omega$. The calculation of the numerator of (35) gives then the exact result

$$\mathcal{N}(\boldsymbol{q}) = 2\pi\kappa^2 N \frac{\hbar q^2}{2m}, \tag{41}$$

a result in which the interaction strength does not contribute[6]. The denominator is written :

$$\mathcal{D}(\boldsymbol{q}) = 2\pi\kappa^2 N\, S(q) \tag{42}$$

hence the expression (36) for $\bar{\omega}(q)$.

The determination of the structure factor $S(q)$ requires the knowledge of the function $g_2(r)$, which has been computed by Lee, Huang, et al. (1957) in the framework of the Bogoliubov approach. This calculation is also detailed in the appendix and we will just give here the behavior of $g_2(r)$ in the neighborhood of $r = a$, since it is the value of $S(q)$ for $q \sim 1/a$ that interests us. Lee, Huang, et al. (1957) find for small r:

$$r \ll \xi : \qquad g_2(r) = \left(1 - \frac{a}{r}\right)^2 + \mathcal{O}(a/\xi). \tag{43}$$

When we expand the square to form the quantity $g_2(r) - 1$, we find the dominant terms $-2a/r$ and a^2/r^2 whose Fourier transforms are respectively proportional to $-1/q^2$ and $1/q$. We then arrive at the structure factor (*cf.* appendix):

$$q\xi \gg 1 : \qquad S(q) \approx 1 - \frac{1}{q^2\xi^2} + \frac{2\pi^2 n a^2}{q} = 1 - \frac{1}{q^2\xi^2}\left(1 - \frac{\pi}{4}qa\right) \tag{44}$$

It only remains to inject this result into the Feynman formula (36) to deduce the center of gravity of the line:

$$\boxed{q\xi \gg 1 : \qquad \hbar\bar{\omega}(q) \approx \epsilon_q \left[1 + \frac{1}{q^2\xi^2}\left(1 - \frac{\pi}{4}qa\right)\right].} \tag{45}$$

[6]This result is known as the f-sum rule or *Thomas–Reiche–Kuhn relation*. This terminology comes from atomic physics and deals with the algebraic sum of the oscillator forces (noted f) of electronic transitions – absorption or emission of photons – in an atom.

This result is the one drawn as a solid line on figure 13 giving the results of the experiment of Lopes, Eigen, et al. (2017a):

$$\alpha = qa\,\frac{\hbar\bar{\omega}(q) - \epsilon_q}{gn} = qa\left(1 - \frac{\pi}{4}qa\right). \tag{46}$$

and it seems in excellent agreement with the experimental data.

2-6 Problem solved?

At first sight, the agreement between the experimental data and the prediction (45) from the Feynman formula seems to solve the problem of the interpretation of the experimental data from Boulder and Cambridge. But a closer look reveals that the situation is not so clear.

A first question that arises is to connect Feynman's result with the spectrum (32) predicted by the Beliaev approach. Since the spectrum (32) concerns the dispersion relation of an elementary excitation while the Feynman result concerns the center of gravity of the line, the discrepancy between the two predictions is possible but it deserves to be explained. To do this, the simplest way is to return to the $\hat{V}^{(+)}$ operator which describes the excitation of the system during the Bragg diffraction. This operator is given in (40) and it is written in second quantization:

$$\hat{V}^{(+)} = \hbar\kappa \sum_{\boldsymbol{k}} a^\dagger_{\boldsymbol{k}+\boldsymbol{q}} a_{\boldsymbol{k}}. \tag{47}$$

When we rewrite the operators $a_{\boldsymbol{k}}, a^\dagger_{\boldsymbol{k}}$ as a function of the operators $a_0 \approx a_0^\dagger \approx \sqrt{N_0}$ and of the operators $b_{\boldsymbol{k}}, b^\dagger_{\boldsymbol{k}}$ for $\boldsymbol{k} \neq 0$, the following terms appear at the same order in $\hbar\kappa$

- A dominant term, proportional to $\sqrt{N}_0$, corresponding to the creation of a single $\boldsymbol{q}$ momentum excitation with $\hbar\omega_q$ energy.
- A second term corresponding to the creation of a pair of excitations $(\boldsymbol{k}_1, \boldsymbol{k}_2)$, of total momentum $\boldsymbol{k}_1 + \boldsymbol{k}_2 = \boldsymbol{q}$.

This single and double excitation structure is described in detail by Griffin (1993). For the problem of interest here, we deduce the form of $\Gamma(\boldsymbol{q},\omega)$:

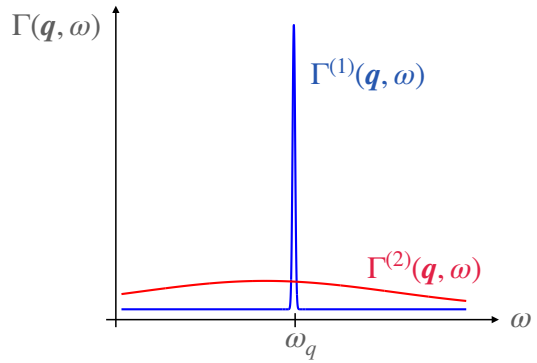

Figure 14. *Generic form of the two-component spectrum expected in an analysis of the Bragg diffraction process using Fermi's golden rule.*

$$\Gamma(\boldsymbol{q},\omega) = \Gamma^{(1)}(\boldsymbol{q},\omega) + \Gamma^{(2)}(\boldsymbol{q},\omega), \tag{48}$$

where $\Gamma^{(1)}$ is a narrow peak, centered on the frequency ω_q of an elementary excitation and $\Gamma^{(2)}$ corresponds to a much wider pedestal. A (schematic!) representation of this spectrum is given in figure 14, the Feynman formula corresponding to the center of gravity of the sum of these two components.

It remains to be understood why the Boulder and Cambridge experiments would be sensitive to the center of gravity of this double-structured line, rather than to the central peak. As far as we know, this question is open[7]. The problem of the interpretation of the experimental results is made even more complex by the fact that this separation between single and double excitation processes is not necessarily relevant on a practical level: we have indeed seen that over the duration of the experiment, an elementary excitation has a quite significant probability of decaying into two excitations of lower energy...

[7] I thank Johannes Hoffmann, Raphael Lopes and Willi Zwerger for the numerous exchanges on this subject.

3 Quantum mixtures and droplets

3-1 Position of the problem

In the experiments that we just described, the LHY energy was a small correction to the dominant mean-field energy and it had very little effect on the equilibrium form of the gas in its ground state. This is of course due to the $na^3 \ll 1$ validity criterion of the LHY calculation. As explained above [*cf.* (7)], this criterion is unavoidable when one takes into account the necessity to reach thermal equilibrium in a sufficiently short time for the three-body losses to be negligible. Despite this constraint, we wish to address here the following question: are there situations where the LHY energy, despite the smallness of na^3, plays a determining role in the equilibrium and in the dynamics of the gas?

Since the LHY contribution cannot be brought to a "standard" value of the mean field energy gn, the other option to make the two terms comparable is to lower the mean field energy. This is the idea put forward by Petrov (2015), and based on a mixture of two fluids. The principle is to start from a situation where the mean field energy for each of the fluids taken separately is positive (intra-species repulsion), while the mean field energy describing the interaction between the two fluids is negative (inter-species attraction). We can then reach a regime where the sum of the mean field energies is almost zero: the LHY energy becomes decisive to calculate the equilibrium shape of the fluid. We will see that this equilibrium corresponds to a "liquid" state, with a density independent of the number of particles. We thus speak about *quantum droplets*.

Another method to lower the mean field energy to the level of LHY energy appeared almost simultaneously to the proposal of Petrov (2015). It amounts to adding an additional term to the mean field and LHY energies describing the s-wave interactions, this term coming from the magnetic dipole-dipole interaction. This approach has been pursued experimentally by the Stuttgart (Ferrier-Barbut, Kadau, et al. 2016; Schmitt, Wenzel, et al. 2016) and Innsbruck (Chomaz, Baier, et al. 2016) groups. These studies then led to the observation of supersolid states in these two groups (Böttcher, Schmidt, et al. 2019; Chomaz, Petter, et al. 2019) and in Florence (Tanzi, Lucioni, et al. 2019). We refer interested readers to recent review

articles by Ferrier-Barbut (2019) and Böttcher, Schmidt, et al. (2021).

3-2 Mean-field stability of a binary mixture

In the following we will focus on the proposal of Petrov (2015), which is based on a binary mixture of two quantum fluids. We start by discussing the stability of such a mixture at the mean field level. We denote 1 and 2 the two components of the mixture, which can correspond to two different atomic species of mass m_1 and m_2, or to the same atomic species but with two different internal states. We denote g_{11} and g_{22} the intra-species mean field interaction parameters and g_{12} the inter-species coupling. We will take $m_1 = m_2$ for simplicity.

We will assume that the couplings g_{11} and g_{22} are positive, i.e. that each component taken separately is stable. On the other hand, we do not make any assumption at this stage about g_{12}. We will see later that the favorable situation corresponds to the case where g_{12} is negative and approximately equal to $-(g_{11}g_{22})^{1/2}$.

We will look at the stability of the mixture according to two criteria:

- There must be no demixing, i.e. the energy of the mixture must be lower than the energy of the system with separate phases.
- The system must be stable, i.e. it must not collapse on itself.

Let's start by evaluating the energy of the phase with demixing, where the species i occupies a volume V_i, with $V_1 + V_2 = V$ where V is the total accessible volume. We have

$$E_{\rm demix} = g_{11}\frac{N_1^2}{2V_1} + g_{22}\frac{N_2^2}{2V_2} \tag{49}$$

where we have neglected the (non-extensive) energy resulting from the surface tension between the two phases. The minimization of this energy with respect to V_1 (at constant total volume V) leads to the equilibrium of pressures $\frac{1}{2}g_{11}n_1^2 = \frac{1}{2}g_{22}n_2^2$ and we arrive at the minimal energy of this separated phase:

$$E_{\rm demix} = g_{11}\frac{N_1^2}{2V} + g_{22}\frac{N_2^2}{2V} + \sqrt{g_{11}g_{22}}\,\frac{N_1N_2}{V}. \tag{50}$$

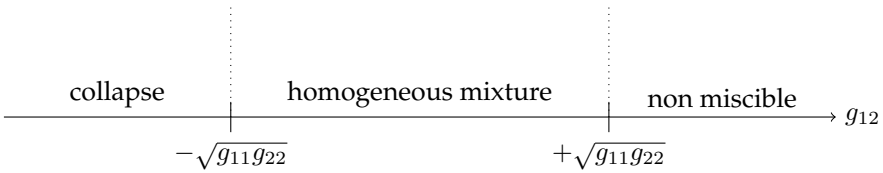

Figure 15. *The three possible scenarios according to the value of g_{12}.*

Let us now consider the mixed phase, where each species occupies the entire accessible volume V. Its mean-field energy is

$$E_{\rm mix} = g_{11}\frac{N_1^2}{2V} + g_{22}\frac{N_2^2}{2V} + g_{12}\frac{N_1N_2}{V}. \tag{51}$$

The comparison with the energy of the separated phase (50) immediately gives the criterion:

$$\boxed{\text{Miscibility if:} \qquad g_{12} < \sqrt{g_{11}g_{22}}} \tag{52}$$

Let us now look at the stability of this mixed phase. For any pair N_1, N_2, the energy (51) must be positive. If it were not the case, we could lower the energy (i.e. make it tend towards $-\infty$) by taking a volume $V \to 0$, which corresponds to a collapse of the system on itself. By rewriting the energy $E_{\rm mix}$ in the form

$$E_{\rm mix} = \frac{1}{2V}\left(\sqrt{g_{11}}\,N_1 - \sqrt{g_{22}}\,N_2\right)^2 + \frac{1}{V}\left(\sqrt{g_{11}g_{22}} + g_{12}\right)N_1N_2, \tag{53}$$

we see that the energy will always be positive if and only if

$$\boxed{\text{Stability if:} \qquad -\sqrt{g_{11}g_{22}} \;<\; g_{12}} \tag{54}$$

To continue the analysis, let us place ourselves for simplicity on the "minimizing" line which cancels the first term of (53), that is with atom numbers N_1 and N_2 chosen such that:

$$\sqrt{g_{11}}\,N_1 = \sqrt{g_{22}}\,N_2 \quad \Leftrightarrow \quad N_1 = N\frac{\sqrt{g_{22}}}{\sqrt{g_{11}}+\sqrt{g_{22}}},\;\; N_2 = N\frac{\sqrt{g_{11}}}{\sqrt{g_{11}}+\sqrt{g_{22}}}. \tag{55}$$

The mean field energy is then written (Petrov 2015):

$$\boxed{E_{\rm mix} = \frac{1}{2}\delta g \frac{N^2}{V}} \tag{56}$$

with

$$\delta g = 2\ (\sqrt{g_{11}g_{22}} + g_{12})\ \frac{\sqrt{g_{11}g_{22}}}{\left(\sqrt{g_{11}} + \sqrt{g_{22}}\right)^2}. \tag{57}$$

If we choose g_{12} very close to $-\sqrt{g_{11}g_{22}}$ (i.e. just at the edge of the collapse boundary of the figure 15), the parameter δg is small. The energy (56) thus has the structure of a? mean field energy for a one-component gas, but with a value of the coupling coefficient δg very reduced compared to the initial systems 1 and 2. This is precisely the effect we are looking for in order for the LHY energy to play a decisive role.

We can extend this study by calculating the excitation spectrum of the homogeneous mixture. Let us assume that $g_{11} = g_{22} \equiv g$ and $N_1 = N_2$ to simplify the writing of the result. Timmermans (1998) obtains in this case the two excitation branches:

$$\boxed{\omega_\pm^2(k) = \omega^2(k) \pm \frac{|g_{12}|}{g} c^2 k^2} \tag{58}$$

where c denotes the speed of sound in each of the condensates taken separately. These two branches correspond to the excitation of total density waves ($n_1 + n_2$ oscillation) and of "spin" waves ($n_1 - n_2$ oscillation). In the low k limit, we find two linear branches

$$\omega_\pm(k) = ck\left(1 \pm \frac{|g_{12}|}{g}\right)^{1/2}, \tag{59}$$

which are both real if and only the stability criterion (54) is satisfied. When this is not the case, the expression (58) allows to determine the k wavenumber which leads to the largest imaginary part of $\omega_\pm(k)$, and thus to the maximal instability.

3-3 LHY energy for a mixture

The LHY energy for a mixture has been calculated by Larsen (1963) and Minardi, Ancilotto, et al. (2019). In the homonuclear case $m_1 = m_2$, this energy is written:

$$E_{\rm LHY} = \frac{8V}{15\pi^2}\frac{m^{3/2}}{\hbar^3}\left(g_{11}n_1\right)^{5/2}\ f\left(\frac{g_{12}^2}{g_{11}g_{22}}, \frac{g_{22}n_2}{g_{11}n_1}\right) \tag{60}$$

where the dimensionless function $f(x, y)$ defined by

$$f(x,y) = \frac{1}{2^{5/2}}\sum_\pm \left[1 + y \pm \sqrt{(1-y)^2 + 4xy}\right]^{5/2} \tag{61}$$

is in practice of order unity. In the vicinity of the instability point $g_{12} = -\sqrt{g_{11}g_{22}}$, we have $x \approx 1$ so that this energy is written:

$$g_{12} \approx -\sqrt{g_{11}g_{22}}: \qquad E_{\rm LHY} = \frac{8}{15\pi^2}\frac{m^{3/2}}{\hbar^3}\frac{\left(g_{11}N_1 + g_{22}N_2\right)^{5/2}}{V^{3/2}}. \tag{62}$$

For a mixture in the proportion $N_2/N_1 = \sqrt{g_{11}/g_{22}}$ defined in (55), this energy simplifies to

$$\boxed{E_{\rm LHY} = \frac{8}{15\pi^2}\frac{m^{3/2}}{\hbar^3}\frac{\left(\bar{g}N\right)^{5/2}}{V^{3/2}} \qquad \text{with} \quad \bar{g} = \sqrt{g_{11}g_{22}}} \tag{63}$$

that is, the LHY energy of a gas with a coupling constant $\bar{g}$ [*cf.* (1)]. The LHY energy is therefore not significantly reduced in the vicinity of the instability point $g_{12} = -\sqrt{g_{11}g_{22}}$, unlike the mean field energy (56).

3-4 Droplet stabilization

To form an edifice stabilized by LHY energy, Petrov (2015) suggested adjusting the value of the interspecies coupling g_{12} in the vicinity of the collapse zone in figure 15, more precisely inside the unstable region. If it were alone, the mean field energy (56) would then lead to a collapse of the gas on itself, since δg is negative. Two terms may oppose this collapse. To estimate them, let us note $V = \ell^3$ the effective volume occupied by the fluid at equilibrium. These two terms are

- The kinetic energy term

$$\boxed{E_{\rm kin} \approx \frac{N\hbar^2}{2m\ell^2} = \frac{N\hbar^2}{2mV^{2/3}}} \tag{64}$$

This single-particle contribution corresponds to the energy needed to confine an atom in a domain of size ℓ;

- The LHY term calculated in (63).

Both of these positive contributions increase as the cloud contracts and thus can effectively counterbalance the mean field term.

To simplify the discussion, we will review the separate action of each of these two terms against the mean field term. If only the kinetic energy and the mean field term are considered, the equilibrium volume of the fluid V must minimize

$$E_{\text{kin+MF}}(V) = \frac{N\hbar^2}{2mV^{2/3}} - \frac{|\delta g|N^2}{2V}. \tag{65}$$

This function of V is plotted in figure 16 and the stationary point that appears is clearly unstable for our three dimensional problem[8]. The desired equilibrium can therefore not occur in practice.

If only the LHY term and the mean field term are considered, the equilibrium volume must minimize

$$E_{\text{LHY+MF}}(V) = \gamma\frac{m^{3/2}}{\hbar^3}\frac{(\bar{g}N)^{5/2}}{V^{3/2}} - \frac{|\delta g|N^2}{2V} \qquad \text{with} \quad \gamma = \frac{8}{15\pi^2}. \tag{66}$$

This function is plotted in figure 17 and it leads to a stable minimum: the LHY energy can thus effectively prevent the collapse of the gas on itself that the mean field tends to cause. More precisely, we find that this minimum corresponds to a density $n = N/V$ given by (up to a numerical coefficient):

$$n\,\bar{a}^3 \sim \left(\frac{|\delta g|}{\bar{g}}\right)^2 \qquad \text{with} \quad \bar{g} = \frac{4\pi\hbar^2\bar{a}}{m}. \tag{67}$$

We arrive at the following important result: the equilibrium volume is such that the density within the droplet $n = N/V$ is independent of the number of atoms. This corresponds to the definition of a liquid, i.e. a state that is both fluid and almost incompressible [this last point is confirmed by

[8]The situation would be different in 1D where the mean field term would vary as $-|\delta g|N^2/2\ell$. We would then find the well known situation which leads to the formation of solitons. The transition between the soliton regime and the droplet regime is discussed by Cheiney, Cabrera, et al. (2018).

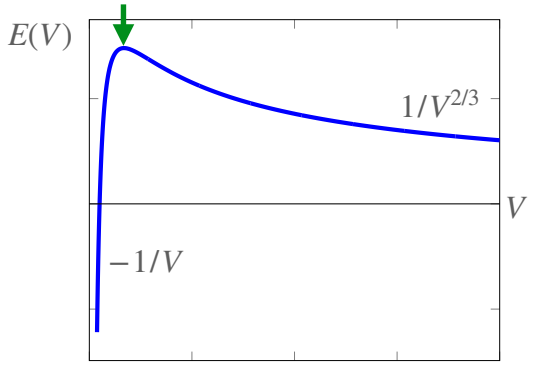

Figure 16. *Competition between the mean field term (56) and the kinetic energy term (64) for a 3D cloud. The equilibrium indicated by the arrow is unstable.*

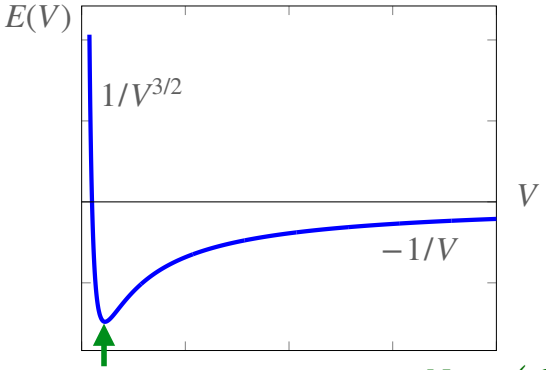

Figure 17. *Competition between the mean field term (56) and the LHY term (63). The equilibrium indicated by the arrow is stable.*

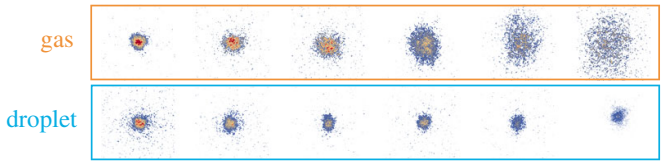

Figure 18. *Evolution of a ^{39}K gas in free space for a mixture of the two hyperfine states $|F = 1, m = 0\rangle$ and $|F = 1, m = -1\rangle$. Top row: expansion (gas regime) obtained for $|\delta g|$ very small, with the kinetic energy playing a significant role; bottom row: droplet regime obtained for $|\delta g|$ larger and resulting essentially from the competition between mean field energy and LHY energy. The images are taken at $t = 0, 2, \ldots, 10$ ms. The initial number of atoms in the droplet is of the order of 200 000 and the* r.m.s. *size of the order of 2μm. The ratio N_1/N_2, on the order of 0.7, is in good agreement with the theoretical prediction. Figure taken from Semeghini, Ferioli, et al. (2018).*

the study of the vibration modes of the droplet (Petrov 2015)]. We note moreover that this density satisfies the validity criterion of the Bogoliubov approximation $n\bar{a}^3 \ll 1$, if we take care to keep $|\delta g|$ small in front of the typical value $\bar{g}$ of the coupling coefficient.

In practice, it is of course appropriate to consider simultaneously the kinetic energy and the LHY contribution to quantitatively study the competition with the negative mean field energy. However, for large numbers of atoms, kinetic energy plays a small role and the prediction (67) can be used as a good approximation.

We will not describe here the experimental observation of these droplets since this subject will be detailed in the seminar and workshop of April 15. Let us just mention that these droplets have been observed in absence of confinement by Semeghini, Ferioli, et al. (2018) in Florence and Guo, Jia, et al. (2021) in Beijing. The experiments of Taruell's group in Barcelona have been performed in a one- or two-dimensional confinement (Cabrera, Tanzi, et al. 2018; Cheiney, Cabrera, et al. 2018). An example of a result from the Florence group is shown in figure 18.

Appendix

Demonstration of the Feynman relation

We start with the time-dependent perturbation $\hat{V}(t) = \hat{V}^{(+)}\ \mathrm{e}^{-\mathrm{i}\omega t} + \mathrm{H.c.}$ which probes the density of the fluid at a particular wave vector $\boldsymbol{q}$:

$$\hat{V}^{(+)} = \hbar\kappa \int \hat{n}(\boldsymbol{r}) \mathrm{e}^{\mathrm{i}\boldsymbol{q}\cdot\boldsymbol{r}}\ \mathrm{d}^3 r \tag{68}$$

where the operator $\hat{n}(\boldsymbol{r})$ is associated with the spatial density in $\boldsymbol{r}$: $\hat{n}(\boldsymbol{r}) = \sum_{j=1}^{N} \delta\left(\boldsymbol{r} - \hat{\boldsymbol{r}}_j\right)$. The operator $\hat{V}^{(+)}$ is therefore:

$$\hat{V}^{(+)} = \hbar\kappa \sum_j \mathrm{e}^{\mathrm{i}\boldsymbol{q}\cdot\hat{\boldsymbol{r}}_j}. \tag{69}$$

The probability per unit of time to excite the system assuming that it is initially in its ground state $|\psi_0\rangle$ is given by the Fermi golden rule:

$$\Gamma(\boldsymbol{q}, \omega) = \frac{2\pi}{\hbar} \sum_f \left|\langle\psi_f|\hat{V}^{(+)}|\psi_0\rangle\right|^2\ \delta(E_f - E_0 - \hbar\omega) \tag{70}$$

and we define the average frequency $\bar{\omega}$ as

$$\bar{\omega}(\boldsymbol{q}) = \frac{\int_{-\infty}^{+\infty} \omega\ \Gamma(\boldsymbol{q}, \omega)\ \mathrm{d}\omega}{\int_{-\infty}^{+\infty} \Gamma(\boldsymbol{q}, \omega)\ \mathrm{d}\omega} = \frac{\mathcal{N}(\boldsymbol{q})}{\mathcal{D}(\boldsymbol{q})} \tag{71}$$

where in fact only the positive frequencies contribute to Γ since the system is initially in its ground state.

Calculation of the numerator $\mathcal{N}(q)$. The integral over ω is written:

$$\begin{aligned} \mathcal{N}(\boldsymbol{q}) &= \frac{2\pi}{\hbar^3} \sum_f \langle\psi_0|\hat{V}^{(-)}|\psi_f\rangle\ \langle\psi_f|\hat{V}^{(+)}|\psi_0\rangle\ (E_f - E_0) \\ &= \frac{2\pi}{\hbar^3} \sum_f \langle\psi_0|\hat{V}^{(-)}|\psi_f\rangle\ \langle\psi_f|\left[\hat{H}, \hat{V}^{(+)}\right]|\psi_0\rangle \end{aligned} \tag{72}$$

which gives

$$\begin{aligned}\mathcal{N}(\boldsymbol{q}) &= \frac{2\pi}{\hbar^3}\langle\psi_0|\,\hat{V}^{(-)}\,\left[\hat{H},\hat{V}^{(+)}\right]|\psi_0\rangle \\ &= -\frac{2\pi}{\hbar^3}\langle\psi_0|\,\left[\hat{H},\hat{V}^{(-)}\right]\,\hat{V}^{(+)}\,|\psi_0\rangle \end{aligned} \tag{73}$$

Because of the isotropy of the system, the result for $\mathcal{N}(\boldsymbol{q})$ is equal to that for $\mathcal{N}(-\boldsymbol{q})$. Since the substitution $\boldsymbol{q}\to-\boldsymbol{q}$ corresponds to the exchange of $\hat{V}^{(+)}$ and $\hat{V}^{(-)}$, we deduce that $\mathcal{N}(\boldsymbol{q})$ is equal to

$$\mathcal{N}(\boldsymbol{q}) = \frac{\pi}{\hbar^3}\langle\psi_0|\,\left[\hat{V}^{(-)},\left[\hat{H},\hat{V}^{(+)}\right]\right]|\psi_0\rangle. \tag{74}$$

The Hamiltonian of the gas is written:

$$\hat{H} = \sum_j \frac{\hat{\boldsymbol{p}}_j^2}{2m} + \frac{1}{2}\sum_{i\neq j} v(\hat{r}_{ij}). \tag{75}$$

Therefore, only the kinetic energy term has a nonzero commutator with the operators $\hat{V}^{(\pm)}$. We find:

$$\left[\hat{H},\hat{V}^{(+)}\right] = \frac{\hbar\kappa}{2m}\,\sum_j\left[\hat{\boldsymbol{p}}_j^2,\mathrm{e}^{\mathrm{i}\boldsymbol{q}\cdot\hat{\boldsymbol{r}}_j}\right] = \frac{\hbar^2\kappa}{2m}\sum_j \boldsymbol{q}\cdot\left(\hat{\boldsymbol{p}}_j\,\mathrm{e}^{\mathrm{i}\boldsymbol{q}\cdot\hat{\boldsymbol{r}}_j} + \mathrm{e}^{\mathrm{i}\boldsymbol{q}\cdot\hat{\boldsymbol{r}}_j}\,\hat{\boldsymbol{p}}_j\right) \tag{76}$$

and

$$\left[\hat{V}^{(-)},\left[\hat{H},\hat{V}^{(+)}\right]\right] = \frac{\hbar^4\kappa^2}{m}\,Nq^2 \tag{77}$$

so that we finally obtain (41).

The link with the Thomas–Reiche–Kuhn relation in atomic physics is made by choosing for simplicity an atom with only one outer electron. For this electron, of position $\hat{x}$ and mass m, we find for an energy eigenstate $|m\rangle$:

$$\sum_n (E_n - E_m)\,|\langle n|\hat{x}|m\rangle|^2 = \frac{\hbar^2}{2m} \tag{78}$$

The proof is similar to the above, with the operators $\hat{V}^{(\pm)}$ replaced by $\hat{x}$.

Calculation of the denominator $\mathcal{D}(q)$.

The integral over ω gives :

$$\begin{aligned}\mathcal{D}(\boldsymbol{q}) &= \frac{2\pi}{\hbar^2}\sum_f \langle\psi_0|\hat{V}^{(-)}|\psi_f\rangle\,\langle\psi_f|\hat{V}^{(+)}|\psi_0\rangle \\ &= \frac{2\pi}{\hbar^2}\langle\psi_0|\,\hat{V}^{(-)}\,\hat{V}^{(+)}\,|\psi_0\rangle \\ &= 2\pi\kappa^2\left(N + \sum_{i\neq j}\langle\psi_0|\mathrm{e}^{\mathrm{i}\boldsymbol{q}\cdot(\hat{\boldsymbol{r}}_i-\hat{\boldsymbol{r}}_j)}|\psi_0\rangle\right)\end{aligned} \tag{79}$$

which leads to (42).

The spatial correlation function $g_2(r)$

The calculation of the $g_2(r)$ function for the ground state of the Bose gas was carried out in detail in the original article by Lee, Huang, et al. (1957). We simply reproduce here the main lines of this calculation, which is a bit tedious but without noticeable difficulty. Different aspects of the behavior of the function $g_2(r)$ have been analyzed in the more recent articles of Naraschewski & Glauber (1999) and Holzmann & Castin (1999).

The correlation function g_2 is written as the square of the norm of a vector:

$$g_2(r) = \frac{1}{n^2}\|\hat{\Psi}(\boldsymbol{r})\hat{\Psi}(0)|0_B\rangle\|^2, \tag{80}$$

where $|0_B\rangle$ denotes the ground state of the gas, i.e. the vacuum of Bogoliubov excitations. Let us replace the field operators $\hat{\Psi}(0)$ and $\hat{\Psi}(\boldsymbol{r})$ by their expression in terms of the creation and destruction operators of elementary excitations

$$\begin{aligned}\hat{\Psi}(\boldsymbol{r}) &= \sqrt{n}_0 + \frac{1}{\sqrt{L^3}}\sum_{\boldsymbol{k}\neq 0}\mathrm{e}^{\mathrm{i}\boldsymbol{k}\cdot\boldsymbol{r}}\,a_{\boldsymbol{k}} \\ &= \sqrt{n}_0 + \frac{1}{\sqrt{L^3}}\sum_{\boldsymbol{k}\neq 0}\mathrm{e}^{\mathrm{i}\boldsymbol{k}\cdot\boldsymbol{r}}\left(u_k b_{\boldsymbol{k}} - v_k b_{-\boldsymbol{k}}^\dagger\right).\end{aligned} \tag{81}$$

We then see that the vector entering in (80) can contain 0, 1 or 2 Bogoliubov

excitations:

$$\begin{aligned}\hat\Psi(\boldsymbol{r})\hat\Psi(0)|0_B\rangle &= \left(n_0 - \frac{1}{L^3}\sum_{\boldsymbol{k}\neq 0} u_k v_k\, \mathrm{e}^{-\mathrm{i}\boldsymbol{k}\cdot\boldsymbol{r}}\right)|0_B\rangle \\ &- \frac{\sqrt{n_0}}{\sqrt{L^3}}\sum_{\boldsymbol{k}\neq 0} v_k\left(1+\mathrm{e}^{-\mathrm{i}\boldsymbol{k}\cdot\boldsymbol{r}}\right)|1_{\boldsymbol{k}}\rangle \\ &+ \frac{1}{L^3}\sum_{\text{pairs }\boldsymbol{k},\boldsymbol{k}'} v_k v_{k'}\left(\mathrm{e}^{-\mathrm{i}\boldsymbol{k}\cdot\boldsymbol{r}}+\mathrm{e}^{-\mathrm{i}\boldsymbol{k}'\cdot\boldsymbol{r}}\right)|1_{\boldsymbol{k}}1_{\boldsymbol{k}'}\rangle \quad (82)\end{aligned}$$

We obtain the correlation function[9]

$$\begin{aligned}g_2(r) &= [1+F(r)]^2 + [1+G(r)]^2 - 1 - 2\frac{n'}{n}[F(r)+G(r)] \quad (83)\\ &= 1 + 2\frac{n_0}{n}[F(r)+G(r)] + F^2(r) + G^2(r) \quad (84)\end{aligned}$$

where we have adopted the same notations as Lee, Huang, et al. (1957):

$$F(r) = \frac{1}{N}\sum_{\boldsymbol{k}\neq 0} v_k^2\, \mathrm{e}^{\mathrm{i}\boldsymbol{k}\cdot\boldsymbol{r}}, \qquad G(r) = -\frac{1}{N}\sum_{\boldsymbol{k}\neq 0} u_k v_k\, \mathrm{e}^{\mathrm{i}\boldsymbol{k}\cdot\boldsymbol{r}}. \quad (85)$$

Asymptotic behaviors. Lee, Huang, et al. (1957) give the short and long range expansions of the functions F and G. In the neighborhood of $r=0$, they find:

$$r \ll \xi : \qquad F(r) \approx \frac{n'}{n}, \qquad G(r) \approx -\frac{a}{r} + \frac{8}{\sqrt{\pi}}\sqrt{na^3} \quad (86)$$

which leads to

$$r \ll \xi : \qquad g_2(r) = \left(1-\frac{a}{r}\right)^2 + \mathcal{O}(a/\xi). \quad (87)$$

At large distances, Lee, Huang, et al. (1957) find:

$$r \gg \xi : \qquad F(r) \sim -G(r) \sim \frac{1}{\pi^2 n\xi}\frac{1}{r^2} \quad (88)$$

which leads to

$$r \gg \xi : \qquad g_2(r) \approx 1 + \mathcal{O}\left(r^{-4}\right). \quad (89)$$

[9] Note that the corresponding equation of the article of Lee, Huang, et al. (1957) contains a term $4n'/n$ instead of $2n'/n$ in factor of the last term of (83). This error was reported by Garcia-Colin (1960).

The structure factor $S(q)$

Once the function g_2 is known, we calculate the Fourier transform of $g_2(r)-1$ to determine $S(q)$ which intervenes directly in the Feynman formula. To carry out this calculation, we start from the expression (84) which we put in the form

$$g_2(r) = 1 + g_{2,a}(r) + g_{2,b}(r) \quad (90)$$

with

$$g_{2,a}(r) = 2\frac{n_0}{n}[F(r)+G(r)] \qquad g_{2,b}(r) = F^2(r)+G^2(r), \quad (91)$$

and we pose

$$S(q) = 1 + S_a(q) + S_b(q) \quad (92)$$

with

$$S_{a/b}(q) = n\int g_{2,a/b}(r)\,\mathrm{e}^{-\mathrm{i}\boldsymbol{q}\cdot\boldsymbol{r}}\,\mathrm{d}^3 r. \quad (93)$$

Contribution of $g_{2,a}(r)$. The calculation of the Fourier transform of $g_{2,a}(r)$ is straightforward: since F and G are defined in (85) as Fourier transforms of v_k^2 and $-u_k v_k$, we find:

$$S_a(q) = -2\frac{n_0}{n} v_q(u_q - v_q). \quad (94)$$

In the $n_0 \approx n$ approximation (quantum depletion neglected when $\sqrt{na^3} \ll 1$), we can notice that this contribution alone leads to the result for the Bogoliubov spectrum given in (24)

$$\frac{\epsilon_q}{1+S_a(q)} \approx \frac{\epsilon_q}{1-2v_q(u_q-v_q)} = \hbar\omega_q. \quad (95)$$

In particular, in the limit $q\xi \gg 1$, we saw in the previous chapter that $u_q \sim 1$ and $v_q \sim 1/2q^2\xi^2 \ll u_q$, so this expression simplifies to

$$q\xi \gg 1 : \qquad S_a(q) \approx -\frac{n_0}{n}\frac{1}{q^2\xi^2} \approx -\frac{1}{q^2\xi^2}. \quad (96)$$

Contribution of $g_{2,b}(r)$. The complete calculation of the Fourier transform of $g_{2,b}(r)$ is more complicated than for $g_{2,a}(r)$ and we just consider here the dominant term for $q\xi \gg 1$ and $\sqrt{na^3} \ll 1$. The only term to take into account then comes from the Fourier transform of $G^2(r)$, which can be evaluated using the expression of G at small r given in (86):

$$S_b(q) \approx n \int G^2(r)\, \mathrm{e}^{-\mathrm{i}\boldsymbol{q}\cdot\boldsymbol{r}}\, \mathrm{d}^3 r \approx n \int \frac{a^2}{r^2}\, \mathrm{e}^{-\mathrm{i}\boldsymbol{q}\cdot\boldsymbol{r}}\, \mathrm{d}^3 r = \frac{2\pi^2 n a^2}{q}. \qquad (97)$$

Summary for the $q\xi \gg 1$ regime. Combining (92), (96) and (97), we arrive at the result (44).

Chapter V

The two-body contact

In the previous chapters, we were interested in the link between two-body physics, described by the scattering length a, and the properties of a N-body system, discussed by the Bogoliubov method. This link was possible for a weakly interacting gas, the small parameter of the problem being $\sqrt{na^3}$. This imposed that the distance between particles $d = n^{-1/3}$ always remained large in front of a.

The purpose of this chapter is to explore the "2-body – N-body" link without making any assumption on the a/d ratio. More precisely, we will not put any constraint on the value of the scattering length a, which can be experimentally adjusted almost at will for atomic species exhibiting a Fano-Feshbach resonance. It can be set to a positive or negative value, from $|a| \lesssim b$ (where b is the range of the potential, itself of the order of a few nanometers) up to values greater than a micrometer, which becomes large compared to the distance between particles: $a \gtrsim d$. On the other hand, we will always assume that the system is dilute, i.e. that the range of the potential b satisfies $b \ll d$. We will also restrict ourselves (with one exception in the next chapter) to cases where only the s-wave interactions play a significant role.

To the three length scales a, b and d that we have just mentioned, we add the thermal wavelength $\lambda = \left(2\pi\hbar^2/mk_{\rm B}T\right)^{1/2}$ (*cf.* figure 1). In the first chapter of this course, we explained how the virial expansion allowed us to approach the weakly degenerate case $\lambda \ll d$. In the following we will concentrate on the strongly degenerate case $\lambda \gtrsim d$.

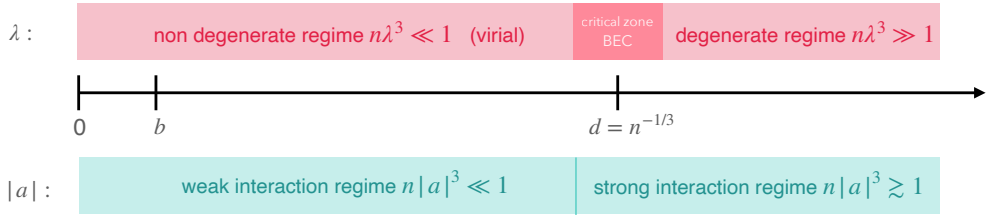

Figure 1. *The four length scales of the problem: potential range b and scattering length a for the two-body problem, mean inter-particle distance d and thermal wavelength λ for the N-body problem. The system will always be assumed to be dilute: $b \ll d$. In this chapter, we will be mainly interested in the degenerate regime, $\lambda > d$, and in the case of a large scattering length $a \gg b$.*

For the case of three-dimensional gases that will interest us here, the "2-body – N-body" link was largely initiated by Shina Tan in a series of three papers. The first two were deposited on arXiv in 2005, but these three papers were only published (together) in 2008 (Tan 2008a; Tan 2008b; Tan 2008c). In this work, Tan established a large number of universal relations verified by a two-component Fermi gas, with interactions described in the zero range limit.

These relations that we are going to study link microscopic quantities, such as the momentum distribution of the gas or its two-body spatial correlation function, to macroscopic quantities, such as its ground state energy

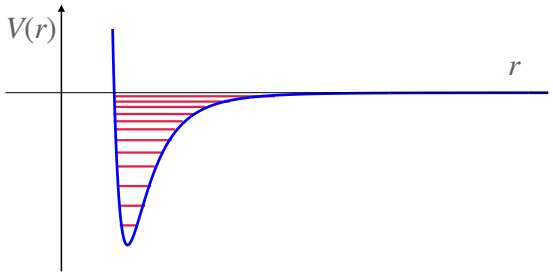

Figure 2. *Two-body interaction potential $V(r)$. The potential well, whose depth is typically several hundred kelvins, contains many ro-vibrational bound states.*

and more generally its free energy or its pressure. They involve a quantity C called "contact", a name justified by the fact that it constitutes a measure of the probability of having two particles close to each other. The interest of relations involving contact is that they do not require precise knowledge of the state of the system, which we would not be able to provide in the case of strong interactions $a \gtrsim d$.

Tan's approach has been further developed and generalized theoretically by many authors, and additional universal relationships have been established. It is not possible to cite them all here. Let us simply mention the articles that, in addition to Tan's, served as the basis for writing this and the next chapter: Baym, Pethick, et al. 2007; Punk & Zwerger 2007; Braaten & Platter 2008; Werner, Tarruell, et al. 2009; Zhang & Leggett 2009; Combescot, Alzetto, et al. 2009; Yu, Bruun, et al. 2009; Braaten, Kang, et al. 2010; Braaten 2011; Werner & Castin 2012a; Werner & Castin 2012b.

1 Scope of the contact concept

1-1 Contribution of bound states

Before approaching the presentation of the contact, it is important to specify the framework in which we will work. A first point concerns the states linked to two (or more) particles. For the atomic species used in the laboratory, the two-body interaction potential $V(r)$ represented in figure 2 has a depth of the order of several hundreds of kelvins and it generally includes many bound states. Apart from a Fano–Feshbach resonance, the energy of the last bound state is of the order of about ten times the van der Waals energy E_{vdW} (see course 2021), i.e. from 0.1 to 1 mK depending on the species. This energy is large compared to the characteristic energies of gases, which are in the range 10 nK–1 μK. This considerable difference is still increased for the more strongly bound states in the potential $V(r)$. It follows that the formation of dimers in these states constitutes a irreversible loss of atoms for the gas. Once these dimers are formed, they generally escape the trap confining the assembly of atoms and they do not enter the realization of the thermodynamic equilibrium. We will therefore ignore them in the following.

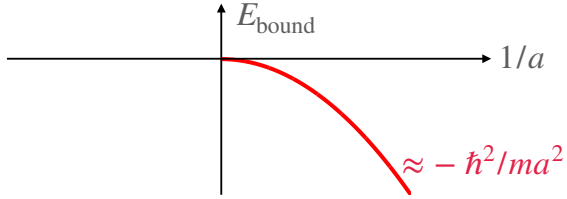

Figure 3. *Energy of the bound state that appears on the $a > 0$ side of a Fano–Feshbach resonance.*

The situation is different for the very weakly bound state which appears in the vicinity of a Fano-Feshbach resonance, more precisely on the $a > 0$ side of the resonance (figure 3). The resonance corresponds to $|a| = +\infty$ (*i.e.* $1/a = 0$) and the energy of the bound state, very low in absolute value, is $\approx -\hbar^2/ma^2$. This binding energy is comparable to the other energy scales of the gas and this bound state must therefore be taken into account for the study of the dynamics and thermodynamics of the N body system.

In the vicinity of this resonance, one can also wonder about the possibility of forming more complex states, with three bodies for example. For fermions of spin $1/2$ with $m_\uparrow \approx m_\downarrow$, the Pauli principle forbids the formation of a three-body state. On the other hand, for bosons or for spin $1/2$ fermions with a large difference between $m_\uparrow$ and $m_\downarrow$, these weakly bound

three-body states exist – this is the Efimov effect – and must also be taken into account [for a review of the three-body problem, see Naidon & Endo (2017)].

1-2 Conditions of application : fermions vs. bosons

We will see that the central element of Tan's approach, the *contact*, is the thermodynamically conjugate quantity of the scattering length a. The contact allows to characterize thermodynamically all the short-range physics of the system, provided that the interactions between particles do not introduce any other energy scale than $\hbar^2/ma^2$ in the relevant energy domain for these quantum gases. In particular, the three-body problem and the Efimov effect should not invalidate this assumption.

As we have indicated in the previous paragraph (§ 1-1), the Efimov effect is absent for a gas of $1/2$ spin fermions with $m_\uparrow \approx m_\downarrow$. The first field of application of the results of this chapter is therefore a gas of N fermions of spin[1] $1/2$. In this case, we will not need any restriction on the sign or the value of the scattering length a characterizing the $\uparrow\downarrow$ interactions.

For a gas of bosons (or for a gas of fermions with a ratio $m_\uparrow/m_\downarrow$ very different from 1), we have explained that the assumption stated above is not always correct. In the vicinity of a scattering resonance, three-body physics can introduce new length and energy scales, which then complicates the problem since a is no longer the only quantity characterizing the interactions. To avoid this difficulty, we will assume in this chapter that the Bose gas is prepared in a configuration such that :

- the scattering length a is positive, to ensure its mean-field stability;
- the density is sufficiently low that $na^3 \ll 1$, i.e. $a \ll d$, so that there is a time range during which the gas can reach its equilibrium state related to two-body interactions, without the three-body states being appreciably populated (see Chapter 4, § 1.1).

Note that these assumptions remain compatible with the use of a Fano–Feshbach resonance, $b \ll a$ provided that we have simultaneously $a \ll d$.

[1] It can of course be a pseudo-spin, the two states being chosen from the set of Zeeman sub-levels of the atoms.

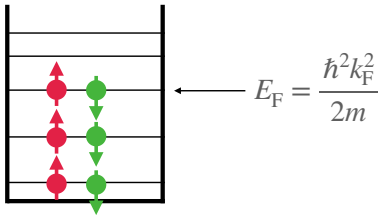

Figure 4. *Ground state of an equilibrated ideal Fermi gas, with the filling of the single-particle states up to the Fermi level.*

1-3 Reminder on the Fermi gas

Since the Fermi gas will play an essential role in this chapter, we will recall here some definitions and properties concerning this system. We will assume that the gas is "balanced", i.e. that there is the same number of atoms in each spin state:

$$N_\uparrow = N_\downarrow \equiv \frac{N}{2}. \tag{1}$$

In the absence of interaction, the ground state of the gas is obtained by filling with two particles (one $\uparrow$, one $\downarrow$) each momentum state from the momentum zero to the momentum $\hbar k_\mathrm{F}$ (figure 4). The value of the Fermi level is deduced from

$$N = \sum_{\boldsymbol{k}}^{|\boldsymbol{k}|<k_\mathrm{F}} 2. \tag{2}$$

Using the usual transition from a discrete sum over $\boldsymbol{k}$ to an integral:

$$N = \frac{L^3}{(2\pi)^3} \int_{|\boldsymbol{k}|<k_\mathrm{F}} 2\, \mathrm{d}^3k = \frac{L^3 k_\mathrm{F}^3}{3\pi^2}, \tag{3}$$

we get

$$k_\mathrm{F} = \left(3\pi^2 n\right)^{1/3} \qquad \text{with} \quad n = \frac{N}{L^3}. \tag{4}$$

The energy of the ground state in absence of interaction is:

$$E = \sum_{\boldsymbol{k}=0}^{|\boldsymbol{k}|<k_\mathrm{F}} 2\, \frac{\hbar^2 k^2}{2m} = \frac{3}{5} N E_\mathrm{F} \qquad \text{with} \quad E_\mathrm{F} = \frac{\hbar^2 k_\mathrm{F}^2}{2m}. \tag{5}$$

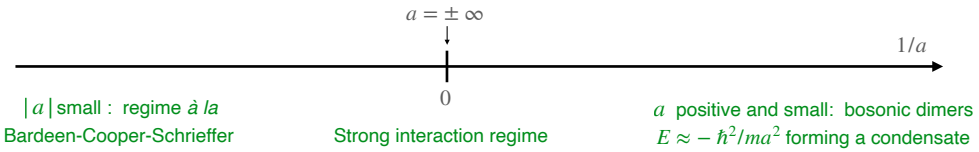

Figure 5. *The different regimes for the ground state of a Fermi gas with s-wave $\uparrow\downarrow$ interactions, characterized by the scattering length a.*

Let us now take into account the interactions. At low temperature, only the s-wave interactions are significant and the Pauli principle forbids this channel for the $\uparrow\uparrow$ and $\downarrow\downarrow$ collisions. On the other hand, interactions between the two components $\uparrow\downarrow$ are possible and they make this system extremely rich. For any value of a, positive or negative, one predicts and observes a transition from the normal state at high temperature to a superfluid state at low temperature [see for example Zwerger (2012)]. In particular, when a Fano–Feshbach resonance is crossed, the following regimes are observed for the ground state (figure 5):

- For a positive and small in front of d, this superfluid state can be approximated by the Bose–Einstein condensation theory, with pairs of fermions that form in real space to constitute bosonic dimers.
- For a negative and small in absolute value, the superfluid state can be described by the BCS (Bardeen–Cooper–Schrieffer) theory.
- In the vicinity of the resonance, we find the strong interaction regime $n|a|^3 \gtrsim 1$.

It is not our intention to review in this chapter all the physics of the interacting Fermi gas. We will only indicate the elements that are essential for the study of the link between binary interactions and macroscopic properties of the fluid.

1-4 Wide or narrow Feshbach resonances?

Tan's approach allows to provide quantitative predictions on strongly interacting systems with a scattering length a large in front of the range of the potential b. In atomic gas physics, the range b is given by the van der Waals length $R_{\rm vdW}$ and a large scattering length a is usually obtained via a Fano–Feshbach resonance. We studied these resonances in last year's course and showed that they can be classified into two categories:

- The large resonances, for which the scattering amplitude is written as a good approximation
$$f(k) \approx \frac{-a}{1+\mathrm{i}ka} \tag{6}$$
for all k such that $k \lesssim b^{-1}$. The scattering length is in this case the only relevant parameter to characterize the binary interactions and everything that follows in this chapter applies without problem.
- Narrow resonances, for which a quadratic term must be taken into account in the denominator of this fraction:
$$f(k) \approx \frac{-a}{1+\mathrm{i}ka+k^2R_*a}, \tag{7}$$
the length R_* being large before the "natural" range $b \approx R_{\rm vdW}$ (Petrov 2004). For these narrow resonances, corresponding to an abnormally large effective range term $r_e = -2R_*$, the following approach is not applicable[2], since the scattering length alone is not sufficient to characterize binary interactions in the $k \lesssim b^{-1}$ domain.

2 Contact and two-body correlations

2-1 Reminder : scattering states close to $E = 0$

We will recall here some useful properties of low energy scattering states. For more details, we refer the reader to the course 2021. We are interested in s-wave collisions (thus isotropic) and the analysis of the process is done by considering the radial equation verified by the reduced wave function $u_k(r) = r\,\psi_k(r)$ of energy $E = \hbar^2k^2/2m_{\rm r}$, where $m_{\rm r} = m/2$ is the reduced

[2] Werner & Castin (2012b) detail how to generalise Tan's approach to take into account the effective range term.

mass :

$$-\frac{\hbar^2}{2m_r}u_k'' + V(r)\,u_k(r) = E\,u_k(r). \tag{8}$$

Outside the range of the potential, this solution is written in terms of the phase shift $\delta_0(k)$:

$$r \gtrsim b : \qquad u_k(r) \propto \sin[kr + \delta_0(k)]. \tag{9}$$

The scattering length is defined by $a = -\lim_{k\to 0}\delta_0(k)$ so that (9) becomes

$$r \gtrsim b, k \to 0 : \qquad u_k(r) \propto a - r. \tag{10}$$

This behavior common to all reduced radial functions $u_k(r)$ for k small is illustrated on figure 6 in the case of a square well. We placed ourselves in the vicinity of a resonance with $a = 10\,b$. The normalized wave function $\psi_0(r)$ has the following behavior:

$$r > b : \qquad \psi_0(r) = \frac{1}{\sqrt{L^3}}\left(\frac{a}{r} - 1\right) = \frac{a}{\sqrt{L^3}}\left(\frac{1}{r} - \frac{1}{a}\right), \tag{11}$$

and the behavior of $\psi_k(r)$ is similar for k sufficiently small. We will see in what follows that it is the behavior in $1/r$ of ψ_0 that plays a determining role.

2-2 A qualitative argument

To begin with, let us consider the wave function of the ground state of a gas of N particles.

- For spinless bosons, we will write this wave function as $\Phi(\boldsymbol{r}_1, \boldsymbol{r}_2, \ldots, \boldsymbol{r}_N)$, with the normalization

$$\int |\Phi(\boldsymbol{r}_1, \boldsymbol{r}_2, \boldsymbol{r}_3, \ldots, \boldsymbol{r}_N)|^2\, \mathrm{d}^3 r_1 \ldots \mathrm{d}^3 r_N = 1. \tag{12}$$

  The particles having been arbitrarily numbered 1,2,..., this wave function gives the probability amplitude to find the particle 1 at the point $\boldsymbol{r}_1$, the particle 2 at the point $\boldsymbol{r}_2$,... and it is symmetric by exchange of two particles.

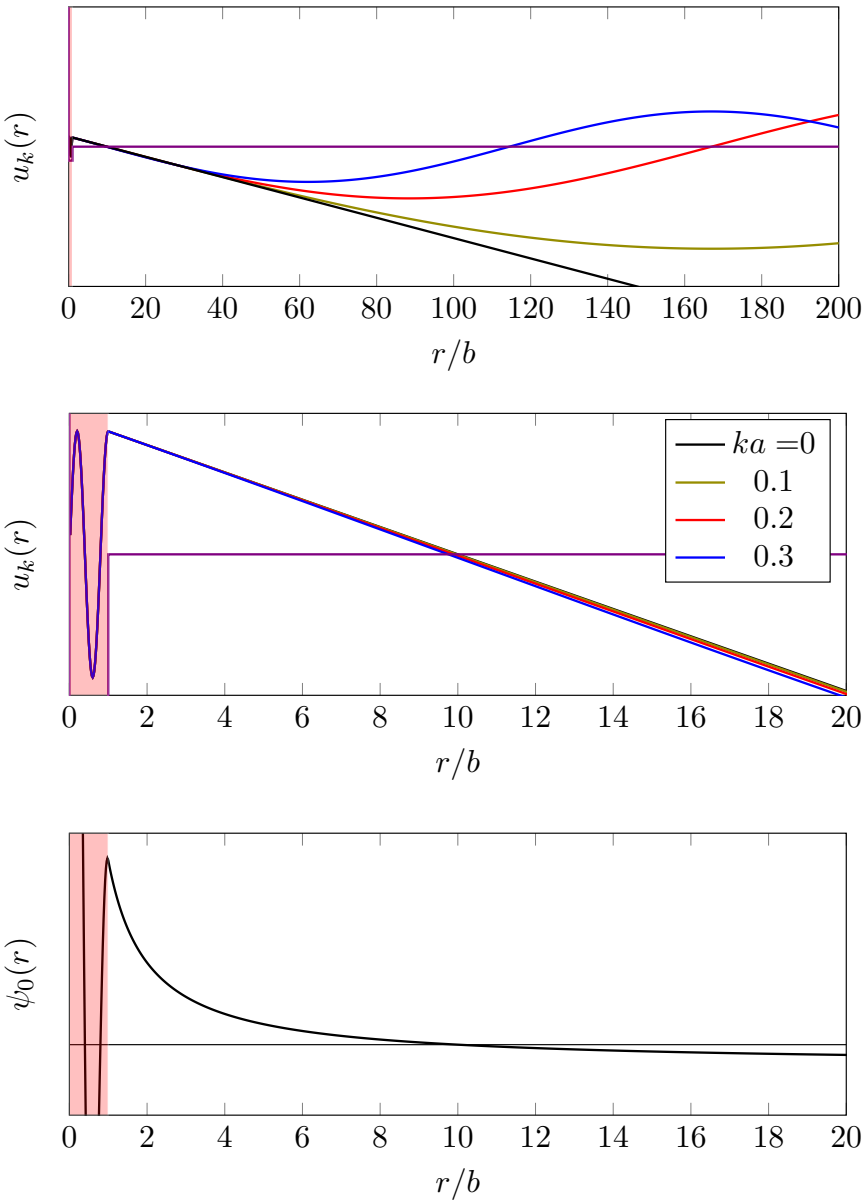

Figure 6. *Reduced radial functions $u_k(r)$ and radial function $\psi_0(r)$ for scattering by a square well with $a = 10\,b$.*

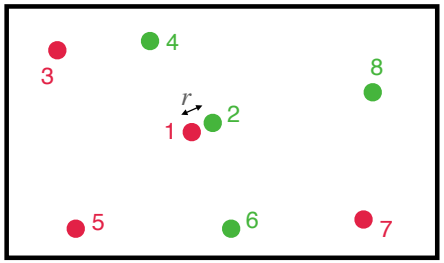

Figure 7. *N fermion system. We are interested in the behavior of the wave function Φ when particles 1 and 2 of opposite spin approach each other, the other particles being far from $\boldsymbol{r}_1$ and $\boldsymbol{r}_2$.*

- For the fermion case, we consider a gas with $N/2$ particles in the $\uparrow$ spin state and $N/2$ particles in the $\downarrow$ spin state. We can write the N-body wave function by assigning the odd indices $\boldsymbol{r}_1, \boldsymbol{r}_3, \ldots$ to the $N/2$ fermions of spin $\uparrow$ and the even indices $\boldsymbol{r}_2, \boldsymbol{r}_4, \ldots$ to the $N/2$ fermions of spin $\downarrow$ with the same normalization as in (12). This wave function is antisymmetric by any permutation of two odd indices, and also antisymmetric by any permutation of two even indices.

Let us fix the positions $\boldsymbol{r}_3, \boldsymbol{r}_4, \ldots, \boldsymbol{r}_N$ and let us be interested in the variation of Φ when $\boldsymbol{r}_1$ and $\boldsymbol{r}_2$ approach each other. More precisely, let us pose

$$\boldsymbol{r}_1 = \boldsymbol{R} + \frac{\boldsymbol{r}}{2}, \qquad \boldsymbol{r}_2 = \boldsymbol{R} - \frac{\boldsymbol{r}}{2}, \tag{13}$$

and consider the limit of small r (typically of the order of b), assuming that the remaining $N-2$ particles are at a distance $\gg b$ from $\boldsymbol{R}$ (figure 7). It is then natural to assume the following result:

$$\Phi(\boldsymbol{r}_1, \boldsymbol{r}_2, \ldots, \boldsymbol{r}_N) \approx \psi_0(r)\ \tilde{\Phi}(\boldsymbol{R}, \boldsymbol{r}_3, \ldots, \boldsymbol{r}_N) \tag{14}$$

where $\psi_0(r)$ is the scattering state for the relative particle of the pair (1,2) at zero energy (see figure 6, bottom). In the case of a strong interaction, $a \sim d$, one expects this form to remain valid as long as $r \ll a, d$, i.e. as long as particles 1 and 2 do not enter the "influence zones" of the other particles, and interact only with each other.

Remark. If we describe the interaction between particles by the pseudo-potential, the qualitative argument we just gave becomes the definition of the domain of wave functions eligible to describe the system (Werner & Castin 2012b). This wave function must be such that for any pair of particles, for example $(1,2)$, we have:

$$r \to 0: \quad \Phi(\boldsymbol{r}_1, \boldsymbol{r}_2, \ldots, \boldsymbol{r}_N) = \left(\frac{1}{r_{12}} - \frac{1}{a}\right) \tilde{\Phi}\left(\boldsymbol{R}, \boldsymbol{r}_3, \ldots, \boldsymbol{r}_N\right) + \mathcal{O}(r_{12}) \tag{15}$$

where $\tilde{\Phi}$ is a regular function of the coordinates of the $N-2$ other particles and of $\boldsymbol{R}$. We have assumed here that $\boldsymbol{R}$ is different from $\boldsymbol{r}_3, \ldots, \boldsymbol{r}_N$.

2-3 Two-body spatial correlation function

The argument presented above was restricted to the case where the positions $\boldsymbol{r}_3, \ldots, \boldsymbol{r}_N$ were not close to the positions $\boldsymbol{r}_1$ and $\boldsymbol{r}_2$ considered to write (14). To make this assumption more quantitative, we will reformulate it in terms of a two-body correlation function.

Let's present the approach on the fermion case. We introduce the "four-point" correlation function (Zhang & Leggett 2009)

$$\mathcal{G}_{2,\uparrow\downarrow}(\boldsymbol{r}'_a, \boldsymbol{r}'_b; \boldsymbol{r}_a, \boldsymbol{r}_b) = \langle \hat{\Psi}^\dagger_\uparrow(\boldsymbol{r}'_a) \hat{\Psi}^\dagger_\downarrow(\boldsymbol{r}'_b) \hat{\Psi}_\downarrow(\boldsymbol{r}_b) \hat{\Psi}_\uparrow(\boldsymbol{r}_a) \rangle \tag{16}$$

which is calculated from the wave function Φ:

$$\begin{aligned} \mathcal{G}_{2,\uparrow\downarrow}(\boldsymbol{r}'_a, \boldsymbol{r}'_b; \boldsymbol{r}_a, \boldsymbol{r}_b) \quad &= \quad \frac{N^2}{4} \int \mathrm{d}^3 r_3 \ldots \mathrm{d}^3 r_N \ \ \Phi^*(\boldsymbol{r}'_a, \boldsymbol{r}'_b, \boldsymbol{r}_3, \ldots, \boldsymbol{r}_N) \\ &\quad \times \quad \Phi(\boldsymbol{r}_a, \boldsymbol{r}_b, \boldsymbol{r}_3, \ldots, \boldsymbol{r}_N). \end{aligned} \tag{17}$$

This correlation function is normalized as:

$$\iint \mathcal{G}_{2,\uparrow\downarrow}(\boldsymbol{r}_a, \boldsymbol{r}_b; \boldsymbol{r}_a, \boldsymbol{r}_b)\ \mathrm{d}^3 r_a\ \mathrm{d}^3 r_b = \frac{N^2}{4}. \tag{18}$$

More precisely, let us fix $\boldsymbol{r}_b = \boldsymbol{r}'_b = 0$ and let us be interested in the "two-point" object:

$$\mathcal{G}_{2,\uparrow\downarrow}(\boldsymbol{r}', \boldsymbol{0}; \boldsymbol{r}, \boldsymbol{0}) = \langle \hat{\Psi}^\dagger_\uparrow(\boldsymbol{r}') \hat{\Psi}^\dagger_\downarrow(\boldsymbol{0}) \hat{\Psi}_\downarrow(\boldsymbol{0}) \hat{\Psi}_\uparrow(\boldsymbol{r}) \rangle \tag{19}$$

We will try to characterize the behavior of this function when $\boldsymbol{r}$ and $\boldsymbol{r}'$ are both close to 0. To do this, we note that $\mathcal{G}_{2,\uparrow\downarrow}(\boldsymbol{r}', \boldsymbol{0}; \boldsymbol{r}, \boldsymbol{0})$ can be considered as the matrix element of a Hermitian operator $\hat{\mathcal{O}}$ in position representation, $\langle \boldsymbol{r}'|\hat{\mathcal{O}}|\boldsymbol{r}\rangle$. This operator can be diagonalized and written as (Yu, Bruun, et al. 2009):

$$\mathcal{G}_{2,\uparrow\downarrow}(\boldsymbol{r}', \boldsymbol{0}; \boldsymbol{r}, \boldsymbol{0}) = \sum_j \gamma_j \; \phi_j^*(\boldsymbol{r}') \; \phi_j(\boldsymbol{r}). \tag{20}$$

The hypothesis at the basis of the contact theory is then formulated as follows: we suppose that for $r \ll d$, the significantly populated $\phi_j(\boldsymbol{r})$ functions are all very close to the two-particle wave function $\psi_0(r)$ introduced in § 2-1. We therefore define the quantity C such that

$$\boxed{r, r' \ll d : \qquad \mathcal{G}_{2,\uparrow\downarrow}(\boldsymbol{r}', \boldsymbol{0}; \boldsymbol{r}, \boldsymbol{0}) \approx \frac{C}{(4\pi)^2 a^2} \psi_0^*(\boldsymbol{r}') \, \psi_0(\boldsymbol{r})} \tag{21}$$

Using (11), this relation is written outside the range b of the potential

$$\boxed{b \lesssim r, r' \ll d, a : \qquad \mathcal{G}_{2,\uparrow\downarrow}(\boldsymbol{r}', \boldsymbol{0}; \boldsymbol{r}, \boldsymbol{0}) \approx \frac{C}{(4\pi)^2 L^3} \; \frac{1}{r'} \; \frac{1}{r}} \tag{22}$$

The quantity C is called the *two-body contact*. It is an extensive quantity whose dimension is the inverse of a length. The central point of the approach developed here is that at short distances, N-body physics intervenes only through this multiplicative constant. Note that we have defined here the contact for the ground state of the system. We will see in the next section how to generalize this definition to the case of $T \neq 0$, once the link with gas thermodynamics is established.

We proceed in a similar way for the bosons by posing

$$\begin{aligned} \mathcal{G}_2(\boldsymbol{r}'_a, \boldsymbol{r}'_b; \boldsymbol{r}_a, \boldsymbol{r}_b) \quad &\equiv \quad \langle \, \hat{\Psi}^\dagger(\boldsymbol{r}'_a) \hat{\Psi}^\dagger(\boldsymbol{r}'_b) \hat{\Psi}(\boldsymbol{r}_b) \hat{\Psi}(\boldsymbol{r}_a) \, \rangle \\ &= \quad N(N-1) \int \mathrm{d}^3 r_3 \ldots \mathrm{d}^3 r_N \; \Phi^*(\boldsymbol{r}'_a, \boldsymbol{r}'_b, \boldsymbol{r}_3, \ldots, \boldsymbol{r}_N) \\ &\qquad \times \quad \Phi(\boldsymbol{r}_a, \boldsymbol{r}_b, \boldsymbol{r}_3, \ldots, \boldsymbol{r}_N). \end{aligned} \tag{23}$$

This function is normalized as follows

$$\iint \mathcal{G}_2(\boldsymbol{r}_a, \boldsymbol{r}_b; \boldsymbol{r}_a, \boldsymbol{r}_b) \, \mathrm{d}^3 r_a \, \mathrm{d}^3 r_b = N(N-1). \tag{24}$$

The hypothesis at the base of the contact theory is then written for bosons:

$$\boxed{r, r' \ll d : \qquad \mathcal{G}_2(\boldsymbol{r}', \boldsymbol{0}; \boldsymbol{r}, \boldsymbol{0}) \approx \frac{C}{(4\pi)^2 a^2} \psi_0^*(\boldsymbol{r}') \, \psi_0(\boldsymbol{r})} \tag{25}$$

or if $a \gg b$:

$$\boxed{b \lesssim r, r' \ll a, d : \qquad \mathcal{G}_2(\boldsymbol{r}', \boldsymbol{0}; \boldsymbol{r}, \boldsymbol{0}) \approx \frac{C}{(4\pi)^2 L^3} \; \frac{1}{r'} \; \frac{1}{r}} \tag{26}$$

Remark. Rigorously, the short-range validity condition comparing r, r' and the range b should be written $b \ll r, r'$. We take here the less restrictive condition $b \lesssim r, r'$ by relying on the numerical results of Yin & Blume (2015), which will be described in § 4-3. These authors consider a Gaussian two-body interaction potential, $V(r) = V_0 \exp(-2r^2/b^2)$, and show for a gas of $N = 10$ particles that the law (26) is reached to a good approximation as soon as r and r' exceed b (see figure 12).

2-4 Pair distribution

Once the forms (22,26) of the $\mathcal{G}_2$ function have been established, we can determine the short range behavior of the pair distribution function, defined here for fermions:

$$G_{2,\uparrow\downarrow}(\boldsymbol{r}) \equiv \int \mathcal{G}_{2,\uparrow\downarrow}(\boldsymbol{r}_a + \boldsymbol{r}, \boldsymbol{r}_a; \boldsymbol{r}_a + \boldsymbol{r}, \boldsymbol{r}_a) \, \mathrm{d}^3 r_a \tag{27}$$

and we find by using the invariance by translation of the system:

$$\boxed{b \lesssim r \ll d, a : \qquad G_{2,\uparrow\downarrow}(\boldsymbol{r}) \approx \frac{C}{(4\pi)^2 r^2}}. \tag{28}$$

An identical result appears for bosons, without the index $\uparrow\downarrow$ of course.

The rapid increase of $G_2(r)$ at short distance can be understood as a signature of bunching of the particles, provided that they are of opposite spins in the case of fermions. To investigate this point further, let us place

ourselves in the $b \to 0$ limit (pseudo-potential) and consider a particle of spin $\uparrow$ at a given point, e.g. the coordinate origin; let us look at the probability δP of finding a particle of spin $\downarrow$ in a ball of infinitesimal radius r centered at 0. If the particles were uncorrelated, this probability would vary as $\delta P \propto r^3$ when $r \to 0$. Given the variation of G_2, we find here $\delta P \propto r$; this probability always tends to 0 when $r \to 0$, but only linearly with r instead of the r^3 law expected for independent particles.

Link with Bogoliubov's approach. In the previous chapter, we computed the function $g_2 = G_2/nN$ and found at short distance the following result:

$$r \ll \xi : \quad g_2(r) \approx \left(1 - \frac{a}{r}\right)^2 \tag{29}$$

or for $r \ll a \ll d$:

$$r \ll a : \qquad G_2(r) \approx \frac{nNa^2}{r^2}. \tag{30}$$

This variation is well in accordance with (28) and we deduce the value of the contact for a weakly interacting Bose gas at $T = 0$:

$$\boxed{\text{Bogoliubov:} \qquad C = (4\pi a)^2 nN} \tag{31}$$

Note that the validity condition $r \ll \xi$ of (29) is less restrictive than the condition $r \ll d$ of the general case (25). Indeed, $\xi = (8\pi na)^{-1/2} = d\,(d/8\pi a)^{1/2}$ is much larger than d in the weak interaction regime.

2-5 Momentum distribution

As announced in the introduction, the contact C is involved in many physical quantities characterizing the fluid. We are interested here in the momentum[3] distribution $n(\boldsymbol{k})$.

Let us consider for example bosons and let us start with the probability amplitude to find the particle 1 with momentum $\boldsymbol{k}$, the particles $2, \dots, N$ being fixed at the points $\boldsymbol{r}_2, \dots, \boldsymbol{r}_N$. This amplitude is written:

$$\mathcal{A}_1(\boldsymbol{k}; \boldsymbol{r}_2, \dots, \boldsymbol{r}_N) = \int \mathrm{d}^3 r_1 \, \mathrm{e}^{-\mathrm{i}\boldsymbol{k}\cdot\boldsymbol{r}_1} \, \Phi(\boldsymbol{r}_1, \boldsymbol{r}_2, \dots, \boldsymbol{r}_N). \tag{32}$$

[3]To avoid the constant $\hbar$ in all that follows, we work rather with the wave vector $\boldsymbol{k}$ than with the real momentum $\hbar\boldsymbol{k}$.

The probability distribution $n_1(\boldsymbol{k})$ for the momentum of particle 1 is obtained by taking the square modulus of this expression, then integrating over all positions $\boldsymbol{r}_2, \dots, \boldsymbol{r}_N$, which gives:

$$\begin{aligned} n_1(\boldsymbol{k}) = \int \; & \mathrm{e}^{\mathrm{i}\boldsymbol{k}\cdot(\boldsymbol{r}_1' - \boldsymbol{r}_1)} \, \Phi^*(\boldsymbol{r}_1', \boldsymbol{r}_2, \dots, \boldsymbol{r}_N) \\ & \times \Phi(\boldsymbol{r}_1, \boldsymbol{r}_2, \dots, \boldsymbol{r}_N) \, \mathrm{d}^3 r_1 \, \mathrm{d}^3 r_1' \, \mathrm{d}^3 r_2 \dots \mathrm{d}^3 r_N, \end{aligned} \tag{33}$$

which naturally brings up the four-point correlation function $\mathcal{G}_2$ considered above.

We are interested here in the behavior of this function at large k, thus coming from the contribution of the small differences $|\boldsymbol{r}_1 - \boldsymbol{r}_1'|$. This contribution becomes important when the couple $(\boldsymbol{r}_1, \boldsymbol{r}_1')$ approaches one of the other positions $\boldsymbol{r}_2, \boldsymbol{r}_3, \dots, \boldsymbol{r}_N$. Consider for example the resonant behavior between $(\boldsymbol{r}_1, \boldsymbol{r}_1', \boldsymbol{r}_2)$, the result then having to be multiplied by $N - 1$ to take into account the other possibilities $(\boldsymbol{r}_1, \boldsymbol{r}_1', \boldsymbol{r}_j)$, $j = 3 \dots N$. We see appearing by using (26):

$$\begin{aligned} & \boldsymbol{r}_1, \boldsymbol{r}_1', \boldsymbol{r}_2 \text{ close:} \quad \int \mathrm{d}^3 r_3 \; \dots \mathrm{d}^3 r_N \; \Phi^*(\boldsymbol{r}_1', \boldsymbol{r}_2, \boldsymbol{r}_3, \dots, \boldsymbol{r}_N) \\ & \times \Phi(\boldsymbol{r}_1, \boldsymbol{r}_2, \boldsymbol{r}_3, \dots, \boldsymbol{r}_N) \approx \frac{1}{N(N-1)} \frac{C}{(4\pi)^2 L^3} \frac{1}{r_{12}'} \frac{1}{r_{12}}. \end{aligned} \tag{34}$$

The contribution of the term $\frac{1}{r_{12}'}\frac{1}{r_{12}}$ to the Fourier transform giving $n_1(\boldsymbol{k})$ is written:

$$\begin{aligned} \int \frac{\mathrm{e}^{\mathrm{i}\boldsymbol{k}\cdot(\boldsymbol{r}_1' - \boldsymbol{r}_1)}}{r_{12}' \, r_{12}} \, \mathrm{d}^3 r_1 \, \mathrm{d}^3 r_1' \, \mathrm{d}^3 r_2 \quad &= \quad \int \frac{\mathrm{e}^{\mathrm{i}\boldsymbol{k}\cdot(\boldsymbol{r}_1' - \boldsymbol{r}_2)}}{r_{12}'} \frac{\mathrm{e}^{\mathrm{i}\boldsymbol{k}\cdot(\boldsymbol{r}_2 - \boldsymbol{r}_1)}}{r_{12}} \, \mathrm{d}^3 r_1 \, \mathrm{d}^3 r_1' \, \mathrm{d}^3 r_2 \\ &= \quad L^3 \left(\frac{4\pi}{k^2}\right)^2 \end{aligned} \tag{35}$$

where we used

$$\int \frac{\mathrm{e}^{\mathrm{i}\boldsymbol{k}\cdot\boldsymbol{r}}}{r} \, \mathrm{d}^3 r = \frac{4\pi}{k^2}. \tag{36}$$

We thus find the dominant behavior for the large momentum for the particle 1:

$$n_1(\boldsymbol{k}) = \frac{1}{N} \frac{C}{k^4} + \dots \tag{37}$$

and it only remains to multiply the result by N to obtain the total momentum distribution of the gas:

$$\boxed{\text{Bosons :} \qquad n(\boldsymbol{k}) = \frac{C}{k^4} + \dots} \tag{38}$$

this distribution being by construction normalized as follows (*cf.* (33)):

$$\text{Bosons :} \qquad \frac{1}{(2\pi)^3} \int n(\boldsymbol{k}) \, \mathrm{d}^3 k = N. \tag{39}$$

We thus find that the momentum distribution behaves like k^{-4} at large k (where the "…" term becomes negligible) and the contact gives directly the weight of this component.

For a spin $1/2$ balanced fermion gas, the contact has been defined so that this relation remains valid for each component:

$$\boxed{\text{Fermions :} \qquad n_\uparrow(\boldsymbol{k}) = n_\downarrow(\boldsymbol{k}) = \frac{C}{k^4} + \dots} \tag{40}$$

with normalization

$$\text{Fermions :} \qquad \frac{1}{(2\pi)^3} \int n_\uparrow(\boldsymbol{k}) \, \mathrm{d}^3 k = \frac{1}{(2\pi)^3} \int n_\downarrow(\boldsymbol{k}) \, \mathrm{d}^3 k = \frac{N}{2}. \tag{41}$$

Recall that we had proved the existence of this wing in the framework of Bogoliubov's theory for the pseudo-potential, in the $na^3 \ll 1$ case. The (considerable!) interest of the present approach is to generalize this result to the case of large scattering lengths, and even to the unitary case $1/a = 0$. Its domain of validity in the case of strong interactions $a \sim d$ can be deduced directly from that found for the pair distribution in the previous paragraph:

$$\frac{1}{a}, \frac{1}{d} \ll k \lesssim \frac{1}{b}. \tag{42}$$

This general law in k^{-4}, valid in the unitary regime and on both sides of this regime, was first predicted by Haussmann (1994).

Remark. It is interesting to note that a $1/k^4$ law appears for a one-dimensional gas described by the Tonks (Minguzzi, Vignolo, et al. 2002) or Lieb–Lininger models, with a prefactor related to the derivative of the ground state energy of the gas in a manner similar to what we will see in § 3 (Olshanii & Dunjko 2003). This law in $1/k^4$ is also valid in two dimensions, both for fermions (Werner & Castin 2012b; Shi, Chiesa, et al. 2015) and for bosons (Werner & Castin 2012a). Note that for 2D bosons, the Efimov problem does not arise (Brodsky, Kagan, et al. 2006) and the difficulties related to the introduction of an additional parameter to describe three-body interactions are absent.

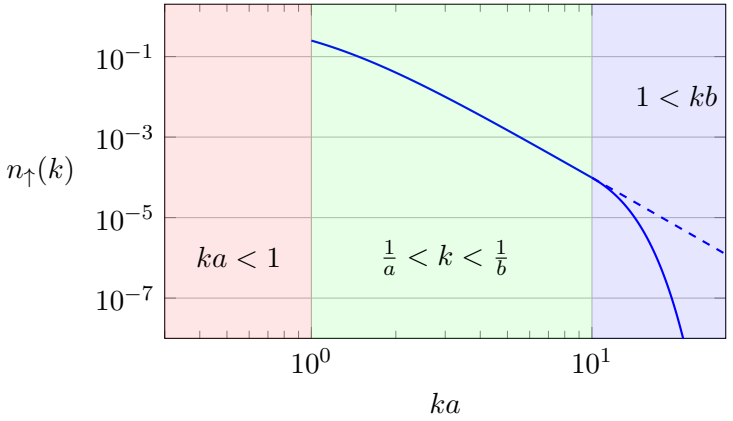

Figure 8. *Typical sketch of the momentum distribution $n(k)$ of a two-component Fermi gas or a Bose gas (neglecting three-body effects) in the limit of a scattering length $a \sim d$ much larger than the range b of the interatomic potential. The law $n(k) \approx C/k^4$ is valid in the central region colored in green.*

3 Thermodynamic definition of contact

3-1 A new thermodynamic variable

In this section we move to an apparently different definition of contact, based on the notion of thermodynamic variables. A fluid at equilibrium is described by its equation of state, which gives the variation of a thermody-

namic potential (its energy E for example) as a function of conjugated thermodynamic variables like entropy/temperature, volume/pressure, number of particles/chemical potential. We thus have the total differential for the energy

$$\mathrm{d}E \;=\; T\,\mathrm{d}S \;-\; P\,\mathrm{d}L^3 \;+\; \mu\,\mathrm{d}N \tag{43}$$

with

$$T = \left(\frac{\partial E}{\partial S}\right)_{L^3,N} \qquad P = -\left(\frac{\partial E}{\partial L^3}\right)_{S,N} \qquad \mu = \left(\frac{\partial E}{\partial N}\right)_{S,L^3}. \tag{44}$$

The interaction potential can be added to the list of these thermodynamic variables, but its characterization generally requires a large number of parameters, which makes this notion of little practical use. The situation changes radically when we are interested in a cold dilute gas, since the interactions can then be described using a single parameter, the scattering length a. It is then relevant to introduce this parameter explicitly in the equation of state, which leads to introduce also its thermodynamic conjugate quantity. In fact, it is more convenient to use the variable $1/a$ and to pose

$$\boxed{\text{Bosons :} \qquad \frac{\hbar^2 C}{8\pi m} = -\left(\frac{\partial E}{\partial(1/a)}\right)_{S,L^3,N}} \tag{45}$$

The thermodynamic description of the fluid is then done according to the usual procedure, using the differential of a thermodynamic potential, the energy for example:

$$\boxed{\mathrm{d}E \;=\; T\,\mathrm{d}S \;-\; P\,\mathrm{d}L^3 \;+\; \mu\,\mathrm{d}N \;-\; \frac{\hbar^2 C}{8\pi m}\,\mathrm{d}\,(1/a)} \tag{46}$$

We will first place ourselves at zero temperature (hence at zero entropy) and show that the quantity C which appears in this expression coincides with the contact introduced in (25). We will generalize this approach to the case of non-zero temperature in § 3-4.

Case of fermions. For spin $1/2$ fermions, the definition is modified by a factor 2 and becomes

$$\boxed{\text{Fermions :} \qquad \frac{\hbar^2 C}{4\pi m} = -\left(\frac{\partial E}{\partial(1/a)}\right)_{S,L^3,N}} \tag{47}$$

This additional factor of 2 allows to absorb the fact that a fermion interacts only with $N/2$ particles (those of opposite spin), while a boson interacts with the $N-1$ other particles. As we have already mentioned, with this definition, the wing of the momentum distribution is equal to C/k^4 for both bosons and each spin component of fermions.

3-2 A useful lemma

To link the contact to the derivative of the energy with respect to the scattering length, we will start by proving a preliminary result. Let us consider a collision between two particles of mass m, that is a reduced mass $m_{\mathrm{r}} = m/2$. The interaction between the two particles is described by the potential $V(r)$ and we consider the zero energy solution $\psi_0(r)$ for the radial equation. Suppose that the interaction potential $V(r)$ is slightly modified:

$$V(r) \;\longrightarrow\; V(r) + \delta V(r). \tag{48}$$

We are interested in the corresponding change δa of the scattering length a and we will establish the following result:

$$\boxed{L^3 \int_0^\infty \delta V(r)\,\psi_0^2(r)\,\mathrm{d}^3 r = \frac{4\pi\hbar^2}{m}\,\delta a} \tag{49}$$

the function $\psi_0(r)$ being normalized so that $\psi_0(r) \approx 1/L^{3/2}$ at infinity [*cf.* (11)].

Proof: As usual, it is convenient to consider the reduced radial wave function $u_0(r) = r\,\psi_0(r)$ which is a solution of the equation :

$$-\frac{\hbar^2}{2m_{\mathrm{r}}} u_0''(r) + V(r)\,u_0(r) = 0. \tag{50}$$

Let us note $\delta u(r)$ the modification of $u_0(r)$ induced by the change δV. We obtain at order 1:

$$-\frac{\hbar^2}{2m_{\rm r}}\delta u''(r) + \delta V(r)\, u_0(r) + V(r)\, \delta u(r) = 0. \tag{51}$$

Let's multiply this equation by $u_0(r)$ and integrate the result between $r = 0$ and $r = r_{\max}$, upper bound that we will take infinite at the end of the calculation:

$$-\frac{\hbar^2}{2m_{\rm r}}\int_0^{r_{\max}} \delta u''(r)\, u_0(r)\, {\rm d}r + \int_0^{r_{\max}} \delta V(r)\, u_0^2(r)\, {\rm d}r + \int_0^{r_{\max}} V(r)\, \delta u(r)\, u_0(r)\, {\rm d}r = 0. \tag{52}$$

To evaluate the first term, recall that $u_0(r)$ and $u_0(r) + \delta u(r)$ satisfy the boundary conditions:

$$u_0(0) = 0,\ \delta u(0) = 0 \tag{53}$$

and

$$r \gg b: \quad u_0(r) \approx \frac{1}{L^{3/2}}(r-a), \quad u_0(r) + \delta u(r) \approx \frac{1}{L^{3/2}}(r - a - \delta a), \tag{54}$$

i.e. $\delta u(r) \approx -\delta a/L^{3/2}$ and $\delta u' \approx 0$ at large r. A double integration by parts of the first term gives

$$\begin{aligned}\int_0^{r_{\max}} \delta u_0''(r)\, u_0(r)\, {\rm d}r &= [u_0\, \delta u']_0^{r_{\max}} - [u_0'\, \delta u]_0^{r_{\max}} + \int_0^{r_{\max}} u_0''(r)\, \delta u(r)\, {\rm d}r \\ &= 0 + \frac{\delta a}{L^3} + \frac{2m_{\rm r}}{\hbar^2}\int_0^{r_{\max}} V(r)\, u_0(r)\, \delta u(r)\, {\rm d}r \end{aligned} \tag{55}$$

Inserting this result in (52) in the limit $r_{\max} \to +\infty$ provides the result announced in (49).

3-3 Variation of a and contact

We are now able to prove that the parameter C introduced as the conjugate variable of $1/a$ is the same as the contact defined in (21,25) from the two-body correlation function. We consider an assembly of N particles with binary interactions, with the Hamiltonian:

$$\hat{H} = \hat{H}_{\rm kin} + \hat{H}_{\rm int} \tag{56}$$

with

$$\hat{H}_{\rm kin} = \sum_j \frac{\hat{\boldsymbol{p}}_j^2}{2m} \qquad \hat{H}_{\rm int} = \sum_{i<j} V(\hat{r}_{ij}). \tag{57}$$

Let us consider an infinitesimal variation of the potential V inducing a variation (also very small) of the scattering length a. We carry out this variation at constant volume and number of particles (remember that we have placed ourselves for the moment at zero temperature and thus at zero entropy). We try to evaluate

$$\left(\frac{\partial E}{\partial a}\right)_{L^3,N}. \tag{58}$$

The Hellmann–Feynman theorem allows to express the variation of the energy in terms of the variation of the Hamiltonian itself:

$$\frac{\partial E}{\partial a} = \langle \frac{\partial \hat{H}}{\partial a}\rangle = \langle \frac{\partial \hat{H}_{\rm int}}{\partial a}\rangle. \tag{59}$$

The last member is calculated by using the link between the variation δV and the variation δa established with the lemma (49). Let us take for example the case of bosons and start from

$$\begin{aligned}\delta\langle \hat{H}_{\rm int}\rangle &= \frac{N(N-1)}{2}\int \delta V(r_{12})\, |\Phi(\boldsymbol{r}_1, \boldsymbol{r}_2, \ldots, \boldsymbol{r}_N)|^2\, {\rm d}^3r_1 \ldots {\rm d}^3r_N \\ &= \frac{1}{2}\int \delta V(r_{12})\, \mathcal{G}_2(\boldsymbol{r}_1, \boldsymbol{r}_2; \boldsymbol{r}_1, \boldsymbol{r}_2)\, {\rm d}^3r_1\, {\rm d}^3r_2 \\ &= \frac{L^3}{2}\int \delta V(r)\, \mathcal{G}_2(\boldsymbol{r}, \boldsymbol{0}; \boldsymbol{r}, \boldsymbol{0})\, {\rm d}^3r. \end{aligned} \tag{60}$$

Because of the presence of δV, the integrand is nonzero only if $r \lesssim b$. We can therefore use the starting hypothesis of the contact theory, namely the equation (25) which we reproduce here for $\boldsymbol{r} = \boldsymbol{r}'$:

$$r \ll d: \qquad \mathcal{G}_2(\boldsymbol{r}, \boldsymbol{0}; \boldsymbol{r}, \boldsymbol{0}) \approx \frac{C}{(4\pi)^2 a^2}|\psi_0(\boldsymbol{r})|^2. \tag{61}$$

Using the lemma (49), we then arrive at:

$$\delta\langle\hat{H}_{\rm int}\rangle = \frac{C\hbar^2}{8\pi m a^2}\delta a, \tag{62}$$

from which we deduce the desired relation:

$$\frac{\partial E}{\partial(1/a)} = -a^2\frac{\partial E}{\partial a} = -a^2\frac{\delta\langle\hat{H}_{\rm int}\rangle}{\delta a} = -\frac{C\hbar^2}{8\pi m}. \tag{63}$$

The thermodynamic quantity C introduced in (45) is thus identical to the contact defined from the function $\mathcal{G}_2$ and used in (61).

3-4 The case of the non-zero temperature

In all the above, we have considered the case of a system at zero temperature and we have expressed the contact in terms of the energy of the ground state of the system. In fact, the approach we have described for the ground state can be performed for any eigenstate Φ_j of the Hamiltonian of the N-body system, provided that its energy is low enough that the interactions remain limited to the s-wave regime. This indeed guarantees that the two-body correlation function deduced from Φ_j behaves as indicated in (21,25).

Let's start by defining a contact C_j for each eigenstate Φ_j of energy E_j as [*cf.* (45-47)]

$$C_j = -\frac{[4/8]\pi m}{\hbar^2}\left(\frac{\partial E_j}{\partial(1/a)}\right)_{N,L^3} \tag{64}$$

with the factor 4 (resp. 8) for fermions (resp. bosons). Let us now suppose that the system is in a statistical mixture of eigenstates, with a density operator

$$\hat{\rho} = \sum_j P_j\,|\Phi_j\rangle\langle\Phi_j|, \tag{65}$$

the P_j obeying for example the Boltzmann law $P_j \propto {\rm e}^{-E_j/k_{\rm B}T}$ for a temperature T. We can define an averaged contact using the weights P_j:

$$C = \sum_j P_j C_j \tag{66}$$

and this contact will allow us to calculate all the quantities we have been interested in so far, such as the momentum distribution, the two-body correlation function or the radio-frequency spectrum that we will discuss in the next chapter. Indeed, the contact intervenes in a linear way in all these expressions.

Inserting the expression of each C_j into (66), we find

$$C = -\frac{[4/8]\pi m}{\hbar^2}\left(\frac{\partial E}{\partial(1/a)}\right)_{N,L^3,\{P_j\}} \qquad \text{with} \quad E = \sum_j P_j E_j. \tag{67}$$

The derivative defining the mean contact must be taken keeping constant the populations of each eigenstate Φ_j, which is the definition of an adiabatic process in quantum thermodynamics. We can therefore replace the previous definition of C by a more conventional formulation, involving the constant entropy derivative of the mean energy of the system:

$$\boxed{\text{fermions/bosons}: \qquad C = -\frac{[4/8]\pi m}{\hbar^2}\left(\frac{\partial E}{\partial(1/a)}\right)_{N,L^3,S}} \tag{68}$$

We can also work at constant T and N, which is the same as replacing the average energy E by the free energy $F = E - TS$:

$$\boxed{\text{fermions/bosons}: \qquad C = -\frac{[4/8]\pi m}{\hbar^2}\left(\frac{\partial F}{\partial(1/a)}\right)_{N,L^3,T}} \tag{69}$$

or at constant T and μ, and use the grand potential Ω:

$$\boxed{\text{fermions/bosons}: \qquad C = -\frac{[4/8]\pi m}{\hbar^2}\left(\frac{\partial \Omega}{\partial(1/a)}\right)_{\mu,L^3,T}}. \tag{70}$$

Note that in this last case, we know that for an extensive system, the grand potential is related to the volume and pressure by the simple relation $\Omega = -PV$, so that the contact per unit volume is written:

$$\boxed{\text{fermions/bosons}: \qquad \frac{C}{L^3} = \frac{[4/8]\pi m}{\hbar^2}\left(\frac{\partial P}{\partial(1/a)}\right)_{\mu,T}} \tag{71}$$

This set of relations is remarkable since it links many microscopic parameters such as $n_\sigma(k)$ or $G_2(r)$ to the thermodynamics of the system, even though it is (at present) impossible to calculate the equation of state of an interacting system at any temperature and for an arbitrary scattering length.

To finish this paragraph, let us indicate that the contact, like the other thermodynamic quantities, can be calculated by a virial expansion in the weakly degenerate regime. One can consult the article of Liu (2013) and references therein.

3-5 Contact and virial theorem

Using dimensional analysis, it is possible to obtain relationships between different thermodynamic quantities such as internal energy, pressure and contact. Let us consider for example the entropy of the system, which is a state function whose differential is written

$$\text{fermions/bosons}: \qquad \mathrm{d}S = \frac{1}{T}\mathrm{d}E + \frac{P}{T}\mathrm{d}L^3 - \frac{\mu}{T}\mathrm{d}N + \frac{\hbar^2 C}{[4/8]\pi m T}\mathrm{d}(1/a). \tag{72}$$

The entropy can be put in the form $S = Nk_\mathrm{B}\, f(E, L^3, N, a)$ where the function f is dimensionless and intensive. We can simplify its writing significantly:

- Since f is intensive, only the three intensive variables E/N, V/N and a have to intervene:

$$S = Nk_\mathrm{B}\, f\left(\frac{E}{N}, \frac{L^3}{N}, a\right). \tag{73}$$

- Since f is dimensionless, we are able to choose its variables also dimensionless. The scattering length a provides the natural energy scale $\hbar^2/ma^2$ and the natural volume scale a^3. We can therefore write the entropy S as

$$S = Nk_\mathrm{B}\, f\left(\frac{E/N}{\hbar^2/ma^2}, \frac{L^3/N}{a^3}\right). \tag{74}$$

Such a writing, a function of only two variables, will allow us to establish a relation between the three conjugate variables of E, L^3 and a, that is T, P and the contact C. We have indeed:

$$\frac{1}{T} = \left(\frac{\partial S}{\partial E}\right)_{L^3,N,a} = Nk_\mathrm{B}\frac{ma^2}{N\hbar^2}\,\partial_1 f \tag{75}$$

where $\partial_1 f$ denotes the derivative of f with respect to its first variable,

$$\frac{P}{T} = \left(\frac{\partial S}{\partial L^3}\right)_{E,N,a} = Nk_\mathrm{B}\frac{1}{Na^3}\,\partial_2 f \tag{76}$$

and

$$\frac{\hbar^2 C}{[4/8]\pi m T} = \left(\frac{\partial S}{\partial(1/a)}\right)_{E,L^3,N} = -2Nk_\mathrm{B}\frac{Ema^3}{N\hbar^2}\,\partial_1 f \;+\; 3Nk_\mathrm{B}\frac{L^3}{Na^2}\partial_2 f. \tag{77}$$

The elimination of $\partial_1 f$ and $\partial_2 f$ between the three preceding equations then leads to (Tan 2008c):

$$\boxed{\text{fermions/bosons}: \qquad PL^3 = \frac{2}{3}E + \frac{\hbar^2 C}{[12/24]\pi m a}.} \tag{78}$$

One can consult the article of Werner (2008) for a generalization of this relation to the case of a gas confined in a potential of arbitrary shape.

Unitary case. In the case $a \to \infty$, the contact tends to a finite value so that we find

$$\boxed{\text{Unitary gas:} \qquad PL^3 = \frac{2}{3}E.} \tag{79}$$

This remarkable relation is a consequence of scale invariance for a infinity: the energy scale $\hbar^2/ma^2$ and volume scale a^3 disappear, so that the equation of state giving the entropy S (or any other thermodynamic function) is a function of only one variable :

$$S = Nk_\mathrm{B}\, f\left(\frac{EmL^2}{\hbar^2 N^{5/3}}\right). \tag{80}$$

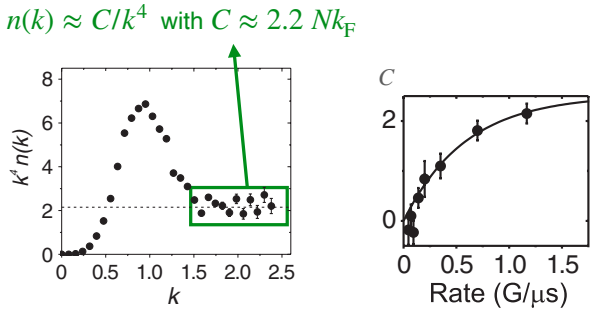

Figure 9. *Left : variation of $k^4\, n(k)$ as a function of k for $(k_{\rm F}a)^{-1} = -0.08\,(4)$. The plateau at large values of k allows to extract the value of the contact C for this value of a. The figure on the right shows the importance of having a very fast change of the scattering length from the value of interest to the zero value used for the time of flight. For the measurements given in the left figure, the magnetic field change is performed with a rate of 1.4 G/μs. Figures extracted from Stewart, Gaebler, et al. (2010).*

The relation (79) is deduced by using:

$$\frac{1}{T} = \frac{k_{\rm B} m L^2}{\hbar^2 N^{2/3}}\, f' \qquad\qquad \frac{P}{T} = \frac{2}{3}\,\frac{k_{\rm B} E m}{\hbar^2 N^{2/3} L}\, f'. \tag{81}$$

where f' denotes the derivative of f.

4 First measurements of the contact

4-1 Momentum distribution of a Fermi gas

Experiments conducted in Boulder by Debbie Jin and her team during the period 2010-12 have shown very convincingly the fact that the contact allows to link measurements of various quantities, made on complex systems such as a Fermi gas around the unitary limit or a strongly interacting Bose gas (Stewart, Gaebler, et al. 2010; Sagi, Drake, et al. 2012; Wild, Makotyn, et al. 2012). We focus here on the results obtained on the Fermi gas.

The experiments described by Stewart, Gaebler, et al. (2010) were conducted on a potassium-40 gas (a fermion), prepared in an equilibrium mixture of its two lowest energy Zeeman states, $|\downarrow\rangle \equiv |F = 9/2, m_F = -9/2\rangle$ and $|\uparrow\rangle \equiv |F = 9/2, m_F = -7/2\rangle$. The gas contains $N = 2\ 10^5$ atoms in total, it is confined in a laser dipole trap and cooled by evaporation to a temperature $T = 0.11\, T_{\rm F}$ with $k_{\rm B} T_{\rm F} = E_{\rm F}$. At the end of the evaporation, the strength of the interactions between the two spin states is adjusted to the desired value by slowly modifying the external magnetic field thanks to a Fano–Feshbach resonance.

Let's focus here on the measurement of the momentum distribution. Once the stationary regime was reached for the desired scattering length, Stewart, Gaebler, et al. (2010) very quickly switched the magnetic field to the value for which $a = 0$, and then measured the spread of the atomic cloud in a time of flight. Since the interaction energy is zero during the time of flight, this spread gives access to the initial momentum distribution. It is essential that the magnetic field change is very fast, to avoid significant conversion of the initial interaction energy into additional kinetic energy. The results of this momentum measurement are shown in figure 9. We see that the wing does indeed vary as k^{-4}, and we thus obtain a first determination of the near-resonant contact $C \approx 2.2 N k_{\rm F}$.

We will return to other characterizations of the contact made by the Boulder group in the next chapter, once we have described another study tool, radio-frequency spectroscopy.

4-2 Scaling laws for contact

In the case of a two-component Fermi gas, we can give some elements on the value of the contact in the asymptotic regimes. We will distinguish the three cases encountered successively when sweeping across a Fano–Feshbach resonance. We limit ourselves here to the case of zero temperature (figure 10) so that all the phases considered below are superfluid.

- On the $a < 0$ side and relatively far from the resonance, we find the BCS regime with $k_{\rm F}|a| \ll 1$. The interaction energy in the ground state

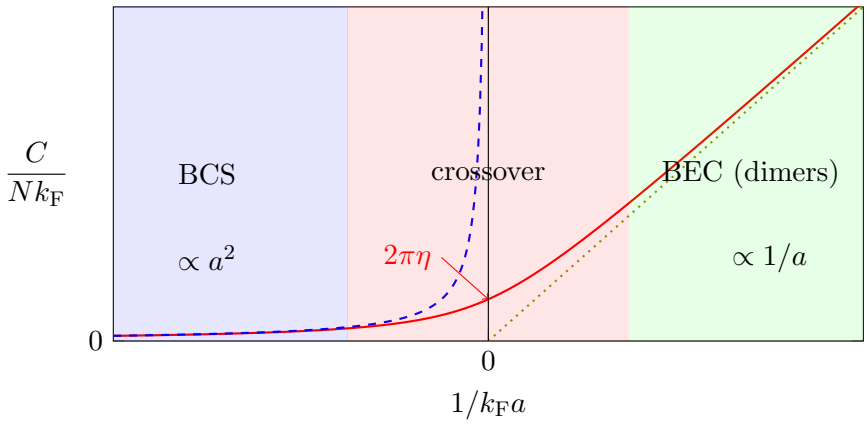

Figure 10. *"Schematic" variation of the C contact with the scattering length for a two-component Fermi gas. The dashed line shows the prediction (86) for a small and positive scattering length a, the gas then consisting of an assembly of dimers. The blue dashed line represents the prediction (**??**) for the BCS limit, for a scattering length a negative and small in absolute value. The purpose of the red solid line is simply to give an idea of the variation of C/Nk_F in the different regimes of k_Fa values, but it does not provide a precise value.*

is simply calculated in a mean field approach[4]

$$E_{\rm int} \approx \frac{1}{L^3}\left(\frac{N}{2}\right)^2 \frac{4\pi\hbar^2 a}{m} \tag{82}$$

which leads for this regime to:

$$\boxed{a<0: \qquad C \approx (2\pi a)^2 n\, N \quad \Leftrightarrow \quad \frac{C}{Nk_F} \approx \frac{4}{3}(k_Fa)^2} \tag{83}$$

We find a similar result to the Bogoliubov approach for bosons (31), except for a factor 4.

- At resonance, i.e. at the threshold of the two-body bound state, the scattering length becomes infinite. There is then no more length scale associated to the interactions and we find the scale invariant situation mentioned above; by simple dimensional analysis and in the case $T=0$, we expect the energy at this point to be written as $E=\frac{3}{5}NE_F\,\xi$ where ξ is a dimensionless (universal) parameter that has to be calculated numerically or measured experimentally. In the vicinity of this point, a first linear correction in $1/a$ is expected and the energy must be in the form (still by dimensional analysis):

$$E \approx NE_F\left(\frac{3}{5}\xi - \frac{\eta}{k_Fa}\right) \tag{84}$$

where η is another dimensionless universal parameter. The contact is then

$$\boxed{a=\pm\infty: \qquad \frac{C}{Nk_F} = 2\pi\eta} \tag{85}$$

There is no known analytical expression for this coefficient η and its theoretical determination is a difficult theoretical problem. In practice, a numerical calculation (quantum Monte Carlo) gives $2.95,\,(10)$ (Drut, Lähde, et al. 2011), in good agreement with the experimental results of Laurent, Pierce, et al. (2017) that we will discuss in the next chapter, and the even more recent ones of Mukherjee, Patel, et al. (2019) and Carcy, Hoinka, et al. (2019).

- In the case where the two-body bound state has appeared[5], the scattering length a is positive. This bound state involves one atom $\uparrow$ and one atom $\downarrow$, and its energy is $\approx -\hbar^2/(ma^2)$. Since the number of atoms is assumed here to be the same for both spin states, the gas contains $N_\uparrow = N_\downarrow = N/2$ dimers and the energy of its ground state is $E=-N\hbar^2/(2ma^2)$, which leads to:

$$\boxed{a>0: \qquad C \approx \frac{4\pi}{a}\,N \quad \Leftrightarrow \quad \frac{C}{Nk_F} \approx \frac{4\pi}{k_Fa}} \tag{86}$$

The contribution of the dimer-dimer interaction, characterized by the scattering length $a_{\rm dd} \approx 0.6\,a$ (Petrov, Salomon, et al. 2004), is in the mean field approximation

$$E_{\rm dd} = \frac{\pi\hbar^2 a_{\rm dd}}{4m} nN \tag{87}$$

[4] Corrections from the BCS theory are exponentially small and are therefore neglected here.

[5] We assume here that there is no formation of aggregates larger than these dimers, see for example Petrov (2003) and Castin, Mora, et al. (2010) and Endo & Castin (2015).

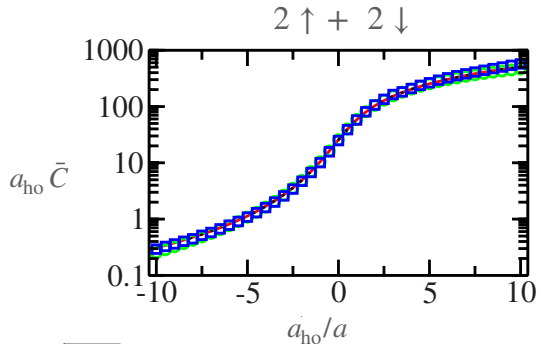

Figure 11. *Variation of the contact with $1/a$ calculated by Blume & Daily (2009). The red solid line represents the value deduced from the derivative of the total energy with respect to $1/a$ [eq. (47)]. The values indicated by green circles [resp. blue squares] are obtained from the pair distribution $G_2(r)$ [resp. the momentum distribution $n(k)$]. The variation of C with $1/a$ is consistent with the one showed in figure 10.*

and its contribution to the contact is of higher order than (86).

4-3 Numerical studies

To test the predictions we have described, Blume & Daily (2009) and Yin & Blume (2015) numerically calculated the energy and position and momentum distributions of a small number of particles confined in an isotropic harmonic trap. The original paper by Blume & Daily (2009) involved $N = 4$ particles, 2 in $\uparrow$ and 2 in $\downarrow$. Yin & Blume (2015) were then able to carry out calculations up to $N = 10$.

The harmonic confinement potential of frequency ω provides the natural length scale for the problem, $a_{\rm ho} = \sqrt{\hbar/m\omega}$. For these calculations, the interaction potential between two atoms is chosen to be Gaussian of range b: $V(r) = -V_0\ \mathrm{e}^{-r^2/2r_0^2}$ with $V_0 > 0$, *i.e.* a range $b \sim 2r_0$. For a given value of r_0, the depth V_0 is adjusted to be close to a zero energy resonance; recall that this is the point where a bound state is about to appear or has just appeared, the scattering length a diverging at this point. The parameter r_0

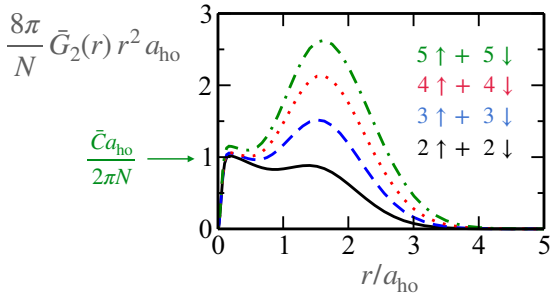

Figure 12. *Function $r^2G_2(r)/N$ giving the spatial correlation of $\uparrow\downarrow$ pairs at the unitary limit $a = \infty$ for different numbers of particles. Figure extracted from Yin & Blume (2015).*

is chosen to be small in front of $a_{\rm ho}$, with typically $r_0/a_{\rm ho} = 10^{-2}$ to 10^{-1}. The limit of the pseudo-potential is obtained by taking the limit $r_0 \to 0$, for a constant scattering length a.

Blume & Daily (2009) have numerically verified that the different ways of calculating the contact, from (i) the total energy, (ii) the two-body spatial correlation function and (iii) the momentum distribution lead to very close values for C. The different results are reported in figure 11. In addition, Blume & Daily (2009) have tested the generalized virial theorem demonstrated by Werner (2008), which also gives access to the value of the contact.

Yin & Blume (2015) have extended this calculation to a number of particles up to $N = 10$. This allows us to have a first intuition of what would be the thermodynamic limit for this system. Figure 12 shows the variations of $r^2G_2(r)/N$ for $N = 4, 6, 8$ and 10 in the unitary regime $a = \infty$. We see that the curves obtained for different values of N cluster together in the distance domain $b \lesssim r \ll a_{\rm ho}$ (with here $r_0 = 0.06\,a_{\rm ho}$), as expected.

4-4 Fano-Feshbach resonance and molecular fraction

As explained in detail in last year's course, a Fano–Feshbach resonance is an extremely powerful tool to modify the scattering length describing the

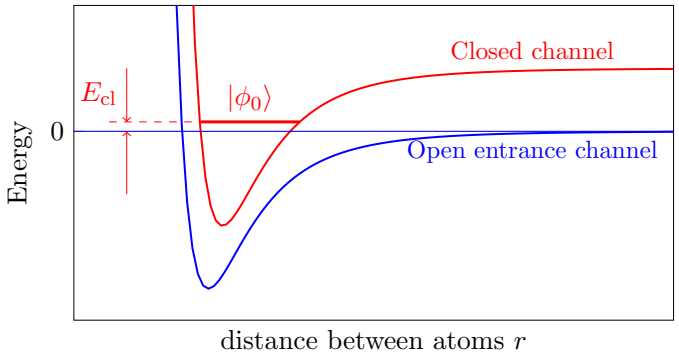

Figure 13. *Principle of a resonance of Fano–Feshbach.*

s-wave collision of two atoms. We start from a gas of atoms with Hamiltonian $\hat{H}_{\rm at}$ leading to scattering length $a_{\rm bg}$. We assume that in addition to the standard interactions described by $a_{\rm bg}$, a pair of colliding atoms ("open" channel) can temporarily form a $|\phi_0\rangle$ state of a closed channel, corresponding to a di-atomic molecule, before separating again (figure 13). The energy of $|\phi_0\rangle$ can be adjusted with respect to the energy reference $E = 0$ of the open channel by varying for example the ambient magnetic field B.

The law giving the scattering length $a(B)$ is assumed to be known, and is usually given in the form:

$$a(B) = a_{\rm bg}\left(1 - \frac{B_1}{B - B_0}\right), \tag{88}$$

which reflects a resonant behavior around $B = B_0$. When $|B - B_0| \gg B_1$, the coupling between the open and closed channel has no significant effect and the scattering length returns to its background value $a_{\rm bg}$. The law (88) is given by the solution of the two-body problem (*cf.* course 2021) and we want to relate this law to the value of the contact C, as proposed by Werner, Tarruell, et al. (2009).

For a gas of spin 1/2 atoms, the Hamiltonian describing the gas can be put in the form

$$\hat{H} = \hat{H}_{\rm at} + \sum_{\boldsymbol{K}}\left(\frac{\hbar^2 K^2}{4m} + E_{\rm dim}(B)\right) b^\dagger_{\boldsymbol{K}} b_{\boldsymbol{K}} + \hat{V}_{\rm at,dim} \tag{89}$$

where $\hat{b}^\dagger_{\boldsymbol{K}}$ creates a molecule of mass $2m$ in the state $|\phi_0\rangle$, with momentum $\hbar\boldsymbol{K}$.

For simplicity, we consider the zero temperature case. We note E the energy of the ground state of the gas and we consider the derivative $\frac{\partial E}{\partial B}$ taken at constant volume and number of particles. The Hellmann–Feynman theorem gives

$$\frac{\partial E}{\partial B} = \langle \frac{\partial \hat{H}}{\partial B}\rangle = \mu \langle N_{\phi_0}\rangle \tag{90}$$

where $\mu = \frac{{\rm d}E_{\rm dim}}{{\rm d}B}$ represents the magnetic moment[6] of $|\phi_0\rangle$ and where $N_{\phi_0} = \sum_{\boldsymbol{K}} b^\dagger_{\boldsymbol{K}} b_{\boldsymbol{K}}$ is the operator giving the number of $|\phi_0\rangle$ molecules present. Moreover, this derivative can be related to the contact since

$$\frac{\partial E}{\partial B} = \frac{\partial E}{\partial a}\frac{{\rm d}a}{{\rm d}B} = \frac{\hbar^2 C}{4\pi m a^2}\frac{{\rm d}a}{{\rm d}B}. \tag{91}$$

The quantity $\frac{{\rm d}a}{{\rm d}B}$ is deduced directly from (88). We thus obtain a relation between the population of the dimer state and the contact:

$$\boxed{\langle N_{\phi_0}\rangle = \frac{\hbar^2}{4\pi m a^2 \mu}\frac{{\rm d}a}{{\rm d}B} C} \tag{92}$$

This result, due to Werner, Tarruell, et al. (2009), can be generalized to the case of non-zero temperature, the derivative of the gas energy being in this case taken at constant entropy. It has been tested by Werner, Tarruell, et al. (2009) on the experimental data obtained by Partridge, Strecker, et al. (2005) (Rice University group) long before the theory was developed.

Rice's experiment was conducted on a ^{6}Li gas, initially prepared in the regime of weakly bound dimers of energy $\sim -\hbar^2/ma^2$, by placing the gas on the $a > 0$ side of the Fano–Feshbach resonance located at $B = 834\,$G. Recall that for a broad Fano–Feshbach resonance, a dimer of energy $-\hbar^2/ma^2$

[6] It has been implicitly assumed here that the magnetic moment of free atoms is zero. If this is not the case, it is sufficient to replace in what follows μ by $\delta\mu$, i.e. the difference between the magnetic moment of $|\phi_0\rangle$ and that of the pair of atoms of the open channel.

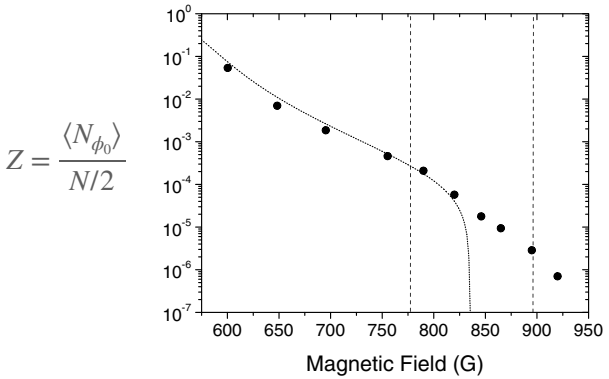

Figure 14. *Variation of the fraction of molecules Z in the closed channel $|\phi_0\rangle$ for a ^{6}Li gas around the Fano–Feshbach resonance located at $B_0 = 834\,G$. The weakly bound dimer condensate regime corresponds to the $B < B_0$ region. Figure extracted from Partridge, Strecker, et al. (2005).*

has only a weak overlap with the molecular state $|\phi_0\rangle$ of the closed channel: the main contribution to this dimer comes from the open channel.

The magnetic field was then slowly swept to bring the gas into the strongly interacting regime. Partridge, Strecker, et al. (2005) measured the fraction of atoms in the "closed" channel of the Feshbach resonance, the $|\phi_0\rangle$ molecular state, thanks to a laser that brought this molecule into an excited electronic state. This resulted in the spontaneous emission of a photon and a loss of particles that could be detected.

The results of the measurement of the fraction $Z = 2\langle N_{\phi_0} \rangle / N$ of atoms in the molecular state $|\phi_0\rangle$ are shown in figure 14. We see that this fraction is always much smaller than 1, as expected for a broad resonance. Werner, Tarruell, et al. (2009) used these data to deduce the value of the contact thanks to (92). The result is shown in figure 15: the agreement between the data of Partridge, Strecker, et al. (2005) and the theoretical modeling is remarkable.

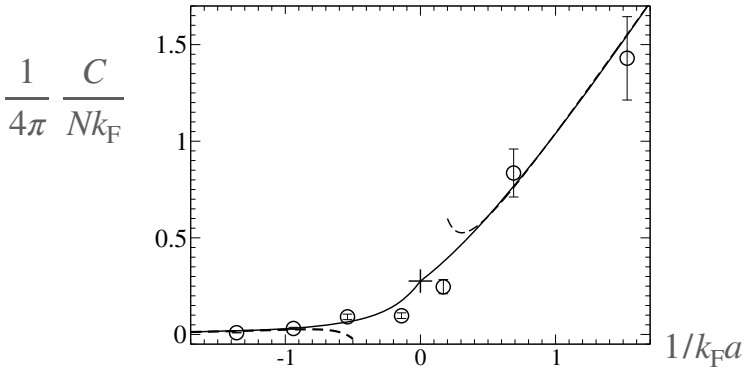

Figure 15. *Points: data from Partridge, Strecker, et al. (2005) re-expressed as a function of contact via (92). Continuous curve: prediction for the contact of a spin 1/2 Fermi gas. Figure extracted from Werner, Tarruell, et al. (2009).*

Chapter VI

The different facets of the two-body contact

We continue in this last chapter our study of the contact C started in chapter 5. Recall that the contact C is a quantity that allows, for a dilute system, to link aspects of two-body physics, such as the pair distribution function $G_2(r)$, to the equilibrium thermodynamics of the gas, its internal energy E for example (see figure 1). For a gas of spin 1/2 fermions, this link between microscopic and macroscopic properties is possible whatever the strength of the interactions – characterized by the scattering length a – and the degeneracy of the gas – characterized by the phase-space density $n\lambda^3$. For a gas of bosons, restrictions are to be put on the density and the scattering length to avoid that microscopic processes involving more than two bodies play a significant role.

Our goal in this chapter is to present a series of measurements of the contact involving spectroscopic techniques or the study of losses induced by collisions between atoms. To set up the formalism to describe these measurements, it is useful to reformulate the results of the previous chapter in terms of the pseudo-potential $\hat{V}_{\rm pp}$, i.e. a potential of range $b = 0$. This reformulation is not trivial: it is accompanied by a divergence of some quantities characterizing the system, its kinetic energy for example. We will show that this divergence is compensated by the divergence of the other component of the energy of the fluid, the interaction energy, the sum of the two energies, i.e. the thermodynamic function *internal energy* E being convergent, as it should be.

Once the formalism for describing a zero range potential is in place, we will move on to model a radio frequency spectroscopy experiment and show how the short range correlations studied in the previous chapter translate into the shape of the resonance line, in particular its wing. We will describe experimental observations of this wing, as well as other manifestations of contact for a fermion gas, such as atomic losses induced by the presence of impurities within the gas.

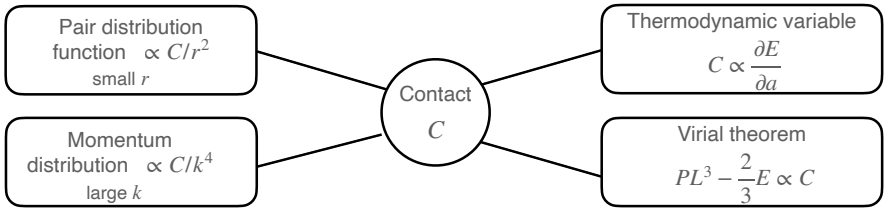

Figure 1. *The different links established by the two-body contact introduced in chapter 5.*

The last part of this chapter will be devoted to the Bose gas. We will briefly explain why Efimov-type three-body processes make the situation more complex than for fermions. We will describe experiments demonstrating two-body contact in different density regimes, limiting ourselves to situations where three-body effects do not play a significant role.

1 Contact and pseudo-potential

1-1 Reminder on the definition of the contact

In the previous chapter, starting from a wave function $\Phi(\boldsymbol{r}_1,\dots,\boldsymbol{r}_N)$ for N particles, we defined the contact C from the two-body correlation function. We are particularly interested in the case of a scattering resonance, when the scattering length a becomes much larger than the range of the potential b.

Let us recall the approach followed in the case of a gas of spin $1/2$ fermions. Let us assume that this gas is balanced, i.e. $N_\uparrow = N_\downarrow = N/2$ and let us assign odd (resp. even) indices to the particles of spin $\uparrow$ (resp. $\downarrow$). The function $\Phi(\boldsymbol{r}_1,\dots,\boldsymbol{r}_N)$ is thus antisymmetric by any exchange of odd indices, and also antisymmetric by any exchange of even indices.

We have introduced the two-body correlation function

$$\begin{aligned}\mathcal{G}_{2,\uparrow\downarrow}(\boldsymbol{r}',\boldsymbol{0};\boldsymbol{r},\boldsymbol{0}) &= \langle\hat\Psi^\dagger_\uparrow(\boldsymbol{r}')\hat\Psi^\dagger_\downarrow(\boldsymbol{0})\hat\Psi_\downarrow(\boldsymbol{0})\hat\Psi_\uparrow(\boldsymbol{r})\rangle \\ &= \frac{N^2}{4}\int \mathrm{d}^3r_3\dots\mathrm{d}^3r_N\ \ \Phi^*(\boldsymbol{r}',\boldsymbol{0},\boldsymbol{r}_3,\dots,\boldsymbol{r}_N) \\ &\qquad\times\quad \Phi(\boldsymbol{r},0,\boldsymbol{r}_3,\dots,\boldsymbol{r}_N),\end{aligned} \tag{1}$$

then, using the zero energy wave function $\psi_0(\boldsymbol{r})$ describing the state of the relative variable in a collision between two particles, we explained that the two-body correlation function could be put in the form

$$r,r'\ll d,a: \qquad \mathcal{G}_{2,\uparrow\downarrow}(\boldsymbol{r}',\boldsymbol{0};\boldsymbol{r},\boldsymbol{0}) \approx \frac{C}{(4\pi)^2a^2}\,\psi_0(r')\,\psi_0(r) \tag{2}$$

where $d=n^{-1/3}$ is the average distance between particles and where the contact C describes the effect of the remaining $N-2$ bodies. We have written a similar relation for an assembly of spinless or polarized bosons.

We are also interested in the associated momentum distribution $n(k)$ and we have shown for spin $1/2$ fermions that :

$$\text{Fermions:}\qquad \frac{1}{a}\ll k\ll\frac{1}{b}: \qquad n_\uparrow(k)=n_\downarrow(k)\approx\frac{C}{k^4}. \tag{3}$$

A natural question at this stage concerns the extension of these results to the case of a potential of range $b=0$, i.e. the pseudo-potential $\hat V_{\rm pp}$. The use of the pseudo-potential allows to simplify the calculations and to find other remarkable scaling laws, as we will see in the case of radio-frequency spectroscopy.

Recall that in reality, inter-atomic potentials have a non-zero range b, of the order of the van der Waals length $R_{\rm vdW}$. If the use of the pseudo-potential leads to a divergent expression for a certain physical quantity, it is important to keep in mind this natural limitation at short distances ($R_{\rm vdW}\lesssim r$) or, equivalently, at large momentum ($k\lesssim R_{\rm vdW}^{-1}$).

1-2 The zero-range limit

In the limiting case of a zero range potential, the tail of the momentum distribution $n(k)=C/k^4$ given in (3) extends to infinity. We immediately deduce that the kinetic energy

$$E_{\rm cin}=\frac{1}{(2\pi)^3}\int\frac{\hbar^2k^2}{2m}\ \left[n_\uparrow(k)+n_\downarrow(k)\right]\ \mathrm{d}^3k \tag{4}$$

diverges since the integrand tends to a constant at infinity:

$$\frac{1}{(2\pi)^3}\ \frac{\hbar^2k^2}{2m}\ \frac{2C}{k^4}\ 4\pi k^2=\frac{\hbar^2C}{2\pi^2m}. \tag{5}$$

The usual remedy to this type of "ultra-violet" divergence is to place a cutoff in the momentum space. If we note $k_{\rm max}$ the upper bound of the integral on k, the kinetic energy is written:

$$\boxed{\text{Fermions:}\qquad E_{\rm kin}=\frac{\hbar^2Ck_{\rm max}}{2\pi^2m}+\dots} \tag{6}$$

where "..." represents a finite and regular contribution. One will notice that the presence of k^{-5} terms could invalidate this assertion, by leading to a divergence in $\log(k_{\rm max})$. Fortunately, it can be shown that the presence of such terms is excluded in the case of the Fermi gas considered here (Tan 2008c).

To make this zero range limit more quantitative, we will now approach the problem by modeling the interaction between atoms by the pseudopotential.

1-3 The pseudo-potential approach

In the case of a binary interaction described by the pseudo-potential

$$\hat{V}_{\rm pp}\left[\psi(\boldsymbol{r})\right] = g\,\delta(\boldsymbol{r})\,\frac{\partial}{\partial r}\left[r\psi(\boldsymbol{r})\right]\Big|_{r=0} \qquad \text{with} \quad g = \frac{4\pi\hbar^2 a}{m}, \tag{7}$$

one can determine exactly the scattering states $\psi_{\boldsymbol{k}}(\boldsymbol{r})$ and the possible bound state $\psi_{\rm bound}(r)$ (*cf.* course 2020-21). A scattering state of energy $E = \hbar^2k^2/2m_r$ ($m_r = m/2$ is the reduced mass) is written

$$\psi_{\boldsymbol{k}}(\boldsymbol{r}) = {\rm e}^{{\rm i}\boldsymbol{k}\cdot\boldsymbol{r}} - \frac{a}{1+{\rm i}ka}\frac{{\rm e}^{{\rm i}kr}}{r} \tag{8}$$

with in particular for zero energy, the normalized wave function:

$$\psi_0(r) = \frac{a}{L^3}\left(\frac{1}{r} - \frac{1}{a}\right). \tag{9}$$

The bound state exists if and only if $a > 0$ and is written:

$$\psi_{\rm bound}(\boldsymbol{r}) = \frac{1}{\sqrt{2\pi a}}\frac{{\rm e}^{-r/a}}{r} \tag{10}$$

energy $E = -\hbar^2/ma^2$.

Let us also recall the action of the pseudo-potential on a function with a divergence in $1/r$:

$$\psi(\boldsymbol{r}) = \frac{\alpha}{r} + \psi_{\rm reg}(\boldsymbol{r}) \quad \Rightarrow \quad V_{\rm pp}\left[\psi(\boldsymbol{r})\right] = g\,\psi_{\rm reg}(0)\,\delta(\boldsymbol{r}) \tag{11}$$

Each eigenstate (8,9,10) has the same behavior in the neighborhood of the origin:

$$\psi(\boldsymbol{r}) \propto \frac{1}{r} - \frac{1}{a} + \mathcal{O}(\boldsymbol{r}) \tag{12}$$

and this behavior, which links the coefficients of the r^{-1} term and the r^0 term, is thus shared by all physically acceptable functions in the presence of the pseudopotential; it constitutes the domain of the Hamiltonian involving this pseudopotential.

This behavior generalizes to a N body system, if the binary interactions are described by the pseudopotential. The fermionic wave function $\Phi(\boldsymbol{r}_1, \boldsymbol{r}_2, \boldsymbol{r}_3, \ldots, \boldsymbol{r}_N)$ introduced above must verify:

$$\Phi(\boldsymbol{r}_1, \boldsymbol{r}_2, \boldsymbol{r}_3, \ldots, \boldsymbol{r}_N) \propto \left(\frac{1}{r_{12}} - \frac{1}{a}\right)\tilde{\Phi}(\boldsymbol{R}, \boldsymbol{r}_3, \ldots, \boldsymbol{r}_N) \tag{13}$$

when the distance r_{12} tends to 0. We have posed here $\boldsymbol{R} = (\boldsymbol{r}_1 + \boldsymbol{r}_2)/2$ and assumed that $\boldsymbol{R}$ was different from all $\boldsymbol{r}_j$, $j = 3, \ldots, N$. The two-body correlation function at short distances[1] is therefore:

$$\mathcal{G}_{2,\uparrow\downarrow}(\boldsymbol{r}', \boldsymbol{0}; \boldsymbol{r}, \boldsymbol{0}) \approx \frac{C}{(4\pi)^2 L^3}\left(\frac{1}{r'} - \frac{1}{a} + \mathcal{O}(r')\right)\left(\frac{1}{r} - \frac{1}{a} + \mathcal{O}(r)\right). \tag{14}$$

Let us now consider the interaction energy. We take again the case of N fermions of spin $1/2$. This interaction energy can be evaluated from

$$E_{\rm int} = \frac{N^2}{4}\int \Phi^*(\boldsymbol{r}_1, \boldsymbol{r}_2, \ldots, \boldsymbol{r}_N)\,\left\{\hat{V}_{\rm pp}(r_{12})\;\left[\Phi(\boldsymbol{r}_1, \boldsymbol{r}_2, \ldots, \boldsymbol{r}_N)\right]\right\}\,{\rm d}^3r_1 \ldots {\rm d}^3r_N \tag{15}$$

Using (14), we find

$$\begin{aligned} E_{\rm int} &= \frac{C}{(4\pi)^2}\int\left(\frac{1}{r} - \frac{1}{a}\right)\,\left[\hat{V}_{\rm pp}\left(\frac{1}{r} - \frac{1}{a}\right)\right]\,{\rm d}^3r \\ &= -\frac{\hbar^2 C}{4\pi m}\int\left(\frac{1}{r} - \frac{1}{a}\right)\delta(\boldsymbol{r})\,{\rm d}^3r, \end{aligned} \tag{16}$$

with an obviously divergent contribution since we have to make the Dirac distribution act on the $1/r$ function.

As for the calculation of the kinetic energy, let us put a cutoff in k at a value $k_{\rm max}$, which amounts to smoothing the divergence of $1/r$ in $r = 0$ on

[1] The behavior given in (14) is a direct consequence of the argument presented in the previous chapter, that $\mathcal{G}_{2,\uparrow\downarrow}(\boldsymbol{r}', \boldsymbol{0}; \boldsymbol{r}, \boldsymbol{0})$ can be seen as the matrix element of a Hermitian operator between $\langle\boldsymbol{r}'|$ and $|\boldsymbol{r}\rangle$. This operator can be put in the diagonal form $\sum\gamma_j\phi_j^*(\boldsymbol{r}')\phi_j(\boldsymbol{r})$ and every function ϕ_j verifies (12) since it belongs to the Hamiltonian domain.

a domain of extension $k_{\rm max}^{-1}$. We can then compute the integral (16) using

$$\frac{1}{r} = \frac{1}{2\pi^2} \int \frac{\mathrm{e}^{\mathrm{i}\boldsymbol{k}\cdot\boldsymbol{r}}}{k^2}\, \mathrm{d}^3k \tag{17}$$

so that

$$\frac{1}{r}\delta(\boldsymbol{r}) = \frac{1}{2\pi^2} \int \frac{\mathrm{e}^{\mathrm{i}\boldsymbol{k}\cdot\boldsymbol{r}}}{k^2}\delta(\boldsymbol{r})\, \mathrm{d}^3k = \frac{2k_{\rm max}}{\pi}\, \delta(\boldsymbol{r}) \tag{18}$$

hence

$$\boxed{\text{Fermions:} \qquad E_{\rm int} = \frac{\hbar^2 C}{4\pi m}\left(-\frac{2k_{\rm max}}{\pi} + \frac{1}{a}\right)} \tag{19}$$

The two linearly divergent contributions in $k_{\rm max}$ of the kinetic energy and the interaction energy are thus equal in absolute value and of opposite signs. They compensate each other exactly when we compute the total energy, that is to say the thermodynamic function considered in the previous chapter: this function is therefore finite, even for a potential of range $b = 0$. A convenient form for this total energy is

$$\boxed{\text{Fermions:} \qquad E = \sum_{\sigma=\uparrow\downarrow} \frac{1}{(2\pi)^3} \int \frac{\hbar^2 k^2}{2m}\, \left[n_\sigma(k) - \frac{C}{k^4}\right]\, \mathrm{d}^3k + \frac{\hbar^2 C}{4\pi m a}} \tag{20}$$

where the divergent parts of the kinetic energy and the interaction energy terms were isolated and offset each other.

For bosons, if we forget about three-body effects, we find

$$\boxed{\text{Bosons without Efimov:} \qquad E = \frac{1}{(2\pi)^3} \int \frac{\hbar^2 k^2}{2m}\, \left[n(k) - \frac{C}{k^4}\right]\, \mathrm{d}^3k + \frac{\hbar^2 C}{8\pi m a}} \tag{21}$$

The Efimov states that appear in the vicinity of a scattering resonance complicate the situation by introducing another component in the momentum distribution, varying as k^{-5} (Castin & Werner 2011). The divergence induced on the kinetic energy is only logarithmic, and it is compensated by an additional term in the interaction energy also originating from three-body effects (Braaten, Kang, et al. 2011).

1-4 The case of a potential in "true" Dirac

A commonly used method (see Chapter 3) to describe a potential of negligible range is to use a true Dirac distribution $\bar{g}\,\delta(\boldsymbol{r})$, associated with the cutoff $k_{\rm max}$ in momentum space, and to choose

$$\frac{1}{g} = \frac{1}{\bar{g}} + \frac{m k_{\rm max}}{2\pi^2\hbar^2}, \qquad \frac{1}{a} = \frac{1}{\bar{a}} + \frac{2k_{\rm max}}{\pi}, \tag{22}$$

where $g = 4\pi\hbar^2 a/m$ is the "physical" coupling constant and $\bar{g} = 4\pi\hbar^2\bar{a}/m$ the "bare" coupling constant.

The constraint (22) is obtained by imposing on the eigenfunction $\psi_0(r) = \frac{1}{r} - \frac{1}{a}$ of zero energy for $\hat{p}^2/2m_{\rm r} + \hat{V}_{\rm pp}$ to be also eigenfunction of zero energy for $\hat{p}^2/2m_{\rm r} + \bar{g}\delta(\boldsymbol{r})$:

$$-\frac{\hbar^2}{m}\boldsymbol{\nabla}^2\left(\frac{1}{r} - \frac{1}{a}\right) + \bar{g}\delta(\boldsymbol{r})\left(\frac{1}{r} - \frac{1}{a}\right) = 0, \tag{23}$$

which implies

$$\delta(\boldsymbol{r})\ \left[\frac{4\pi\hbar^2}{m} + \bar{g}\left(\frac{2}{k_{\rm max}} - \frac{1}{a}\right)\right] = 0 \tag{24}$$

where we used $\boldsymbol{\nabla}^2(1/r) = -4\pi\delta(\boldsymbol{r})$ and $\frac{1}{r}\big|_0 = 2k_{\rm max}/\pi$ [*cf.* (18)].

In a calculation, intermediate results may involve the "bare" coupling constant $\bar{g}$ and/or the cutoff $k_{\rm max}$, but the physical quantities must be calculated by taking the limit $k_{\rm max} \to \infty$ and they must be expressed using g only. When this is not possible, it means that we are in the presence of a problem whose answer depends explicitly on the range b of the potential.

We can see that the interaction energy (19) is written in these conditions

$$\text{Fermions:} \qquad E_{\rm int} = \frac{\hbar^4 C}{m^2\bar{g}} \tag{25}$$

and a similar expression for bosons with no Efimov:

$$\text{Bosons without Efimov effect:} \qquad E_{\rm int} = \frac{\hbar^4 C}{2m^2\bar{g}} \tag{26}$$

It is therefore not a physical quantity, just like the kinetic energy (6) which explicitly involves $k_{\rm max}$. On the other hand, the total energy involves only the physical coupling constant g.

Let us now check that we can directly find the result (25-26) for a "true" Dirac potential. Let us consider spinless bosons to simplify the notations. The Hamiltonian is written in these conditions

$$\hat{H} = \hat{H}_{\rm kin} + \hat{H}_{\rm int} \tag{27}$$

with

$$\hat{H}_{\rm int} = \frac{\bar{g}}{2}\hat{K} \qquad \text{et} \qquad \hat{K} = \int \hat{\psi}^\dagger(\boldsymbol{r})\hat{\psi}^\dagger(\boldsymbol{r})\hat{\psi}(\boldsymbol{r})\hat{\psi}(\boldsymbol{r})\ \mathrm{d}^3 r \tag{28}$$

hence the interaction energy

$$E_{\rm int} = \langle \hat{H}_{\rm int}\rangle = \frac{\bar{g}}{2}\ \langle \hat{K}\rangle. \tag{29}$$

The quantity $\langle K\rangle$ involves the value of the function $\mathcal{G}_2(\boldsymbol{r}_1', \boldsymbol{r}_2'; \boldsymbol{r}_1, \boldsymbol{r}_2)$ when the four points are identical, i.e. for a uniform system:

$$\langle \hat{K}\rangle = L^3\ \mathcal{G}_2(0,0;0,0). \tag{30}$$

Let us take again the expression (14) of $\mathcal{G}_2$ at short distances. We must use the "value in 0" of the function $1/r$, which we gave in (18). Let us transfer this value into the expression (2) of $\mathcal{G}_2$:

$$\mathcal{G}_2(0,0) = \frac{C}{(4\pi)^2 L^3}\left(\frac{2k_{\rm max}}{\pi} - \frac{1}{a}\right)^2 = \frac{\hbar^4 C}{L^3 m^2}\ \frac{1}{\bar{g}^2}. \tag{31}$$

The correlation function $\mathcal{G}_2$ taken in $\boldsymbol{r}_1 = \boldsymbol{r}_2$ is thus not a physical quantity for an interacting gas, since it involves the bare coupling $\bar{g}$ and not the physical coupling g. It diverges when we take the limit $k_{\rm max} \to \infty$. The situation for an interacting gas is thus radically different from the case of the ideal gas (Naraschewski & Glauber 1999).

Let us now return to the interaction energy (29)

$$E_{\rm int} = \frac{\bar{g}}{2}\ \langle \hat{K}\rangle = \frac{\bar{g}}{2}\ L^3\ \frac{\hbar^4 C}{L^3 m^2}\ \frac{1}{\bar{g}^2}. \tag{32}$$

This result coincides with the one announced in (26).

To summarize, the use of the couple $(\bar{g}, k_{\rm max})$, followed by the limit $k_{\rm max} \to \infty$ under the condition (22) linking $\bar{g}, k_{\rm max}$ to the real coupling g allows us to carry out calculations in a relatively simple and transparent way. This is the method we will use in the next part dedicated to radio-frequency spectroscopy.

2 Contact and radio frequency spectroscopy

2-1 Position of the problem

Radio frequency spectroscopy is a powerful way to analyze the properties of a quantum gas. While for an isolated atom, the absorption spectrum is composed of discrete lines, the spectrum of an interacting gas is generally a continuum whose line shape, center of gravity, and wings provide information about the nature of the N-particle states that may exist within the fluid.

We will focus here on the case of a gas of spin $1/2$ fermions. The idea is to illuminate the gas with an electromagnetic wave of frequency ω which can induce a transition from one of the two internal atomic states, $\uparrow$ for example, to a third state which we will note e (figure 2). The fact of choosing a "radio-frequency" wave, thus of long wavelength, means that the passage from $\uparrow$ to e is not accompanied by any transfer of momentum, contrary to what would happen if we used a light beam (Bragg spectroscopy). The momentum states that will play a role in the following are those which are populated in the stationary state of the gas, in particular during the interaction between two close atoms.

We are going to study here the variation with ω of the transfer rate $\Gamma(\omega)$ from $\uparrow$ to e, and we are going to look at two quantities:

- The average position of the resonance involves the contact and is written in the limit of large scattering lengths $|a_{e\downarrow}|, |a_{e\downarrow}| \gg b$:

$$\boxed{\langle\omega\rangle \equiv \frac{\int \omega\,\Gamma(\omega)\,\mathrm{d}\omega}{\int \Gamma(\omega)\,\mathrm{d}\omega} \approx \omega_0\ +\ \left(\frac{1}{a_{\uparrow\downarrow}} - \frac{1}{a_{e\downarrow}}\right)\ \frac{\hbar C}{4\pi m N_\uparrow}} \tag{33}$$

  where ω_0 denotes the $\uparrow e$ transition frequency of an isolated atom (we will assume here $\omega_0 > 0$ to fix the ideas).

- When the atoms in the state e do not interact with the $\downarrow$ atoms ($a_{e\downarrow}$=0), the mean displacement (33) diverges. It can be shown that this is due to the appearance of a large detuned wing for $\Gamma(\omega)$, which also in-

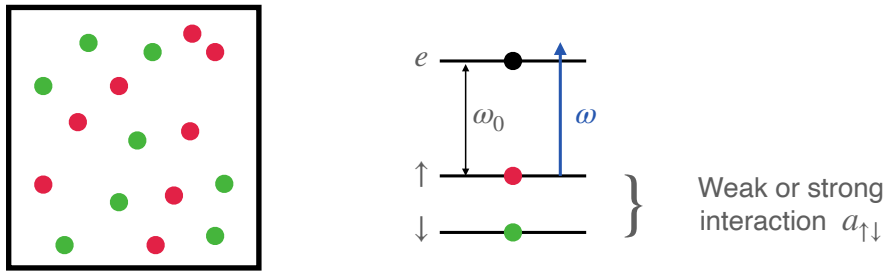

Figure 2. *Principle of radio-frequency spectroscopy for a two-component Fermi gas. A radio-frequency wave couples one of the two spin states, here ↑, to a third internal state denoted e.*

volves the contact:

$$\boxed{\frac{\Gamma(\omega)}{\int \Gamma(\omega)\,\mathrm{d}\omega} \approx \frac{1}{4\pi^2 N_\uparrow}\sqrt{\frac{\hbar}{m}}\,\frac{C}{(\omega-\omega_0)^{3/2}}} \tag{34}$$

We will see that this wing is closely related to the $1/k^4$ decay of the momentum distribution.

These results were obtained from a succession of works described in Yu & Baym (2006), Baym, Pethick, et al. (2007), Punk & Zwerger (2007), Haussmann, Punk, et al. (2009), and Pieri, Perali, et al. (2009) and Braaten, Kang, et al. (2010).

2-2 Center of mass of the spectrum

The calculation of the rate $\Gamma(\omega)$ is done by using the Fermi golden rule, or in an equivalent way, the linear response approach. The perturbation created by the radio frequency wave is described by the operator

$$\hat{H}_{\mathrm{rf}}(t) = \frac{\hbar\Omega}{2}\,\mathrm{e}^{-\mathrm{i}\omega t}\,\hat{Y} + \mathrm{H.c.} \qquad \text{with} \quad \hat{Y} = \int \hat{\Psi}_e^\dagger(\boldsymbol{r})\,\hat{\Psi}_\uparrow(\boldsymbol{r})\,\mathrm{d}^3 r, \tag{35}$$

where Ω is the Rabi frequency of the radio-frequency, proportional to its oscillating electromagnetic field. We have made here the rotating wave approximation (RWA) by keeping only the quasi-resonant part (in $\mathrm{e}^{-\mathrm{i}\omega t}$ with $\omega > 0$) for the passage from ↑ to e.

The transfer rate is then written [see for example Cohen-Tannoudji, Diu, et al. (1986), XIII-C-3]

$$\Gamma(\omega) = \frac{\pi}{2}\Omega^2 \sum_{\Phi_f} |\langle\Phi_f|\hat{Y}|\Phi_i\rangle|^2\,\delta[\omega - (E_f - E_i)/\hbar]. \tag{36}$$

In this expression, the state $|\Phi_i\rangle$, of energy E_i, represents the initial state with $N_\uparrow$ and $N_\downarrow$ particles in the two spin states ↑ and ↓, and no particles in the e state. The sum covers all possible final states $|\Phi_f\rangle$ (of energy E_f). These states have $N_\uparrow - 1$ particles in the ↑ state, 1 particle in the e state, and $N_\downarrow$ particles in the ↓ state.

To show (33), let us first look at the denominator $\int \Gamma(\omega)\,\mathrm{d}\omega$. The integral over ω of the Dirac distribution gives 1; using the closure relation $\hat{1} = \sum_{\Phi_f} |\Phi_f\rangle\langle\Phi_f|$, we arrive at:

$$\begin{aligned}\int \Gamma(\omega)\,\mathrm{d}\omega &= \frac{\pi}{2}\Omega^2\,\langle\Phi_i|\,\hat{Y}^\dagger\,\hat{Y}\,|\Phi_i\rangle \\ &= \frac{\pi}{2}\Omega^2 \int \langle\Phi_i|\hat{\Psi}_\uparrow^\dagger(\boldsymbol{r})\,\hat{\Psi}_e(\boldsymbol{r})\,\hat{\Psi}_e^\dagger(\boldsymbol{r}')\,\hat{\Psi}_\uparrow(\boldsymbol{r}')|\Phi_i\rangle\,\mathrm{d}^3 r\,\mathrm{d}^3 r'.\end{aligned} \tag{37}$$

For fermions, we have the anti-commutation relation $[\hat{\Psi}_e(\boldsymbol{r}), \hat{\Psi}_e^\dagger(\boldsymbol{r}')]_+ = \delta(\boldsymbol{r} - \boldsymbol{r}')$. As the $|\Phi_i\rangle$ state does not contain a particle in the e state, we deduce:

$$\int \Gamma(\omega)\,\mathrm{d}\omega = \frac{\pi}{2}\Omega^2 \int \langle\Phi_i|\hat{\Psi}_\uparrow^\dagger(\boldsymbol{r})\,\hat{\Psi}_\uparrow(\boldsymbol{r})|\Phi_i\rangle\,\mathrm{d}^3 r = \frac{\pi}{2}\Omega^2 N_\uparrow. \tag{38}$$

The calculation of the numerator of (33), $\int \omega\,\Gamma(\omega)\,\mathrm{d}\omega$, is slightly more complicated. We use the presence of $\delta[\omega - (E_f - E_i)/\hbar]$ to establish

$$\hbar\omega\langle\Phi_i|\hat{Y}^\dagger|\Phi_f\rangle = (E_f - E_i)\langle\Phi_i|\hat{Y}^\dagger|\Phi_f\rangle = \langle\Phi_i|[\hat{Y}^\dagger, \hat{H}]|\Phi_f\rangle, \tag{39}$$

where $\hat{H}$ denotes the Hamiltonian in the absence of radio-frequency coupling. This leads to (still using a closure relation on $|\Phi_f\rangle$):

$$\int \omega\,\Gamma(\omega)\,\mathrm{d}\omega = \frac{\pi}{2\hbar}\Omega^2 \int \langle\Phi_i|\left[\hat{\Psi}_\uparrow^\dagger(\boldsymbol{r})\,\hat{\Psi}_e(\boldsymbol{r}), \hat{H}\right]\,\hat{\Psi}_e^\dagger(\boldsymbol{r}')\,\hat{\Psi}_\uparrow(\boldsymbol{r}')|\Phi_i\rangle\,\mathrm{d}^3 r\,\mathrm{d}^3 r', \tag{40}$$

where the Hamiltonian contains the internal energy $\hbar\omega_0$ of the state e, the kinetic energy terms for the three components $\uparrow$, $\downarrow$ and e, and the three interaction terms $\uparrow\downarrow$, $e\downarrow$ and $e\uparrow$.

Let us first observe that the commutators of $\hat{\Psi}^\dagger_\uparrow(\boldsymbol{r})\hat{\Psi}_e(\boldsymbol{r})$ with the kinetic energy terms as well as with the $e\uparrow$ coupling have a zero contribution for the initial state considered.

We will treat here the interaction terms using "true" Dirac potentials, according to the procedure explained in §1-4. We introduce for this purpose the bare couplings $\bar{g}_{\uparrow\downarrow}$, $\bar{g}_{e\downarrow}$, $\bar{g}_{e\uparrow}$ associated to the same cutoff $k_{\max}$ in momentum space. In the calculation of the commutator involved in (40), the only non-zero contributions come from the internal energy $\hbar\omega_0$ of e and from the couplings $e\downarrow$ and $\uparrow\downarrow$. We then arrive at

$$\langle\omega\rangle = \omega_0 + \frac{1}{\hbar N_\uparrow}\,(\bar{g}_{e\downarrow} - \bar{g}_{\uparrow\downarrow})\,\langle\hat{K}_{\rm int}\rangle. \tag{41}$$

The operator $\hat{K}$, defined by:

$$\hat{K} = \int \hat{\psi}^\dagger_\uparrow(\boldsymbol{r})\hat{\psi}^\dagger_\downarrow(\boldsymbol{r})\hat{\psi}_\downarrow(\boldsymbol{r})\hat{\psi}_\uparrow(\boldsymbol{r})\,\mathrm{d}^3r \tag{42}$$

is the fermionic version of the operator introduced in (28) for bosons. Its average is $\hbar^4 C/(m^2\bar{g}^2_{\uparrow\downarrow})$ [*cf.* (30,31)], which leads to:

$$\langle\omega\rangle = \omega_0 + \frac{\bar{a}_{e\downarrow}}{\bar{a}_{\uparrow\downarrow}}\left(\frac{1}{\bar{a}_{\uparrow\downarrow}} - \frac{1}{\bar{a}_{e\downarrow}}\right)\frac{\hbar C}{4\pi m N_\uparrow}. \tag{43}$$

Using the identity between the bare couplings $(\bar{g},\bar{a})$ and the physical couplings (g,a):

$$\frac{1}{\bar{a}_{\uparrow\downarrow}} - \frac{1}{\bar{a}_{e\downarrow}} = \frac{1}{a_{\uparrow\downarrow}} - \frac{1}{a_{e\downarrow}}, \tag{44}$$

this relation can also be written:

$$\langle\omega\rangle = \omega_0 + \frac{\bar{a}_{e\downarrow}}{\bar{a}_{\uparrow\downarrow}}\left(\frac{1}{a_{\uparrow\downarrow}} - \frac{1}{a_{e\downarrow}}\right)\frac{\hbar C}{4\pi m N_\uparrow} \tag{45}$$

Finally, we can write the ratio $\bar{a}_{e\downarrow}/\bar{a}_{\uparrow\downarrow}$ as:

$$\frac{\bar{a}_{e\downarrow}}{\bar{a}_{\uparrow\downarrow}} = \frac{k_{\max} - \frac{\pi}{2a_{\uparrow\downarrow}}}{k_{\max} - \frac{\pi}{2a_{e\downarrow}}} \quad \to 1 \qquad \text{when} \quad k_{\max}\to\infty. \tag{46}$$

We then arrive at the result announced in (33). Recall that the limit $k_{\max}$ must be understood physically as $k_{\max}\sim 1/b$ since beyond this value, the range of the potential must be taken into account. The result (46) is therefore only physically relevant if the scattering lengths are such that $|a_{\uparrow\downarrow}|, |a_{e\downarrow}| \gg b$. One can consult the article by Baym, Pethick, et al. (2007) for a discussion of situations where this inequality is not satisfied.

One might be surprised not to see an interaction term proportional to $g_{e\uparrow}$ in the above. The reason is that the action of the radio frequency consists in making each of the $N_\uparrow$ atoms switch from the $|\uparrow\rangle$ state to the $\cos\theta\,|\uparrow\rangle + \sin\theta\,|e\rangle$state (with $\theta\ll 1$ in our perturbative approach). These $N_\uparrow$ atoms all remain in the same internal state, they are thus polarized fermions and they do not interact with each other (Gupta, Hadzibabic, et al. 2003). The situation would of course be different if we considered bosons.

2-3 The wing of the radio frequency spectrum

We consider in this paragraph the case where the atoms in the e state do not interact with the atoms in $\uparrow$ and $\downarrow$. In particular, the fact of posing $a_{e\downarrow}=0$ leads to the divergence of (33). We want to show here that this divergence of the integral $\int \omega,\Gamma(\omega)\mathrm{d}\omega$ comes from the appearance of a wing in $(\omega-\omega_0)^{-3/2}$, whose expression is given in (34).

Since the atoms in the state e evolve freely, the form of the possible final states Φ_f involved in the Fermi golden rule (36) is simple: they are product states $|e:\boldsymbol{k}\rangle\otimes|\Phi_f^{(N-1)}\rangle$, of energy $E_f = \frac{\hbar^2k^2}{2m} + E_f^{(N-1)}$. A generic matrix element involved in (36) is then written:

$$\langle\Phi_f|\hat{Y}|\Phi_i\rangle = \int \frac{\mathrm{e}^{-\mathrm{i}\boldsymbol{k}\cdot\boldsymbol{r}}}{\sqrt{L^3}}\langle\Phi_f^{(N-1)}|\hat{\Psi}_\uparrow(\boldsymbol{r})|\Phi_i\rangle\,\mathrm{d}^3r. \tag{47}$$

When $\omega-\omega_0$ is large, an isolated $\uparrow$ atom is almost insensitive to radio frequency. The dominant final states are those where the radio-frequency makes the internal state of an atom $\uparrow$, initially very close to an atom $\downarrow$, change. Depending on the value of a, these two atoms could, before the r.f. transition, form a bound state or be in a scattering state. In both cases, the center of mass momentum of this pair was small, while the momentum

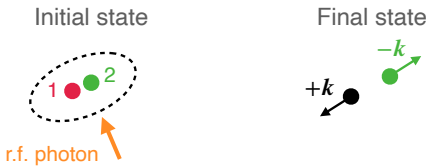

Figure 3. *Process contributing to the wing $\propto (\omega-\omega_0)^{3/2}$ of the radio frequency spectrum.*

distributions of each of the two partners (or equivalently, the momentum distribution of the relative variable) could be broad.

During the transition from $\uparrow$ to e, the total momentum of the pair is unchanged and thus remains negligible. The total initial energy of the pair, E_i, is assumed to be small in front of the detuning $\hbar(\omega-\omega_0)$, even if its two components, kinetic and interaction (which are of opposite signs), are each comparable to the detuning[2]. Once the radio frequency photon has been absorbed and the $\uparrow$ atom has been transferred to the e state, the two atoms do not interact anymore (figure 3). They share equally the excess energy $\hbar(\omega-\omega_0)$, each of the two atoms gaining the kinetic energy $\hbar^2k^2/2m$. The distribution $\delta[\omega-(E_f-E_i)/\hbar]$ can then be approximated by $\delta(\omega-\omega_0-\hbar k^2/m)$.

Once this approximation is done, we can again use a closure relation on the $|\Phi_f^{(N-1)}\rangle$ states. The sum of the squares of the matrix elements of type (47) gives

$$\Gamma(\omega)\approx\frac{\pi\Omega^2}{2}\sum_{\boldsymbol{k}}\sum_{\Phi_f^{(N-1)}}|\langle e:\boldsymbol{k}|\otimes\langle\Phi_f^{(N-1)}|\hat{Y}|\Phi_i\rangle|^2\,\delta\left(\omega-\omega_0-\frac{\hbar k^2}{m}\right) \quad (48)$$

or

$$\Gamma(\omega)\approx\frac{\pi\Omega^2}{2}\sum_{\boldsymbol{k}}\int\frac{\mathrm{e}^{\mathrm{i}\boldsymbol{k}\cdot(\boldsymbol{r}'-\boldsymbol{r})}}{L^3}\langle\Phi_i|\hat{\Psi}_\uparrow^\dagger(\boldsymbol{r}')\,\hat{\Psi}_\uparrow(\boldsymbol{r})|\Phi_i\rangle \times\delta\left(\omega-\omega_0-\frac{\hbar k^2}{m}\right)\mathrm{d}^3r\,\mathrm{d}^3r'. \quad (49)$$

[2] A similar reasoning appears in the analysis of the energy increase induced by atomic losses in an interacting gas (Bouchoule, Dubois, et al. 2021). The loss of atoms that have a close neighbor leads to a divergence of the rate of energy increase for a zero range potential.

We recognize the momentum distribution for the $\uparrow$ state:

$$n_\uparrow(\boldsymbol{k})=\int\mathrm{e}^{\mathrm{i}\boldsymbol{k}\cdot(\boldsymbol{r}'-\boldsymbol{r})}\,\langle\Phi_i|\hat{\Psi}_\uparrow^\dagger(\boldsymbol{r}')\,\hat{\Psi}_\uparrow(\boldsymbol{r})|\Phi_i\rangle\,\mathrm{d}^3r\,\mathrm{d}^3r' \quad (50)$$

so that $\Gamma(\omega)$ is written:

$$\Gamma(\omega)\approx\frac{\pi\Omega^2}{2}\frac{1}{(2\pi)^3}\int n_\uparrow(\boldsymbol{k})\,\delta\left(\omega-\omega_0-\frac{\hbar k^2}{m}\right)\mathrm{d}^3k. \quad (51)$$

We then insert the asymptotic law $n_\uparrow(\boldsymbol{k})\approx C/k^4$ and arrive at

$$\int n_\uparrow(\boldsymbol{k})\,\delta\left(\omega-\omega_0-\frac{\hbar k^2}{m}\right)\mathrm{d}^3k=2\pi C\sqrt{\frac{\hbar}{m}}\frac{1}{(\omega-\omega_0)^{3/2}} \quad (52)$$

and

$$\Gamma(\omega)\approx\frac{\Omega^2}{8\pi}\sqrt{\frac{\hbar}{m}}\,\frac{C}{(\omega-\omega_0)^{3/2}} \quad (53)$$

which is consistent with the prediction (34).

Note that in practice, $a_{e\downarrow}$ is never strictly zero. Braaten, Kang, et al. (2010) show that for $\omega\gtrsim\hbar/ma_{e\downarrow}^2$, the slow decay in $(\omega-\omega_0)^{-3/2}$ switches to a faster decay in $(\omega-\omega_0)^{-5/2}$, which ensures the convergence of the integral giving the center of mass of the line [see also Chin & Julienne (2005)]. Corrections related to the range $b\sim R_{\mathrm{vdW}}$ of the potential can also play a role for very large detunings.

3 Experimental studies on the Fermi gas

3-1 Radio-frequency spectroscopy

We presented in the previous chapter a first part of the results obtained by the Boulder group in 2010 for the measurement of the contact, using the momentum distribution of a ^{40}K fermion gas with $|\downarrow\rangle\equiv|F=9/2,m_F=-9/2\rangle$ and $|\uparrow\rangle\equiv|F=9/2,m_F=-7/2\rangle$ (Stewart, Gaebler, et al. 2010). Let us now describe the second study carried out by the same group using radio frequency spectroscopy, performed from the $|\uparrow\rangle$ state to the $|e\rangle\equiv|F=9/2,m_F=-5/2\rangle$ state. The transfer rate as a function of the detuning

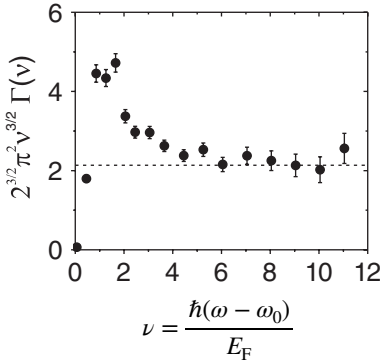

Figure 4. *Variation of $\nu^{3/2}\ \Gamma(\nu)$, where $\Gamma(\nu)$ is the rate of transfer from $|\uparrow\rangle$ to $|e\rangle$ by a radio frequency detuned by ν from resonance, ν being expressed here in units of $E_F/2\pi\hbar$. The plateau observed for large values of ν allows to determine the contact for the chosen value of a [$(k_F a)^{-1} = -0.03$ for these data].Figure extracted from Stewart, Gaebler, et al. (2010).*

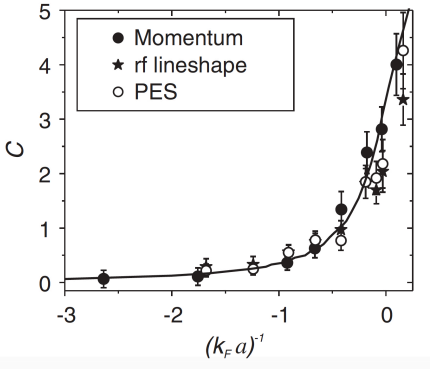

Figure 5. *Summary of the values obtained for the contact (in units of Nk_F) by measuring the momentum distribution (black dots) and by radio frequency spectroscopy (stars). The third data set uses photoemission spectroscopy (PES). The solid curve is the theoretical prediction of Werner, Tarruell, et al. (2009). Figure taken from Stewart, Gaebler, et al. (2010).*

$\omega - \omega_0$ is shown in figure 4. We see that this rate varies as expected as $(\omega - \omega_0)^{-3/2}$ at large detunings, and the proportionality coefficient thus provides another determination of the contact.

Figure 5 combines the two datasets for the contact obtained by Stewart, Gaebler, et al. (2010) from the momentum distribution and from radio frequency spectroscopy. A third dataset was obtained with the photoemission spectroscopy technique which we will not describe here. All these data are compatible with each other and their variation with $1/a$ is in good agreement with the qualitative discussion in the previous chapter.

Recently, the MIT group led by M. Zwierlein has further investigated the contact at the unitary point $a = \pm\infty$ using radio frequency spectroscopy (Mukherjee, Patel, et al. 2019). The MIT researchers varied the temperature of the gas to study the behavior of the contact when crossing the transition between the superfluid and normal states ($T_c \approx 0.17\,T_F$). These measurements, plotted in figure 6 (top), were performed in a uniform gas, confined in a box-like potential, which avoids the broadening of the spectrum that occurs in a harmonic trap because of the spatial density variations. The obtained spectra provide a lot of information about the physics involved. For example, the shift of the line maximum gives access to the energy of the Cooper pairs whose formation becomes energetically favorable for $T \lesssim 0.5\,T_F$. For the spectrum obtained at the lowest temperature, we clearly see a $(\omega - \omega_0)^{-3/2}$ wing (figure 6, bottom), with a slightly faster decay for very large detunings, related to the non-zero interactions between the e atoms and the $\downarrow$ atoms [see the discussion after equation (53)].

The contact deduced from the wing analysis of the radio frequency spectrum by the MIT group is shown in figure 7, along with results obtained simultaneously by the Swinburne group using the measurement of the dynamical structure factor $S(\boldsymbol{q}, \omega)$. The results of both groups are in excellent agreement and provide in particular the value in the zero temperature limit $C/Nk_F \approx 3$.

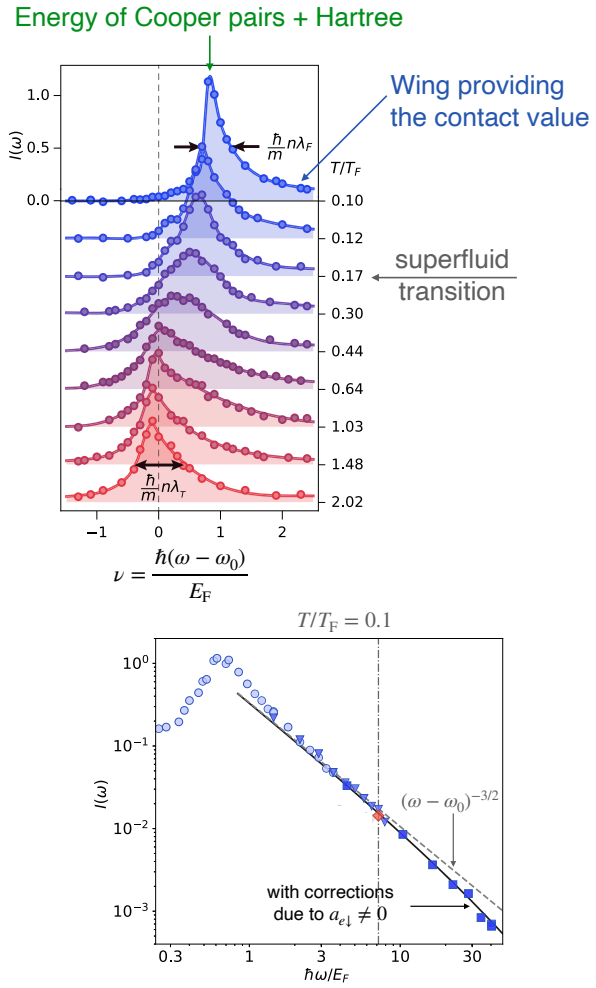

Figure 6. *Top: series of radio frequency spectra measured on a unitary Fermi gas ($|a| = +\infty$) for different temperatures. Bottom : spectrum measured at low temperature with the wing in $(\omega - \omega_0)^{-3/2}$, and corrections related to residual interactions between e and $\downarrow$. The analysis of these data gives $C = 3.07\,(6)$. Figures taken from Mukherjee, Patel, et al. (2019).*

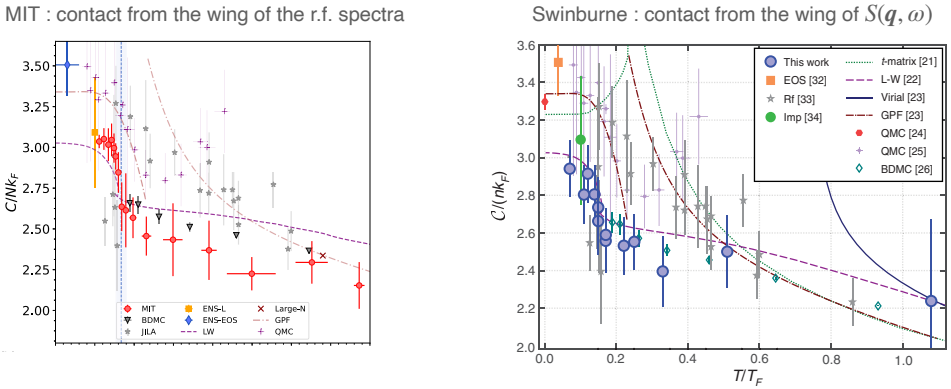

Figure 7. *Contact values for an equilibrium Fermi gas in the unitary regime as a function of temperature. Left figure taken from Mukherjee, Patel, et al. (2019). Right figure taken from Carcy, Hoinka, et al. (2019). Theoretical BDMC (bold-diagrammatic Monte Carlo) data were obtained by Rossi, Ohgoe, et al. (2018). The value of Laurent, Pierce, et al. (2017) discussed in § 3-2 is indicated by an orange square (green dot) on the left (right) plot.*

3-2 Measurement of contact by atom loss

Laurent, Pierce, et al. (2017) have developed an original approach to measure the contact in a ^{6}Li gas of spin 1/2 confined in an optical trap, by inserting a few ^{7}Li atoms playing the role of impurities (see also see Spiegelhalder, Trenkwalder, et al. (2009b) and Khramov, Hansen, et al. (2012)). The principle of the measurement is to study how impurities promote the formation of $^6\mathrm{Li}_2$ dimers. We are therefore interested in the three-body process:

$$^6\mathrm{Li}\uparrow + {}^6\mathrm{Li}\downarrow + {}^7\mathrm{Li} \longrightarrow {}^6\mathrm{Li}_2 + {}^7\mathrm{Li}. \tag{54}$$

The presence of the impurity allows for the conservation of energy and momentum in this process.

Since the dimer that is formed has a small extension ($b \sim R_{\mathrm{vdW}}$), the rate at which this process occurs gives information about the probability density for having the two ^{6}Li atoms close together, at a distance of $\sim b$ from each other: this is precisely the quantity to which the contact gives

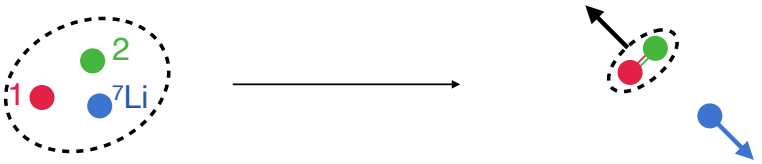

Figure 8. *The impurity assisted dimer formation process. At the end of the process, the energy released is converted into kinetic energy. This energy is large enough for the impurity to escape from the trap confining the particles.*

access. As the ^{7}Li atom has a large kinetic energy after the dimer formation, it escapes from the trap. The loss rate of the ^{7}Li atoms thus allows to infer the value of the contact in the ^{6}Li gas.

For a quantitative treatment of the problem, we introduce the three-body operator:

$$\iiint g(\boldsymbol{r}_\mathrm{i},\boldsymbol{r}_\uparrow,\boldsymbol{r}_\downarrow)\,\hat\Psi_\mathrm{d}^\dagger\left(\frac{\boldsymbol{r}_\uparrow+\boldsymbol{r}_\downarrow}{2}\right)\,\hat\Psi_\mathrm{i}^\dagger(\boldsymbol{r}_\mathrm{i})\,\hat\Psi_\mathrm{i}(\boldsymbol{r}_\mathrm{i})\,\hat\Psi_\uparrow(\boldsymbol{r}_\uparrow)\,\hat\Psi_\downarrow(\boldsymbol{r}_\downarrow)\,\mathrm{d}^3r_\mathrm{i}\,\mathrm{d}^3r_\uparrow\,\mathrm{d}^3r_\downarrow. \tag{55}$$

We see appearing in this operator the density of impurities in $\boldsymbol{r}_i$, $\hat n_\mathrm{i}(\boldsymbol{r}_\mathrm{i}) = \hat\psi_\mathrm{i}^\dagger(\boldsymbol{r}_\mathrm{i})\hat\psi_\mathrm{i}(\boldsymbol{r}_\mathrm{i})$; moreover, the dimer is created in the middle of the segment joining the two fermions $\uparrow$ and $\downarrow$ initially present. The function g, which depends on the details of the interaction potentials between the three atoms, takes significant values only when the three atoms are in the same volume of extension $\sim b$.

To calculate the rate of dimer production (and thus impurity loss), one can use an approach based on Fermi's golden rule. The treatment is detailed in the *Supplemental Material* of Laurent, Pierce, et al. (2017) and it is close to what we have developed for the calculation of the radio frequency spectrum. The result can be written

$$\dot N_\mathrm{i} = -\gamma(C/L^3)\,N_\mathrm{i}, \tag{56}$$

where the coefficient γ involves the coupling function g entering (55), but does not depend on the value of the scattering length a for the fermion gas.

The strategy adopted by Laurent, Pierce, et al. (2017) was to first calibrate the γ coefficient by making measurements of the loss rate $\dot N_\mathrm{i}$ in a regime where the contact is well known. In practice, these calibration measurements were made for a small and positive, favoring a dimer gas. The temperature was chosen well above the degeneracy temperature, so that the gas distribution in the trap was well described by a simple Boltzmann law.

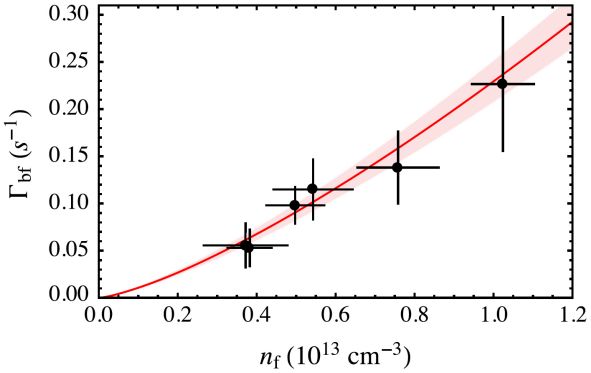

Figure 9. *Variation of ^{7}Li impurity loss rate as a function of the density of the ^{6}Li fermion gas. These data were taken at resonance ($a = \infty$ for the $\uparrow$ and $\downarrow$ fermion interaction) and the solid red line indicates the expected $n^{4/3}$ variation law. Figure extracted from Laurent, Pierce, et al. (2017).*

Once the γ coefficient was known, Laurent, Pierce, et al. (2017) placed their ^{6}Li gas at resonance ($a = \infty$) to study the contact in a strong interaction regime at a temperature as low as possible, in practice $T/T_\mathrm{F} \approx 0.1$. We have seen above [see for example figure 7] that in the unitary regime, we expect for the contact the following law

$$\frac{C}{L^3} = 2\pi\eta\; k_\mathrm{F} n \propto n^{4/3}. \tag{57}$$

According to (56), this same law in $n^{4/3}$ is expected for the impurity loss rate. We check on figure 9 that this is indeed the case. The fit of the experimental data provides the value $2\pi\eta \approx 3.1(4)$ for the coefficient in (57), in good agreement with the results shown in figure 7.

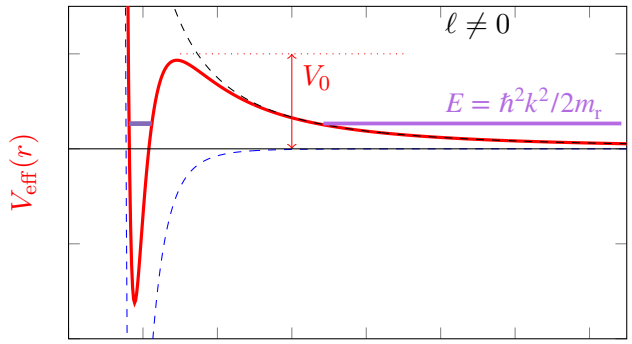

Figure 10. *Resonance for a $\ell \neq 0$ channel due to the presence of a quasi-bound state.*

3-3 The p wave contact

In this chapter we have been interested so far in s-wave interactions, characterized by a scattering length a, and we have introduced the contact as the thermodynamic quantity conjugate of a (or more precisely $1/a$), to within a multiplicative factor. This interest in s-wave interactions is justified: whether one takes a gas of polarized bosons or a gas of spin $1/2$ fermions, the momentum channel $\ell = 0$ is generally dominant over all others at low temperature. Recall that this is due to the centrifugal barrier $\hbar^2 \ell(\ell+1)/mr^2$ which exists in all $\ell \neq 0$ channels. This barrier is notably larger than the energy of the particles, so that the scattering in these channels is generally negligible.

Nevertheless, there are situations where scattering in a channel other than the s-wave can play an important role. Consider for example a polarized Fermi gas, so that there are no s-wave collisions. Suppose further that there exists a scattering resonance for the p-wave channel $\ell = 1$. Such a resonance can occur if there is a near zero energy quasi-bound state in the well formed by the attractive van der Waals potential and the repulsive centrifugal barrier (see figure 10): this is called a *shape resonance*. This resonance can also be induced by a coupling between two collision channels, one open, the other closed, according to the usual scheme of Fano–Feshbach resonances.

We discussed in the 2021 lecture series the main characteristics of a p-wave scattering process:

- In the region $b \lesssim r \ll 1/k$, the expected form for the radial part $\chi(r)$ of the wave function $\psi(r,\theta,\varphi) = \chi(r)\, Y_{\ell,m}(\theta,\varphi)$ is a linear combination of r^{-2} and r^1 (compare to the combination of r^{-1} and r^0 for the s wave). We introduce the scattering volume v to fix the relative weight of these two terms (it plays a similar role to that of the scattering length a for the s wave):
$$b \ll r \ll 1/k : \qquad \chi(r) \propto \frac{1}{r^2} - \frac{r}{3v}. \tag{58}$$
- The p-wave scattering amplitude is given by $f(k,\theta) = 3\cos(\theta)\, f_1(k)$ with:
$$p \text{ wave} : \qquad \frac{1}{f_1(k)} = -\frac{1}{k^2 v} + \frac{k_e}{2} - \mathrm{i}k + \dots \tag{59}$$
The dominant term also involves the scattering volume v. The next term $k_e/2$ is an effective range term and the last term written here, the pure imaginary $-\mathrm{i}k$, is a consequence of the unitarity of the scattering process (optical theorem).

Note that the situation is notably different from the case of the s wave scattering:
$$s \text{ wave} : \qquad \frac{1}{f_0(k)} = -\frac{1}{a} - \mathrm{i}k + \frac{1}{2} r_e k^2 + \dots \tag{60}$$
where the effective range term was a priori small in front of $-\mathrm{i}k$, itself small in front of the scattering length contribution. For a p-wave interacting system, it is preferable to keep the two independent parameters v and k_e to obtain a faithful characterization of the scattering process. Let us also note that for a Fano–Feshbach resonance induced by an external magnetic field $\boldsymbol{B}$, this field breaks the rotational invariance of the problem; it is then necessary to introduce v_m and $k_{e,m}$ with $m = -1, 0, +1$ corresponding to the three possible orientations of the angular momentum relative to $\boldsymbol{B}$.

The variation in $1/r^2$ of the relative wave function (58) suggests

- that the two-body correlation function will be dominated at short distances (while respecting $b \lesssim r$) by a term varying as $1/r^4$;
- that the probability amplitude to find the momentum $\boldsymbol{k}$ will be proportional to the Fourier transform of $1/r^2$, i.e. $1/k$, leading to a momentum probability distribution varying as $1/k^2$.

Detailed analyses conducted by Yoshida & Ueda (2015), Yu, Thywissen, et al. (2015), and Yu, Thywissen, et al. (2016) confirm this intuition. By introducing the variable conjugate to the scattering volume

$$C_{v,m} = -\frac{8\pi m}{\hbar^2}\left(\frac{\partial E}{\partial(1/v_m)}\right)_{S,N,V,k_e} \tag{61}$$

we then find for the distribution of pairs at short distance[3]:

$$\rho_2(\boldsymbol{r}_1,\boldsymbol{r}_2) = \frac{1}{4\pi L^3}\frac{1}{r^4}\sum_m |Y_{1,m}(\hat{\boldsymbol{r}})|^2 C_{v,m}, \tag{63}$$

where the function $Y_{1,m}(\hat{\boldsymbol{r}})$ is the spherical harmonic depending on the angular variables (θ,φ) marking the direction of the unit vector aligned with $\boldsymbol{r} = \boldsymbol{r}_1 - \boldsymbol{r}_2$. Similarly, we find for the momentum distribution

$$n(\boldsymbol{k}) = \frac{4\pi}{k^2}\sum_m |Y_{1,m}(\hat{\boldsymbol{k}})|^2 C_{v,m}. \tag{64}$$

Yu, Thywissen, et al. (2015) further discuss the introduction of the contact C_{k_e} related to the effective range term k_e, which for example adds a r^{-2} component to the pair distribution function and a k^{-4} component to the momentum distribution [see also Yu, Thywissen, et al. (2016)].

Note that the momentum distribution (64) is not normalizable, the decrease in k^{-2} at infinity being too slow. Setting a cutoff in k is therefore essential to make sense of this distribution. As explained by Yoshida & Ueda (2015), this divergence is related to the fact that unlike the s-wave case, there is no physical limit of a zero range potential leading to a p-wave resonant interaction (see also Pricoupenko (2006)).

[3] In the case where the three contacts C_m are equal, the following relation on the spherical harmonics is useful:

$$\sum_m |Y_{1,m}(\boldsymbol{u})|^2 = \frac{3}{4\pi}. \tag{62}$$

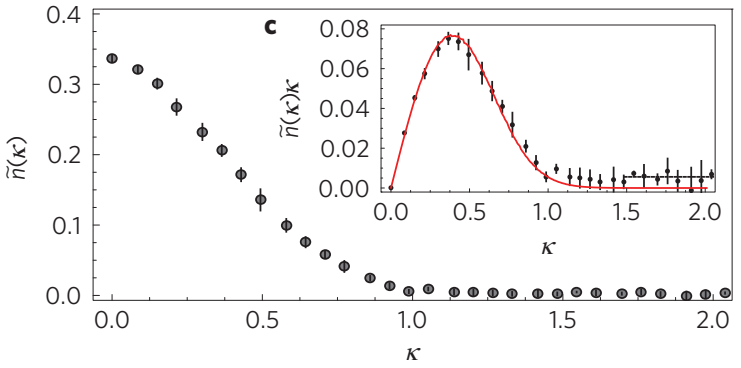

Figure 11. *Momentum distribution of a polarized Fermi gas (^{40}K) in the vicinity of a p-wave Feshbach resonance for $v_{m=\pm1}$ ($B = 198.3\,G$). This distribution is measured by time of flight, with integration along the imaging z axis (chosen parallel to the magnetic field). The expected $1/k^2$ law translates here into a variation in $1/\kappa$, with $\kappa \propto \left(k_x^2 + k_y^2\right)^{1/2}$, because of the integration along the imaging beam axis. Figure extracted from Luciuk, Trotzky, et al. (2016).*

The evidence of a k^{-2} component in the momentum distribution was provided by the Toronto group led by J. Thywissen (Luciuk, Trotzky, et al. 2016) and the result is shown in figure 11. The set of data of Luciuk, Trotzky, et al. (2016), obtained both by radio-frequency spectroscopy and by the measurement of $n(k)$, is plotted in figure 12 for the two contacts C_v and C_{k_e}. As expected, we see that these contacts take significant values in the regime where a quasi-bound state is close to the characteristic energy of the atoms, i.e. the Fermi energy.

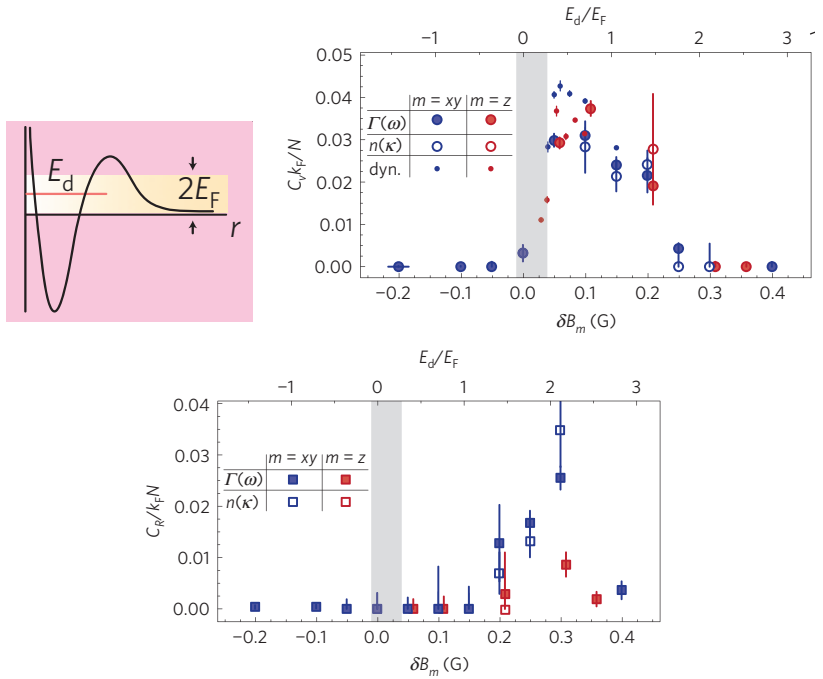

Figure 12. *Contacts C_v and C_{k_e}, associated with the parameters v and k_e (C_{k_e} is noted here C_R), and inferred from radio-frequency spectroscopy and from the momentum distribution. Figure extracted from Luciuk, Trotzky, et al. (2016).*

4 Two-body contact for Bose gases

4-1 The various regimes for Bose gases

We are interested here in the case of a gas of spinless or polarized bosons, with s-wave interactions characterized by the scattering length a. As always for this course, we assume that the gas is dilute so that $nb^3 \ll 1$, where b is the range of the potential. The extension of Tan's results to the case of bosons was carried out as early as the late 2000s by Combescot, Alzetto, et al. (2009) (who neglected the three-body effects), and then by Braaten, Kang, et al. (2011), Werner & Castin (2012a), and Smith, Braaten, et al. (2014) (who have taken them into account). The first Bose gas experiments were conducted in the Boulder group by Wild, Makotyn, et al. (2012) and will be described in §4-3.

We will start by summarizing the different possible situations:

- The case of a gas in weak interaction, $na^3 \ll 1$ with $a > 0$. At low temperature, this case can be described by the Bogoliubov approximation; at higher temperature, the Hartree-Fock method or the virial expansion can be used.

  On the theoretical level, if the interaction potential between atoms is completely repulsive, with a range $b \sim a$ (this is the case for a hard sphere potential for example), no instability is to be feared. On a practical level however, there are always bound states in the interatomic potential for the species used in the laboratory, which can induce losses[4] of atoms escaping from the trap as diatomic molecules. These molecules are formed in a three-body collision, in which two partners form the bound state and the third carries away the energy released in the creation of the dimer. We recall that these losses are absent for a spin 1/2 Fermi gas because the Pauli principle forbids to have three fermions close to each other if only two spin states $\uparrow$ and $\downarrow$ are available.

  Fortunately, as explained in Chapter 3 (§1.1), the condition $na^3 \ll 1$ guarantees that there is a time range during which the gas has reached its equilibrium state without the losses mentioned above playing an appreciable role.

- The case of a weak interaction ($n|a|^3 \ll 1$) with $a < 0$. At low temperature and in three dimensions, the use of the mean field theory leads to a dynamical instability of the gas and to its collapse.

- The strong interaction regime, $n|a|^3 \gtrsim 1$, with a positive or negative. In this case, which requires $|a| \gg b$, a series of weakly bound three-body states can appear. The number of these states is infinite for

[4] In fact, these losses are themselves an interesting process, as they may exhibit a universal character, as shown theoretically by Braaten & Hammer (2013a) and Laurent, Leyronas, et al. (2014), and studied experimentally by Rem, Grier, et al. (2013), Fletcher, Gaunt, et al. (2013), and Eismann, Khaykovich, et al. (2016). Furthermore, these losses can lead to a violation of Tan relations, as shown in the one-dimensional case by Bouchoule & Dubail (2021).

$a = \pm\infty$: this is the well-known Efimov (1971) effect [see Naidon & Endo (2017) for a review]. These states can have a large extension and it is easy to form them during collisions in the gas. Therefore, the contribution of these states must be taken into account in determining the thermodynamic equilibrium of the system.

To characterize the thermodynamics of the system, it is then necessary to introduce, in addition to the two-body contact, another parameter called the *three-body contact* (Braaten, Kang, et al. 2011; Werner & Castin 2012a; Smith, Braaten, et al. 2014). The first experimental measurement of this three-body contact was made by Fletcher, Lopes, et al. (2017). We will not discuss these experiments here because their explanation requires the development of a specific formalism, which we defer to a future lecture series.

Moreover, in this regime, the formation of dimers mentioned above becomes problematic. In the regime close to $T = 0$, the gas does not have time to reach its equilibrium state before having lost a significant fraction of its constituents. The study of the thermodynamic equilibrium of a strongly interacting Bose gas can therefore only be done in the non-degenerate regime (Li & Ho 2012; Fletcher, Gaunt, et al. 2013; Rem, Grier, et al. 2013; Chevy & Salomon 2016).

4-2 Predictions for the two-body contact

We have plotted in table 1 the expected values for the two-body contact of a Bose gas in the regimes mentioned above. In the non resonant case and at $T = 0$, we are dealing with an "ordinary" Bose–Einstein condensate. The value of the contact is directly deduced from the mean field prediction for the energy of the condensate:

$$E_{\mathrm{m.f.}} = \frac{1}{2} gnN \qquad \text{with} \quad g = \frac{4\pi\hbar^2 a}{m} \quad \Rightarrow \quad C = (4\pi a)^2 nN. \tag{65}$$

Let's stay in the non resonant case and go to the non degenerate case. Using the virial expansion, we saw in chapter 1, § 2.3, that the interaction energy is simply doubled compared to the value (65). The contact is therefore also doubled, this increase being simply a signature of the bunching effect discovered by Hanbury-Brown & Twiss (1956).

	$T = 0$	Non degenerate $n\lambda^3 \ll 1$
Off resonance	$(4\pi na)^2$	$2 \times (4\pi na)^2$
On resonance	$\sim n^{4/3}$	$32\pi(n\lambda)^2$

Table 1. *Predicted values for the two-body contact per unit volume C/L^3 of a Bose gas.*

Let us now turn to the resonant case. The zero temperature value is given here as a mere scaling law $\sim n^{4/3}$ (Diederix, Heijst, et al. 2011; Sykes, Corson, et al. 2014; Smith, Braaten, et al. 2014), but is difficult to test it experimentally. Indeed, as explained in § 4-1, it is not possible to produce a Bose gas at equilibrium in this regime, given the large three-body loss rate. In contrast, the prediction in the last box of the table, corresponding to a non degenerate gas with resonant interactions, is experimentally testable (Fletcher, Lopes, et al. 2017). We now briefly explain how to arrive at this value.

We use the virial expansion, already discussed in chapter 1 of this lecture series, which gives the expansion of the grand potential Ω in powers of the fugacity $z = \exp(\mu/k_{\mathrm{B}}T)$:

$$\Omega = -PV = -\frac{k_{\mathrm{B}}TV}{\lambda^3} \sum_{j=1}^{\infty} b_j(T) z^j \tag{66}$$

which we truncate to order 2. We use the thermodynamic definition of contact (recall that $b_1(T) = 1$ for any temperature):

$$C = \frac{8\pi a^2 m}{\hbar^2} \left(\frac{\partial \Omega}{\partial a}\right)_{T,V,\mu} = -16\pi^2 nN\lambda a^2 \left(\frac{\partial b_2}{\partial a}\right)_T \tag{67}$$

where we used $z = n\lambda^3$ at this order of the calculation.

Let us now take the part of $b_2(T)$ related to the interactions and calculated in chapter 1:

$$b_2^{(\mathrm{int})} = \frac{2^{3/2}}{\pi} \int_0^{+\infty} \frac{\mathrm{d}\delta_0}{\mathrm{d}k} \mathrm{e}^{-\hbar^2 k^2/mk_{\mathrm{B}}T} \, \mathrm{d}k \; + \; \Theta(a) \, 2^{3/2} \mathrm{e}^{-E_{\mathrm{lie}}/k_{\mathrm{B}}T}. \tag{68}$$

Recall that the first contribution comes from the continuum formed by the scattering states; it involves the phase shift $\delta_0(k)$ of an s wave collision,

given by:

$$\frac{\mathrm{d}\delta_0}{\mathrm{d}k} = \frac{-a}{1+k^2a^2}. \tag{69}$$

The second contribution, due to the possible bound state intervening in the resonance, of energy $E_{\rm bound} = -\hbar^2/ma^2$, is present only in the domain $a > 0$, hence the Heaviside function $\Theta(a)$.

The calculation consists in taking the derivative of b_2 with respect to a, then considering the limit $a = \pm\infty$. It does not present any difficult step, even if it is a bit long [see for example Braaten & Hammer (2013b)]. We arrive at the same value in both limits $a \to -\infty$ (no bound state) and $a \to +\infty$ (the bound state contributes). This value is given in table 1. Note that although the contact $C(a)$ itself is continuous and finite in $1/a = 0$, its left and right derivatives do not coincide due to the singularity introduced by the function $\Theta(a)$. The curve $C(a)$ thus exhibits a cusp at resonance.

4-3 Two-body contact and rf spectroscopy

The first experimental determination of the contact for bosons was carried out by Wild, Makotyn, et al. (2012) on a condensed gas of ^{85}Rb. Using a Feshbach resonance ($B = 155\,$G), the scattering length was varied between $300\,a_0$ and $1300\,a_0$, i.e. from 3 to 13 times the range $b \sim R_{\rm vdW}$ of the van der Waals potential. This determination was based on radio-frequency spectroscopy, similar to that described for fermions in §2, with the search for a $(\omega-\omega_0)^{-3/2}$ component in the wing of the r.f. spectrum [*cf.* §2-3]. A typical result is shown in figure 13 (left).

Wild, Makotyn, et al. (2012) then studied (still in the zero temperature limit) the variation of the contact with the scattering length a. Using the link between the contact and $\partial E/\partial a$, one deduces from the result of Lee, Huang, et al. (1957) the expected value for C:

$$C = (4\pi a)^2 n N_0 \left(1 + \frac{64}{3\sqrt{\pi}}\sqrt{na^3}\right). \tag{70}$$

The experimental result is plotted in figure 13 (right). The mean field prediction (only the "1" in the parenthesis above) is plotted as a solid line. The dashed line shows the prediction including the $\sqrt{na^3}$ correction. For these

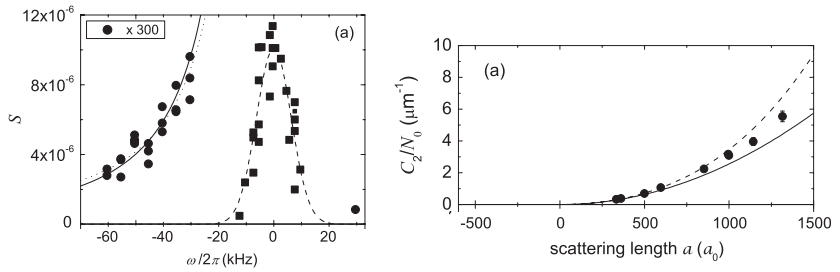

Figure 13. *Left: radio-frequency spectrum measured on a ^{85}Rb condensate. One deduces the value of the contact from the wing of the spectrum, fitted by a $(\omega-\omega_0)^{-3/2}$ law. Right: variation of the contact with the scattering length a. Figure extracted from Wild, Makotyn, et al. (2012).*

data, the average density was $\sim 6\times10^{12}\,\mathrm{cm}^{-3}$ and the maximum value of $\sqrt{na^3}$ was ~ 0.04. The precise origin of the discrepancy between the experimental data and the prediction (70) is not known, but Wild, Makotyn, et al. (2012) mention the dependence of the measured value for C with $\dot{B}$. The quantity $\dot{B}$ designates here the speed with which the magnetic field is brought to its final value to fix the value of the scattering length. One can therefore suspect that slight non-equilibrium effects have affected these measurements.

Wild, Makotyn, et al. (2012) also looked for a signature of the three-body contact in their data. The contribution of this contact was expected to be a wing of the r.f. spectrum varying as $G(\omega)/\omega^2$, where $G(\omega)$ is a log-periodic function depending on the three-body parameter. However, no measurable contribution of this three-body physics was observed in the Boulder experiment, in contrast with the subsequent experiment of Fletcher, Lopes, et al. (2017).

4-4 Measurement of the contact by Ramsey spectroscopy

Zou, Bakkali-Hassani, et al. (2021) have carried out a measurement of the contact of a Bose gas in the non-resonant case, sweeping a wide range of temperatures from the quasi-non-degenerate regime (phase-space density

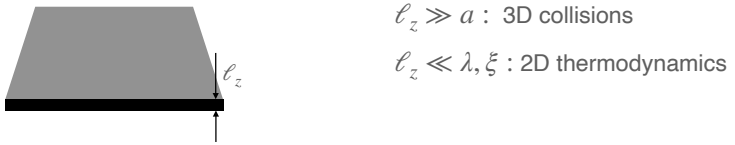

Figure 14. *Quasi- two-dimensional gas used for two-body contact measurement by Zou, Bakkali-Hassani, et al. (2021).*

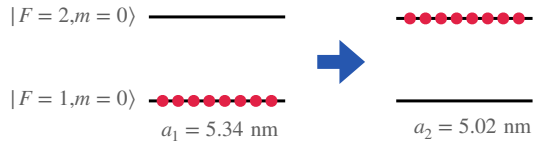

Figure 15. *Transfer between two internal states of ^{87}Rb to determine the value of the two-body contact.*

$\mathcal{D} \sim 2$) to the case of a practically pure condensate ($\mathcal{D} \sim 70$). This measurement has been carried out in a quasi-bidimensional configuration (figure 14): the gas thickness along the "frozen" dimension is small in front of the thermal wavelength and the healing length, but it remains large in front of the scattering length a, so that the 3D modeling of a collision process adopted so far continues to be relevant.

The experimental procedure takes advantage of the fact that the scattering lengths describing the interactions between atoms in a ^{87}Rb gas are all close to each other for the different possible internal states composing the ground electronic level. Starting from a gas in the internal state $|1\rangle = |F = 1, m = 0\rangle$ ($a_{11} = 100.9\, a_0$), Zou, Bakkali-Hassani, et al. (2021) have measured the energy ΔE to be supplied to the gas[5] for achieving a full transfer of the atoms to the state $|2\rangle = |F = 2, m = 0\rangle$ ($a_{22} = 94.9\, a_0$) [*cf.* figure 15]. The contact is then deduced directly from its thermodynamic definition:

$$C = \frac{8\pi m a^2}{\hbar^2} \left(\frac{\partial E}{\partial a}\right)_{N,V,S} \approx \frac{8\pi m a^2}{\hbar^2} \frac{\Delta E}{\Delta a} \tag{71}$$

with $\Delta a = a_2 - a_1$. The transition takes place (approximately) at constant entropy because of the small variation of a.

The transfer from $|1\rangle$ to $|2\rangle$ is done by a Ramsey method, with two short $\pi/2$ microwave pulses separated by a waiting time of duration $\tau = 10\,\text{ms}$. We scan the frequency ν of the microwave inducing the transfer and we look for which value of ν the transfer is optimal. An example of Ramsey signal is shown in figure 16, left. We can verify that at the top of the central fringe (whose position depends on the gas density), the transfer from $|1\rangle$ to $|2\rangle$ is indeed total.

The link with the contact[6] is obtained thanks to (71) and the result is shown in figure 16, right. The results of Zou, Bakkali-Hassani, et al. (2021) are in good agreement with the existing theories in the two limiting cases of a non-degenerate gas (virial expansion) and a strongly degenerate gas (classical field method or Bogoliubov approximation). In the critical zone where the superfluid transition occurs (phase-space density ~ 8), there is to our knowledge no theory that has reproduced quantitatively these experimental results.

[5] after subtraction of the energy $Nh\nu_0$, where $h\nu_0$ is the internal energy change for an isolated atom.

[6] To apply the result (71), it is important that the three scattering lengths a_{11}, a_{12}, a_{22} are close to each other, i.e. close to the SU(2) symmetry for this two-state system. The constraint on a_{12} comes from the fact that during the waiting time τ between the two pulses, the two states $|1\rangle$ and $|2\rangle$ are simultaneously present in the trap [see Zou, Bakkali-Hassani, et al. (2021) for a detailed description of the evolution of the gas during this phase].

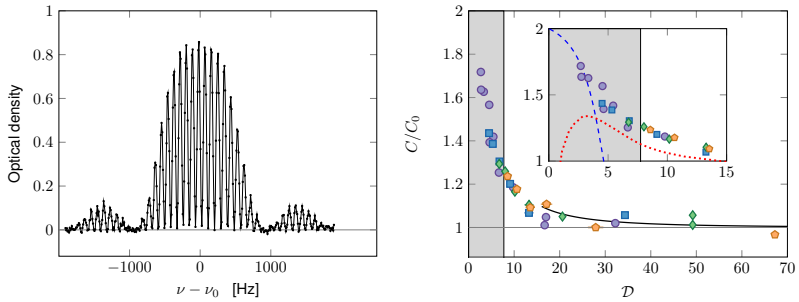

Figure 16. *Left: Ramsey spectroscopy signal, allowing to determine the energy to be supplied to a ^{87}Rb gas to make its internal state switch from $|F = 1, m = 0\rangle$ to $|F = 2, m = 0\rangle$ and thus change its scattering length by the amount $\Delta a = a_{22} - a_{11}$. Right: Value of the contact deduced from (71), plotted in units of the contact C_0 for the Bogoliubov regime. The dashed curve gives the result of the virial expansion (Ren 2004). The dotted curve corresponds to the predictions of a classical field theory (Prokof'ev & Svistunov 2002). Figure extracted from Zou, Bakkali-Hassani, et al. (2021).*

References

Altmeyer, A, S Riedl, C Kohstall, MJ Wright, R Geursen, M Bartenstein, C Chin, J Hecker-Denschlag & R Grimm (2007), "Precision measurements of collective oscillations in the BEC-BCS crossover", in *Physical review letters* 98.4, p. 040401.

Baym, Gordon, CJ Pethick, Zhenhua Yu & Martin W Zwierlein (2007), "Coherence and clock shifts in ultracold Fermi gases with resonant interactions", in *Physical review letters* 99.19, p. 190407.

Beliaev, ST (1958a), "Application of the methods of quantum field theory to a system of bosons", in *SOVIET PHYSICS JETP-USSR* 7.2, pp. 289–299.

– (1958b), "Energy spectrum of a non-ideal Bose gas", in *Sov. Phys. JETP* 7.2, pp. 299–307.

Beth, Erich & George E Uhlenbeck (1937), "The quantum theory of the non-ideal gas. II. Behaviour at low temperatures", in *Physica* 4.10, pp. 915–924.

Blume, D. & K. M. Daily (2009), "Universal relations for a trapped four-fermion system with arbitrary s-wave scattering length", in *Phys. Rev. A* 80 (5), p. 053626.

Bogoliubov, N. N. (1947), "On the theory of superfluidity", in *J. Phys. (USSR)* 11, p. 23.

Bookjans, Eva M., Christopher D. Hamley & Michael S. Chapman (2011), "Strong Quantum Spin Correlations Observed in Atomic Spin Mixing", in *Phys. Rev. Lett.* 107 (21), p. 210406.

Böttcher, Fabian, Jan-Niklas Schmidt, Jens Hertkorn, Kevin Ng, Sean Graham, Mingyang Guo, Tim Langen & Tilman Pfau (2021), "New states of matter with fine-tuned interactions: quantum droplets and dipolar supersolids", in *Reports on Progress in Physics* 84, p. 012403.

Böttcher, Fabian, Jan-Niklas Schmidt, Matthias Wenzel, Jens Hertkorn, Mingyang Guo, Tim Langen & Tilman Pfau (2019), "Transient supersolid properties in an array of dipolar quantum droplets", in *Physical Review X* 9.1, p. 011051.

Bouchoule, I. & J. Dubail (2021), "Breakdown of Tan's Relation in Lossy One-Dimensional Bose Gases", in *Phys. Rev. Lett.* 126 (16), p. 160603.

Bouchoule, Isabelle, Léa Dubois & Léo-Paul Barbier (2021), "Losses in interacting quantum gases: Ultraviolet divergence and its regularization", in *Phys. Rev. A* 104 (3), p. L031304.

Braaten, Eric (2011), "Universal Relations for Fermions with Large Scattering Length", in *BCS-BEC Crossover and the Unitary Fermi Gas*, ed. by Wilhelm Zwerger, Springer.

Braaten, Eric & H.-W. Hammer (Nov. 2013a), "Universal Relation for the Inelastic Two-Body Loss Rate"en, in *Journal of Physics B: Atomic, Molecular and Optical Physics* 46.21arXiv: 1302.5617, p. 215203.

Braaten, Eric & HW Hammer (2013b), "Universal relation for the inelastic two-body loss rate", in *Journal of Physics B: Atomic, Molecular and Optical Physics* 46.21, p. 215203.

Braaten, Eric, Daekyoung Kang & Lucas Platter (2010), "Short-Time Operator Product Expansion for rf Spectroscopy of a Strongly Interacting Fermi Gas", in *Phys. Rev. Lett.* 104 (22), p. 223004.

– (2011), "Universal Relations for Identical Bosons from Three-Body Physics", in *Phys. Rev. Lett.* 106 (15), p. 153005.

Braaten, Eric, Masaoki Kusunoki & Dongqing Zhang (2008), "Scattering Models for Ultracold Atoms", in *Annals of Physics* 323.7, pp. 1770–1815.

Braaten, Eric & Lucas Platter (May 2008), "Exact Relations for a Strongly Interacting Fermi Gas from the Operator Product Expansion"en, in *Physical Review Letters* 100.20, p. 205301.

Brodsky, I. V., M. Yu. Kagan, A. V. Klaptsov, R. Combescot & X. Leyronas (2006), "Exact diagrammatic approach for dimer-dimer scattering and

bound states of three and four resonantly interacting particles", in *Phys. Rev. A* 73 (3), p. 032724.
Cabrera, CR, L Tanzi, J Sanz, B Naylor, P Thomas, P Cheiney & L Tarruell (2018), "Quantum liquid droplets in a mixture of Bose-Einstein condensates", in *Science* 359.6373, pp. 301–304.
Campana, LS, A Caramico D'Auria, L Cesare & U Esposito (1979), "On the validity of the Bogoliubov approximation for a high-density Bose model", in *Lettere al Nuovo Cimento (1971-1985)* 24.5, pp. 147–150.
Carcy, C., S. Hoinka, M. G. Lingham, P. Dyke, C. C. N. Kuhn, H. Hu & C. J. Vale (2019), "Contact and Sum Rules in a Near-Uniform Fermi Gas at Unitarity", in *Phys. Rev. Lett.* 122 (20), p. 203401.
Carlen, Eric A, Markus Holzmann, Ian Jauslin & Elliott H Lieb (2021), "Simplified approach to the repulsive Bose gas from low to high densities and its numerical accuracy", in *Physical Review A* 103.5, p. 053309.
Castin, Y. & R. Dum (1998), "Low-temperature Bose-Einstein condensates in time-dependent traps: Beyond the $U(1)$ symmetry-breaking approach", in *Phys. Rev. A* 57 (4), pp. 3008–3021.
Castin, Yvan, Christophe Mora & Ludovic Pricoupenko (2010), "Four-Body Efimov Effect for Three Fermions and a Lighter Particle", in *Phys. Rev. Lett.* 105 (22), p. 223201.
Castin, Yvan & Félix Werner (2011), "Single-particle momentum distribution of an Efimov trimer", in *Phys. Rev. A* 83 (6), p. 063614.
Castin, Yvan & Félix Werner (May 2013), "Troisième coefficient du viriel du gaz de Bose unitaire", in *Canadian Journal of Physics* 91, pp. 382–389.
Cayla, Hugo, Salvatore Butera, Cécile Carcy, Antoine Tenart, Gaétan Hercé, Marco Mancini, Alain Aspect, Iacopo Carusotto & David Clément (2020), "Hanbury Brown and Twiss Bunching of Phonons and of the Quantum Depletion in an Interacting Bose Gas", in *Physical Review Letters* 125.16, p. 165301.
Ceperley, D., G. V. Chester & M. H. Kalos (1978), "Monte Carlo study of the ground state of bosons interacting with Yukawa potentials", in *Phys. Rev. B* 17 (3), pp. 1070–1081.
Cheiney, P, CR Cabrera, J Sanz, B Naylor, L Tanzi & L Tarruell (2018), "Bright soliton to quantum droplet transition in a mixture of Bose-Einstein condensates", in *Physical review letters* 120.13, p. 135301.
Chevy, F., V. Bretin, P. Rosenbusch, K. W. Madison & J. Dalibard (2001), "Transverse Breathing Mode of an Elongated Bose–Einstein Condensate", in *Phys. Rev. Lett.* 88, p. 250402.
Chevy, F & C Salomon (2016), "Strongly correlated Bose gases", in *Journal of Physics B: Atomic, Molecular and Optical Physics* 49.19, p. 192001.
Chin, Cheng & Paul S. Julienne (Jan. 2005), "Radio-frequency transitions on weakly bound ultracold molecules"en, in *Physical Review A* 71.1, p. 012713.
Chomaz, L, S Baier, D Petter, MJ Mark, F Wächtler, Luis Santos & F Ferlaino (2016), "Quantum-fluctuation-driven crossover from a dilute Bose-Einstein condensate to a macrodroplet in a dipolar quantum fluid", in *Physical Review X* 6.4, p. 041039.
Chomaz, L, D Petter, P Ilzhöfer, G Natale, A Trautmann, C Politi, G Durastante, RMW Van Bijnen, A Patscheider, M Sohmen, et al. (2019), "Long-lived and transient supersolid behaviors in dipolar quantum gases", in *Physical Review X* 9.2, p. 021012.
Cohen-Tannoudji, Claude, Bernard Diu & Franck Laloë (2021), *Mécanique quantique-Tome 3*, EDP sciences.
Cohen-Tannoudji, Claude, Bernard Diu & Frank Laloe (1986), "Quantum Mechanics, Volume 2", in *Quantum Mechanics* 2, p. 626.
Combescot, R., F. Alzetto & X. Leyronas (2009), "Particle distribution tail and related energy formula", in *Phys. Rev. A* 79 (5), p. 053640.
Diederix, J. M., T. C. F. van Heijst & H. T. C. Stoof (2011), "Ground state of a resonantly interacting Bose gas", in *Phys. Rev. A* 84 (3), p. 033618.
Donnelly, R. J., J. A. Donnelly & R. N. Hills (1981), "Specific heat and dispersion curve for helium II", in *Journal of Low Temperature Physics* 44.5, pp. 471–489.
Drut, Joaquín E., Timo A. Lähde & Timour Ten (2011), "Momentum Distribution and Contact of the Unitary Fermi Gas", in *Phys. Rev. Lett.* 106 (20), p. 205302.
Duan, L.-M., A. Sørensen, J. I. Cirac & P. Zoller (2000), "Squeezing and Entanglement of Atomic Beams", in *Phys. Rev. Lett.* 85 (19), p. 3991.
Efimov, V (1971), "Weakly-bound states of three resonantly-interacting particles", in *Sov. J. Nucl. Phys* 12.589, p. 101.
Eismann, Ulrich, Lev Khaykovich, Sébastien Laurent, Igor Ferrier-Barbut, Benno S. Rem, et al. (2016), "Universal Loss Dynamics in a Unitary Bose Gas", in *Phys. Rev. X* 6 (2), p. 021025.
Endo, Shimpei (2020), "Virial expansion coefficients in the unitary Fermi gas", in *SciPost Physics Proceedings* 3, p. 049.
Endo, Shimpei & Yvan Castin (2015), "Absence of a four-body Efimov effect in the $2+2$ fermionic problem", in *Phys. Rev. A* 92 (5), p. 053624.

– (2016a), "The interaction-sensitive states of a trapped two-component ideal Fermi gas and application to the virial expansion of the unitary Fermi gas", in *Journal of Physics A: Mathematical and Theoretical* 49.26, p. 265301.
– (2016b), "Unitary boson-boson and boson-fermion mixtures: third virial coefficient and three-body parameter on a narrow Feshbach resonance", in *The European Physical Journal D* 70.11, p. 238.
Evrard, Bertrand, An Qu, Jean Dalibard & Fabrice Gerbier (2021), "From Many-Body Oscillations to Thermalization in an Isolated Spinor Gas", in *Phys. Rev. Lett.* 126 (6), p. 063401.
Fedichev, PO, MW Reynolds & GV Shlyapnikov (1996), "Three-body recombination of ultracold atoms to a weakly bound s level", in *Physical review letters* 77.14, p. 2921.
Ferrier-Barbut, Igor (2019), "Ultradilute quantum droplets", in *Physics Today* 72.4, pp. 46–52.
Ferrier-Barbut, Igor, Holger Kadau, Matthias Schmitt, Matthias Wenzel & Tilman Pfau (2016), "Observation of quantum droplets in a strongly dipolar Bose gas", in *Physical review letters* 116.21, p. 215301.
Feynman, R. P. (1954), "Atomic Theory of the Two-Fluid Model of Liquid Helium", in *Phys. Rev.* 94 (2), pp. 262–277.
Fletcher, Richard J., Alexander L. Gaunt, Nir Navon, Robert P. Smith & Zoran Hadzibabic (2013), "Stability of a Unitary Bose Gas", in *Phys. Rev. Lett.* 111 (12), p. 125303.
Fletcher, Richard J, Raphael Lopes, Jay Man, Nir Navon, Robert P Smith, Martin W Zwierlein & Zoran Hadzibabic (2017), "Two-and three-body contacts in the unitary Bose gas", in *Science* 355.6323, pp. 377–380.
Foldy, Leslie L (1961), "Charged boson gas", in *Physical Review* 124.3, p. 649.
Garcia-Colin, Leopoldo S (1960), "Pair Distribution Function of a Hard Sphere Bose System Calculated by the Pseudo-Potential Method", in *Journal of Mathematical Physics* 1.2, pp. 87–96.
Gardiner, C. W. (1997), "Particle-number-conserving Bogoliubov method which demonstrates the validity of the time-dependent Gross-Pitaevskii equation for a highly condensed Bose gas", in *Phys. Rev. A* 56 (2), pp. 1414–1423.
Gavoret, J & Ph Nozieres (1964), "Structure of the perturbation expansion for the Bose liquid at zero temperature", in *Annals of Physics* 28.3, pp. 349–399.
Gavoret, Jean (1963), "Application de la théorie des perturbations à l'étude d'un liquide de Bose au zéro absolu", in *Annales de Physique*, vol. 13, 8, EDP Sciences, , pp. 441–491.
Girardeau, M (1962), "Ground state of the charged Bose gas", in *Physical Review* 127.5, p. 1809.
Glyde, H. R., R. T. Azuah & W. G. Stirling (2000), "Condensate, momentum distribution, and final-state effects in liquid ^{4}He", in *Phys. Rev. B* 62 (21), pp. 14337–14349.
Glyde, H. R., S. O. Diallo, R. T. Azuah, O. Kirichek & J. W. Taylor (2011), "Atomic momentum distribution and Bose-Einstein condensation in liquid ^{4}He under pressure", in *Phys. Rev. B* 84 (18), p. 184506.
Griffin, Allan (1993), *Excitations in a Bose-condensed liquid*, 4, Cambridge University Press.
Gross, C., T. Zibold, E. Nicklas, J. Estève & M. K. Oberthaler (2010), "Nonlinear atom interferometer surpasses classical precision limit", in *Nature* 464, 1165 EP –.
Guarrera, Vera, Peter Würtz, Arne Ewerbeck, Andreas Vogler, Giovanni Barontini & Herwig Ott (2011), "Observation of local temporal correlations in trapped quantum gases", in *Physical review letters* 107.16, p. 160403.
Guggenheim, E Ao (1945), "The principle of corresponding states", in *The Journal of Chemical Physics* 13.7, pp. 253–261.
Guo, Zhichao, Fan Jia, Lintao Li, Yinfeng Ma, Jeremy M. Hutson, Xiaoling Cui & Dajun Wang (2021), "Lee-Huang-Yang effects in the ultracold mixture of ^{23}Na and ^{87}Rb with attractive interspecies interactions", in *Phys. Rev. Research* 3 (3), p. 033247.
Gupta, S, Z Hadzibabic, MW Zwierlein, CA Stan, K Dieckmann, CH Schunck, EGM Van Kempen, BJ Verhaar & W Ketterle (2003), "Radio-frequency spectroscopy of ultracold fermions", in *Science* 300.5626, pp. 1723–1726.
Halinen, Jani, Vesa Apaja & Mikko Saarela (2000), "Role of short-and long-range interactions in quantum Bose fluids", in *Physica B: Condensed Matter* 284, pp. 3–4.
Hanbury-Brown, R. & R. Q. Twiss (1956), "Correlation between photons in two coherent beams of light", in *Nature* 177, pp. 27–29.
Haussmann, R. (1994), "Properties of a Fermi liquid at the superfluid transition in the crossover region between BCS superconductivity and Bose-Einstein condensation", in *Phys. Rev. B* 49 (18), pp. 12975–12983.

Haussmann, Rudolf, Matthias Punk & Wilhelm Zwerger (2009), "Spectral functions and rf response of ultracold fermionic atoms", in *Physical Review A* 80.6, p. 063612.
Ho, Tin-Lun & Erich J. Mueller (2004), "High Temperature Expansion Applied to Fermions near Feshbach Resonance", in *Phys. Rev. Lett.* 92 (16), p. 160404.
Ho, Tin-Lun & Qi Zhou (2010), "Obtaining the phase diagram and thermodynamic quantities of bulk systems from the densities of trapped gases", in *Nature Physics* 6.2, pp. 131–134.
Hofmann, Johannes & Wilhelm Zwerger (2017), "Deep Inelastic Scattering on Ultracold Gases", in *Phys. Rev. X* 7 (1), p. 011022.
Hohenberg, P. C. & P. M. Platzman (1966), "High-Energy Neutron Scattering from Liquid He^4", in *Phys. Rev.* 152 (1), pp. 198–200.
Holzmann, Markus & Yvan Castin (1999), "Pair correlation function of an inhomogeneous interacting Bose-Einstein condensate", in *The European Physical Journal D-Atomic, Molecular, Optical and Plasma Physics* 7.3, pp. 425–432.
Hou, Y. & J. E. Drut (2020), "Fourth- and Fifth-Order Virial Coefficients from Weak Coupling to Unitarity", in *Phys. Rev. Lett.* 125 (5), p. 050403.
Hou, Y, KJ Morrell, AJ Czejdo & JE Drut (2021), "Fourth-and fifth-order virial expansion of harmonically trapped fermions at unitarity", in *Physical Review Research* 3.3, p. 033099.
Hugenholtz, N. M. & D. Pines (1959), "Ground-State Energy and Excitation Spectrum of a System of Interacting Bosons", in *Phys. Rev.* 116 (3), pp. 489–506.
Kaplan, David B. & Sichun Sun (2011), "New Field-Theoretic Method for the Virial Expansion", in *Phys. Rev. Lett.* 107 (3), p. 030601.
Khramov, Alexander Y., Anders H. Hansen, Alan O. Jamison, William H. Dowd & Subhadeep Gupta (2012), "Dynamics of Feshbach molecules in an ultracold three-component mixture", in *Phys. Rev. A* 86 (3), p. 032705.
Klempt, C., O. Topic, G. Gebreyesus, M. Scherer, T. Henninger, P. Hyllus, W. Ertmer, L. Santos & J. J. Arlt (2010), "Parametric Amplification of Vacuum Fluctuations in a Spinor Condensate", in *Phys. Rev. Lett.* 104 (19), p. 195303.
Ku, Mark JH, Ariel T Sommer, Lawrence W Cheuk & Martin W Zwierlein (2012), "Revealing the superfluid lambda transition in the universal thermodynamics of a unitary Fermi gas", in *Science* 335.6068, pp. 563–567.
Landau, L. D. & E. M. Lifshitz (1975), *Physique Statistique*, Editions Mir.
Larsen, David M (1963), "Binary mixtures of dilute bose gases with repulsive interactions at low temperature", in *Annals of Physics (New York)(US)* 24.
Laurent, Sébastien, Xavier Leyronas & Frédéric Chevy (2014), "Momentum Distribution of a Dilute Unitary Bose Gas with Three-Body Losses", in *Phys. Rev. Lett.* 113 (22), p. 220601.
Laurent, Sébastien, Matthieu Pierce, Marion Delehaye, Tarik Yefsah, Frédéric Chevy & Christophe Salomon (2017), "Connecting Few-Body Inelastic Decay to Quantum Correlations in a Many-Body System: A Weakly Coupled Impurity in a Resonant Fermi Gas", in *Phys. Rev. Lett.* 118 (10), p. 103403.
Law, C. K., H. Pu & N. P. Bigelow (1998), "Quantum Spin Mixing in Spinor Bose-Einstein Condensates", in *Phys. Rev. Lett.* 81, p. 5257.
Lebowitz, J. L. & O. Penrose (1964), "Convergence of Virial Expansions", in *Journal of Mathematical Physics* 5.7, pp. 841–847.
Lee, Tsin D, Kerson Huang & Chen N Yang (1957), "Eigenvalues and eigenfunctions of a Bose system of hard spheres and its low-temperature properties", in *Physical Review* 106.6, p. 1135.
Leggett, A. J. (2001), "Bose–Einstein condensation in the alkali gases", in *Rev. Mod. Phys.* 73, p. 333.
– (2006), *Quantum Liquids*, Oxford University Press.
Leyronas, X. (2011), "Virial expansion with Feynman diagrams", in *Phys. Rev. A* 84 (5), p. 053633.
Li, Weiran & Tin-Lun Ho (2012), "Bose Gases near Unitarity", in *Phys. Rev. Lett.* 108 (19), p. 195301.
Lieb, Elliott H, Robert Seiringer, Jan Philip Solovej & Jakob Yngvason (2005), *The mathematics of the Bose gas and its condensation*, vol. 34, Springer Science & Business Media.
Liu, Xia-Ji (2013), "Virial expansion for a strongly correlated Fermi system and its application to ultracold atomic Fermi gases", in *Physics Reports* 524.2, pp. 37–83.
Liu, Xia-Ji, Hui Hu & Peter D. Drummond (2009), "Virial Expansion for a Strongly Correlated Fermi Gas", in *Phys. Rev. Lett.* 102 (16), p. 160401.
Lopes, Raphael, Christoph Eigen, Adam Barker, Konrad G. H. Viebahn, Martin Robert-de Saint-Vincent, Nir Navon, Zoran Hadzibabic & Robert P. Smith (2017a), "Quasiparticle Energy in a Strongly Interacting Ho-

mogeneous Bose-Einstein Condensate", in *Phys. Rev. Lett.* 118 (21), p. 210401.

Lopes, Raphael, Christoph Eigen, Nir Navon, David Clément, Robert P. Smith & Zoran Hadzibabic (2017b), "Quantum Depletion of a Homogeneous Bose-Einstein Condensate", in *Phys. Rev. Lett.* 119 (19), p. 190404.

Luciuk, Christopher, Stefan Trotzky, Scott Smale, Zhenhua Yu, Shizhong Zhang & Joseph H Thywissen (2016), "Evidence for universal relations describing a gas with p-wave interactions", in *Nature Physics* 12.6, pp. 599–605.

Mias, George I., Nigel R. Cooper & S. M. Girvin (2008), "Quantum noise, scaling, and domain formation in a spinor Bose-Einstein condensate", in *Phys. Rev. A* 77 (2), p. 023616.

Minardi, F, F Ancilotto, A Burchianti, C D'Errico, C Fort & M Modugno (2019), "Effective expression of the Lee-Huang-Yang energy functional for heteronuclear mixtures", in *Physical Review A* 100.6, p. 063636.

Minguzzi, A., P. Vignolo & M.P. Tosi (2002), "High-momentum tail in the Tonks gas under harmonic confinement", in *Physics Letters A* 294, pp. 222–226.

Mohling, F. & A. Sirlin (1960), "Low-Lying Excitations in a Bose Gas of Hard Spheres", in *Phys. Rev.* 118 (2), pp. 370–378.

Moroni, S., D. E. Galli, S. Fantoni & L. Reatto (1998), "Variational theory of bulk ^{4}He with shadow wave functions: Ground state and the phonon-maxon-roton spectrum", in *Phys. Rev. B* 58 (2), pp. 909–924.

Mukherjee, Biswaroop, Parth B. Patel, Zhenjie Yan, Richard J. Fletcher, Julian Struck & Martin W. Zwierlein (2019), "Spectral Response and Contact of the Unitary Fermi Gas", in *Phys. Rev. Lett.* 122 (20), p. 203402.

Naidon, Pascal & Shimpei Endo (May 2017), "Efimov physics: a review", in *Reports on Progress in Physics* 80.5, p. 056001.

Naraschewski, M & RJ Glauber (1999), "Spatial coherence and density correlations of trapped Bose gases", in *Physical Review A* 59.6, p. 4595.

Nascimbène, Sylvain, Nir Navon, KJ Jiang, Frédéric Chevy & Christophe Salomon (2010), "Exploring the thermodynamics of a universal Fermi gas", in *Nature* 463.7284, pp. 1057–1060.

Nation, PD, JR Johansson, MP Blencowe & Franco Nori (2012), "Colloquium: Stimulating uncertainty: Amplifying the quantum vacuum with superconducting circuits", in *Reviews of Modern Physics* 84.1, p. 1.

Navon, Nir, Swann Piatecki, Kenneth Günter, Benno Rem, Trong Canh Nguyen, Frédéric Chevy, Werner Krauth & Christophe Salomon (2011), "Dynamics and thermodynamics of the low-temperature strongly interacting Bose gas", in *Physical review letters* 107.13, p. 135301.

Ngampruetikorn, Vudtiwat, Meera M. Parish & Jesper Levinsen (2015), "High-temperature limit of the resonant Fermi gas", in *Phys. Rev. A* 91 (1), p. 013606.

Nozières, P. & D. Pines (1990), *The Theory of Quantum Liquids, Superfluid Bose Liquids*, Addison-Wesley.

Olshanii, Maxim & Vanja Dunjko (2003), "Short-Distance Correlation Properties of the Lieb-Liniger System and Momentum Distributions of Trapped One-Dimensional Atomic Gases", in *Phys. Rev. Lett.* 91 (9), p. 090401.

Olshanii, Maxim & Ludovic Pricoupenko (2001), "Rigorous Approach to the Problem of Ultraviolet Divergencies in Dilute Bose Gases", in *Phys. Rev. Lett.* 88 (1), p. 010402.

Papp, SB, JM Pino, RJ Wild, S Ronen, Carl E Wieman, Deborah S Jin & Eric A Cornell (2008), "Bragg spectroscopy of a strongly interacting rb 85 bose-einstein condensate", in *Physical review letters* 101.13, p. 135301.

Partridge, G. B., K. E. Strecker, R. I. Kamar, M. W. Jack & R. G. Hulet (2005), "Molecular Probe of Pairing in the BEC-BCS Crossover", in *Phys. Rev. Lett.* 95 (2), p. 020404.

Pethick, Christopher & Henrik Smith (2008), *Bose-Einstein condensation in dilute gases*, 2nd ed, Cambridge ; New York: Cambridge University Press.

Petrov, D. S. (Jan. 2003), "Three-body problem in Fermi gases with short-range interparticle interaction"en, in *Physical Review A* 67.1, p. 010703.

– (2004), "Three-Boson Problem near a Narrow Feshbach Resonance", in *Phys. Rev. Lett.* 93, p. 143201.

Petrov, D. S., C. Salomon & G. V. Shlyapnikov (2004), "Weakly Bound Dimers of Fermionic Atoms", in *Phys. Rev. Lett.* 93 (9), p. 090404.

Petrov, DS (2015), "Quantum mechanical stabilization of a collapsing Bose-Bose mixture", in *Physical Review Letters* 115.15, p. 155302.

Pezzè, Luca, Augusto Smerzi, Markus K. Oberthaler, Roman Schmied & Philipp Treutlein (2018), "Quantum metrology with nonclassical states of atomic ensembles", in *Rev. Mod. Phys.* 90 (3), p. 035005.

Pieri, Pierbiagio, Andrea Perali & Giancarlo Calvanese Strinati (2009), "Enhanced paraconductivity-like fluctuations in the radiofrequency spectra of ultracold Fermi atoms", in *Nature Physics* 5.10, pp. 736–740.

Pitaevskii, L. & S. Stringari (2016), *Bose–Einstein Condensation and Superfluidity*, 2nd edition, Oxford: Oxford University Press.

Pitaevskii, L. P. & A. Rosch (1997), "Breathing mode and hidden symmetry of trapped atoms in two dimensions", in *Phys. Rev. A* 55, R853.
Pricoupenko, Ludovic (2006), "Modeling Interactions for Resonant p-Wave Scattering", in *Phys. Rev. Lett.* 96 (5), p. 050401.
Prokof'ev, N. V. & B. V. Svistunov (2002), "Two-dimensional weakly interacting Bose gas in the fluctuation region", in *Phys. Rev. A* 66, p. 043608.
Pu, H. & P. Meystre (2000), "Creating Macroscopic Atomic Einstein-Podolsky-Rosen States from Bose-Einstein Condensates", in *Phys. Rev. Lett.* 85 (19), pp. 3987–3990.
Punk, M & W Zwerger (2007), "Theory of rf-spectroscopy of strongly interacting fermions", in *Physical review letters* 99.17, p. 170404.
Rakshit, D., K. M. Daily & D. Blume (2012), "Natural and unnatural parity states of small trapped equal-mass two-component Fermi gases at unitarity and fourth-order virial coefficient", in *Phys. Rev. A* 85 (3), p. 033634.
Rem, B. S., A. T. Grier, I. Ferrier-Barbut, U. Eismann, T. Langen, et al. (2013), "Lifetime of the Bose Gas with Resonant Interactions", in *Phys. Rev. Lett.* 110 (16), p. 163202.
Ren, Hai-cang (2004), "The virial expansion of a dilute Bose gas in two dimensions", in *Journal of statistical physics* 114.1-2, pp. 481–501.
Ronen, Shai (2009), "The dispersion relation of a Bose gas in the intermediate-and high-momentum regimes", in *Journal of Physics B: Atomic, Molecular and Optical Physics* 42.5, p. 055301.
Rossi, R., T. Ohgoe, K. Van Houcke & F. Werner (2018), "Resummation of Diagrammatic Series with Zero Convergence Radius for Strongly Correlated Fermions", in *Phys. Rev. Lett.* 121 (13), p. 130405.
Rupak, Gautam (2007), "Universality in a 2-Component Fermi System at Finite Temperature", in *Phys. Rev. Lett.* 98 (9), p. 090403.
Sadler, LE, JM Higbie, SR Leslie, M Vengalattore & DM Stamper-Kurn (2006), "Spontaneous symmetry breaking in a quenched ferromagnetic spinor Bose–Einstein condensate", in *Nature* 443.7109, pp. 312–315.
Sagi, Yoav, Tara E Drake, Rabin Paudel & Deborah S Jin (2012), "Measurement of the homogeneous contact of a unitary Fermi gas", in *Physical review letters* 109.22, p. 220402.
Schmitt, Matthias, Matthias Wenzel, Fabian Böttcher, Igor Ferrier-Barbut & Tilman Pfau (2016), "Self-bound droplets of a dilute magnetic quantum liquid", in *Nature* 539.7628, pp. 259–262.
Semeghini, G, G Ferioli, L Masi, C Mazzinghi, L Wolswijk, F Minardi, M Modugno, G Modugno, M Inguscio & M Fattori (2018), "Self-bound quantum droplets of atomic mixtures in free space", in *Physical review letters* 120.23, p. 235301.
Shi, Hao, Simone Chiesa & Shiwei Zhang (2015), "Ground-state properties of strongly interacting Fermi gases in two dimensions", in *Phys. Rev. A* 92 (3), p. 033603.
Smith, D. Hudson, Eric Braaten, Daekyoung Kang & Lucas Platter (2014), "Two-Body and Three-Body Contacts for Identical Bosons near Unitarity", in *Phys. Rev. Lett.* 112 (11), p. 110402.
Sokol, P.E. (1995), "Bose–Einstein Condensation", in , ed. by A. Griffin, D. W. Snoke & S. Stringari, Cambridge University Press, chap. 4. Bose-Einstein condensation in liquid helium.
Spiegelhalder, F. M., A. Trenkwalder, D. Naik, G. Hendl, F. Schreck & R. Grimm (2009a), "Collisional Stability of ^{40}K Immersed in a Strongly Interacting Fermi Gas of ^{6}Li", in *Phys. Rev. Lett.* 103 (22), p. 223203.
– (2009b), "Collisional Stability of ^{40}K Immersed in a Strongly Interacting Fermi Gas of ^{6}Li", in *Phys. Rev. Lett.* 103 (22), p. 223203.
Steinhauer, J., R. Ozeri, N. Katz & N. Davidson (2002), "Excitation spectrum of a Bose–Einstein condensate", in *Phys. Phys. Lett.* 88.12, p. 120407.
Stewart, JT, JP Gaebler, TE Drake & DS Jin (2010), "Verification of universal relations in a strongly interacting Fermi gas", in *Physical Review Letters* 104.23, p. 235301.
Stringari, S (2004), "Collective oscillations of a trapped superfluid Fermi gas near a Feshbach resonance", in *EPL (Europhysics Letters)* 65.6, p. 749.
Sykes, AG, JP Corson, JP D'Incao, AP Koller, CH Greene, Ana Maria Rey, KRA Hazzard & JL Bohn (2014), "Quenching to unitarity: Quantum dynamics in a three-dimensional Bose gas", in *Physical Review A* 89.2, p. 021601.
Tan, Shina (2008a), "Energetics of a strongly correlated Fermi gas", in *Annals of Physics* 323.12, pp. 2952–2970.
– (2008b), "Generalized virial theorem and pressure relation for a strongly correlated Fermi gas", in *Annals of Physics* 323.12, pp. 2987–2990.
– (2008c), "Large momentum part of a strongly correlated Fermi gas", in *Annals of Physics* 323.12, pp. 2971–2986.
– (2008d), "Three-boson problem at low energy and implications for dilute Bose-Einstein condensates", in *Phys. Rev. A* 78 (1), p. 013636.
Tanzi, Luca, Eleonora Lucioni, Francesca Famà, Jacopo Catani, Andrea Fioretti, Carlo Gabbanini, Russell N Bisset, Luis Santos & Giovanni Mod-

ugno (2019), "Observation of a dipolar quantum gas with metastable supersolid properties", in *Physical review letters* 122.13, p. 130405.
Tenart, Antoine, Gaétan Hercé, Jan-Philipp Bureik, Alexandre Dareau & David Clément (2021), "Observation of pairs of atoms at opposite momenta in an equilibrium interacting Bose gas", in *Nature Physics*, pp. 1–5.
Timmermans, Eddy (1998), "Phase separation of Bose-Einstein condensates", in *Phys. Phys. Lett.* 81.26, p. 5718.
Uhlenbeck, George E & Erich Beth (1936), "The quantum theory of the non-ideal gas I. Deviations from the classical theory", in *Physica* 3.8, pp. 729–745.
Walls, D. F. & G. J. Milburn (1988), *Quantum optics*, Berlin: Springer-Verlag.
Walls, Daniel F & Gerard J Milburn (2007), *Quantum optics*, Springer Science & Business Media.
Werner, F., L. Tarruell & Y. Castin (Apr. 2009), "Number of closed-channel molecules in the BEC-BCS crossover"en, in *The European Physical Journal B* 68.3, pp. 401–415.
Werner, Félix (Aug. 2008), "Virial theorems for trapped cold atoms"en, in *Physical Review A* 78.2, p. 025601.
Werner, Félix & Yvan Castin (2006), "Unitary Quantum Three-Body Problem in a Harmonic Trap", in *Phys. Rev. Lett.* 97 (15), p. 150401.
Werner, Félix & Yvan Castin (Nov. 2012a), "General relations for quantum gases in two and three dimensions. II. Bosons and mixtures", in *Physical Review A* 86.5, p. 053633.
– (July 2012b), "General relations for quantum gases in two and three dimensions: Two-component fermions"en, in *Physical Review A* 86.1, p. 013626.
Wild, RJ, P Makotyn, JM Pino, EA Cornell & DS Jin (2012), "Measurements of Tan's contact in an atomic Bose-Einstein condensate", in *Physical review letters* 108.14, p. 145305.
Wu, Tai Tsun (1959), "Ground State of a Bose System of Hard Spheres", in *Phys. Rev.* 115 (6), pp. 1390–1404.
Xu, K., Y. Liu, D. E. Miller, J. K. Chin, W. Setiawan & W. Ketterle (2006), "Observation of Strong Quantum Depletion in a Gaseous Bose-Einstein Condensate", in *Phys. Rev. Lett.* 96 (18), p. 180405.
Yan, Yangqian & D. Blume (2016), "Path-Integral Monte Carlo Determination of the Fourth-Order Virial Coefficient for a Unitary Two-Component Fermi Gas with Zero-Range Interactions", in *Phys. Rev. Lett.* 116 (23), p. 230401.
Yin, XY & D Blume (2015), "Trapped unitary two-component Fermi gases with up to ten particles", in *Physical Review A* 92.1, p. 013608.
Yoshida, Shuhei M. & Masahito Ueda (2015), "Universal High-Momentum Asymptote and Thermodynamic Relations in a Spinless Fermi Gas with a Resonant p-Wave Interaction", in *Phys. Rev. Lett.* 115 (13), p. 135303.
Yu, Z. & G. Baym (2006), "Spin-correlation functions in ultracold paired atomic-fermion systems: Sum rules, self-consistent approximations, and mean fields", in *Phys. Rev. A* 73 (6), p. 063601.
Yu, Zhenhua, Georg M. Bruun & Gordon Baym (2009), "Short-range correlations and entropy in ultracold-atom Fermi gases", in *Phys. Rev. A* 80 (2), p. 023615.
Yu, Zhenhua, Joseph H. Thywissen & Shizhong Zhang (2015), "Universal Relations for a Fermi Gas Close to a p-Wave Interaction Resonance", in *Phys. Rev. Lett.* 115 (13), p. 135304.
– (2016), "Erratum: Universal Relations for a Fermi Gas Close to a p-Wave Interaction Resonance [Phys. Rev. Lett. 115, 135304 (2015)]", in *Phys. Rev. Lett.* 117 (1), p. 019901.
Zhang, Shizhong & Anthony J. Leggett (2009), "Universal properties of the ultracold Fermi gas", in *Phys. Rev. A* 79 (2), p. 023601.
Zou, Y-Q, B Bakkali-Hassani, C Maury, É Le Cerf, S Nascimbene, J Dalibard & J Beugnon (2021), "Tan's two-body contact across the superfluid transition of a planar Bose gas", in *Nature communications* 12.1, pp. 1–6.
Zwerger, Wilhelm, ed. (2012), *The BCS-BEC crossover and the unitary fermi gas*en, Lecture notes in physics 836, OCLC: 844865150, Heidelberg: Springer.